AMIRA INTERNATIONAL

Progress Report

Confidential

P544 – Proterozoic Sediment Hosted Copper Deposits

December 2001

Centre for Ore Deposit Research – University of Tasmania
Colorado School of Mines

AMIRA International Limited ACN 004 448 266 ABN 60 176 687 975
9th Floor 128 Exhibition Street Melbourne 3000 Australia Phone: +61 3 9679 9999 Facsimile: +61 3 9679 9900
email: AMIRA@amira.com.au Website www.amira.com.au

Proterozoic sediment-hosted copper deposits

AMIRA/ARC project P544

Meeting 4
December 2001

CODES SRC

UNIVERSITY
OF TASMANIA

Produced by the
Centre for Ore Deposit Research
University of Tasmania
GPO Box 252-79,
Hobart Tasmania Australia 7001

December 2001

Cover photo — Lower Roan equivalent in South Australia: contact betweeen the Mount Painter Complex (basement) and the basal unit of the Arkaroola Subgroup, the Paralana Quartzite.

another Pongratz & Hlaing Production 2001

Contents

Introduction

ARC/AMIRA Project P544 "Proterozoic sediment-hosted copper deposits" has a number of important objectives which include:

1. To understand the processes responsible for transporting, concentrating and fixing Cu and other ore constituents during sedimentary basin evolution.
2. To document the various stages and paragenesis of copper deposition and remobilisation during basin evolution.
3. To develop a range of geological, geochemical and isotopic vectors that point toward ore, both on a district and a deposit scale.
4. To determine what is different about the setting and geological evolution of the African Copperbelt, compared to Australian Proterozoic sedimentary basins, that may explain the difference in Cu (and Co) endowment in these areas.
5. To apply research results from both Africa and Australia to produce better empirical exploration models for Proterozoic sediment-hosted Cu deposits.

The reports presented here are the results of work carried out by CODES researchers in Zambia and South Australia during 2001, and they begin to address some, or all of the project objectives. It is the first annual report prepared with the CODES research team at 'full strength', now that Rob Scott has joined the team, and both Zambian PhD projects are underway.

Presentation of these results was to have been made at a sponsors' meeting in Hobart in February, but this will now take place at a combined meeting and field trip in May. Activities by CSM researchers will also be reported on at the sponsors' meeting in Adelaide.

The first contribution (Selley & Bull: **Basin architecture during deposition of the lower to middle Umberatana Group, northern Flinders Ranges, South Australia: implications for Cu mineralisation**) describes mapping traverses through the Adelaide Fold Belt in the northern Flinders Ranges. Marked lateral facies variations in the Tapley Hill Formation indicate a period of accelerated basin growth during early to middle Umberatana Group times. Collapse of thick Burra Group sequences into the underlying Curdimurka Subgroup rocks and related diapir emplacement, provides a mechanism that allows deep seated saline Cu-bearing fluids to interact with the organic carbon rich rocks of the Tapley Hill Formation.

The second of the South Australian contributions (Mackay: **Sedimentology and structure of the Curdimurka Subgroup, Willouran Range, South Australia**) is a progress report on the results of field work in the Willouran Ranges for Mackay's PhD research which commenced early in 2001. The Willouran Ranges contain excellent exposures of the Callanna and Burra Groups (the two lowermost units in the Adelaide Fold Belt sequences), and the work presented here indicates that the area has undergone at least two early phases of compressional deformation. Furthermore, in the areas visited to date, the Callanna and Burra Groups are always in tectonic contact.

The report by McGoldrick: **Copper mineralisation at Emmie Bluff, South Australia 1: Setting, host rocks, ore textures and multi-element geochemistry**,

describes the results of geochemical and petrographic investigations of the two spatially separate styles of Cu mineralisation at Emmie Bluff on the Stuart Shelf. While the data do not prove a genetic link between the two mineralisation types, they are consistent with all mineralisation forming at, or after, about 600 Ma from oxidised fluids moving (laterally) out of the Adelaide Fold Belt sequences. These fluids would flow through both basement and cover rocks of the Stuart Shelf , and Cu would be trapped at suitably chemically reactive sites (eg., magnetite 'skarn' rocks in the basement, organic carbon rich rocks in the cover).

Zambian research results are described in the subsequent four reports, and the Zambian section concludes with outlines of the two CODES PhD projects commenced in the latter half of 2001.

The report by Selley & Bull: **Stratigraphy and basin geometry at the Chibuluma West copper–cobalt deposit, Zambia** describes a condensed sequence of Lower Roan sediments from the southern margin of the Chambishi 'basin'. This package was deposited within a series of WNW-trending, asymmetric depocentres and basin growth was controlled by an array of NNE-dipping growth faults. Tilt-block rotation resulted in uplift of basement-cored blocks, which continued to amplify during sedimentation. Emergence of the transfer zone late during deposition of the Lower Roan, resulted in reworking of basal strata into restricted depocentres and lapping of Upper Roan units directly onto basement. Basin inversion caused further amplification of basement-cored blocks and emplacement within the Lower Roan stratigraphy along mylonitic footwall cut-out thrusts. Roan sub-basins were tightened into WNW-trending synclines, separated by basement inliers.

The next report, Selley & Cooke: **Mineral zonation and sulfur isotope systematics of the Chibuluma West copper–cobalt deposit, Zambia** is also based on core from Chibuluma West deposit. Small scale stratiform ore textures and their relationship to layer parallel albitic flooding and dilation along bedding surfaces are described. New laser ablation S isotope data are presented for Cu and Fe sulfides, which indicate the Chibuluma sulfides are anomalously isotopically heavy compared to published values from other Copperbelt deposits. There is a systematic relationship between stratigraphic position and S isotopic compositions, but no obvious correlation with metal grades and sulfide mineral zonation. The data have several important implications for ore formation

- bornite and chalcopyrite are not in isotopic equilibrium
- direct biogenic sulfate reduction was not an important process at Chibuluma
- grainscale isotopic heterogeneity precludes a single homogenous aqueous S source

The report by Scott: **Structural setting and paragenesis of the Mufulira copper deposit, Zambia** uses new observations from selected underground exposures and stratigraphic thickness data extracted from mine sections to better understand the nature and significance of the basement contact at Mufulira. Three underground exposures were selected because of their proximity to so-called 'palaeo-highs', and observations from these locations suggest the Lower Roan bedding parallels the basement contact, or onlaps it at a low angle. There is little indication of significant shearing or faulting at this contact. Thickness relationships for C-Orebody and the Footwall Formation in the central basin are consistent with deposition of the Footwall Formation into an actively forming half-graben. As no Footwall Formation unit can be correlated between various sub-basins, it is likely significant relief existed prior to the onset of Katangan sedimentation, and this was maintained by faulting until just prior to deposition of the Ore Formation.

The Konkola (Kirilabomwe) deposits are the most 'sedimentary'-looking of all the Copperbelt deposits and the report by Scott & Pollington: **Character, paragenesis and zonation of the copper ores at Konkola (Kirilabomwe), Zambia**, describes the relationship between Cu sulfides and the strong

bedding parallel fabric in the host siltstones at Konkola. They conclude that any structurally induced upgrading or remobilization of sulfides is very minor and occurred during localised layer parallel dilation and shearing related to regional folding (e.g., Kirilabomwe Anticline). Another important conclusion from their work is that although primary chalcocite occurs throughout the Ore Shale, there is a prominent zone of secondary (supergene) chalcocite (+hematite) mineralisation at the top and bottom margins of this unit.

The Zambian part of the report concludes with outlines of PhD projects at Nkana and Konkola North (Mawson Croaker: **Geology and genesis of the Nkana deposit, Zambia** & Nicky Pollington: **Sedimentology, mineral paragenesis and geochemistry of the Konkola North Copper deposit, Zambia)** and deposit summaries covering Nkana and Konkola North. These deposit summaries are the first of a series which we intend to produce for all the Zambian Copperbelt deposits.

The final report by Bull et al.: **Provisional stratigraphic comparison of three copper mineralized basins; the Zambian Copperbelt, the Polish Kupferschiefer and the Adelaide Fold Belt** is our first serious attempt to compare the Zambian Copperbelt and the Adelaide Fold Belt. Several members of the research team had the opportunity to visit the Polish Kupferschiefer in August. From this visit it was clear the basin setting of the European Permo-Triassic shared many common features with the Neoproterozoic of Zambia and South Australia, but there were also important differences. This report describes these features and discusses their implications for Cu metallogeny in the Zambian Copperbelt and the Adelaide Fold Belt. The report concludes by proposing a number of testable hypotheses that should help refine basin analysis aspects of our research in the Zambian Copperbelt.

In conclusion, I would like to compliment the research team for a very productive year and thank everyone for their efforts so far. I believe we have made very good progress toward a more contemporary understanding of the Zambian Copperbelt, and are beginning to recognise some of the key questions regarding Cu metallogeny in the Neoproterozoic in South Australia. Finally, I would like to acknowledge June Pongratz efforts in layout and setting all the reports to yield yet another fine Pongratz Production.

Peter McGoldrick
January 2002

Basin architecture during deposition of the lower to middle Umberatana Group, Adelaide Fold Belt, South Australia: implications for Cu mineralisation

David Selley & Stuart Bull
Centre for Ore Deposit Research, University of Tasmania

Summary

A pronounced phase of basin growth is recorded by lower and middle Umberatana Group strata of the Adelaide Fold Belt. Basin style is characterised by the generation of asymmetric, wedge-shaped accommodation spaces atop significantly rotated blocks comprising Warrina Supergroup. Block rotation occurred in response to extension along a complex array of shallowly dipping, listric normal faults, most probably soling out within evaporitic strata of the lower Curdimurka Subgroup. Basin growth initiated at least as early as the Sturtian glacial period, but accelerated during deposition of the middle Tapley Hill Formation. Sedimentation during this period included voluminous influx of coarse-grained megabreccias and conglomerates, which cut down progressively through lower Umberatana and Burra group strata, possibly as low as the upper Curdimurka Subgroup.

Basin growth was driven by the combined effects of accelerated Rodinean breakup and gravitational collapse of thick Burra Group sequences into the underlying Curdimurka Subgroup. Rotational uplift of the Curdimurka Subgroup, probable emplacement of diapirs and enhancement of fluid flow coeval with Umberatana Group sedimentation, provided the mechanisms for interaction of deep seated saline Cu-bearing fluids with reactive host media of the Tapley Hill Formation.

Introduction and rationale

In this report we presents results from a traverse across the Torrens Hinge Zone to the major depocentres located east of the Norwest Fault in the Willouran Ranges. Research was focussed at lower and middle levels of Umberatana Group, which record a pronounced acceleration of basin subsidence as well as mobilisation of deep level salt derived largely from the evaporite-rich Curdimurka Subgroup. The principal aim of the study is to decipher basin evolution during deposition of the carbonaceous Tapley Hill Formation, which hosts numerous small stratiform, breccia and vein style copper deposits within the Northern Adelaide Fold Belt, and larger stratiform and stratabound copper deposits on the neighbouring Stuart Shelf. Can the density of copper deposits found at this stratigraphic level be recording a "diagenetic" phase of mineralisation related to a fundamental reorganisation of basin geometry and fluid circulation systems, or does it simply reflect a favourably reactive host medium for basinal fluids expelled during basin dewatering or Delamarian inversion?

Stratigraphic architecture and basin evolution

A fundamental change in basin geometry and stratigraphic architecture occurs at the Warrina–Heysen supergroup boundary (Fig. 1). Preiss (1983, 2000) interpreted this boundary to record an abrupt transition from rift-style basin growth to a protracted phase of sag-dominated sedimentation. In terms of global tectonics, this period of basin evolution is thought to define the onset of Rodinean breakup at ~700 Ma. The following section contrasts basin

evolutionary stages of the Warrina Supergroup and the lowest levels of the Heysen Supergroup (lower to middle Umberatana Group) in the northwestern Adelaide Fold Belt. Data and interpretation concerning the Warrina Supergroup come largely from published sources. Umberatana Group data were sourced from a combination of our own field work, aerial photo interpretation and published work specific to the Willouran Ranges (importantly Murrell, 1977; Coats and Dalgarno, 1983; Krieg et al., 1991).

Warrina Supergroup

Early rift basins filled with Warrina Supergroup strata (Callanna and Burra Groups) were narrow, fault bounded and deeply subsident, with restricted depocentres and sediment dispersal patterns. In the northwestern Adelaide Fold Belt, sedimentary and minor mafic and felsic volcanogenic units accumulated within a narrow NW striking, fault-bounded depocentre (Willouran Trough). The depocentre has a minimum strike length of 200 km (Fig. 2) and is bounded in part along its southwestern flank by the Norwest Fault, and to the south east by an ENE-trending splay off the Paralana "transfer system" (Paul et al., 1999; Selley, 2000). It is defined by a pronounced negative gravity anomaly which is most likely attributable to thick accumulations of low density clastic sediments of the Curdimurka Subgroup. Along the southwestern margin of the depocentre, the negative gravity anomaly transgresses the Norwest Fault, possibly indicating that during Willouran rift phases at least, the main basin-bounding structure lay further west than the current expression of this structure. Broadly, the gravity anomaly wanes to the southeast, a feature which is interpreted to reflect progressive thinning of the Warrina Supergroup in the region of the Paralana "transfer system" (or Central Flinders Domain) and supported by published isopach maps of Burra Group thickness (Paul et al., op. cit.).

The stratigraphic architecture of the Warrina Supergroup in the Willouran Trough comprises a series of stacked rift sequences (maximum thickness of 15 km) with relatively simple and cyclical internal structure (Fig. 1). Variation in the lithological character of each rift cycle is fairly subtle (Forbes and Preiss, 1987). Rift pulses are recorded by prograding arkosic clastic wedges, fed largely from marginal alluvial fan systems to the west, passing basinward to finer grained clastic and carbonate deposits (Coats and Preiss, 1987; Forbes and Preiss, op. cit.). Older rift phases of the Callanna Group are distinguished from younger phases by a more restricted basin environment and thick accumulations of cherty to evaporitic carbonates and thinly bedded evaporitic siliciclastic units deposited in sabkhas and hypersaline tidal flats respectively (Coats and Preiss, op. cit.). However, details of Callanna Group stratigraphic architecture are obscured by the combination of pervasive deformation (enhanced by salt tectonics during basin growth and inversion), and limited exposure at this stratigraphic level (Bull et al., this volume). For example, it is known that mafic volcanism formed part of the early rift phases in the Willouran Trough, but the evidence for this is confined to isolated basaltic and doleritic xenoliths within diapiric breccias.

The Burra Group records broadening of rifting during the Torrensian and a transition to shallow marine conditions in rift depocentres. The Norwest Fault was demonstrated by Paul (et al., 1999) to have been active as a major basin bounding growth fault at this time, with an order of magnitude increase in thickness of the Burra Group across this structure in the Leigh Creek area (southeastern Willouran Trough). Less pronounced but clear thickness variation also occurs across the Norwest Fault in the Willouran Ranges (northeastern Willouran Trough): calculation of Burra Group thicknesses from 1:250,000 geological survey maps reveals an abrupt increase of 3 km to in excess of 9 km from the footwall to the hangingwall of the Norwest Fault. There is also considerable thickness variation within the hangingwall of the Norwest Fault, which Belperio (1990) attributed to the development of a complex mosaic of second-order sub-basins. Although sub-basin development is probable in this region, we will argue below that

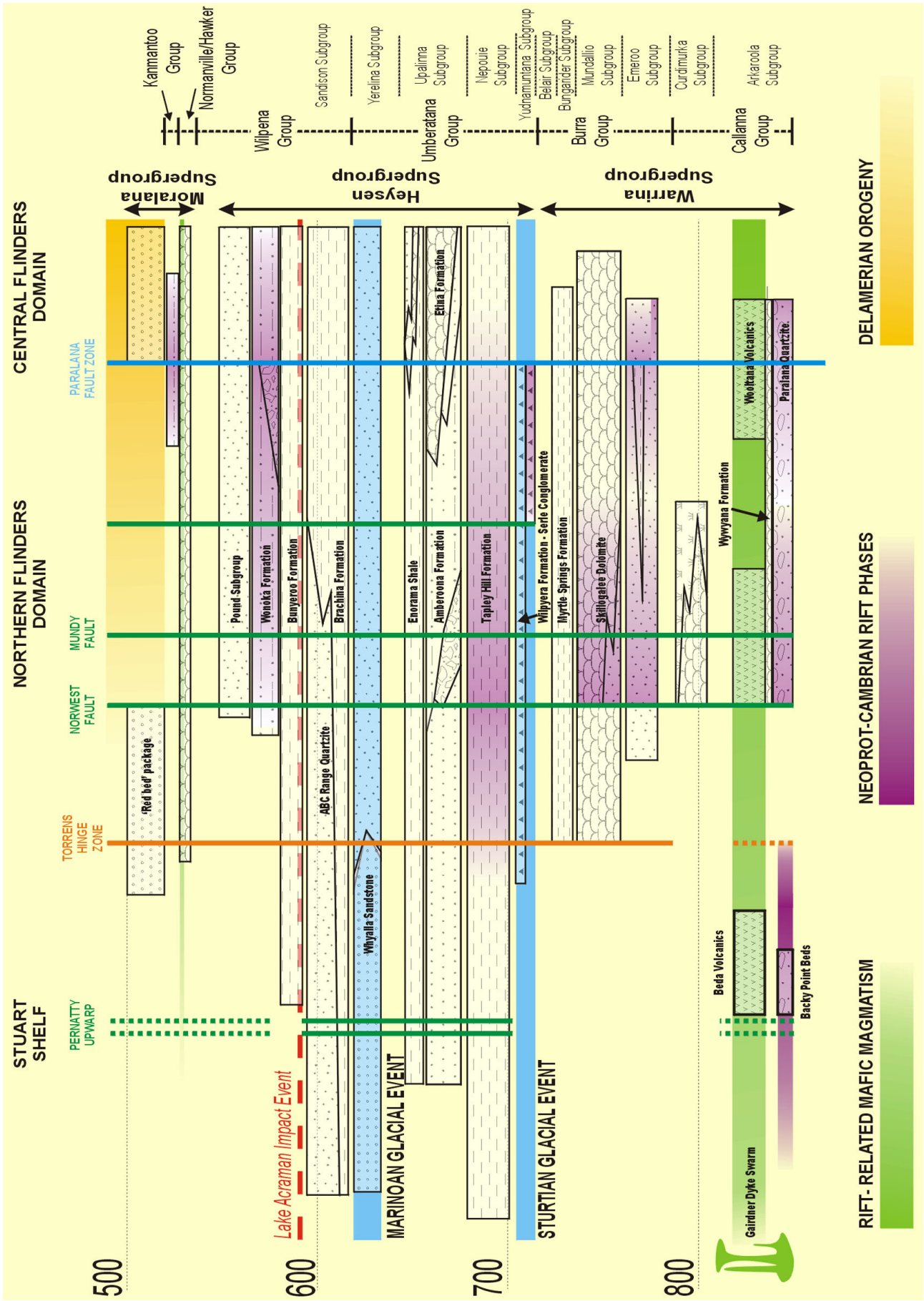

Figure 1
Event stratigraphy plot of Neoproterozoic and Cambrian packages of the northern Adelaide Fold Belt. Plot summaries elements of facies and basin architecture, limits of basin growth and inversion, and fundamental time lines (ie. glacial and impact events). Modified after Selley (2000).

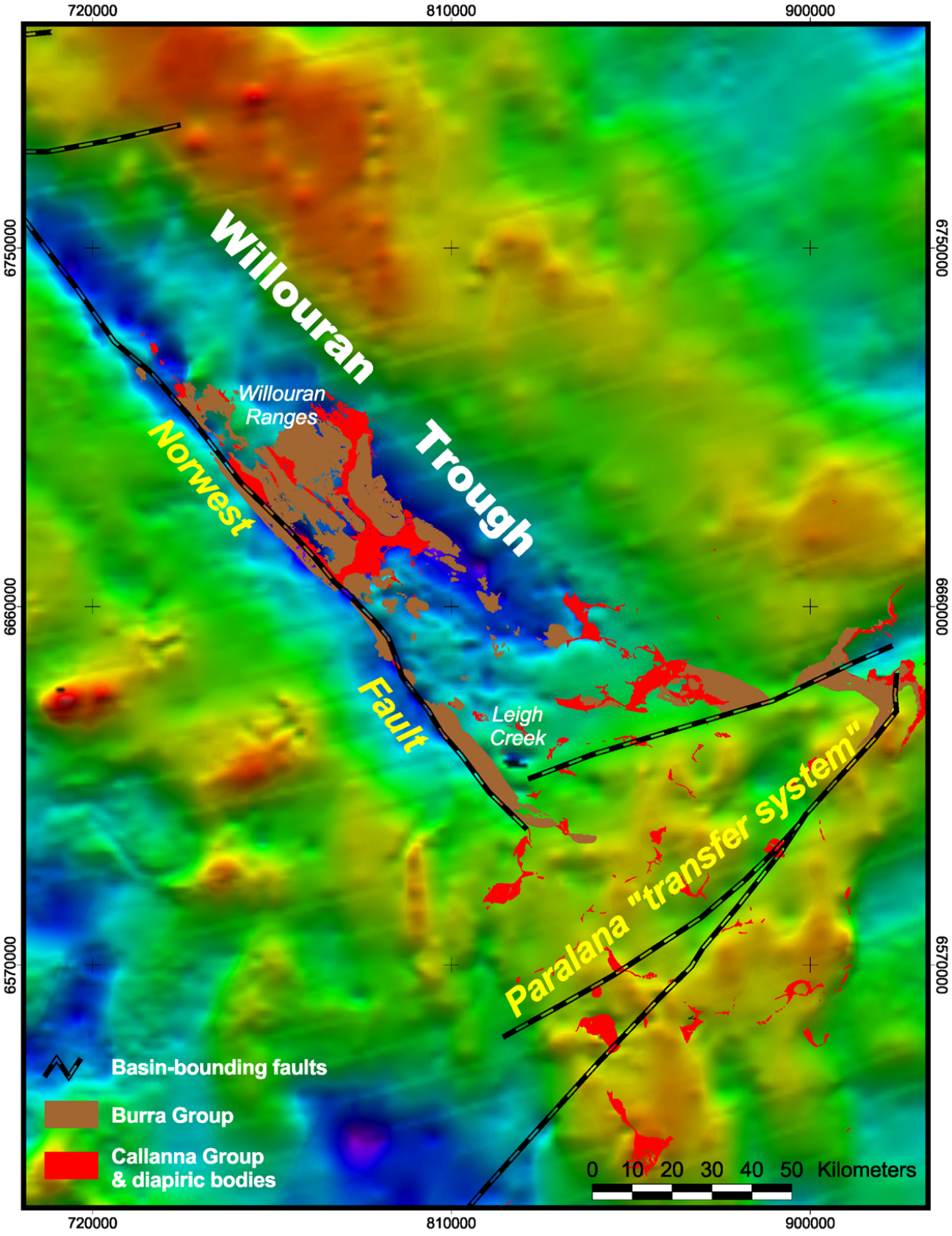

Figure 2.
Outcrop distribution of Callanna and Burra groups (Warrina Supergroup) overlain upon residual gravity image of the northern Adelaide Fold Belt. Note the coincidence of the thick accumulation of Warrina Supergroup strata with a prominent gravity low: ie. Willouran Trough. Strata at this level appear to thin southeastward into the Central Flinders domain, a partly platformal region interpreted to be controlled by the Paralana "transfer system". Outcrop and geophysical data supplied by PIRSA.

much of the observed thickness variation can be explained by the combination of post-depositional, low angle extensional "stripping" of the Burra Group and significant erosion during lower and middle Umberatana Group sedimentation. We consider that the Burra Group in the Willouran Ranges comprised a broadly southwesterly thickening wedge against the Norwest Fault prior to Umberatana Group sedimentation.

Although the Burra Group has locally been dramatically affected by salt tectonics, particularly within a broad corridor which lies 20–35 km northwest of the Norwest Fault trace, the internal structure of individual "blocks" is considerably less complex than the underlying Callanna Group. The trace of bedding in aerial photographs has a characteristic "tram-track" geometry, which supports the notion of a crude layer-cake stratigraphy.

Umberatana Group

Accelerated basin subsidence and dramatic increase in the complexity of basin geometry is shown by the stratigraphic architecture and sedimentology of the lower and middle Umberatana Group (Fig. 1). Depositional contacts between the Warrina Supergroup and the Umberatana Group are varied and complex. They range from semi-conformable relationships of basal Sturtian glacial deposits with the Burra Group, to very high angle erosional unconformities with deformed Burra Group or Callanna Group, to long-lived, apparently non-erosional onlap surfaces where successively higher levels of the Umberatana Group abut tilted and elevated blocks of Warrina Supergroup strata. The internal architecture of the Umberatana Group is further complicated by either localised or stacked (amalgamated) angular unconformities and pronounced lateral thickness variation. This architecture contrasts markedly with the relatively simple "layer-cake" stratigraphy of the Burra Group.

Throughout the lower and middle Umberatana Group, sedimentation was predominantly marine and sub-wave base, reflecting the increased rate of generation of accomodation space at this time. The onset of sedimentation occurred during the Sturtian glacial period, and is characterised by rapid influx of pebbly sandstones, lithicwacke and recessive shale, siltstone and thinly bedded sandstone packages represented in the Willouran Ranges by the Bolla Bollana Tillite, Wilyerpa Formation and locally the Serle Conglomerate. However, little of the glacial sequence was observed during the current study of middle Umberatana Group depocentres, largely because it has been extensively removed by erosion during deposition of this overlying succession (see below).

In the one locality it was observed, the Bolla Bollana tillite comprised a massive to laminated brown siltstone with scattered pebbles to boulders. Most of the clasts, including all of the boulders, were distinctive polished and/or faceted gray/white quartzite. Rare distinctive coarse-grained felsic porphyry pebbles/cobbles were also present (Fig. 3a). An extensive sequence of Wilyerpa Formation was also observed on one traverse. It comprised sub- to tens of metre-scale interbeds of massive to laminated to rippled siltstone and sandstone and open framework conglomerate (tillite; Fig. 3b).

The basal unit of the Tapley Hill Formation, the Tindelpina Shale Member, was observed at a number of localities. It consists of distinctive fissile, dark gray/black dolomitic and pyritic shale (Fig. 3c) with thin turbiditic sandstone interbeds. The remainder of the Tapley Hill Formation succession comprises less fissile but otherwise similar reduced, sub-wave base, laminated and locally rippled siltstones with varying proportions of interbedded turbiditic sandstones (Fig. 3d). It is conformably overlain by the Amberoona Formation, which is marked by a return to more fissile and carbonaceous (deeper water?) siltstones and shales (Fig. 3e) that have a distinctive fragmented outcrop pattern on aerial photographs.

Interbedded with the ambient turbidite and suspension deposits of the middle Umberatana

Group succession, are substantial amounts of pebble to boulder breccia. Bedforms indicate emplacement by various mass flow processes, from spalling of discrete blocks into fine-grained deposits (talus) to debris flows to high density turbidites. The clast assemblage records intrabasinal reworking (evidenced by numerous clasts of the distinctive faceted and polished quartzite from the basal glacial succession and rare clasts of granite) and erosion down to at least upper Burra Group levels. On the current 1:250,000 scale geological mapping, these breccia units are assigned to both the Tapley Hill and Amberoona Formations, however, it will be argued below that they represent a discrete tectonic event, and hence are a time line, that provides valuable insight into interpretation of the basin history.

Umberatana depocentres in the Willouran Ranges

In the northern Willouran Ranges and Torrens Hinge Zone (Fig. 4), the lower to middle Umberatana Group is preserved within at least three broadly NW trending depocentres: (1) a grossly northeastward deepening sub-basin located in the Torrens Hinge Zone (ie. footwall block of the Norwest Fault), (2) a narrow depocentre which follows the trace of the Bungerider Fault System, and (3) a major depocentre associated with the Kingston Fault Zone and extending northeastward to the present limit of exposure within the Willouran Trough. The latter two of these depocentres occur within the hangingwall of the Norwest Fault and exhibit both complex growth and inversion geometries. For example, thrust slices of Warrina Supergroup strata, probably emplaced upon original basin-bounding growth faults, punctuate Umberatana Group strata close to the western margin of each depocentre.

Additional sub-basins occur along the southern termination of the Willouran Ranges: i.e. south of Witchelina homestead (Fig. 4). They probably represent extensions of the Bungerider and/or Kingston depocentres, but are now separated from them by an ENE-trending "ridge" of thrust and diapirically modified Curdimurka Subgroup. A substantial depocentre probably also existed in the immediate hangingwall of the Norwest Fault, however intense inversion has resulted in erosion down to Warrina Supergroup levels.

In this section, we describe facies architecture and structural geometry of the two closely studied depocentres positioned within the hangingwall of the Norwest Fault.

Bungerider Depocentre

The Bungerider depocentre is preserved as a narrow NW trending trough which terminates at its northwestern and southeastern extremities against inliers of Callanna Group strata (Figs 4, 5). To the northwest, Umberatana Group strata pinch out near the confluence of WNW-trending Burra Group and the Rischbieth Complex (a structurally complex inlier of Callanna Group). To the southeast, the depocentre broadens somewhat, but terminates abruptly against Callanna Group strata thrust emplaced along the NE trending South Hill Structure.

Figure 3
Umberatana Group facies
(a) Bolla Bollana Tillite; coarse-grained felsic porphyry clast within laminated siltstone.
(b) Metre-scale Pebbly sandstone unit (tillite?) in Wilyerpa Formation.
(c) Typical Tindelpina Shale Member outcrop; turbiditic sandstone bed under hammer overlain interbedded with fissile carbonaceous shale (right of view).
(d) Typical Tapley Hill Formation outcrop; interbedded thin- to medium-bedded, massive to laminated sandstone and laminated siltstone (beneath hammer handle).
(e) Typical fissile siltstone of the Amberoona Formation.
(f) Typical rubbly exposure of thick, massive, middle Umberatana breccia unit; note large dolomite boulders (upper left and right), and faceted quartzite boulders (to right of hammer) interpreted to record reworking of underlying glacial deposits.


(a)

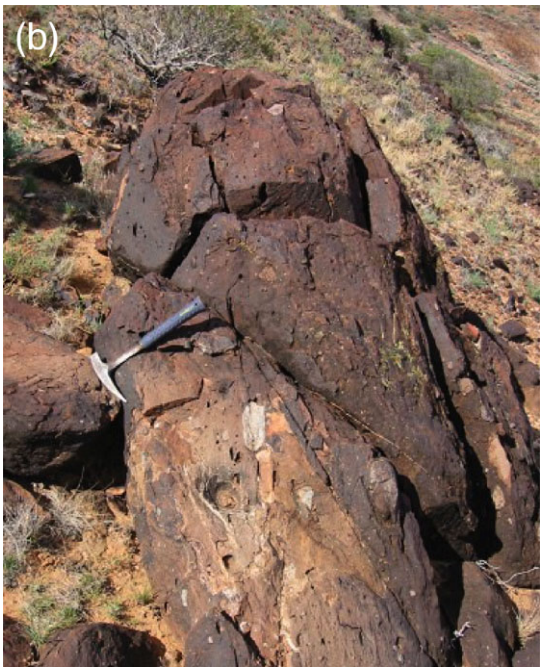
(b)


(c)


(d)


(e)


(f)

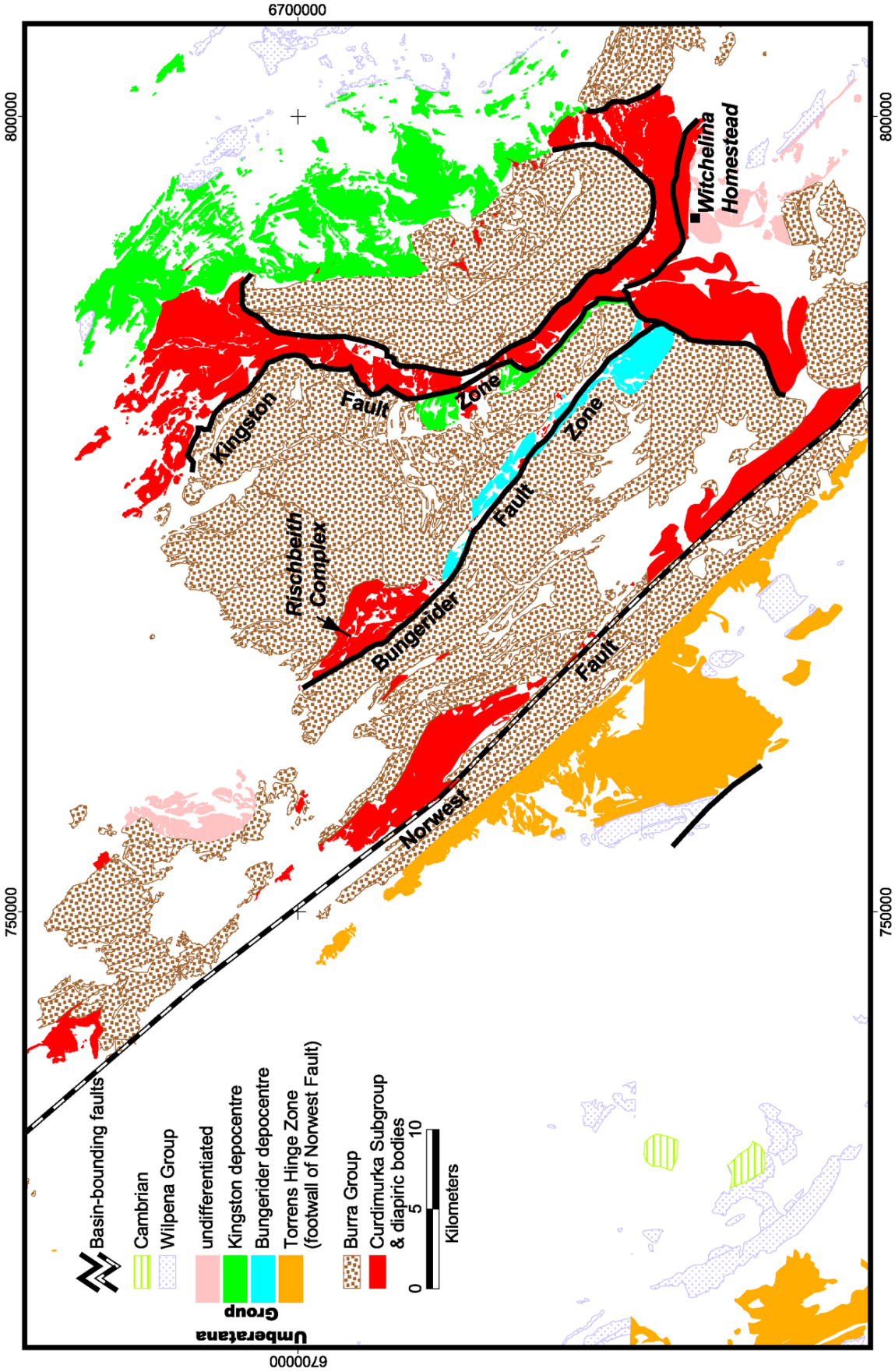

Figure 4
Distribution of Warrina and lower Heysen supergroup strata in the Willouran Ranges and Torrens Hinge Zone. The Umberatana Group is interpreted to have accumulated in at least three distinct depocentres or sub-basins (see text for details). Modified from PIRSA digital copies of Curdimurka, Marree, Andamooka and Copley 1:250,000 geological map sheets.

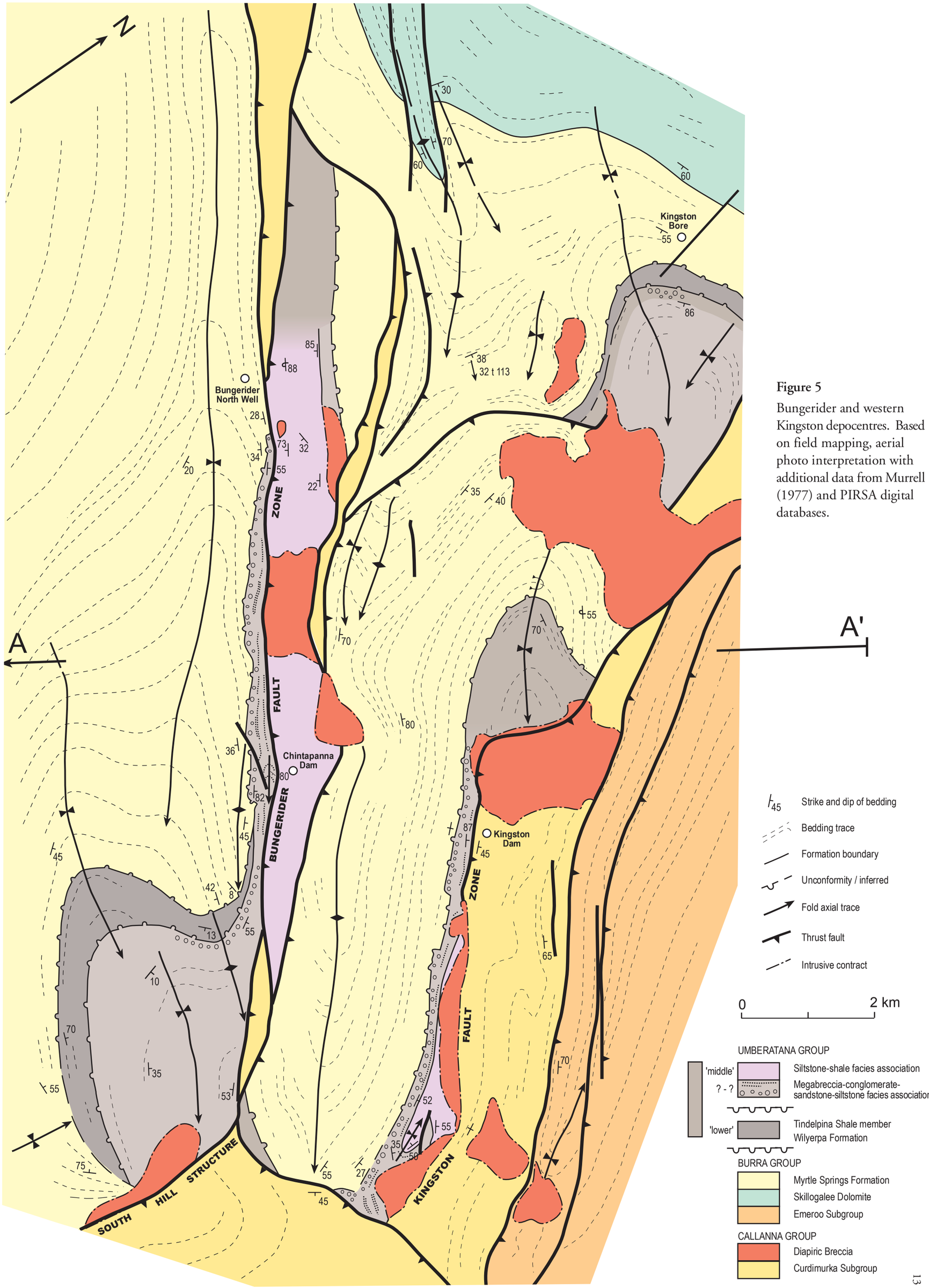

Figure 5

Bungerider and western Kingston depocentres. Based on field mapping, aerial photo interpretation with additional data from Murrell (1977) and PIRSA digital databases.

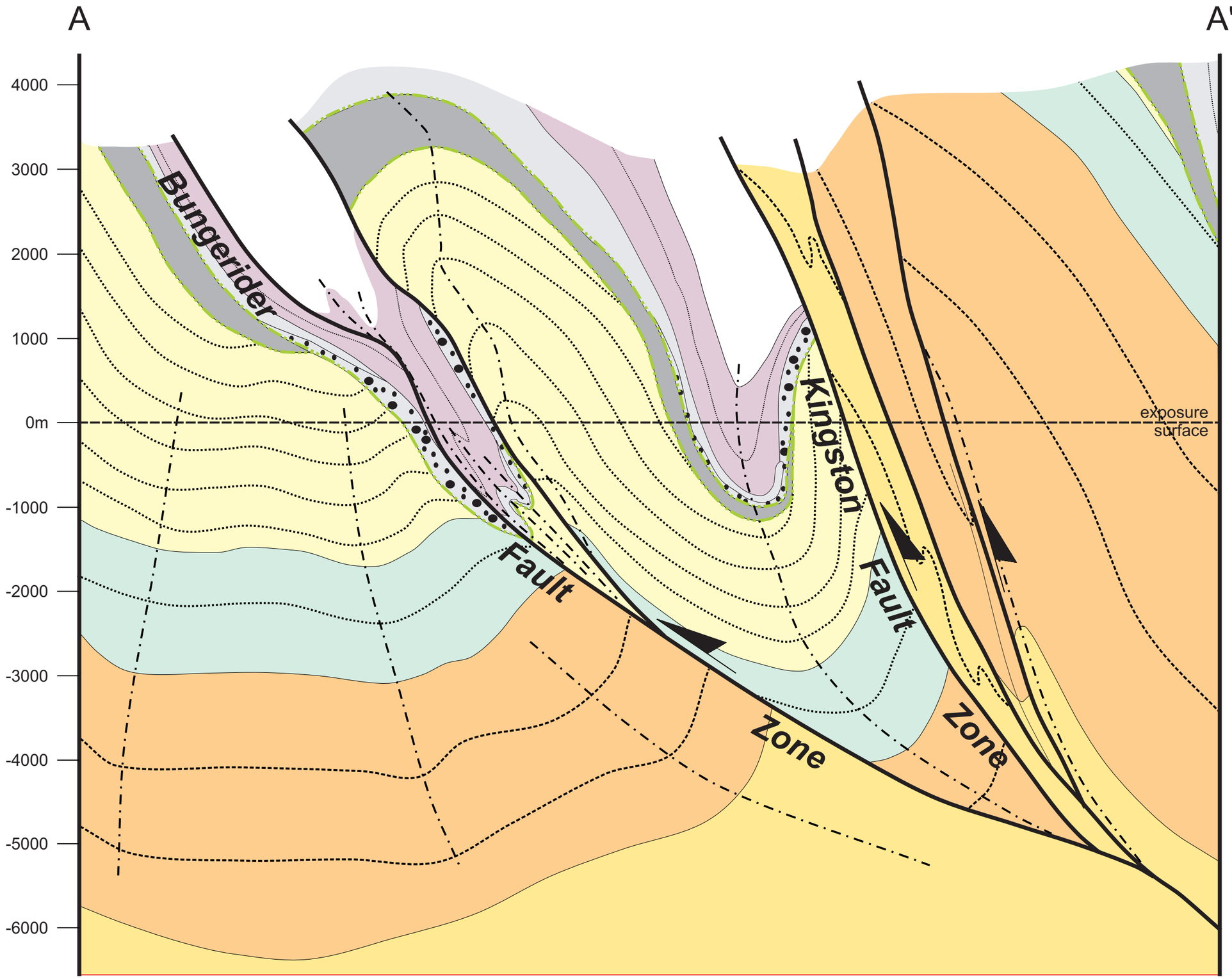

Figure 6
Interpretive, unbalanced cross sections of the Bungerider and western Kingston depocentres.

Our data come mainly from the central part of the depocentre, where middle (or possibly lower) Umberatana Group units occupy the core of a fragmented syncline (Figs 5, 6). Unconformable contacts with the Myrtle Springs Formation (uppermost formation of the Burra Group) are preserved on the limbs of the syncline, with only mild modification due to Delamarian inversion. By contrast, the core is thrusted out by the NE-dipping Bungerider Fault Zone and forms the locus for a string of sandstone-dominated Callanna Group inliers, emplaced as diapirs or fault-bounded slices along or adjacent to the thrust surface. To the northwest, the Bungerider Fault Zone truncates the western limb of the syncline and SW-dipping (presumably SW-facing) Umberatana Group occurs in faulted contact with either Myrtle Springs Formation or Callanna Group inliers. To the southeast, lower levels of the Umberatana Group are preserved on the western margin of the depocentre (including the Sturtian glacials) and the basal unconformity transgresses broadly folded Myrtle Springs Formation. A change in the geometry of the depocentre in this region is manifested by the outcrop pattern of the Umberatana Group which steps westward into the core of an isolated, non-cylindrical syncline. This is a common geometric phenomenon in the western Willouran Ranges, the significance of which will be discussed further below. The eastern side of the depocentre is poorly exposed to the southeast, but inferred to have been thrusted out by a NE-dipping structure which strikes slightly clockwise of the main synclinal axis of the trough.

Significant variation in basin architecture can be demonstrated both along strike and across the axis of the depocentre. From the South Hill Structure, northwestward to Bungerider Well, the eastern side of the depocentre exhibits a complex architecture involving amalgamated high angle unconformities both at the base and within the Umberatana Group, and poorly structured to chaotic facies associations. These features have been previously documented in detail by Murrell (1977), Coats and Dalgarno (1983) and Krieg et al. (1991) — we include some of their data with our own with an aim to developing a basin evolution model for the region.

Lower Umberatana Group

Lower Umberatana Group strata are thickest (and largely restricted) within the synclinal embayment near the southeastern termination of the Bungerider depocentre (Fig. 5). They comprise silt-matrix bouldery diamictite and normally graded (?turbiditic) pebbly sandstone and lithicwacke of the Sturtian glacials, and overlying siltstones and shale of the basal Tapley Hill Formation (Tindelpina Shale Member). Stratal packages wedge out progressively on both limbs of the syncline between erosional unconformities at the bases of the lower and middle Umberatana Group. The angular unconformity at the base of the Sturtian glacials increases from only a few degrees in the core of the syncline to >25° at the northwestern pinch-out of this facies. Restoration of the Burra Group to the onset of Umberatana Group sedimentation reveals consistent shallow to moderate S to SW bedding dips in this region. On the southern limb of the synclinal embayment however, Burra Group strata dipped to the N or NNW at the time of basal Umberatana sedimentation. Variable dip of the Burra Group below the basal Umberatana surface indicates localised folding of the former about a broadly SW plunging synclinal closure prior to or during Umberatana sedimentation. This fold orientation appears restricted to the immediate footwall of the South Hill Structure and continued to amplify during lower Umberatana Group sedimentation as evidenced by progressive thinning of this sequence onto either limb.

Middle Umberatana Group

Unconformably overlying lower Umberatana and Burra group strata is a package characterised by anomalously coarse-grained facies and historically correlated with the Amberoona Formation (Murrell, 1977; Coats and Dalgarno, 1983; and Krieg et al.,1991). On both flanks of the main NW-trending synclinal trough, this formation comprises a broadly upward fining sequence. However the facies architecture

exhibited across the trough is highly asymmetric, with distinct thickening of basal coarse-grained facies on the southwestern limb. Megabreccia deposits, intimately associated with and overlain by medium to thickly bedded, tabular to strongly channelised, internally massive dolomitic sandstone and pebble grade conglomerate occur at the base of the package in a number of areas. This facies association is best developed within the footwall of the Bungerider Fault Zone (SW flank of the depocentre) from Chintapanna Dam to Bungerider North Well, where it partly occupies a steeply sided erosional canyon approximately 5 km in width and up to 200 m deep (Fig. 7a, b). The canyon cuts down abruptly through lower Umberatana strata into the Myrtle Springs Formation. The basal megabreccia is locally in excess of 100m in thickness and comprises blocks of upper Burra Group siliciclastics and carbonates, and conglomerate, siltstone and numerous well rounded bounders of quartzite, granite and quartz porphyry reworked from the Sturtian glacial deposits, set within a massive dolomitic sandstone-siltstone matrix. Rare chocolate brown, highly lensoidal and imbricated pebble conglomerate channel deposits occur within the megabreccia, and impart a crude stratification. Depositional mechanisms were complex and included spalling of talus blocks into silty media, high density debris flow and tractional carpets within narrow linear channels. Limited data on the orientations of channels and canyon margins indicate that drainage systems were oriented northeast, i.e. roughly orthogonal to the basin axis.

The angular unconformity with Burra Group is very high, ubiquitously >40°, but locally approaching 90°. In all areas examined, restoration of Burra Group at middle Umberatana times reveals moderate to steep bedding dips towards the SW.

There is a overall decrease in grainsize above the megabreccia-sandstone sequence. The overlying package is dominated by dolomitic siltstone and shale, with parallel and ripple stratified dolomitic sandstone, rare thin dolarenite beds, tabular buff coloured dolostone and largely intrabasinally derived breccia and conglomerate occurring at regular intervals (Fig. 7c). Although this package is truncated against the Bungerider Fault Zone in the central part of the trough, the work of Murrell (1977) would suggest that it thickens abruptly to the southeast (within the synclinal embayment adjacent to the South Hill Structure), where it unconformably overlies lower Umberatana strata. Semi-coherent to intensely boudinaged dolomitic sandstone and dolomite layers located on the southwestern limb of the main synclinal trough pass laterally and appear reworked into a thick accumulation of channelised debris flows, normally graded dolomite-clast conglomerate and pebbly sandstone within the embayment to the southeast. Asymmetric forward rotated boudins within slide sheets and metric scale thrust stacks with pooled conglomerate lenses at their

Figure 7
Facies types of "middle" Umberatana Group strata from the Bungerider depocentre.
(a) Southeastern margin of canyonised megabreccia-conglomerate-sandstone facies association: footwall of the Bungerider Fault Zone. View to SE, with sub-vertically dipping, NE-facing Umberatana strata in the fore-ground, juxtaposed with moderately NE-dipping Myrtle Springs Formation in the background.
(b) Detail of canyon margin shown in (a). A block of wavy laminated quartz sandstone of the Myrtle Springs Formation enclosed within homogenised dolomitic siltstone of the Umberatana Group.
(c) Base of normally graded, channelised conglomerate. Clasts appear predominantly intra basinally-derived, with locally-sourced angular blocks of buff coloured dolomite within a basal breccia interval, passing upward into more structured granule conglomerate.
(d) Irregular syn-depositional topography developed above imbricate stack of dolomitic siltstone and sandstone blocks. View to NW, with stacked blocks to left and overlying conglomerate lens (right) pooled within depression localised at leading edge of thrust sheet. Thrust transport (hence inferred palaeoslope) was to SE.
(e) Convoluted, originally parallel stratified, fine-grained dolomitic sandstone: hangingwall of the Bungerider Fault Zone.
(f) Thin, tabular beds of dolarenite, emplaced as mass flow. Intervening recessive material is dolomitic siltstone and shale.
(g) Resistant benches of dolomitic siltstone and shale, punctuated by orange-brown dolomitic sandstones. Typifies transition to upper fine-grained portion of the middle Umberatana Group within the hangingwall of the Bungerider Fault Zone.

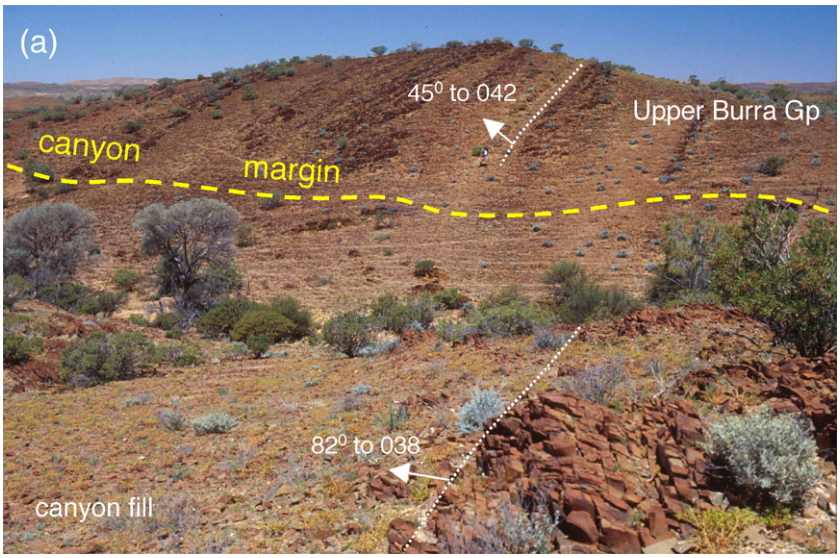
(a)
45⁰ to 042
Upper Burra Gp
canyon
margin
82⁰ to 038
canyon fill


(b)


(c)

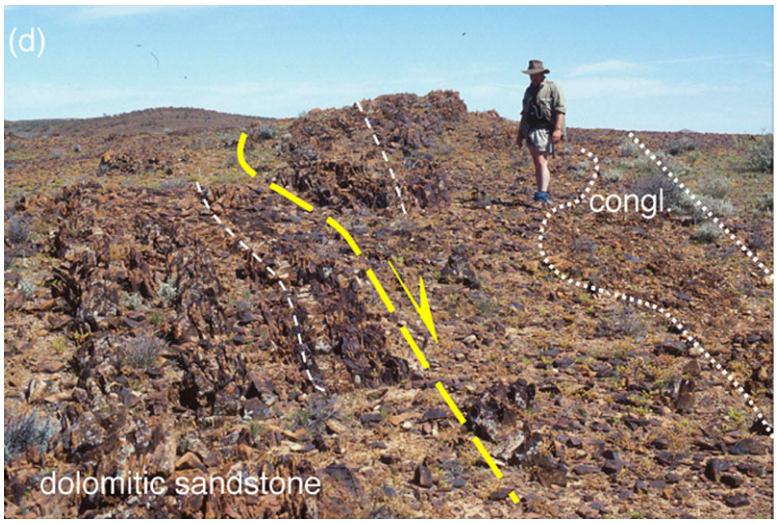
(d)
congl.
dolomitic sandstone


(e)


(f)


(g)

leading edges (Fig. 7d), indicate consistent southeast-directed transport (and hence SE-dipping palaeo-slope) in this region. This facies architecture indicates that the depocentre adjacent to the South Hill Structure continued to generate accommodation space at least until middle Umberatana times.

Similar facies associations to those described above occur within the hangingwall of the Bungerider Fault Zone (northeastern limb of the trough), however they are generally finer grained and highly condensed compared to those deposited in the footwall. Furthermore, although angular discordance exists between the base of the middle Umberatana and the Burra Group, it only locally exceeds 15°. The basal contact of the middle Umberatana Group is preserved only along the northwestern end of the depocentre, where pre-Umberatana Burra Group dips were shallow to the north. The basal megabreccia-sandstone package is locally preserved, however it pinches out rapidly and was not found to exceed 5 m in thickness. Similarly, the overlying shale-siltstone-sandstone-dolomite package is relatively condensed, thinly bedded, fine-grained and apparently lacking in dolomitic conglomerate and breccia (Fig. 7e). The bulk of the sequence comprises a thick upper succession of purple-grey dolomitic siltstone and rare thin dolomitic sandstone layers (Fig. 7f, g). Slope instability is recorded throughout the sequence by small scale slump folds and pseudonodules within sandy facies.

Discussion on basin evolution

Several key elements concerning the structure and stratigraphic architecture of the Bungerider depocentre provide clues to geometry and kinematics of basin growth.

- Amalgamated high angle unconformities within the Umberatana Group on the footwall side of the Bungerider Fault Zone: indicate significant, progressive rotation of Burra Group and lower Umberatana Group strata.
- Asymmetry of facies architecture and geometry of unconformities across the profile of the depocentre (ie. from SW to NE): indicates generation of asymmetric accommodation space and sediment supply.
- Deep level erosion of the Burra Group, with sediment dispersal patterns oriented transversely to the axis of the trough (middle Umberatana megabreccias).
- Abundance of chaotic facies associations, characterised by both extra- and intra-basinally derived debris flows.
- Emplacement of deep seated stratigraphy, either as thrust slices or diapiric bodies along the core of the depocentre during basin inversion.

Many of these features are incompatible with typical rift basins bounded by steeply or moderately dipping growth faults, but are characteristic of supra-detachment basins generated by high degrees of extension above low angle, listric extensional faults (such as those developed in the Basin and Range province: Friedmann and Burbank, 1995). Interpreted present day structural geometry across the axis of the trough and basin geometry restored to the level of the middle Umberatana Group are shown as cross-sections in Figures 6 and 8. It should be noted that the sections are oversimplified as they do no take into account pre-Umberatana Group basin geometry (and consequently any thickness of facies variation in the Warrina Supergroup), nor do they account for the effects of salt diapirism either during basin growth or inversion. The sections show the Bungerider depocentre as having formed above a NE-dipping low angle detachment fault, now inverted and manifested as the Bungerider Fault Zone. The low angle and listric fault geometry is a requirement for the development of significant footwall block rotation and uplift as evidenced by deep incision and amalgamation of high angle Umberatana Group unconformities. The >40° unconformity between the middle Umberatana and Burra groups preserved on the footwall block is entirely consistent with a supra-detachment style setting. The broadly SW-dip of the Burra Group at Umberatana times is interpreted to record block rotation resulting from displacement above NE-dipping listric detachments. However the

90° unconformity recorded locally along the southwestern margin is most probably unfeasible in this environment. Either an additional uplifting and rotational force imposed by salt diapirism, or structural modification of an originally shallower unconformity during basin inversion could account for this geometry.

Thick basal middle Umberatana debris flows are interpreted to have been shed northeastward and partly preserved on the uplifted footwall block. These units thinned and fined toward the basin depocentre to form relatively insignificant deposits on the hangingwall block (northeastern limb of the depocentre). Here the basal angular unconformity was subdued and a thick succession of basinal facies siltstone and shale accumulated. That the entire lower Umberatana Group has been removed from the hangingwall block however, (assuming that it was originally deposited here) indicates it must also have been uplifted and subjected to erosion at middle Umberatana times. We speculate then that the footwall block may have remained as a partly emergent wedge until or during megabreccia sedimentation and that the major basin-bounding fault lay somewhere to the northeast. The latter is perhaps represented by the complex curviplanar array of thrusts which truncate the eastern margin of the Bungerider depocentre and cut down into the Burra Group further to the north (Figs 5, 6, 8).

Additional basin complexity occurs adjacent to the South Hill Structure, where accommodation space persisted throughout the lower and middle Umberatana Group in the form of a narrow trough with probable NE trend. Although this falls outside our immediate study area, we speculate that the South Hill Structure was also active as a detachment surface and imparted localised control on geometry of the Bungerider sub-basin system.

Kingston Depocentre

The Kingston depocentre has broadly compatible facies architecture with that of the Bungerider depocentre, however the Umberatana Group is considerably thicker, with more complete preservation of lower formations. Furthermore, the effects of salt migration and structural modification of the Callanna Group are more pronounced and almost certainly had a directly influenced basin shape and evolution: i.e. generation and progressive migration of rapidly subsident depocentres, geometry of basin-bounding fault zones.

The principal controlling structure of the depocentre is interpreted to be the acuate, but broadly NW-striking, steeply NE-dipping Kingston Fault Zone. It merges with the South Hill Structure to the southeast and passes under Quaternary cover to the northwest (Figs 5, 9). Significant northeast-side-up reverse displacement associated with Delamarian inversion has juxtaposed a substantial hangingwall thickness of lower and upper Warrina Supergroup strata with middle Umberatana to upper Burra Group levels in the footwall. The fault trace is further complicated by a series of diapiric breccias (much like the Bungerider Fault Zone), which stope out much of the fault surface and footwall stratigraphy.

Umberatana Group strata are preserved with a narrow, semi-continuous belt situated in the immediate footwall of the Kingston Fault Zone (between the South Hill Structure and Kingston Bore), and as an anomalously thick, steeply NE-dipping and facing package which unconformably overlies Burra and Callanna group rocks 5–10 km northeast of the Kingston Fault Zone (Figs 5, 9). We have investigated the footwall sequence of the Umberatana Group at a number of localities along its strike, however our field work in the main part of the depocentre was restricted to the northern end, around the Breaden Hill mining centre. Although we have been able to extrapolate southeastward from Breaden Hill using aerial photos and digital copies of PIRSA 1:250,000 scale maps, the thickest part of the Umberatana Group lies on the Marree 1:250,000 sheet, for which explanatory notes and structural data are yet to be released. Our interpretation of facies and basin architecture should therefore be considered provisional until completion of this study next field season.

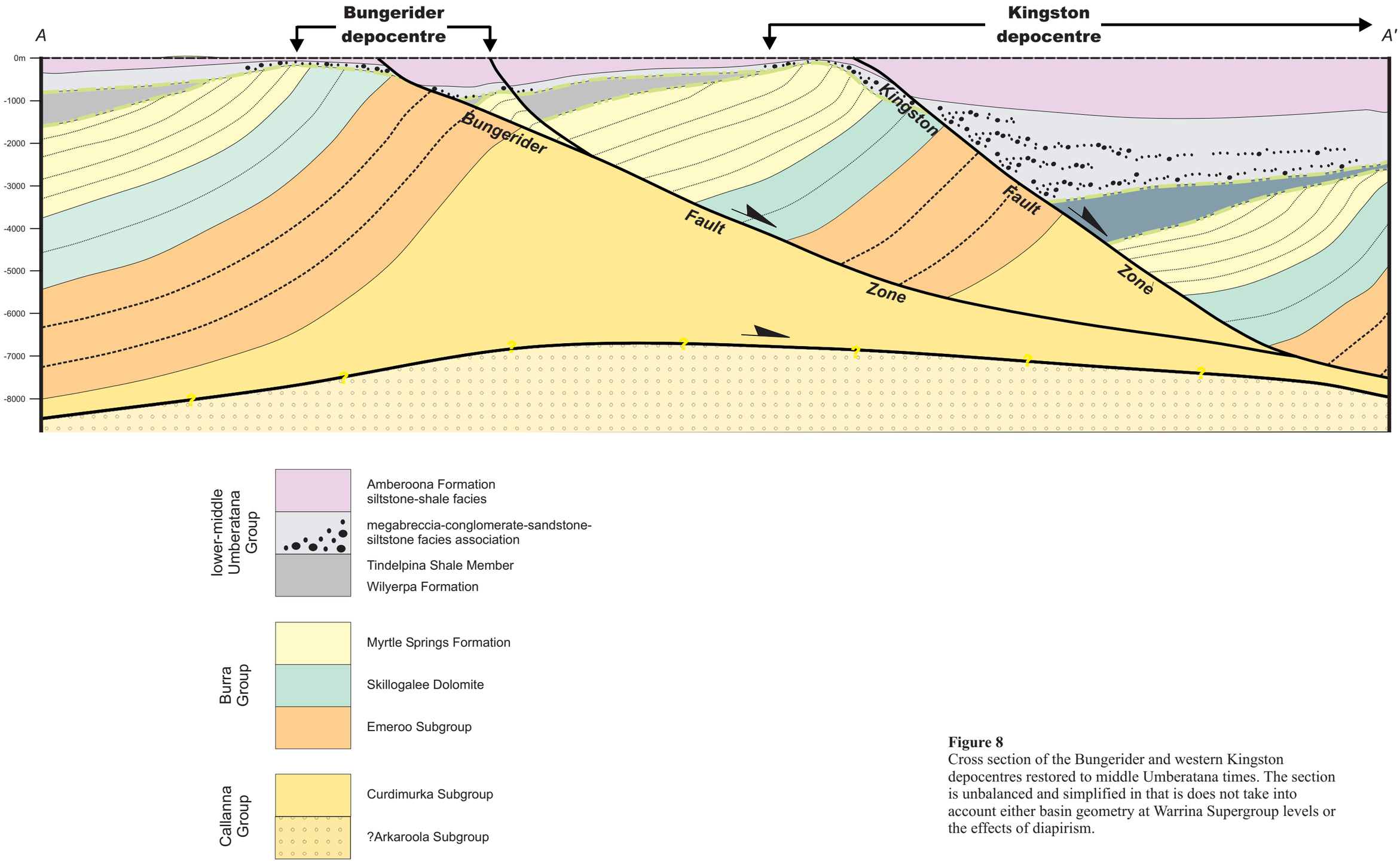

Figure 8
Cross section of the Bungerider and western Kingston depocentres restored to middle Umberatana times. The section is unbalanced and simplified in that is does not take into account either basin geometry at Warrina Supergroup levels or the effects of diapirism.

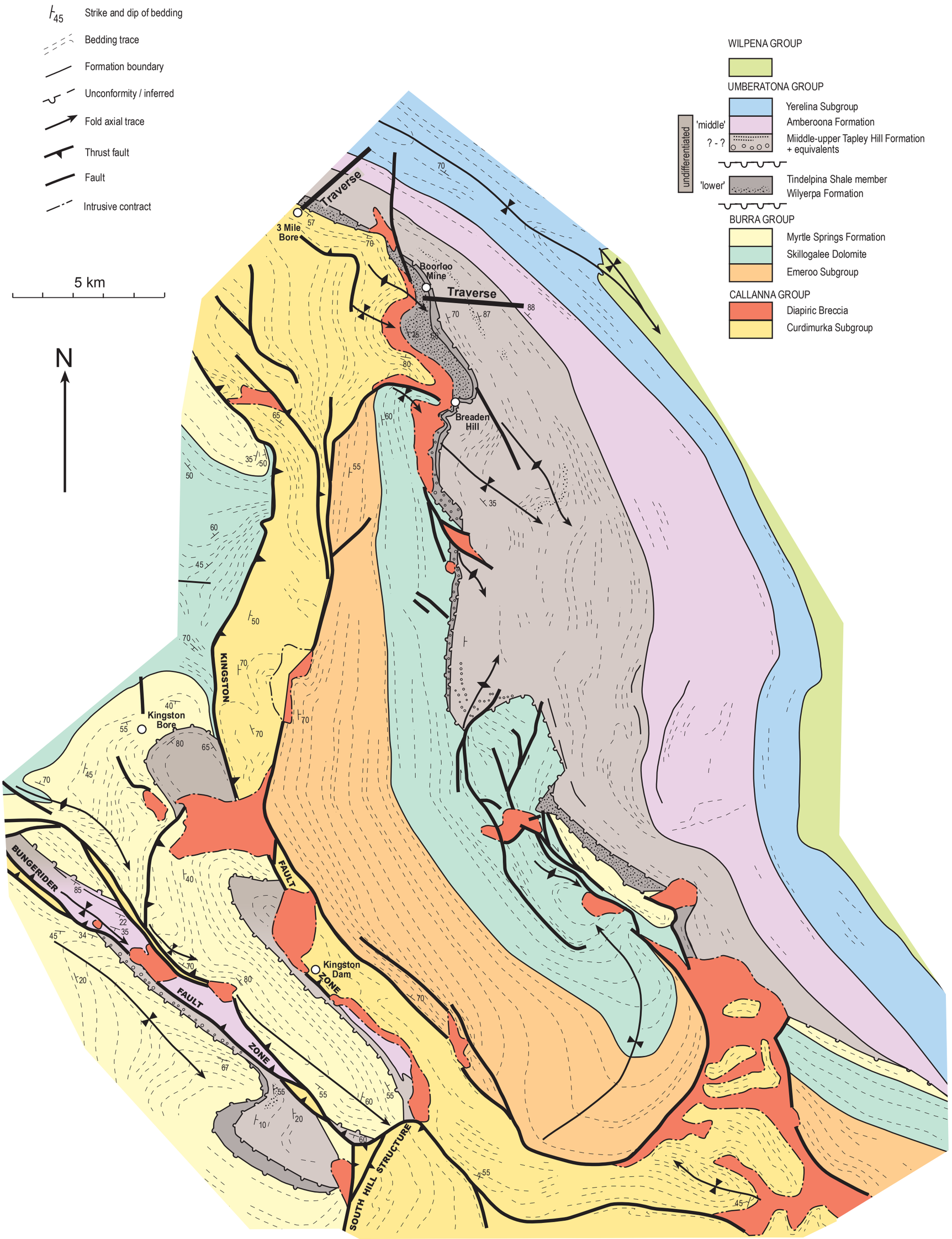

Figure 9

Geological map of the Willouran Ranges. Based on field mapping, aerial photo interpretation with additional data from Murrell (1977) and PIRSA digital databases.

Footwall of the Kingston Fault Zone

Distinct similarities occur between the Umberatana Group preserved within the footwall of the Kingston Fault Zone and the southwestern flank of the Bungerider depocentre. Firstly, the lower Umberatana Group is either very thin or removed entirely. With the exception of the synclinal domain near Kingston Bore where carbonaceous shales of the lower Tapley Hill Formation (Tindelpina Member) crop out, basal middle Umberatana megabreccia deposits lie with angular unconformity upon the upper Burra Group. Within the central part of the belt, the megabreccia reaches a maximum thickness of 80 m and contains clasts derived from the lower Umberatana Group, upper Burra Group and possibly diapirically uplifted blocks of the basal Curdimurka Subgroup (Fig. 10a, b). The angular relationship between the megabreccia and the underlying Myrtle Springs Formation is considerably less than that upon the footwall of the Bungerider Fault Zone however, and is generally less than 25°. Where a distinct angular unconformity can be established, the sediments of the Burra Group dipped moderately to shallowly to the southwest at middle Umberatana times.

The megabreccia package is overlain by up to 200 m of interbedded dolomitic siltstone, thin to thickly bedded, intrabasinally-derived mass flow deposits (Fig. 10c, d) and brecciated dolomite towards the top, before passing abruptly into typical Amberoona Formation purple-grey pencil shales and siltstones. It is not possible to constrain the thickness of the upper basinal facies as it is ubiquitously truncated against the Kingston Fault Zone or stoped out by diapiric breccia (Fig. 10e, f).

Hangingwall of the Kingston Fault Zone

To the northeast of the Kingston Fault Zone, the Umberatana Group is exposed within a broad lensoidal belt with approximately 30 km strike length (however original breadth of the depocentre was undoubtably considerably greater). For the most part, the package overlies and thickens towards the core of a kidney-shaped ?fault-bounded block of Burra Group (Fig. 9). To the northwestern and southeastern limits of the belt however, the lower Umberatana Group thins dramatically and occurs in contact with inliers of Callanna Group strata. Whereas the northwestern inlier comprises relatively intact, albeit internally thrust-thickened stratigraphy (apparently uplifted with respect to the neighbouring Burra Group), the southeastern inlier has very limited strike extent, appears internally chaotic and may have been emplaced at least partially by diapiric uplift. The belt of Callanna Group immediately below the Burra Group block is, by contrast, "condensed" with significant thinning or complete removal of some units. Similar to the footwall of the Bungerider Fault Zone, the Warrina Supergroup is characterised by complex non-cylindrical fold patterns. This is shown most dramatically at the southern termination of the Burra Group block, where the trace of shallowly plunging syncline possesses a near 90° rotation in trend (Fig. 9). This geometry is most likely explained by initial ENE folding due to relative diapiric uplift of the adjacent Callanna Group and subsequent reorientation into a NW orientation during Delamarian inversion.

Our field studies in the vicinity of, and northwest of Breaden Hill involved a near complete package of lower and middle Umberatana strata. The basal contact near Breaden Hill has been substantially modified by diapirism and a 500 m wide veneer of dolomite, marble, dolerite and sandstone blocks set within a brecciated dolomitic matrix, separate Sturtian glacial deposits from both the Callanna and Burra groups (Fig. 9). To the northwest, steeply NE-dipping Sturtian glacials are juxtaposed with moderately to shallowly SSW-dipping and facing Callanna Group. The angular relationship between the two packages is thus in the order of 90°, however exposure was not sufficient to discriminate between a tectonic or erosional contact.

Two traverses were schematically logged from the Sturtian glacials to just above the base of the Amberoona Formation: one approximately 2.5 km

north of Breaden Hill and a second to the northeast of 3 Mile Bore (roughly 6 km to the northwest). Significant thickness variation occurs between the two, with the lower to middle Umberatana Group thinning from roughly 4000 m on the first traverse to 2500 m on the second. This variation was accommodated in part by a N-trending growth fault, clearly identifiable on aerial photographs, which generated substantial thickness increase within the Tapley Hill Formation and lower Amberoona Formation on the southeastern hangingwall block (Fig. 9). The effect of this structure on basin growth during deposition of the Sturtian glacials is unclear, however lateral facies variation at this level does appear to exist. For example, on the first traverse the Wilyerpa Formation (representing the Sturtian glacials in this region) comprises up to 500 m of interbedded siltstone, sandy diamictite, ripple and planar laminated dolomitic sandstone and massive quartzwacke (Fig. 11a). At Breaden Hill, an unconstrained thickness (due to diapiric stoping) of massive quartzwacke-pebbly sandstone-channelised conglomerate facies association becomes conspicuous (Fig. 11b). It would appear from PIRSA maps that this facies association continues to thicken progressively (and possibly coarsen) to the southeast where it has been mapped as the Serle Conglomerate.

At the top of the Sturtian glacials, there was an abrupt cessation of clastic input, as indicated by a sharp transition to dark grey, carbonaceous and locally pyritic siltstones, shales and minor dolomite of the basal Tapley Hill Formation (Tindelpina Shale Member). This change in lithofacies most probably records flooding of uplifted tilt blocks in response to eustatic readjustment following ice sheet melting (cf. Coats and Preiss, 1987). The Tindelpina Shale Member represents the most important host for copper mineralisation and will be discussed further in the following section. The member pinches out northwestward from 70 m thickness to zero between the two traverses beneath an angular unconformity surface (Fig. 9). Overlying the unconformity is a thick (1700 m on the southern traverse) succession of dark grey siltstone interbedded with thinly bedded, fine grained, ripple and parallel laminated sandstone (Fig. 11g), which represents the middle and upper portions of the Tapley Hill Formation. The package is punctuated throughout by numerous cross-stratified and well imbricated, crudely channelised granule conglomerate, coarse grained lithic sandstone and massive dolomitic sandstone beds (Fig. 11c, d, e). Lensoid to tabular bodies of megabreccia ranging from 2–5 m in thickness occur both at the base and approximately 140 m higher in the package. Although considerably thinner, these units are both texturally and compositionally analogous to megabreccia units contained within the footwalls of the Bungerider and Kingston fault zones, and similarly contain evidence of erosion at least as low as the Sturtian

Figure 10
Facies types and structural geometry within the footwall of the Kingston Fault Zone.
(a) Block of internally brecciated arkosic sandstone contained within the basal megabreccia unit near Kingston Dam. The composition and internal texture of the block is remarkably similar to that exhibited by diapiric bodies comprising lower Curdimurka Subgroup strata (cf. Figure 10b). Possible evidence for uplift and emergence of diapiric bodies during Umberatana sedimentation.
(b) Brecciated basal Curdimurka Subgroup contained within an intrusive breccia body emplaced along the trace of the Kingston Fault Zone.
(c) Normally graded pebble to granule conglomerate with well-developed clast imbrication.
(d) Coarse-grained lithic sandstone with crude parallel and cross stratification, and out-sized, ?intrabasinally-derived dolostone clasts at the base.
(e) Southeasterly view of the Kingston Fault Zone near Kingston Dam. The fault trace cuts down progressively into Umberatana Group strata. There is little angular discordance between the similarly NE-facing Curdimurka Subgroup and Umberatana Group. This geometric relationship is taken to indicate original low angle (ie. layer sub-parallel) contacts between these units and the fault surface.
(f) Diapiric body intruding the Kingston Fault Zone. There is no obvious offset of the diapir, indicating that emplacement continued until the later stages of basin inversion.


(a)


(b)


(c)


(d)

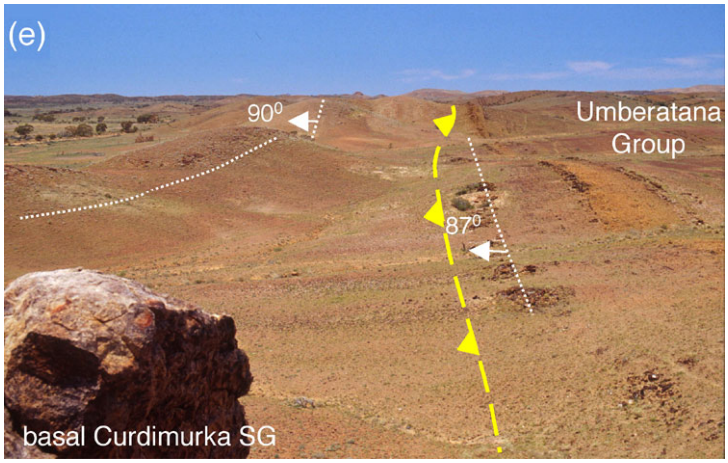
(e)
90⁰
Umberatana Group
87⁰
basal Curdimurka SG

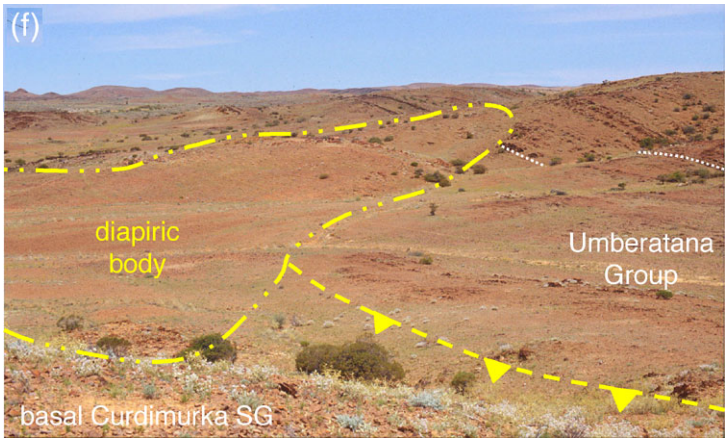
(f)
diapiric body
Umberatana Group
basal Curdimurka SG

with the basal megabreccia-massive sandstone-granule conglomerate-siltstone facies association within the footwall of this structure, indicates substantial basin growth towards the northeast. The basic geometry of the system is envisaged to be analogous to that of the Bungerider depocentre, with abrupt northeasterly thickening of the Tapley Hill Formation from 280 m to roughly 3000 m across a major, first order basin-bounding growth fault which most probably coincides with the present trace of the Kingston Fault Zone (Figs 6, 8). As with the Bungerider depocentre, the footwall sequence is partly preserved and dominated by a condensed, coarse-grained package that incises SW-dipping lower Umberatana and upper Burra Group strata. Near Kingston Bore, the Kingston Fault Zone presently truncates bedding within both the footwall (NE-facing Umberatana Group) and hangingwall (Callana Group) successions at very low to moderate angles. Both successions are NE-dipping and facing, which when coupled with low bedding cut-out angles, indicate a shallow to moderate NE-dip of the original extensional fault geometry (Fig. 10e).

Basin geometry associated with the hangingwall block involved additional complexity imposed by second-order basin growth about a broadly NE-trending basin axis, centred roughly mid-way between elevated inliers of Callanna Group strata. This is shown by transgression and progressive thickening of the basal to middle Umberatana Group across abrupt fault-bounded contacts between the Burra and Callanna groups at either end of the belt. Given the absence of evidence for substantial tectonic displacement at the base of the Umberatana Group, the transgressive nature of the Sturtian glacials indicates that the Callanna Group must have be elevated relative to the neighbouring Burra Group block prior to, or early in, the history of Umberatana sedimentation. Furthermore, removal of the upper Burra Group prior to deposition of the Serle Conglomerate indicates substantial uplift and erosion of the central block also predated or occurred synchronously with glacial sedimentation. Although we have little data from the critical level of the stratigraphy (i.e. Sturtian glacials), we envisage that deep level erosion of the Burra Group occurred in response to tilt-block rotation above the presumably listric trace of Kingston Fault Zone, resulting in uplift of the Warrina Supergroup to the northeast. In support of this interpretation is the positioning of a pronounced negative gravity anomaly well east of the Kingston Fault Zone, that we consider to represent and thickened hangingwall wedge of Callanna Group strata. Thus, the extensional architecture which controlled basin growth during the lower and middle Umberatana, may have originated at Sturtian glacial times or earlier.

Generation of the second order sub-basin within the hangingwall of the Kingston Fault Zone is provisionally interpreted to record gravitational collapse of the Burra Group into underlying evaporitic Callanna Group strata. Apparent thinning of the Callanna Group adjacent to the Kingston Fault Zone may record extensional stripping or extrusion

Figure 11
Facies types of the lower and middle Umberatana Group, hangingwall of the Kingston Fault Zone.
(a) Sandy diamictite within the lower exposed parts of the Wilyerpa Formation.
(b) Poorly structured conglomerate lens within the upper part of the Wilyerpa Formation at Breaden Hill. Note the presence of recrystallised buff-coloured dolostone clasts. These clasts appear compositionally similar to nearby diapirically emplaced blocks and may record emergence of diapirs by the onset of Umberatana sedimentation.
(c) Thin bed of Tapley Hill Formation breccia containing clasts of dolostone and granite, the latter considered to have been reworked from Sturtian glacial deposits.
(d) Crudely stratified, channelised pebble to granule conglomerate near the base of the Tapley Hill Formation.
(e) Parallel stratified dolomitic sandstone within the middle Tapley Hill Formation.
(f) Thick sequence of grossly tabular coarse-grained lithic sandstone deposits at the top of the middle Tapley Hill Formation.
(g) Dark grey mudstone, siltstone and fine-grained, ripple-laminated quartz sandstone from the middle Tapley Hill Formation: typical products of "background" sedimentation.
(h) Extensive, thick sheet of purple-grey dolomitic shale and siltstones of the Amberoona Formation.

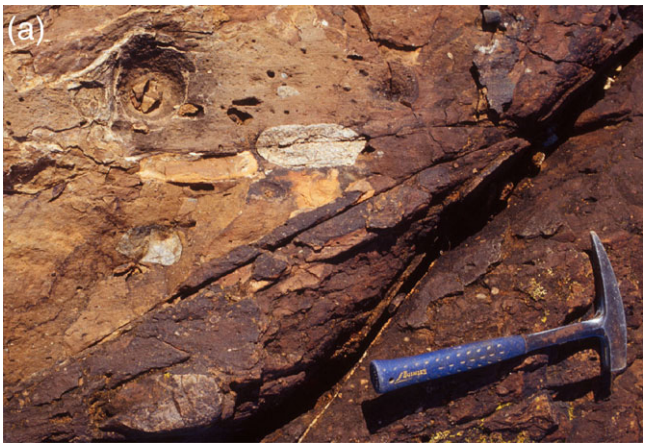
(a)


(b)


(c)

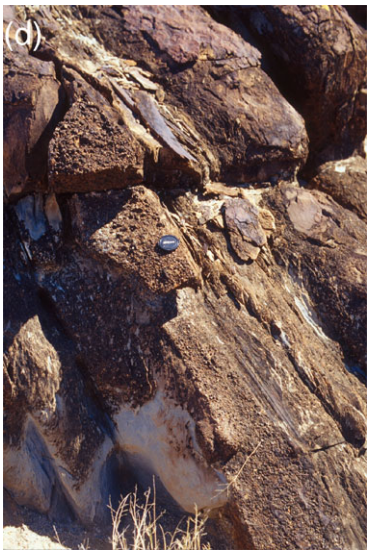
(d)


(e)


(f)


(g)


(h)

glacial deposits. The coarse-grained components of the sequence exhibit several grossly coarsening and fining upward cycles, which culminate in a ~150 m thick package of coarse-grained lithic sandstone and debris flow breccia units approximately 1100 m above the base (Fig. 11f). Above this level, the Tapley Hill Formation fines markedly to dark grey fissile shale and siltstone with relatively rare and thin coarse sandstone intervals. This upper member passes transitionally, but rapidly into purple-grey dolomitic pencil shales and siltstones of the Amberoona Formation (Fig. 11h), with no evidence of angular discordance.

Extrapolation of the lower to middle Umberatana Group southward on aerial photos reveals a progressive increase in thickness to a conservative estimate of 5500 m (assuming average 30 E-dip and no internal folding of the sequence: cf. Rayner and Rowlands, 1980). The bulk of the basin growth is recorded by the Tapley Hill Formation, which appears to thicken by more than 50% from the Breaden Hill traverse to a maximum of nearly 3000m (Fig. 9). At the southern end of the belt, the Umberatana Group appears to thin again above an elevated block of middle to upper Burra Group, emplaced above a shallow, folded thrust surface. Apparent transport on this thrust surface was to the north. A coarse-grained clastic wedge within the lower Tapley Hill Formation accumulated on the northern side of the block (PIRSA digital copy of the Marree 1:250,000 sheet), implying uplift during lower Umberatana Group sedimentation at least.

The basal contact of the Umberatana Group south of Breaden Hill appears highly erosive with incision to middle levels of the Burra Group. Coarse-grained Sturtian glacial deposits step southward across progressively thinning inliers of ?diapirically emplaced Callanna Group onto Skillogalee Dolomite. Assuming that the contact is not tectonic (cf. Rayner and Rowlands, 1980), the entire thickness of the Myrtle Springs Formation (uppermost Burra Group) has been removed via erosion, a thickness in the order of 1000 m based on sections along strike to the south.

Correlation of Umberatana Group stratigraphy

Comparison of the Kingston hangingwall succession to those described in earlier sections reveals an obvious similarity between the middle and upper portions of the Tapley Hill Formation, and the base of the "middle Umberatana" (Amberoona Formation) megabreccia–massive sandstone–granule conglomerate–siltstone facies association from the Bungerider and Kingston footwall areas. Both successions are unconformably underlain (locally at least) by carbonaceous shale of the Tindelpina Shale Member and apparent conformably overlain by "typical" Amberoona siltstones and shales. They both contain abundant mass flow deposits, sourced from relatively deep stratigraphic levels and emplaced as debris flows and turbidites. The principal differences include the obvious thickness contrasts (both of the package as a whole and individual breccia units) and the dark grey, more carbonaceous character of Kingston hangingwall sequence. Both are readily explained, however, by deposition of the Kingston hangingwall sequence upon a more rapidly subsiding basin floor with associated deeper water (more anoxic) conditions.

Although we presently lack sufficient data to unequivocally correlate the sequences, the implications should be considered. Firstly, if we accept that the megabreccia facies belongs to the Tapley Hill Formation rather than the Amberoona Formation, then the main phase of block rotation and uplift, consequent deep level erosion and thus arguably acceleration of extension, occurred not during the middle Umberatana as historically thought, but soon after the end of the Sturtian glaciation period. Secondly, correlation of the sequences would provide a direct tie-line between sediments deposited on the footwall and the hangingwall of the Kingston Fault Zone, aiding accurate basin reconstruction.

Discussion on basin evolution

Correlation of the Tapley Hill Formation exposed within the hangingwall of the Kingston Fault Zone

of material at this level, accommodated laterally by thrust stacking and or diapiric uplift of the neighbouring inliers. Extension was potentially accommodated by a NE-trending (?originally SE-dipping) splay off the Kingston Fault Zone (Fig. 9) that presently defines the northern margin of the Burra Group block and sub-parallels the trace of bedding within the Callanna Group to the north. In support of this interpretation is the coincident position of the "hinge" across which the Umberatana Group thickens to the south.

Copper mineralisation

Relatively few Cu deposits occur in the Willouran Ranges compared other parts of the Adelaide Fold Belt (in particular the Central Flinders Domain). All but one occur within the thickened succession east of the Norwest Fault and form four geographically distinct clusters (Fig. 12): (1) periphery and core of the Rischbieth Complex, western Willouran Ranges, (2) central and northern trace of the Kingston Fault Zone, (3) south of Witchelina homestead, and (4) northeastern Willouran Ranges near Breaden Hill. Although these deposits involve a variety of stratigraphic and lithological hosts, a number of geological criteria are common to each. Firstly and most conspicuous is a spatial association of Cu mineralisation with either the Curdimurka Subgroup, or diapiric breccias inferred to have been derived from it. Deposits occur either within Curdimurka strata or within 1km of a contact with this unit. This leads on to the second common factor, the tendency of deposits to occur close to faulted, or in some cases unconformable boundaries of major stratigraphic packages. For example, within the areas northeast of the Willouran Ranges and south of Witchelina homestead, Cu appears confined to the lower part of the Tapley Hill Formation and/or immediately adjacent Curdimurka Subgroup rocks. Finally in the cases of the northeast Willouran and Kingston Fault areas at least, Cu occurs in the vicinity of structures, which we have argued above, to have acted as major basin-bounding faults at Umberatana times.

In the following section we provide a brief description on the style of mineralisation from workings visited at the Breaden Hill – Boorloo mining centre and the Warra Warra mining centre located on the eastern flank of the Rischbieth Complex.

Breaden Hill–Boorloo mining centre

Deposits in the Breaden Hill–Boorloo area form a narrow linear belt, positioned close to the base of the Tapley Hill Formation (Fig. 12). The belt has a strike extent of roughly 7 km and coincides broadly with the exposed trace of a discontinuous carbonate-quartz matrix diapiric breccia unit, emplaced at the base of the Umberatana Group and transgressing the lower fault-bounded contact of the Callanna and Burra groups. As argued in the previous section, the lower faulted contact is likely to have been active as an extensional fault during earliest Umberatana sedimentation. The age of diapir emplacement is as yet poorly constrained, however field and air photo observations such as apparent thickness changes of lower Umberatana Group strata about diapiric bodies, positioning of breccias adjacent to Umberatana growth faults, and rare blocks of recrystallised dolomite (not dissimilar to the matrix of the diapirs) contained with conglomerates of the Wilyerpa Formation (Fig. 11b), provide equivocal evidence for a phase of uplift and emergence coeval with Umberatana sedimentation.

Greatest density of workings occur at Breaden Hill, where numerous small pits (rarely larger than 3 m^2) exploit Cu-oxide mineralisation hosted in a brecciated, strongly bleached, silicified and carbonate altered shale-siltstone unit, interpreted as the base of the Tindelpina Shale Member. Mineralisation is restricted to zones of coarsely recrystallised dolomite, quartz and haematite breccia that pierce underlying lithic sandstones of the Wilyerpa Formation (Fig. 13a–f). Contact relationships between the breccia and the shale-siltstone unit range from incoherent block-in-matrix texture to injections of breccia along thrust surfaces or as discrete cross-cutting veins. Cu ore occurs mainly as malachite disseminated throughout veins or pods of dolomite-quartz-haematite breccia, cross-cutting and bedding-parallel planar quartz-

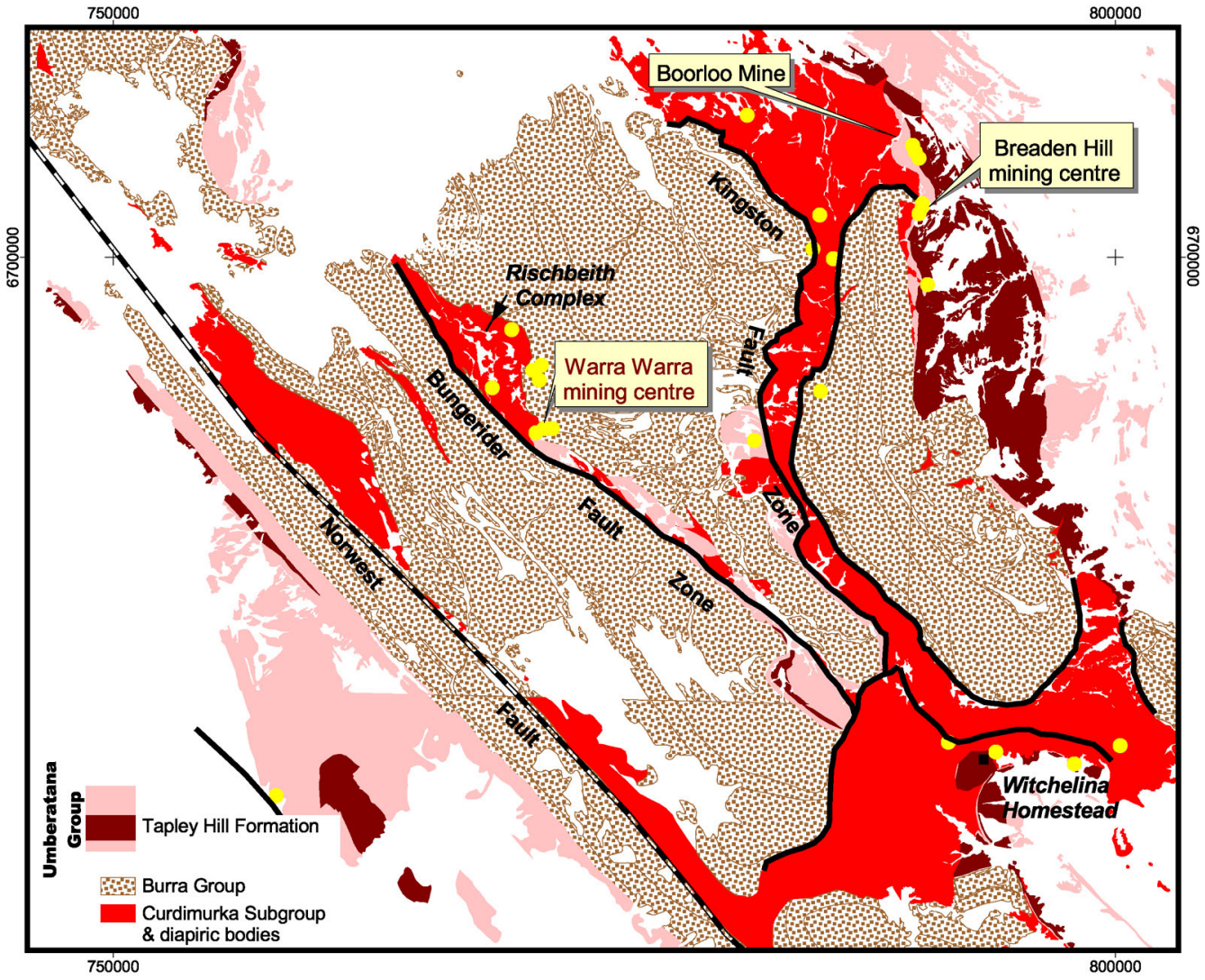

Figure 12
Distribution of Cu deposits throughout the Willouran Ranges.

Figure 13 (see page 37)
Styles of Cu mineralisation within the Breaden Hill mining centre.
(a) Blocks of bleached (?originally carbonaceous) Tindelpina Shale Member floating within mineralised, dolomitic matrix.
(b) Close-up of (a) showing malachite throughout recrystallised dolomitic matrix and pervasive Fe-carbonate spotting within shale blocks.
(c) Stratiform Cu within shale unit bounded on left by brittle, dolomitic fault zone (yellow line) and to right by sub-planar quartz-carbonate-malachite vein (orange line).
(d) Stratiform Cu within basal Tindelpina Shale Member at periphery of tabular dolomite breccia sill.
(e) Dolomitic breccia overthrust upon basal Tindelpina Shale Member.
(f) Close-up of (e) showing stratiform Cu mineralisation within shales immediately adjacent to thrusted contact with dolomite breccia.

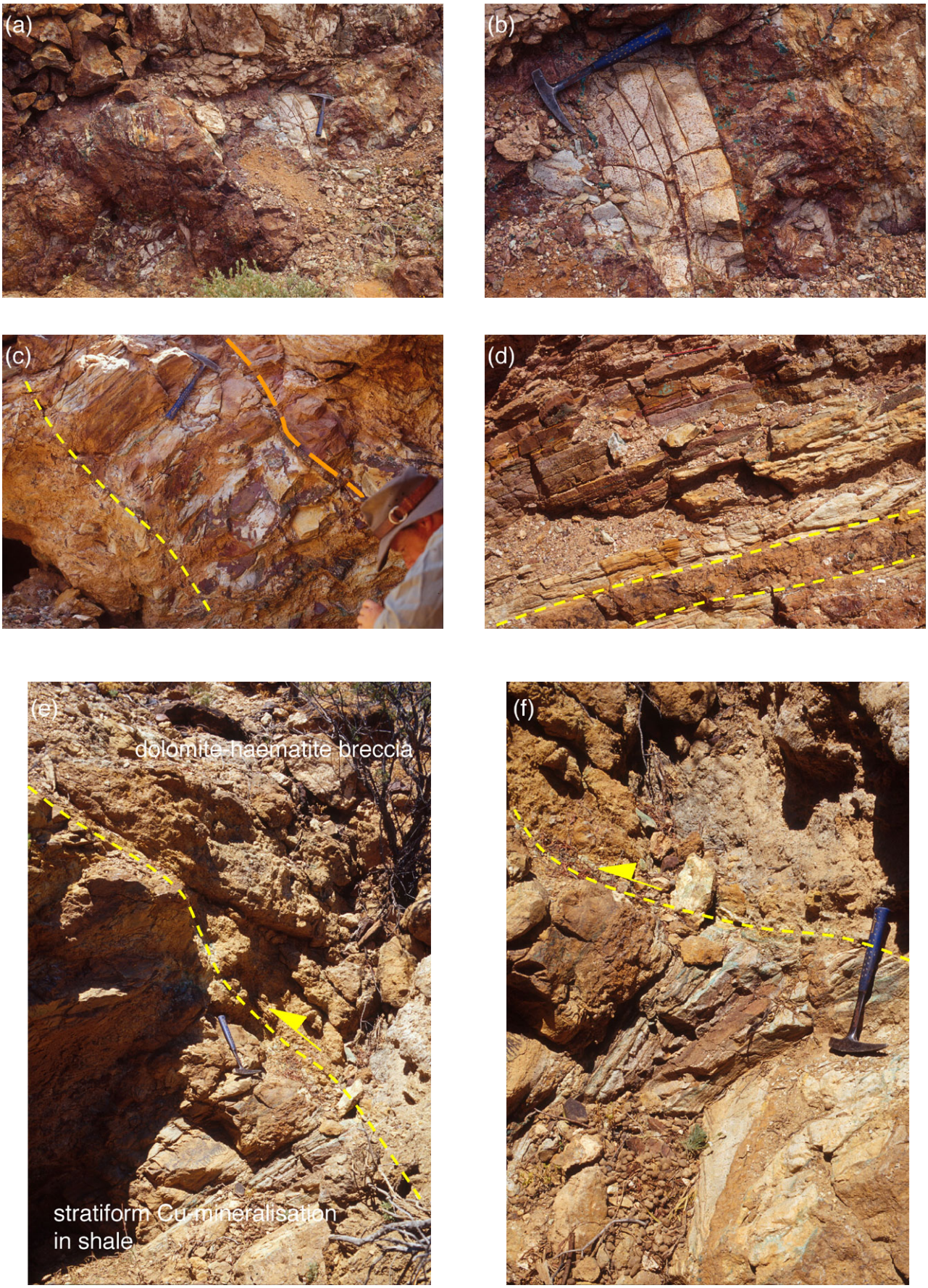
(a)
(b)
(c)
(d)
(e)
dolomite-haematite breccia
stratiform Cu mineralisation
in shale
(f)

carbonate veins, and stratiform to disseminated concentrations within shale. Stratiform mineralisation is seen as spotty concentration of malachite within and at the fringes of delicate calcite and Fe-carbonate seams or veinlets. Inter-seam domains are intensely pitted, with rare preservation of carbonate rhombs and less common goethitic cubic pits, possibly after pyrite. In places, stratiform mineralisation has a strike extent of 2 m or more, however it is invariably structurally-controlled, thickening and intensifying within the wall rocks adjacent to faults, veins or breccia zones. Although similar veins and breccias occur within Wilyerpa Formation sandstones, neither the veins nor the host rock are mineralised.

The main Boorloo workings are focused on discontinuous, N–S striking and moderately E-dipping ferruginous quartz-carbonate veins and stockworks within mudstone-clast conglomerate and siltstone near the top of the Wilyerpa Formation. Veins are associated with a similarly oriented brittle-ductile shear zone on the contact of siltstone and sandstone. The shear zone contains stringers and clots of Fe-carbonate, with abundant specular haematite. Vein stockworks occur within narrow (<1 m) fracture zones and comprise chalcocite veins with malachite rims and peripheral quartz-carbonate-malachite grain aggregates. Where thicker vein sets intersect mudstone-clast conglomerate, the sandy matrix contains disseminations of malachite and some bright apple green ?Cu mineral.

In addition to the vein-hosted deposits at Boorloo, a number of very small exploration pits occur along the base of the Tindelpina Shale Member. This contact has been tested by Utah in the 1970s by a series of drill holes. Sub-economic intercepts of primary copper sulphides from this drilling have been reported by Rayner and Rowlands (1980) and are summarised below. Cu mineralisation is restricted to the carbonaceous and pyritic Tindelpina Shale Member and the intercalated breccia-pebble conglomerate-ripple laminated sandstone-siltstone facies association of the middle Tapley Hill Formation. A single ore-grade intersection of 1m @ 2.5% Cu occurs in association a 10cm quartz-chalcopyrite-pyrite vein, however up to 134 m of low grade mineralisation (0.57% Cu) occurs mainly as disseminations of chalcopyrite and pyrite throughout the matrices of coarse-grained facies and less abundant stratiform, disseminated and vein-related concentrations in silty and mudstone facies.

Warra Warra mining centre

The Warra Warra mining centre consists of a cluster of small workings that occur in the middle Burra Group, over a 4 km strike length parallel to the eastern boundary of the structurally complex and diapiric Rischbieth Complex (Fig. 12). On the scale of the 1:250,000 scale geological mapping, the workings are associated with an area of intersecting E-W and NNW-trending faults cutting the host Skillogalee Dolomite. These structures are of the same orientation, but lesser in density, than those that define the Rischbieth Complex in mostly older Curdimurka stratigraphy immediately to the west. In the best exposed workings, the Cu mineralisation occurs within a steeply SE-dipping succession of interbedded dolomitic siltstones, sandstones and microbially laminated dolomites. It consists of stratabound malachite, localised within a silicified wavy-laminated siltstone horizon, which in detail occurs in broadly bedding-parallel quartz veins and associated wallrock fracture networks. Bedding drag and localised folding at the margins of the veined and brecciated zone in the main pit indicate that it occupies a fault zone.

Regional Cu distribution in the northwestern Adelaide Fold Belt

Cu occurrences in the northern Adelaide Fold Belt are shown in Figure 14. They form two main concentrations: a tabular belt that coincides broadly with the limits of the Willouran Trough and a densely mineralised belt positioned close to both the basal Neoproterozoic unconformity and the trace of the Paralana Fault Zone near Mt Painter. Cu deposits in the first of these areas are most densely distributed about the southeastern limit of the Willouran Trough, where the Heysen Supergroup dominates the present

level of exposure. Density of deposits drops off progressively to the south, where lower and middle Heysen Supergroup strata thin and upper Heysen Supergroup (Pound Subgroup) and Cambrian units become dominant. By contrast, the relatively low abundance of Cu deposits in the Willouran Ranges coincides with particularly thick and well exposed portions of the Burra Group. Thus, it can be argued that there is a crude stratigraphic control on Cu distribution between the bases of the Umberatana Group and the Pound Subgroup. This relationship does not hold for all areas however, as relatively thick accumulations of lower Umberatana Group sediments within the Yudnamutana Trough (northeastern Adelaide Fold Belt) are largely devoid of Cu mineralization (with the exception of the vicinity of the Mt Painter Inlier). The clear difference between the Willouran and Yudnamutana troughs is the thick accumulation of Curdimurka Subgroup strata and the generation of diapiric breccias in the former.

Within the Willouran Trough, Cu occurs almost exclusively within and at the peripheries of diapiric bodies where they intersect favourably reactive strata. Although mineralization occurs across a wide variety of stratigraphic levels, a significant proportion is hosted within variably carbonaceous shales and siltstones of the Tapley Hill Formation and similar, but less reduced lithotypes of the Bunyeroo Formation. The fundamental importance of interaction with rocks of the Curdimurka Subgroup is shown to the west of Leigh Creek, where the exposed package of Burra and Umberatana Group strata is unique in that it is both largely unaffected by diapirism and lacking in Cu mineralisation. It is also noteworthy that this contact between the Burra and Umberatana groups is effectively conformable, which is rare in the northwestern Adelaide Fold Belt. These relationships indicate that the Umberatana basin evolved in a relatively stable environment in this region, with out significant block rotation and uplift.

Basin Model

Although this study is at an early stage, the combined ease of data acquisition from field mapping and aerial photographs, and the wealth of existing knowledge concerning stratigraphic architecture, allow us to construct a provisional model for basin evolution during lower and middle Umberatana deposition. Below we summarise elements of basin geometry as gleaned from our study of facies and stratigraphic architecture in the Willouran Ranges. We also speculate on the mechanisms which controlled basin growth at Umberatana times and contrasted with those associated with Warrina Supergroup deposition. We conclude by considering the effects of basin growth on fluid circulation within the Warrina Supergroup and its possible implications for Cu mineralisation.

Facies and stratigraphic architecture as a record of basin growth and geometry

The lower to middle Umberatana Group records pronounced and sustained basin growth following deposition of thick rift-controlled clastic wedges and platformal successions of the Burra Group. Basin geometry was controlled by a complex network of

Figure 14
Distribution of Cu deposits in the northern Adelaide Fold Belt.
(a) Stratigraphic control on Cu mineralisation. Distinct correlation of Cu deposits within members of the Curdimurka Subgroup, Umberatana and Wilpena groups (below the Pound Subgroup).
(b) Cu deposits coupled with residual gravity image. Clear association of Cu with central and southern limits of the Willouran Trough: ie. with thick accumulations of Curdimurka Subgroup.
(c) Stratigraphic control on Cu mineralisation. Fairly systematic exclusion of Cu deposits from exposures of Burra Group, Pound Subgroup and Cambrian strata.
(d) Stratigraphic control on Cu mineralisation. Strong partitioning of Cu deposits into Curdimurka Subgroup and diapiric breccia bodies, Tapley Hill Formation and Bunyeroo Formation.

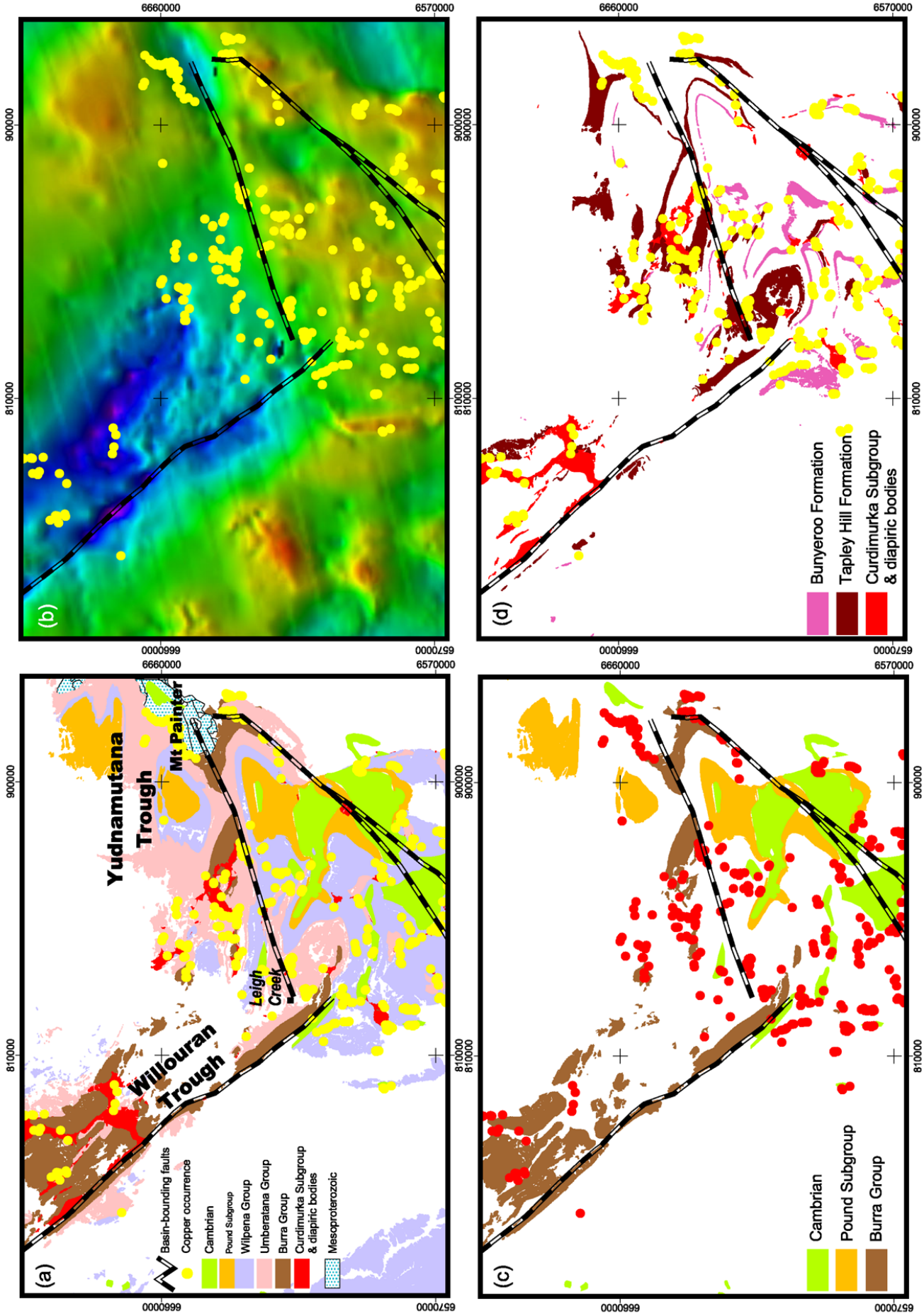
(a)
(b)
(c)
(d)
Yudnamutana Trough
Willouran Trough
Mt Painter
Leigh Creek
Basin-bounding faults
Copper occurrence
Cambrian
Pound Subgroup
Wilpena Group
Umberatana Group
Burra Group
Curdimurka Subgroup & diapiric bodies
Mesoproterozoic
Bunyeroo Formation
Tapley Hill Formation
Curdimurka Subgroup & diapiric bodies
6660000
6570000
900000
810000
666000
657000

corrugated, shallowly dipping, listric extensional faults which were subsequently reactivated as major thrusts during Delamarian basin inversion. The arcuate nature of many of these fault zones partly contributed to the highly varied orientation of folds nucleated during various phases of basin growth and further complicated during the inversion phase.

Basin growth appears to have been episodic and characterised by significant block rotation and consequent uplift within the footwalls of major sub-basin bounding structures. Onset of this style of growth occurred at least as early as the Sturtian glacials and is evidenced by significant erosion of the Burra Group accompanied by relative uplift of the Callanna Group to the east of the Kingston Fault Zone. A moderate angular unconformity also occurs towards the base of the Sturtian glacials within the footwall of the Bungerider Fault Zone. In the latter case, upper Burra Group strata are shown to have dipped moderately to the SW during lower Umberatana sedimentation, a geometry consistent with footwall block rotation above a shallowly NE-dipping listric fault. Major NW striking faults such as the Bungerider and Kingston Fault Zones are interpreted to have acted as first-order sub-basin bounding structures. These may have been partly inherited from Warrina Supergroup basin architecture (the latter having formed under broadly NE-SW extension: Preiss, 2000). Additional complication in basin geometry resulted from extension across structures oriented obliquely to these first-order faults. Second-order depocentres are considered to have trended roughly NE (although further work is required to confirm this) and include the synclinal embayment at the southeastern end of the Bungerider depocentre, and the broad ENE-plunging synclinal structure within the hangingwall of the Kingston Fault Zone. Possible controls on these two second-order depocentres were a NE-trending segment of the South Hill Structure and NE-trending splay off the Kingston Fault Zone respectively. Second-order sub-basin bounding structures may have originated as transfers under continued NE–SW extension. Alternatively, the regional stress field may have changed from that operating during Warrina Supergroup sedimentation to more meridionally-directed extension (consistent with early Sturtian extension in the Yudnamutana Trough), with NE-oriented growth faults nucleated to accommodate stresses imposed obliquely on pre-existing NW-trending faults.

Abrupt termination of clastic supply recorded at the base of the Tapley Hill Formation is interpreted to indicate rapid flooding of uplifted footwall blocks in response to ice melting representing the end of the Sturtian glacial event. Relatively stable tectonic conditions during deposition of the Tindelpina Shale Member may have also contributed to the paucity of coarse-grained detrital input and the predominance of "deep" water carbonaceous shale accumulation.

Resurgence of tectonic activity is heralded by voluminous input of ?footwall-derived coarse-grained debris of the middle Tapley Hill Formation within the hangingwall of the Kingston Fault Zone. A broadly upward thickening cycle of conglomerates and lithic sandstones recording erosion at least as low as the Sturtian glacials, punctuated background siltstone and fine ripple laminated sandstone sedimentation. We speculate that chronostratigraphic facies variants of the Tapley Hill Formation accumulated as anomalously coarse-grained and condensed packages on the footwalls of the Bungerider and Kingston Fault Zones. In these positions, the basal middle Tapley Hill Formation unconformity amalgamated with that at the base of the Sturtian glacials to incise substantially tilted Burra Group strata. Detritus was supplied by canyonised footwall-derived drainage systems oriented transversely to NW trending, first-order depocentres. Preserved within these canyons is a thick basal megabreccia containing clasts of lower Umberatana Group and upper Burra Group. Although no evidence of upward shallowing was recognised in the thick section of upper Tapley Hill Formation located in the hangingwall of the Kingston Fault Zone, possible shallowing is recorded by a progressive upward increase in dolomite content within condensed sections further west.

If our correlation of megabreccia-bearing sequences with the Tapley Hill Formation is correct, the Amberoona Formation within the Willouran Trough at least, records relative tectonic inactivity. Sedimentation was dominated by purple-grey siltstones and shales, with minor carbonate and sandstone. Although data is sparse, we consider that footwall block again became submerged and onlapped by fine-grained basinal deposits. It remains unclear whether this flooding of intra-basinal highs resulted from eustatic sea level rise or collapse of gravitationally unstable footwall blocks. As the Amberoona transgression is a basin-wide phenomenon, a non-tectonic cause would appear more likely.

Possible mechanisms of basin growth and implications for Cu mineralisation

The abrupt change in basin geometry recorded across the Warrina-Heysen Supergroup boundary may be explained by one or both of two competing processes. Firstly, the breakup of the Rodinean supercontinent may have resulted in an accelerated rate of extension that could not be accommodated by growth along the relatively steep basin-controlling structures which operated throughout Warrina Supergroup deposition. Generation of low angle detachment-style faults is a mechanism by which high rates of extension can be accommodated. Such structures are evidenced in the Willouran Ranges by anomalously high angles and rates of block rotation and substantial fragmentation of the pre-Umberatana stratigraphy.

The second important factor that influenced basin growth at Umberatana times was mobility of evaporitic strata in the Callanna Group. We have reasonable evidence that the Curdimurka Subgroup was locally elevated to the level of the middle or upper Burra Group (either as semi-coherent blocks or diapiric breccias) at the onset of Umberatana sedimentation. Relationships do not indicate that the Callanna Group was actively elevated however. Rather the Burra Group was removed or collapsed into depressions generated by evacuated or tectonically thinned Callanna Group. We envisage that extension became decoupled at the level of evaporitic units within the Curdimurka Subgroup, effectively separating a basement-lower Callanna Group package from an upper Curdimurka-Burra-Umberatana group package. This may in part explain why deep levels of the Callanna Group are rarely exposed, even though the appearance of lower level mafic rocks in diapiric breccias can be interpreted to indicate its presence. In this model, extension was driven in part by the far field stress-system, but also by the gravitational and mechanical instability of a salt-bearing substrate overlain by up to 9 km of Burra Group strata. Highly rotational blocks riding above listric faults soled near the base of the Curdimurka Subgroup, would have the combined effects of generating significant accommodation space in the hangingwalls of major faults and significant uplift (potentially as deep as Curdimurka Subgroup) in footwall blocks. Once initiated the process would be self-sustaining as thick asymmetric sediment accumulation during Umberatana time would continue to drive gravitational instability and block rotation. This process would persist until a time at which the rate of far field extension subsided, perhaps with the onset of sag (?Amberoona Formation).

Strong evidence exists for the Curdimurka Subgroup having acted as a source for Cu-bearing fluids. Within the northwestern Adelaide Fold Belt at least, Cu deposits appear almost exclusively related to inliers of Curdimurka Subgroup, diapiric breccias containing dismembered Curdimurka stratigraphy and reactive younger stratigraphic elements at their peripheries. In contrast, Cu is effectively absent where thick sequences of Curdimurka Subgroup did not accumulate, or where the basin geometry was such that this succession was insulated from Umberatana Group or younger sequences by intervening intact Burra Group stratigraphy. Although we are not in a position to prove that mineralisation occurred during the basin-forming phase, our basin model provides a means by which interaction of permeable source rocks and reactive host rocks could have occurred. Generation of extensive fault systems within the Curdimurka Subgroup, coupled with diapirism, had

the ability to generate substantial secondary permeability with these Cu-rich source rocks. Furthermore, the weight of collapse of the Burra Group and consequent ponding of Umberatana Group strata would have provided an effective driving mechanism for both initiating and sustaining laterally extensive fluid circulation cells. If the thickness of overburden was a contributing factor for extension and salt evacuation, it would be logical to conclude that salt (if contained within a fault-bounded depression such as the Willouran Trough) and potentially hydrothermal fluids, would migrate towards areas of thinner cover (e.g. the margin of the Central Flinders Domain).

References

Belperio A. P. 1990. Palaeoenvironmental interpretation of the Late Proterozoic Skillagolee Dolomite in the Willouran Ranges, South Australia. *In* Jago J. B. & Moore P. S. eds. The evolution of a Late Precambrian-Early Palaeozoic rift complex: The Adelaide Geosyncline. *Geological Society of Australia, Special Publication* 16, 85-105.

Bull S. W., Mackay W. & Selley D. 2001. Provisional stratigraphic comparison of three Cu mineralized basins; the Zambian Copper Belt, the Polish Kupferschiefer and the Adelaide Fold Belt. *This volume*.

Coats R. P. & Dalgarno R. 1983. Large Scale Slumping in the Umberatana Group, Willouran Ranges. *In:* Adelaide Geosyncline Sedimentary Environments and Tectonic Settings Symposium, Adelaide, 1983. *Geological Society of Australia Abstracts 10*: 63-64.

Coats R. P & Preiss W. V. 1987. The Warrina Supergroup. *In*: Preiss W. V. (compiler). The Adelaide Geosyncline-late Proterozoic stratigraphy, sedimentation, palaeontology and tectonics. *Geological Survey of South Australia, Bulletin* 53: 43-72 p.

Forbes B. G. & Preiss W. V. 1987. The Burra Group. *In*: Preiss W. V. (compiler). The Adelaide Geosyncline-late Proterozoic stratigraphy, sedimentation, palaeontology and tectonics. *Geological Survey of South Australia, Bulletin* 53: 73-124 p.

Friedmann S. J. & Burbank D. W. 1995. Rift basins and supradetachment basins: intracontinental extensional end-members.
Basin Research. 7: 109-127.

Krieg G. W., Rogers P. A., Callen R. A., Freeman P. J., Alley N. F. & Forbes B. G. 1991. Curdimurka 1:250,000 Geological Series – Explanatory Notes. *Department of Mines and Energy South Australia publication*, 60 p.

Murrell B. 1977. Stratigraphy and tectonics across the Torrens Hinge Zone between Andamooka and Marree, South Australia. *Unpublished PhD. University of Adelaide*, 192p.

Paul E., Flottmann T. & Sandiford M. 1999. Structural geometry and controls on basement-involved deformation in the northern Flinders Ranges, Adelaide Fold Belt, South Australia. *Australian Journal of Earth Sciences* 46, 343-354.

Preiss W. V. 1983. Depositional and tectonic contrasts between Burra Group and Umberatana Group sedimentation. *In:* Adelaide Geosyncline Sedimentary Environments and Tectonic Settings Symposium, Adelaide, 1983. *Geological Society of Australia Abstracts 10*: 13-16.

Preiss W. V. 2000. The Adelaide Geosyncline of South Australia and its significance in Neoproterozoic continental reconstruction. *Precambrian Research* 100, 21-63.

Rayner R. A. & Rowlands N. J. 1980. Stratiform copper in the Late Proterozoic Boorloo Delta, South Australia. *Mineralium Deposita*. 15: 138-149.

Selley D. 2000. Geological framework and copper mineralisation in South Australia. *AMIRA P544 December 2000 report*.

PhD project: Sedimentology and structure of the Curdimurka Subgroup, Willouran Range, South Australia

Wallace Mackay
Centre for Ore Deposit Research, University of Tasmania

Summary

In the period covered by this report, the aims of this study were finalised. The aims address the presence of evaporites in the Curdimurka Subgroup, the role that they may have played in the structural development of the Willouran Range area and their possible influence on basinal fluids.

A literature review on previous work in the Willouran Range concluded that there was further scope for work on the geology of the Willouran Range, based on flaws and omissions within the previous work. In particular, gaps within the knowledge of the sedimentology and structure of the Curdimurka Subgroup were identified.

An aerial photograph interpretation, concentrating mainly on the structure concluded that the Willouran Range area had undergone at least two phases of compressional deformation; an early low-angle thrusting event resulting in over-turned folds and a second event resulting in imbricate thrusting and related folding. An extensional event which affected the Burra Group was also hypthesised.

Field work was conducted in September and October. The field work identified three groups of problems which could be addressed within the context of this study; structural, sedimentological and an over-lapping group of problems. Work began on addressing these problems along the Norwest Fault, at the southern end of the South Hill Structure and to the west of Boorloo Creek. The work arrived at five conclusions:

- Along the Norwest Fault, an early phase of thrusting was recognised, which now appears as a series of strike-slip faults.
- At the southern end of the South Hill Structure, the Curdimurka Group has been thrust above the Burra Group.
- The contact between the Curdimurka Subgroup and the overlying Groups, where observed, is tectonic.
- Structure within the Curdimurka Subgroup is complex, with isoclinal folding, conical folds and, extensional structures and quartz veins.
- Evaporites were deposited throughout the Curdimurka Subgroup, and they are now seen as pseudomorphs of evaporite minerals (gypsum, anhydrite, halite and several unidentified minerals).

Aims of the project

The primary aim of the project is to identify the depositional setting of the Curdimurka Subgroup in the Willouran Range, South Australia. Secondary aims are:

- to identify the overall structure of the Willouran Range,
- to determine the origin of breccias within the Willouran Range and,

- determine (at least theoretically) the influence of the Curdimurka Subgroup on the basinal fluids and their ability to transport metals, and,

- compare and contrast Curdimurka Subgroup in the Willouran Ranges and the best preserved section of Callanna Group rocks at Arkaroola.

Within the aims is the tacit recognition of the presence of evaporites within the Curdimurka Subgroup, and their presence controls the aims. The importance of identifying the depositional setting is that it may control the mineralogy of the evaporites deposited and hence affect the chemistry of fluids derived from, or influenced by, their dissolution. Likewise, the presence of evaporites and their mineralogy may influence or even control the structural history of the Willouran Range area and breccia formation. Hence, the identification of the depositional setting is the primary aim and from this the secondary aims are derived.

It is the occurrence of evaporites in the Willouran Range and the recognition of the association between evaporites and base metal mineralisation which is the *raison d' être* for this study. Warren (1999) provides a summary of the association between sediment-hosted copper and evaporites, an association which Kirkham (2001) has emphasised. The presence of evaporites in the Zambian Copperbelt and the Kupferschiefer in Poland demonstrates a spatial association but the work of Warren (1999) demonstrates that evaporites are fundamental to orebody formation by acting as:

- a brine and ion source,
- a seal and trap to basinal fluids,
- a focus for fluid flow.

By understanding the evaporites in the Willouran Range, their mineralogy, diagenesis and influence on the structural history, it may be possible to assess the potential for sediment-hosted mineralisation within the Adelaide Fold Belt and obtain a better understanding of how the mineralisation in the Zambian Copperbelt may have formed. Figure 1 shows the project area.

Work completed: May–November 2001

The work completed in the period between May and November, 2001 included a literature review for the Willouran Range, an aerial photograph interpretation and mapping in the Willouran Range.

Literature Review

A literature review of previous studies in the Willouran Range was completed. By necessity, it included some background on the Adelaide Fold Belt, to provide information in the regional geology and to identify the main issues and current research trends.

At the regional scale, it is clear that the presence of diapirs within the Adelaide Fold Belt is accepted, but their role in basin development remains controversial (e.g., Mount, 1975; Lemon, 1988; Dyson, 1992, 1996, 2001).

The review concluded that within the Willouran Range area, there have been detailed studies of the Curdimurka Subgroup conducted in the late 1970s to early 1980s as part of an exploration programme for copper (Rowlands et al., 1979, 1980, 1981), a PhD study (Murrell, 1977) and the formalisation of the Callanna Group (Forbes et al., 1981). Forbes (1990) is the most recent work which provides an overview of the geology of the Willouran Range, with emphasis on the Curdimurka Subgroup. In addition, there has been mineral exploration within the area for much of the past forty years, but the reporting of this work has been only cursory in nature; the work of Utah Development Company (UDC; Rowlands et al., 1979, 1981) being the exception. While recognising the value of the previous work, there are key flaws within that work and some major omissions and it is these flaws and omissions which provide the opportunity to build on the previous work.

A flaw in the sedimentological analysis of Rowlands

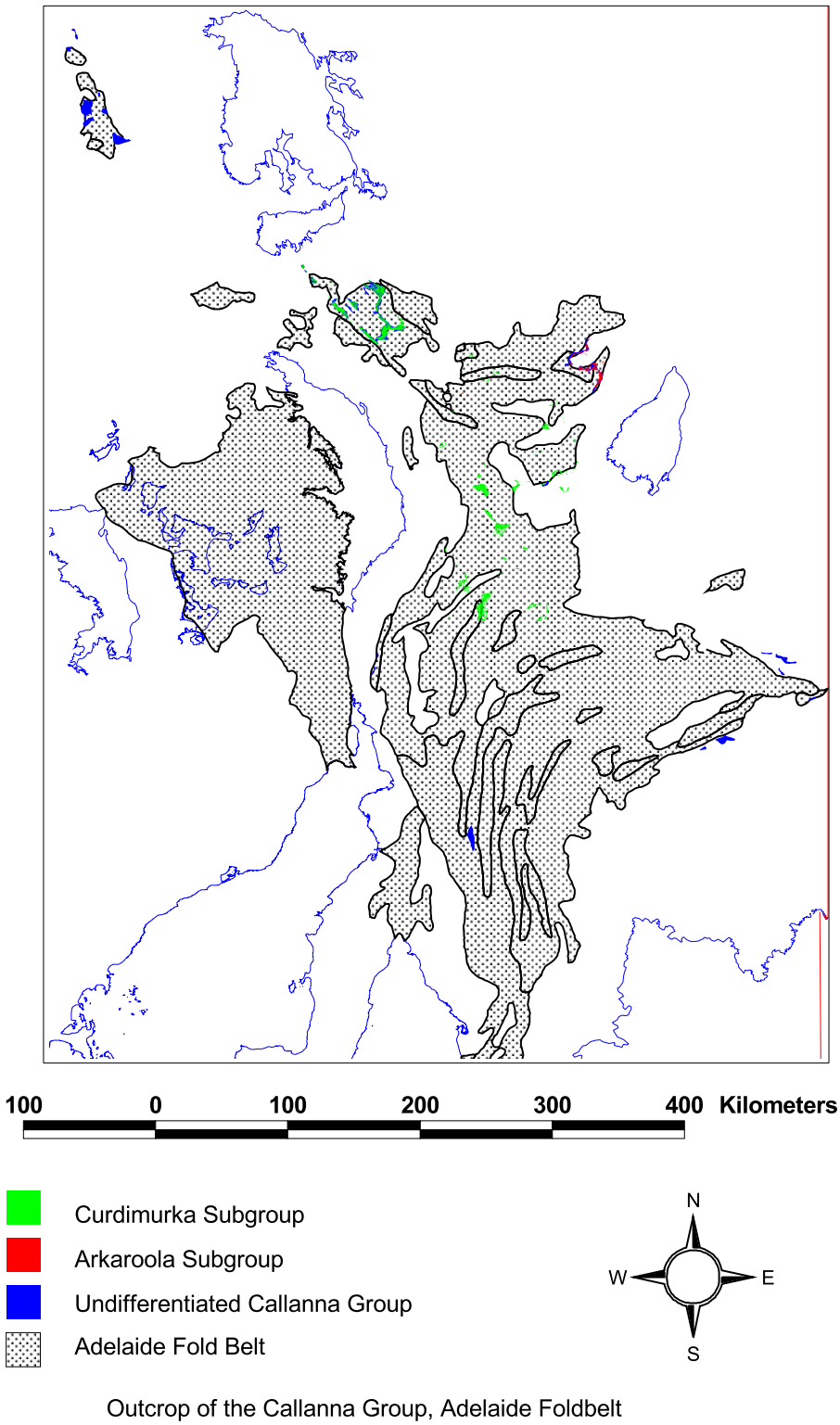

Figure 1
Area of outcrop of the Callanna Group, with the mapping area outlined.

et al. (1979, 1980, 1981) is that the mapping was interpretative, aimed at proving that the depositional environment of the Curdimurka Subgroup was a sabhka. UDC was using an exploration model for sediment-hosted copper mineralisation based on that of Renfro (1974). Hence the geology is described in terms of a sabhka model, with no attempt to justify that model.

The key omission is the lack of integration between structural and sedimentological studies and between individual structural studies. In particular, a number of structural features have been recognised (e.g., Sprigg, 1949; Murrell, 1977; Parker, 1983) but there has been no comprehensive structural study aimed at developing a structural history of the Willouran Range.

Finally, the breccias within the Willouran Range have been a source of controversy since they were first described by Howchin (1924). There have come to be three main interpretations as to the origin of the breccias; decollement structures associated with thrusting (Sprigg, 1949), mega-slumping (Murrell, 1977) or olithostromes (Rowlands et al., 1979, 1980) and diapirs (Preiss, 1987; Forbes, 1990). There is agreement that the common factor in the deformation is the presence of the carbonate and evaporite-rich Callanna Group, which facilitated deformation and was itself brecciated.

Aerial photograph interpretation

An aerial photograph interpretation was undertaken, aimed at understanding the structure of the Willouran Range area. The need for the study was evident after the literature review demonstrated that there was insufficient understanding of the structure. From the study, a hypothesis of the structural history was developed which could be tested in the field.

The study concluded that there is evidence for both extensional deformation and compressional deformation. The extensional deformation is seen best in the Burra Group, but it is also probable that the Curdimurka Subgroup shows the effects of the same extensional event. It was this event which saw the deposition of the Umberatana Group (see also Selley and Bull, this volume).

Two compressional events are seen; a southeast-northwest directed thrusting and a west-directed thrusting. Southeast-northwest thrusting has occurred along the major fault zones, but is best seen along the Norwest Fault. Westerly imbricate thrusting has resulted in the dissection and rotation of the basin to give the present outcrop pattern.

An additional two deformations are possible. Previous workers (Murrell, 1977; Parker, 1983) suggest that the Curdimurka Subgroup was deformed prior to the deposition of the Burra Subgroup. The second possible deformation is seen as a series of regionally anomalous WNW-trending folds within the Skillogalee Dolomite and the Myrtle Springs Formation in the vicinity of the Rischbieth Structure.

From the aerial photograph interpretation, the main areas for the investigation during the first major field trip were identified and the results of the mapping are discussed next.

Field work — September and October.

Introduction

The field work was conducted with the aim of getting to know the area, to identify some of the problems to be addressed and to begin testing the ideas from the aerial photography interpretation. Figure 2 shows the geology of the study area and the position of traverses.

Although not all areas were visited, the key problems relevant to this study were identified. They can be divided into two sub-headings, structural and sedimentological with a third, over-lapping set of problems. Problems associated with structure are,:

- the large-scale structure of the Willouran Range area and its relationship to regional deformation of the Adelaide Fold Belt;

- the structure within the Curdimurka Subgroup, to determine if the Curdimurka Subgroup was deformed prior to or during deposition of the Burra Group;

- the relationships between the various quartz veins observed and to the broader structure and mineralisation.

Sedimentological problems recognised are:

- the nature of the evaporites;

- identification of depositional cycles within the Curdimurka Subgroup;

- the depositional environment and basin evolution recorded by the Curdimurka Subgroup.

A third group of problems can be related to both structure and sedimentology:

- the nature and origin of breccias;

- the relationship between what is mapped as Dome Sandstone along the Norwest Fault and South Hill Structure and the Dome Sandstone in its type section;

- contact relationships between the Curdimurka Subgroup and overlying groups.

Structural studies

The Norwest Fault — Work across the Norwest Fault indicates there are a number of steeply plunging structures along its length, related to the Norwest Fault (Fig. 3). In the Black Knob Structure, sediments stratigraphically above the Dome Sandstone have been folded into a syncline with a steep plunge to the northwest and an axial plane dipping steeply to the northeast. Dome Sandstone recurs stratigraphically above these sediments. To the southeast, a traverse was mapped across a fold interpreted from aerial photographs to be associated with the Black Knob Structure. Poles to bedding across an anticline and syncline pair show that the structure plunges at a moderate angle (about 60º) to the southeast, with an axial plane dipping steeply to the northeast. Finally a traverse across a fold interpreted to be a detached syncline showed that the fold has a steep plunge to the northwest, with an axial plane dipping steeply to the northwest. A traverse about a small sinistral fault offsetting the Dome Sandstone was also mapped. The traverse confirmed that the Dome Sandstone has been offset by about 200 m, at a low angle to bedding with some overturning of bedding at the tips of the fold.

These observations are consistent with an early thrust phase along the Norwest Fault, with the Black Knob Structure being an antiformal stack, thrusting being from northwest to southeast, or dextral as seen in outcrop today. The fold seen in the last traverse is the result of initial northwest to southeast thrusting, resulting in an over-turned syncline, which became detached with continuing northwest to southeast thrusting. Subsequent southeast to northwest movement resulted in the overriding sheet being withdrawn from above the overturned syncline and moved to its present position.

It should also be noted that the Dome Sandstone along the Norwest Fault, although silicified by (presumably) Tertiary weathering, has been re-crystallised and silicified in places, almost to the point of it being indistinguishable from vein quartz, indicating that the Norwest Fault has been a major focus for fluid flow.

Mapping in 2002 will be carried out to confirm these suggestions and provide information on the timing of thrusting.

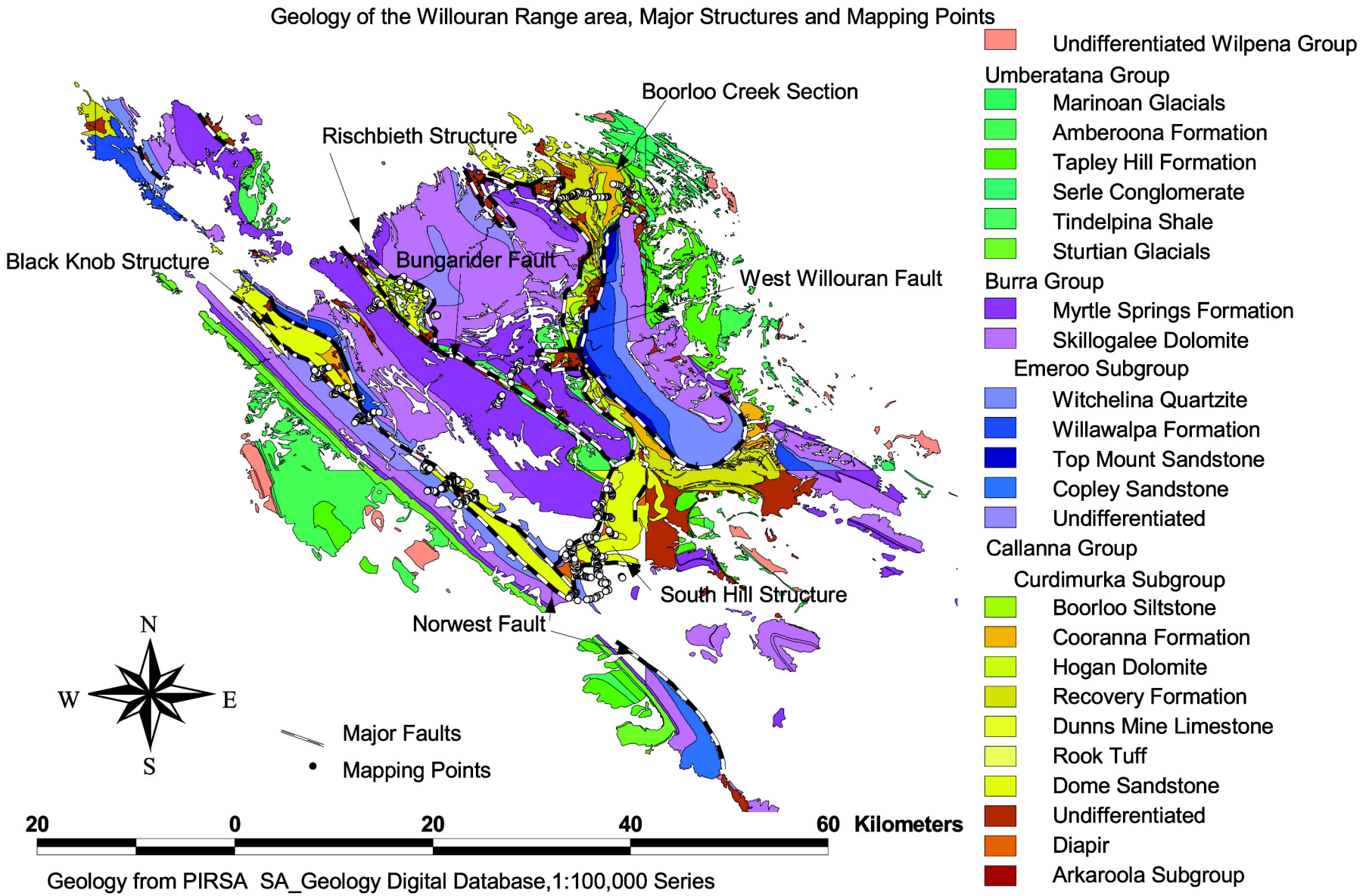
Geology of the Willouran Range area, Major Structures and Mapping Points
Boorloo Creek Section
Rischbieth Structure
Black Knob Structure
Bungarider Fault
West Willouran Fault
South Hill Structure
Norwest Fault
N
W
E
S
Major Faults
Mapping Points
20
0
20
40
60 Kilometers
Geology from PIRSA SA_Geology Digital Database,1:100,000 Series
Undifferentiated Wilpena Group
Umberatana Group
Marinoan Glacials
Amberoona Formation
Tapley Hill Formation
Serle Conglomerate
Tindelpina Shale
Sturtian Glacials
Burra Group
Myrtle Springs Formation
Skillogalee Dolomite
Emeroo Subgroup
Witchelina Quartzite
Willawalpa Formation
Top Mount Sandstone
Copley Sandstone
Undifferentiated
Callanna Group
Curdimurka Subgroup
Boorloo Siltstone
Cooranna Formation
Hogan Dolomite
Recovery Formation
Dunns Mine Limestone
Rook Tuff
Dome Sandstone
Undifferentiated
Diapir
Arkaroola Subgroup

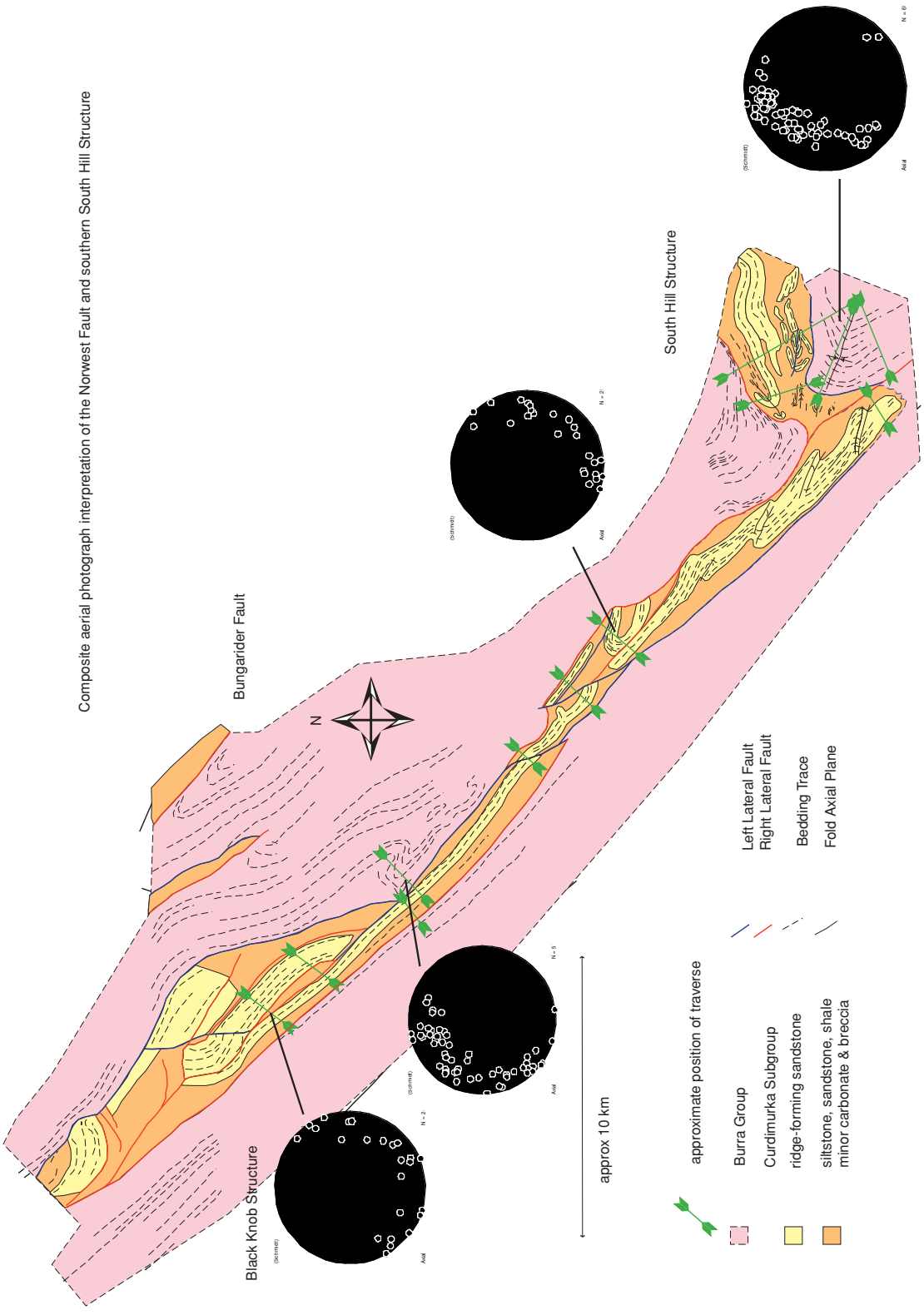

Figure 3
Composite aerial photograph interpretation of the Norwest Fault and southern South Hill Structure, with poles to bedding for individual structures.

The Bungarider Fault — Work along the Bungarider Fault was limited by access and rain, but two traverses were completed and an area along the northeastern edge of the Rischbieth Structure was examined. The first traverse was from the Myrtle Springs Formation, northeast into the Rischbieth Structure. The traverse was across a broad syncline within the Myrtle Springs Formation, with an anomalous 'Z' fold being noted, once again suggesting low angle movement (relative to bedding) affecting the Burra Group. A small-scale thrust was observed in the vicinity of the contact between the Burra Group and the Curdimurka Subgroup. In addition, folding associated with cleavage development was noted, confined to individual beds within the Burra Group. The folding is not associated with the large scale folding seen in aerial photographs. This style of folding was also seen in the Myrtle Springs Formation to the southeast, along the Bungarider Fault in the second traverse.

Along the northeastern contact of the Rischbieth Structure, the Skillogalee Dolomite does thin into the contact. In the vicinity of the contact, extensional quartz veins are common, most commonly as a series of regularly spaced veins, confined to specific horizons within the Skillogalee Dolomite.

Mapping in 2002 will concentrate on the contact relationships between the Curdimurka Subgroup and the Burra Group. Parker (1983) mapped the Rischbieth Structure in detail and although the mapping will be ground-truthed, it is not intended to remap the area in detail.

The South Hill Structure — On the South Hill Structure, most of the work completed to date has concentrated on the southern and western side of the structure, with the aim of determining its relationship to the Norwest Fault (Fig. 3). A series of traverses were mapped across the structure to gather structural information of both the Curdimurka Subgroup and the basal Burra Group. Of particular interest was the relationship between the Burra Group and the Curdimurka Subgroup.

Mapping showed that an area at the southern end of the South Hill Structure marked on geological maps as a diapir, is an area of folding and faulting. Its relationship to diapirism is tenuous, although it is accepted that salt tectonics played a role in the development of the structure. Smaller scale mapping will be required in this area to determine the structure. At a larger scale, mapping indicates that the South Hill Structure in the area mapped is a thrust-related fold. Detailed interpretation of the mapping in this area is incomplete, but it appears that there are a series of northwesterly directed thrusts, which have thrust the Curdimurka Subgroup over the Burra Group.

Structure within the Curdimurka Subgroup — Initial observations of the structure within the Curdimurka Subgroup indicate that it is more complicated than previous mapping infers. The Recovery Formation in particular shows intense deformation, with the Cooranna Formation also showing a considerable amount of internal deformation.

Isoclinal folding is common and was observed in all formations above the Rook Tuff. Figure 4 shows isoclinal folds which, because of the variation in fold plunges, are ascribed to soft-sediment deformation. Folding associated with faulting (at a low angle to bedding) is common and upright conical folds with shallow plunges were observed within the Recovery Formation.

Extensional deformation is seen within the Dunns Mine Limestone, where beds show millimetre- to centimetre-scale extensional fractures (Fig. 5). Quartz and quartz-carbonate veining is locally common, with conjugate vein sets occurring over hundreds of metres within the Recovery Formation.

Quartz Veining

Quartz veins are of interest because they may provide information on the chemistry of basinal fluids and stress fields at different times in the development of the basin. Two types have been identified to date; quartz-carbonate veins and quartz only veins. Figure 6 shows typical quartz veins types.

The quartz-carbonate veins are typically coarse grained, with white quartz along the vein margins and carbonates in the vein centres. Carbonates are usually calcite and siderite, with the proportions of each being variable. Coarse-grained pyrite has been observed with quartz-carbonate veins in several places, mentioned above. Mineralisation at the Euchre Pack Mine (in the Dunns Mine Limestone and the Warra Warra Mine (in the Burra Group) is hosted by quartz-carbonate veins, the mineralisation occurring as a late-stage in-fill within the veins and adjacent country-rock.

Sedimentology of the Curdimurka Subgroup

Evaporite deposition dominates the sedimentology of the Curdimurka Subgroup. A total of six different types of pseudomorphs after (presumed) evaporite minerals have been recognised, including halite, anhydrite, gypsum and what previous workers have identified as shortite. Figure 7 shows some of the evaporite textures seen.

Evaporites appear to have comprised up to 80% of the rock mass in some beds, forming an inter-locking mesh of crystals. Other pseudomorphs occur as scattered, individual crystals on bedding surfaces. Throughout the deposition of the Curdimurka Subgroup above the Rook Tuff, the depth of sedimentation appears to have varied about water (sea or lake) level, with dessication cracks being common, and no evidence of deeper water deposition of evaporites, such as bottom-growth textures, although this may be due to destruction of early textures during diagenesis. Iron oxide after pyrite is common, with in some places pyrite having comprised up to 20% of the rock mass. The pyrite was euhedral, and usually cubic, with grainsize up to 6 mm.

A key aspect of the study will be the differentiation between the various sandstone bodies. At present, it is assumed that the sandstone along the Norwest Fault and the South Hill Structure is the Dome Sandstone. The sandstone is sufficiently different from the Dome Sandstone in its type area at The Dome, to question this assumption. Along the Norwest Fault, the sandstone is typically more silicified, coarser grained and appears to form more sheet-like bodies than the Dome Sandstone at the Boorloo Creek Section, which is generally finer grained, but with coarse-grained channel deposits within it. The variation may be due to changes in facies but a complicating factor is the similarity in places between what is mapped as Dome Sandstone along the Norwest Fault and sandstones mapped at the base of the Burra Group (the Emeroo Subgroup).

Contact Relationships between the Curdimurka Subgroup and the Burra Group

The contact between the Burra Group and the Curdimurka Subgroup is rarely seen, usually being covered by alluvium or regolith.

On the western side of the South Hill Structure, the contact is tectonic and marked by dolomitisation and quartz-carbonate veining. Iron-oxides after pyrite are common with the veins, with the pyrite having been coarse-grained (to 1 cm) and euhedral, usually as pyritohedrons. The quartz veins are coarse-grained and white, with crystal long axes showing rotation with vein growth. Elsewhere around the South Hill Structure, as the contact is approached, there may be folding within the Curdimurka Subgroup, with the folds having an axial plane sub-parallel to the contact. A breccia occurs within the Curdimurka Group close to the contact with the Burra Group. It comprises arenite fragments, retains a layering which is likely bedding and is usually associated with thick chert-rich dolomite beds. The angular variation in dip across the contact is variable with bedding being roughly parallel in some areas, to there being a large difference in others, particularly on the southeastern edge of the South Hill Structure.

At Boorloo Creek, a breccia occurs at the top of the Boorloo Siltstone. It contains megaclasts of limestone (the Black Knob Marble), volcanics (the Noranda Volcanics) and coarse-grained, basic igneous rocks. In addition, there was considerable quartz-carbonate veining at the edge of the breccia along one traverse.

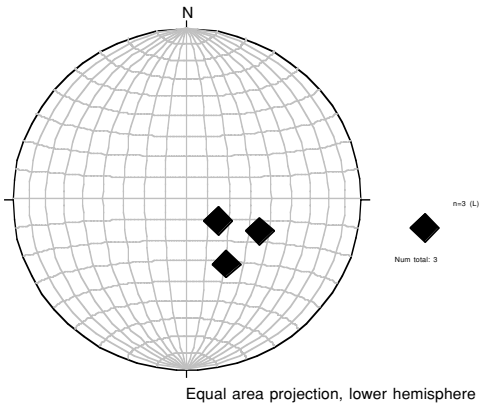

Figure 4.
Isoclinal folds from within the Recovery Formation, Curdimurka Subgroup. Stereonet shows measured plunges of folds in (b).

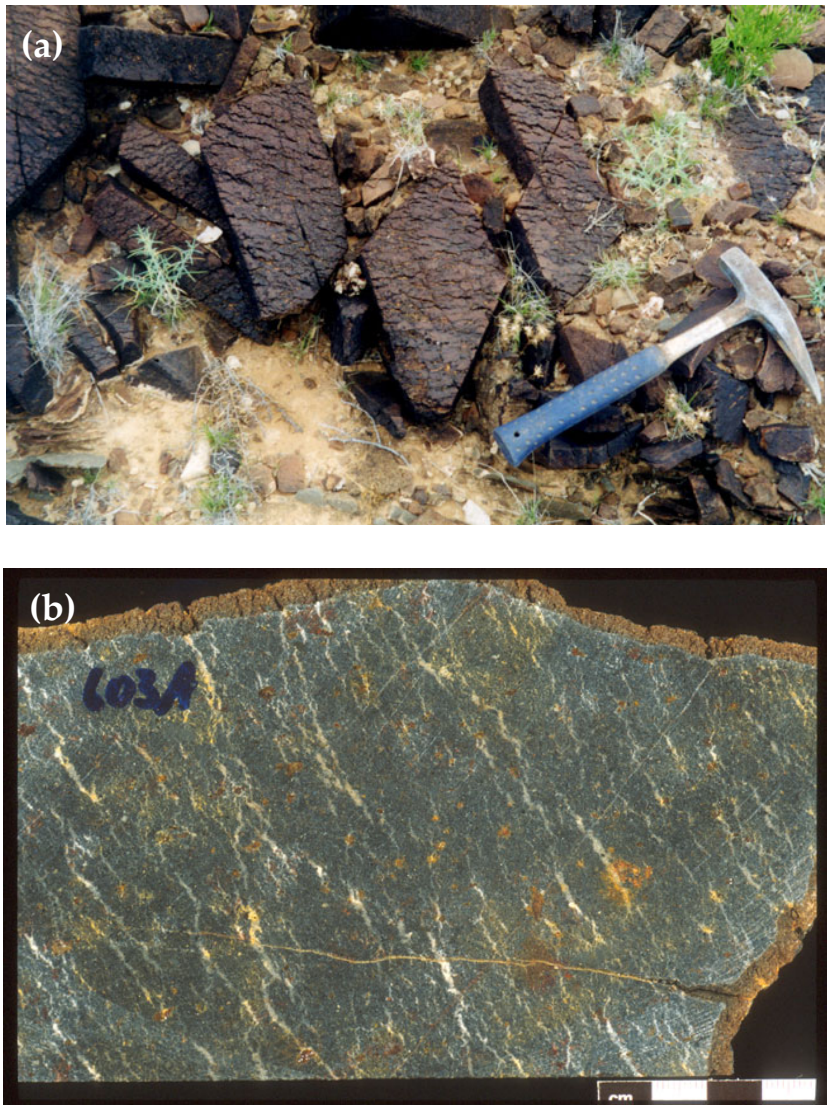

Figure 5
Extensional fractures within the Dunns Mine Limestone, Curdimurka Subgroup. (a) Outcrop showing extensional fractures in sandstone within the Dunns Mine Limestone. (b) Cut slab showing extensional fractures in-filled with carbonates.

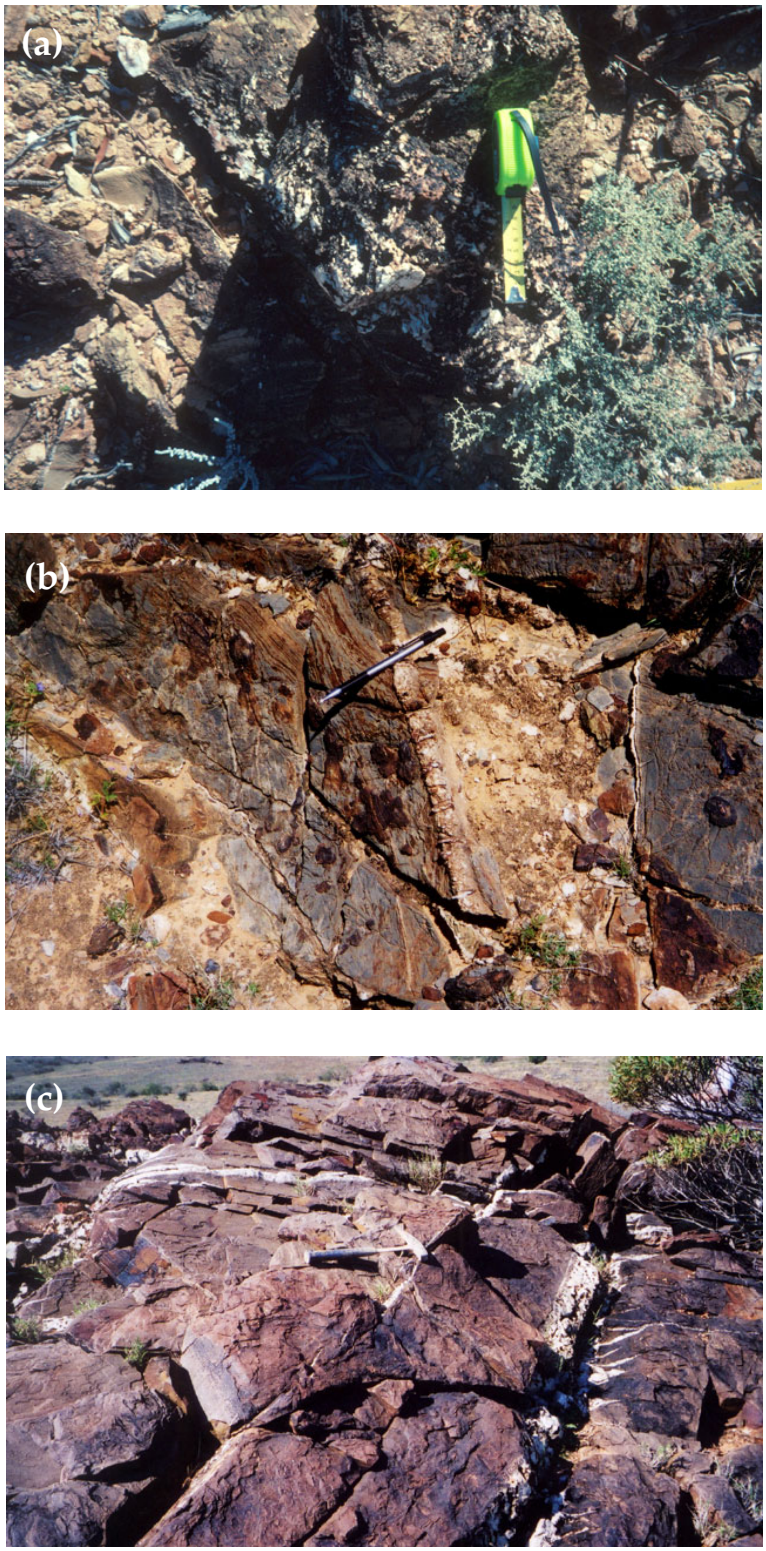

Figure 6
Quartz veins in the Willouran Range. (a) Extensional veins at the contact between the Curdimurka Subgroup and the Burra Group, South Hill Structure. (b) A quartz-carbonate vein in the Recoveery Formation cut by extensional quartz veins. (c) Conjugate veins in the Wilyerpa Formation (Umberatana Group) 100 m above the top o fthe breccia at the contact between the Curdimurka Subgroup and the Umeberatana Group, Boorloo Creek.

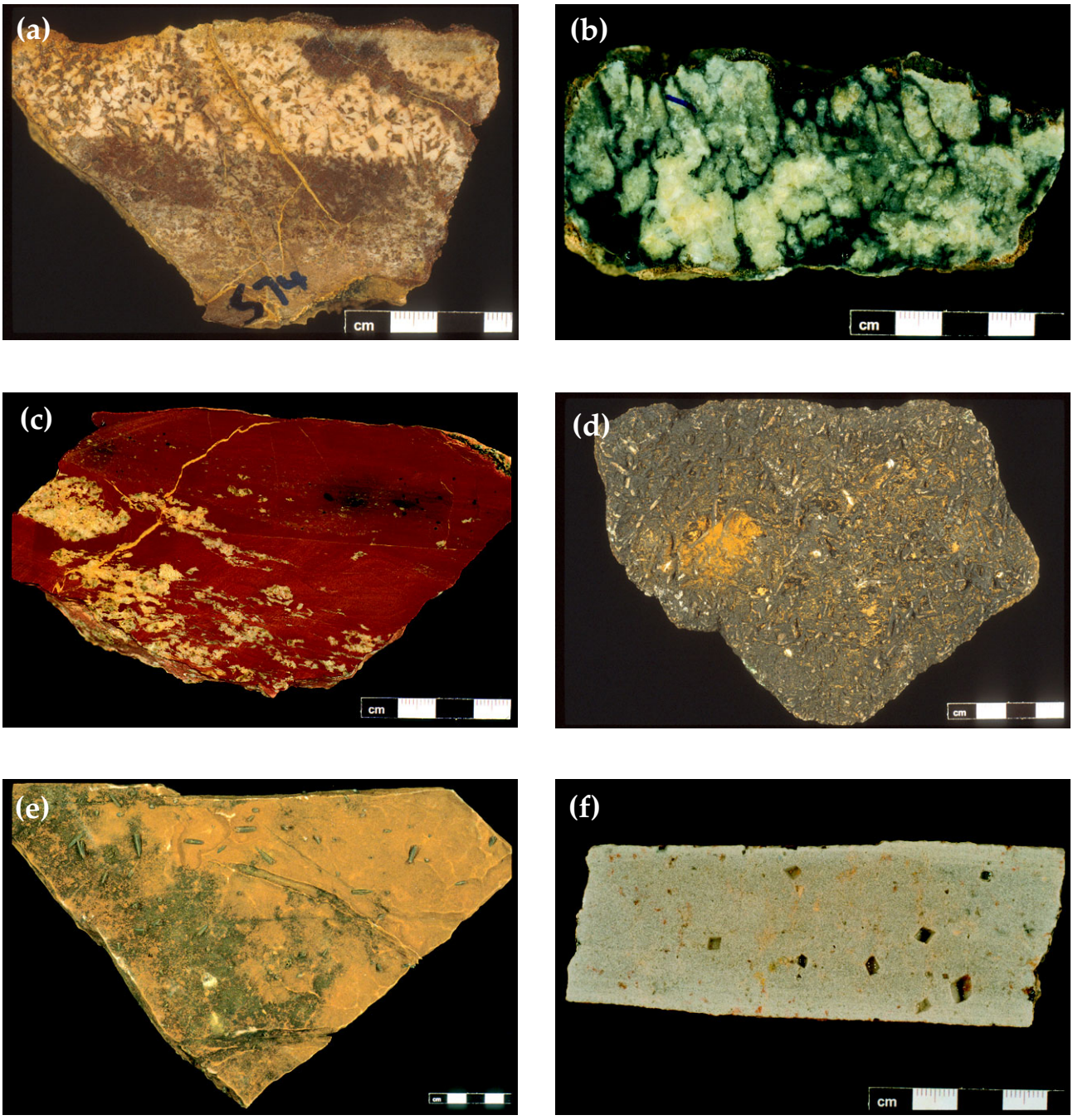

Figure 7
Evaporite textures from the Curdimurka Subgroup. (a) Carbonate after gypsum in limestone. (b) Chickenwire texture, with carbonate replacing anhydrite. (c) Carbonate replacing anydrite in red siltstone. (d) Interlocking crystal mesh (original evaporite mineral and replacing mineral to be identified). (e) Individual crystals of a precursor yet to be identified, replaced by carbonate. (f) Polygonal voids in quartz-feldspar sandstone.

Selley and Bull (this volume) consider this breccia to be due to diapirism.

Along the southwestern edge of the Norwest Fault, there is no apparent difference in dip of bedding across the fault, with the presence of the fault being inferred by changes in facing; from northeast in the Curdimurka Subgroup to southwest in the Burra Group. On the northeastern margin of the fault, the Burra Group usually wraps into a fault at the top of the Curdimurka Subgroup.

Future Work

Mapping

This years field work has demonstrated that to answer the problems posed, mapping will need to be conducted at smaller scales than was possible this year. To allow the problems to be addressed in the time available, key areas for more detailed work have been identified, with larger scale mapping to be conducted between the areas. As such, and to aid in the discussion and planning of further work, the field area has been divided into ten areas. Table 1 provides the areas identified for further work in 2002 and Figure 8 shows the areas. The areas outlined maintain the structural relationships, so that; the Stony Range and the Black Knob Structure map the Norwest Fault; the Bungarider and Rischbieth Structure map the Bungarider Fault and the Boorloo Creek and Willouran Range areas map the East Willouran Fault. Noname, Witchelina Diapir, South Hill Structure and Euramina all map separate structures. Detailed mapping will be conducted at scales of 1:10,000 or less, with traverses being mapped at scales of 1:20,000 or more.

Other Work

The literature reviews, reading on evaporites and field work to date suggest directions of work in the laboratory to support the field work. Identification of the original evaporite mineralogy is considered to

Table 1
Areas for further work (see also Figure 8).

Area	Mapping	Main Interest
Boorloo Creek	detailed mapping	sedimentology of the Curdimurka Subgroup structure within Curdimurka Subgroup
Rischbieth Structure	detailed mapping	structural relationships with the Burra Group
Black Nob Structure	detailed mapping	structural relationships with the Burra Group
Witchelina Diapir	detailed mapping	sedimentology of the Curdimurka Subgroup salt tectonics
South Hill Structure	detailed mapping	structural relationships with the Burra Group brecciation
Stony Range	traverse	structure across and along the Norwest Fault
Bungarider	traverse	structure across and along the Bungarider Fault
Willouran Range	traverse	contact relationships between the Curdimurka Subgroup and the Burra Group
Noname	traverse	structural relationships between the Curdimurka Subgroup and the Burra Group
Euramina	traverse	brecciation

be crucial to understanding the environment of deposition and this work will begin in the next few months. Work will comprise petrographical studies of the Curdimurka Subgroup, especially on those samples with pseudomorphs identified in hand-specimen, electron microprobe studies and X-Ray diffraction to identify remnant evaporite phases (if present). The petrographical studies will also be aimed at the differentiation between the different sandstones within the mapping area.

References

Dyson, I.A., 1992. Geology of the Upalinna Diapir, central Flinders Ranges. South Australia Geological Survey Quarterly Geological Notes, 124, pp 2 - 19.

Dyson, I.A., 1996. A model for diapirism in the Adelaide Geosyncline. MESA Journal, 3, pp 33 - 35.

Dyson, I.A., 2001. The diapir-base metal association in the northern Flinders Ranges. MESA Journal, 22, pp 37 - 43.

Forbes, 1990. Geology of the Willouran Range. *In* Jago, J.B., and Moore, P.S., (eds). The evolution of a late Precambrian - early Palaeozoic rift complex: The Adelaide Geosyncline. Australian Geological Society Special Publication No. 16, pp 68 - 84.

Forbes, B.G., Murrell, B. and Preiss, W.V., 1981. Subdivision of lower Adelaidean, Willouran Ranges. South Australian Geological Survey Quarterly Geological Notes, 79, pp 7-16.

Howchin, W., 1924. The Sturtian Tillite in the Willouran Ranges near Marree (Hergott) and in the northeastern portions of the Flinders Ranges. Report of the Australian Association for the Advancement of Sciences 17, pp 67 - 76.

Kirkham, R.V., 2001. Sediment hosted stratiform copper (ssc), other stratabound base metal deposits and the importance of basinal brines and/or evaporites, halotectonics and halokinesis. In Piestrzynski et al. (eds), Mineral deposits at the beginning of the 21st century. pp 15-18.

Lemon, N.M, 1988. Diapir recognition and modelling with examples from the late Proterozoic Adelaide Geosyncline, Central Flinders Ranges, South Australia. University of Adelaide, PhD Thesis (unpublished).

Mount, T.J., 1975. Diapirs and diapirism in the Adelaide Geosyncline, South Australia. PhD Thesis, University of Adelaide (unpublished).

Murrell, B., 1977. Stratigraphy and tectonics across the Torrens Hinge Zone between Andamooka and Marree, South Australia. University of Adelaide, PhD Thesis (unpublished).

Parker, A.J., 1983. Tectonic development of the Adelaide Fold Belt. Geological Society of Australia, Abstracts 10., pp 23-28.

Preiss, W.V., 1987. The Adelaide Geosyncline: Late Proterozoic stratigraphy, sedimentation, palaentology and tectonics. The Geological Survey of South Australia, Bulletin 53, 438p.

Renfro, A.R., 1974. Genesis of evaporite-associated stratiform metalliferous deposits; a sabhka process. Economic Geology, 69, 33-45.

Rowlands, N.J., Jarvis, D.M., Rayner, R.A. and Blight, P. 1979. S.A. stratiform copper project, EL. 461 Willouran Ranges. Third annual report on exploration activities (period 21.12.78 - 24.12.79). Utah Development Company Report No. 317 (unpublished)

Rowlands, N.J., Blight, P.G., Jarvis, D.M., and von der Borch, C.C., 1980. Sabhka and playa environments in late Proterozoic grabens, Willouran Ranges, South Australia. Journal of the Geological Society of Australia, 27. pp 55 - 68

Rowlands, N.J., Jarvis, D.M., Benade, D.R., Circosta, G. and Blight, P.G., 1981. S.A. Stratiform copper project, EL 461. Fourth annual report on exploration activities (period 24. 12. 79 - 3. 4. 81). Utah Development Company Report No. 338 (unpublished).

Sprigg, R.C., 1949. Thrust structures of the Witchelina area, South Australia. Royal Society of South Australia, Transcripts, 73, 40-47.

Warren, J., 1999. Evaporites: their evolution and economics. Blackwell Science Ltd, Oxford. 438p.

Copper mineralisation at Emmie Bluff, South Australia 1: Setting, host rocks, ore textures and multi-element geochemistry

Peter McGoldrick
Centre for Ore Deposit Research, University of Tasmania

Summary

Two different styles of Cu mineralisation, separated by a vertical distance of about 600 m, are known from the Emmie Bluff area in South Australia. The deeper Cu is hosted by ironstones and has similarities to Olympic Dam. Stratabound Cu occurs in Neoproterozoic sedimentary cover. This report briefly describes the two types of mineralisation, and presents new multi-element geochemical data to help compare the two types. While these data cannot prove a genetic link between the two types, they are not inconsistent with a single oxidised saline relatively low temperature fluid being responsible for both. If this fluid was sourced from the Adelaide Fold Belt, then the maximum age of both mineralisation styles is about 600 Ma (ABC Quartzite – Brachina Formation times). Zinc and Pb, together with the Fe and Mn content of dolomitic sediments may be useful indicators of Cu mineralisation.

Introduction

The Emmie Bluff area, 40 km south of Andamooka (Fig.1), was explored by MIM and JV partners in the 1980s and early 1990s. In an area of less than 5 km^2 blind Cu mineralisation was discovered in hematite and magnetite-pyrite altered 'basement' rocks and also in Neoproterozoic sedimentary 'cover' rocks of the Stuart Shelf. Gow et al. (1994) recognised physico-chemical similarities in the fluids responsible for the Emmie Buff basement Cu mineralisation and those thought to be responsible for giant Olympic Dam deposit (Haynes et al., 1995). Unlike Olympic Dam, there are no constraints on the minimum age of the basement mineralisation at Emmie Bluff, which begs the question of whether as well as a spatial link, there might be a genetic link between basement and cover mineralisation.

The purpose of this report is to:

- briefly describe the basement mineralisation
- describe the important features of Cu mineralisation in the cover rocks
- document major and trace element lithogeochemistry of samples from both mineralisation types
- discuss the constraints these observations place on the origin of and relationship between the two mineralisation types
- determine if lithogeochemical features can be used as vectors toward Cu mineralisation

Methods

Five drill holes from the Emmie Bluff area were examined at the PIRSA core-repository in Adelaide. No attempt was made to re-log these cores, as MIM logs were available. A digital photographic record was made of each core and selected material was collected for petrographic and textural studies. Limited assay data (for Cu, Co, Zn, Pb, Ag and a few Au analyses) were available from MIM records, but archive pulps were not locatable, so the mineralised intervals in these holes were re-sampled. Quarter core was shipped to Hobart, crushed, and milled in a case-hardened mild steel mill. High-quality analyses for 11 major and 20 trace elements (Table 1) were carried out using the 'in house' XRF facility in the

Table 1
Major elements (light grey) and trace elements (dark grey) analysed by XRF; with nominal detection limits (ppm)

Na	Mg											Al	Si	P	S
180	70											40	10	100	20
K	Ca	Sc	Ti	V	Cr	Mn	Fe	Co	Ni	Cu	Zn			As	
3	6	2	40	1.5	1	10	2	2	1	2	1			3	
Rb	Sr	Y	Zr		Mo										
1	1	1	1		1										
	Ba				W							Tl	Pb	Bi	
	4				2							1.5	1.5	2	
							Th		U						
							1.5		1						

School of Earth Sciences, University of Tasmania. Analyses of selected samples for total C , organic C, and rare earths are yet to be undertaken, and will be presented in a subsequent report.

Ironstone-hosted Cu mineralisation

The following description of the basement Cu mineralisation is taken from (Gow et al., 1994) and MIM Technical Report 2724: Relinquishment Report for EL 1808 "Sandy Point" (1996), supplemented by the writer's own observations. Basement mineralisation occurs, on average , 800 m below the surface hosted in an Fe oxide-rich interval 150 m thick and about 3 km in diameter. To the south the Fe-rich rocks are described as "a highly fractured zone of discordant magnetite-rich skarn" hosted in a sericitised rhyodacite. To the north (e.g., in DDH SAE6) the ironstones are mostly ferruginised metasiltstones (Fig. 2) and associated ferruginised porphyritic granite. Mineralisation is mostly low grade and occurs as chalcopyrite-bornite and minor covellite associated with a low temperature hematite-quartz-chlorite-pyrite assemblage. Typical assays are presented on Table 2.

For the present study six, 1 m long samples of quarter core were collected from SAE6 for geochemical analysis. Three of these samples were from the intensely hematised, Cu-rich interval between 937.1 and 952 m, and the other three from weakly hematitc, quartz-chlorite rock (meta-arkose?) deeper in the hole. Geochemical data for these samples is available in the Appendix CD to this report, and selected trace elements are compared to Cu in a series of cross-plots on Figure 3. If the two samples with less than 100 ppm Cu are repesentative of 'barren' irontones,

Table 2
Indicative Cu grades from basement mineralisation in DDHs SAE3, SAE4, and SAE6

SAE6	15 m at 1.23wt%Cu	from 937 m
	104 m at 0.27wt% Cu	from 960 m
SAE4	18 m at 0.64wt% Cu in hematite-rock beneath the Pandurra Formation followed by 50 m at 0.57wt% Cu	
SAE3	massive hematite including 18 m at 0.7wt% Cu	

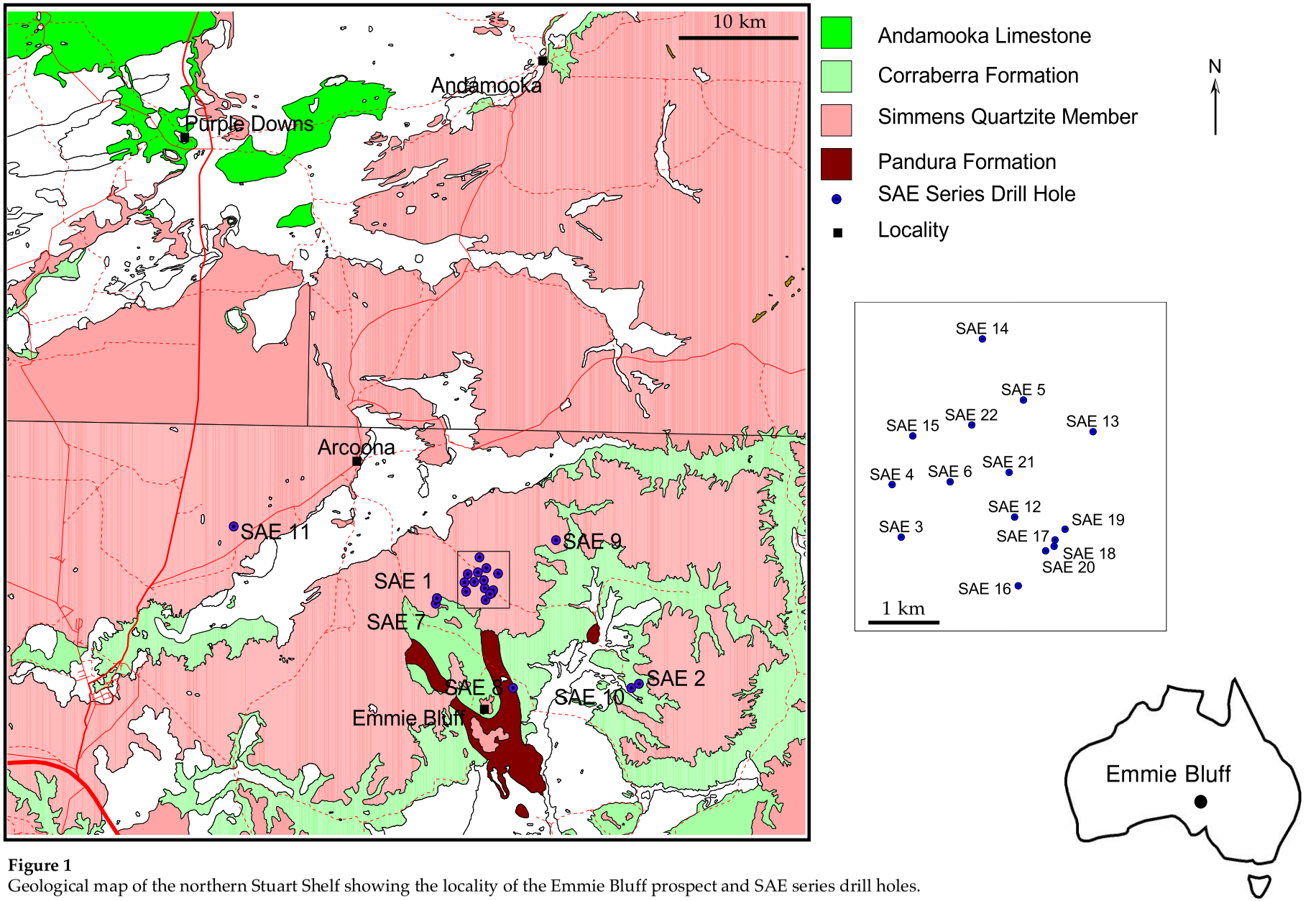

Figure 1
Geological map of the northern Stuart Shelf showing the locality of the Emmie Bluff prospect and SAE series drill holes.

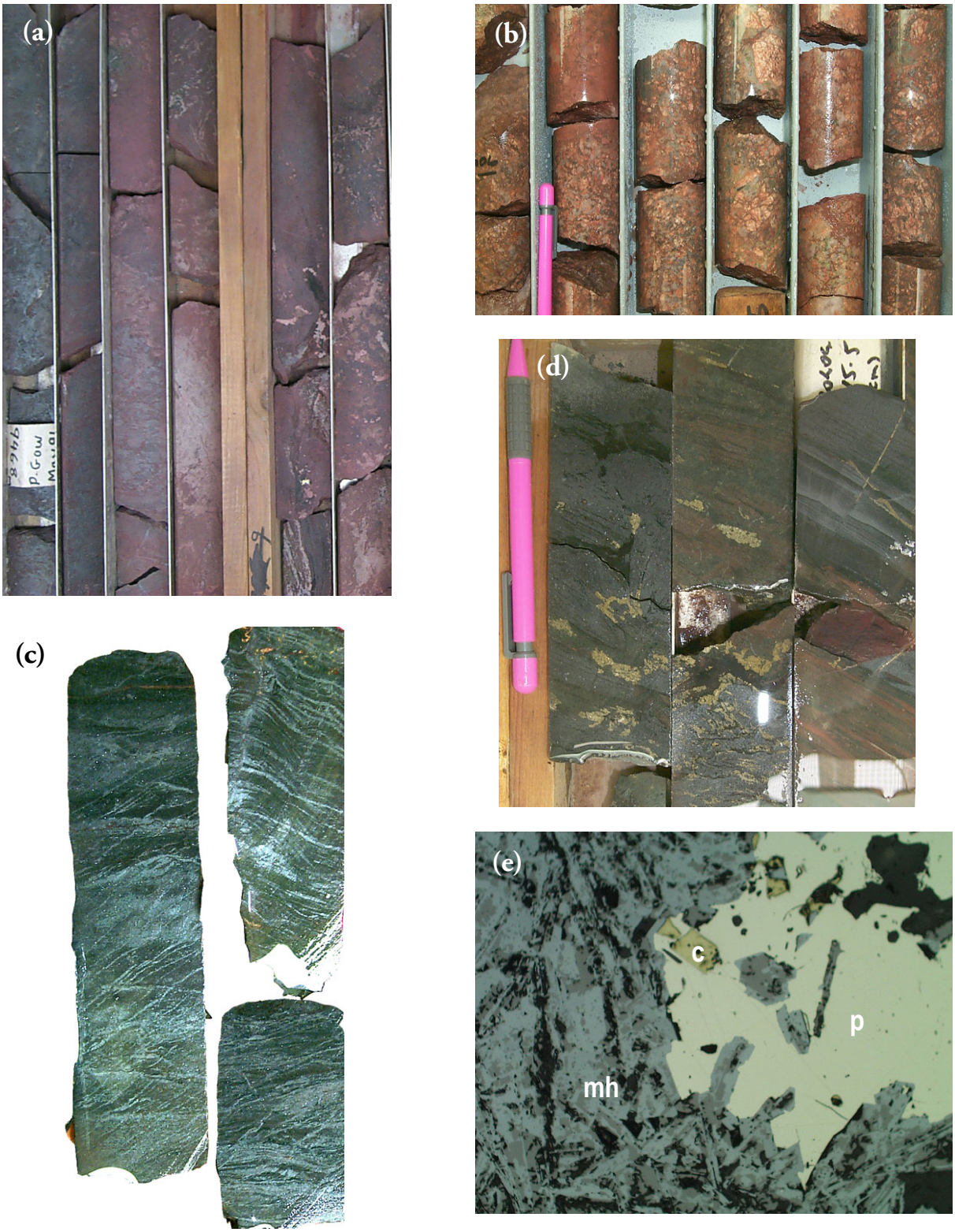

Figure 2
Photographs and photomicrographs of the Emmie Bluff ironstones and ironstone-hosted mineralisation.
(a) Copper-mineralised massive hematitic ironstones from DDH SAE 6 (about 940 m).
(b) Hematite-altered porphyritic granite from DDH SAE 6 (about 960 m).
(c) Massive hematite-magnetite rock with ? relict bedding indicating replacement of siltstones by Fe-oxides.
(d) Examples of Cu mineralized ironstones from SAE 6.
(e) Reflected light photomicrograph of 'typical' ironstone mineralisation showing bladed magnetite-hematite (mh) aggregates partly replaced by pyrite (p) containing minor chalcopyrite (c) - field of view 200 microns.

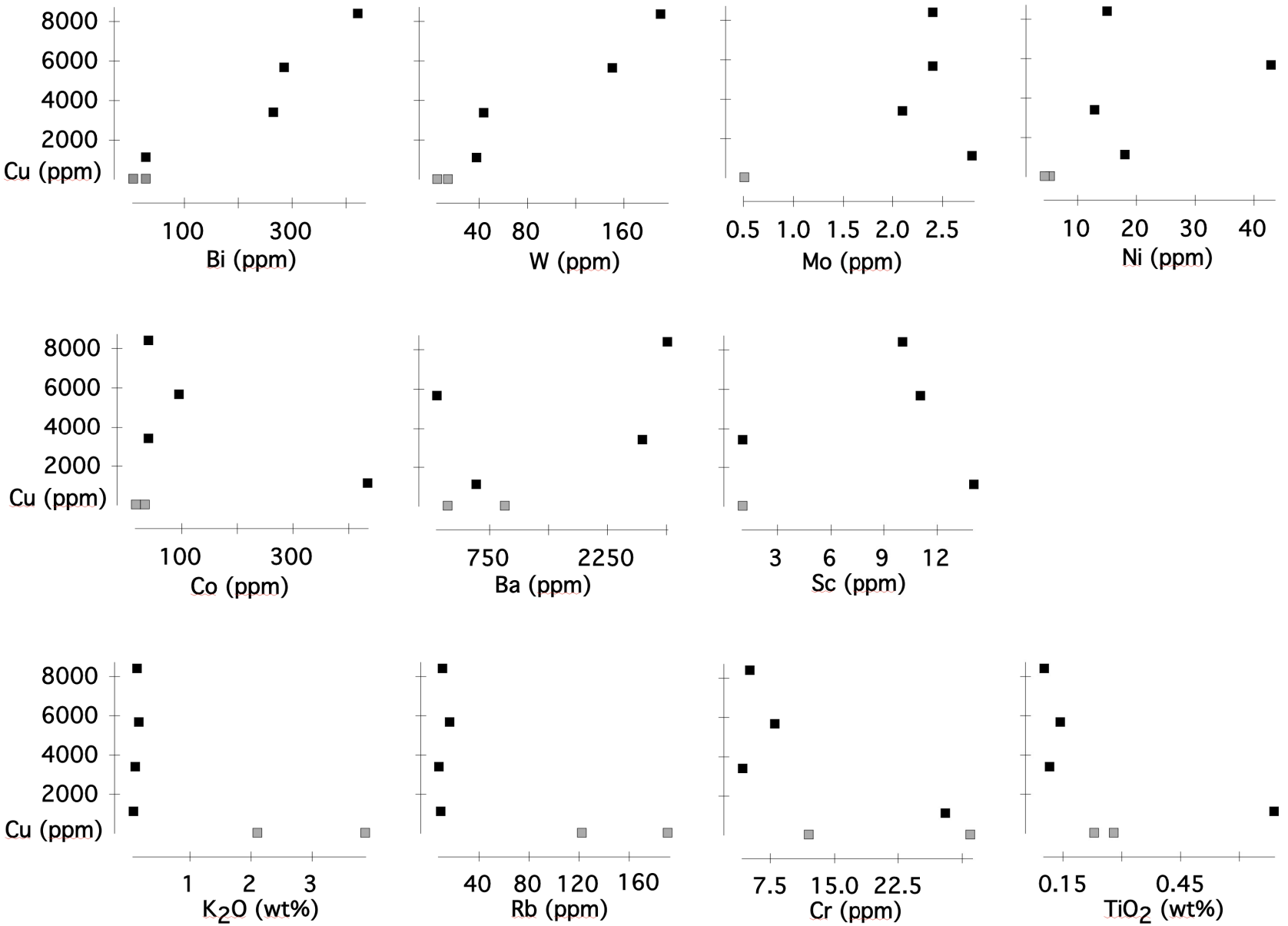

Figure 3
Cross plots for six ironstone samples from drill-hole SAE6 displaying the relationship between Cu and selected trace elements; two low-Cu (barren ironstone) samples are highlighted with grey symbol.

then cursory inspection of these plots indicate that the Cu-rich samples have elevated levels of Bi, W, Mo, Ni, compared to the 'barren' ironstones, and may have elevated Co, Ba and Sc. Conversely, K, Rb (and arguably TiO_2 and Cr) are low in the Cu-mineralised ironstones. It should be noted that, although Mo is enriched in the mineralized samples, the absolute levels of Mo are very low.

Copper mineralisation in the cover rocks

After 1990, the main focus of MIMs activity at Emmie Bluff was the Cu mineralisation in the cover rocks. In all, this mineralisation was intersected in ten diamond drill holes at an average depth of 400 m over an area of about four square kilometers (Fig. 1).

In 1998, data from these drill holes was used by Hamish Patterson & Associates to calculate a resource of 25 mt at 1.3 wt% Cu (cited in Gunson Resources prospectus, April 2000).

Copper sulfides occur, almost exclusively, in a condensed sequence of carbonaceous, dolomitic silstones and shales. At Emmie Bluff the Tapley Hill Formation(THF) occurs in a 2 km wide, NW-SE elongate trough. Maximum thickness is about 40 m (Fig. 4). MIM drilling to the NE and SW, and 1998 drilling to the SE by Stuart Metals (MGD1) reveals that the THF to be absent. Both the THF, and the Cu mineralisation are open to the NW (Fig. 4).

The THF rests disconformably on coarse clastics of the Mesoproterozoic Pandurra Formation (Fig. 4). This unit comprises up to a thousand metres of arenaceous red bed sediments mostly deposited in a fluviatile environment (Cowley, 1993). The upper surface of the Pandurra Formation has been affected by deep weathering processes, and at Emmie Bluff the basal THF includes material re-worked from the regolith formed on and from the Pandurra Formation.

At Emmie Bluff the THF is overlain conformably by reddened clastics including very coarse, poorly sorted sands, grits and conglomerates (Fig. 5) similar in appearance to the underlying Pandurra Formation. These have been correlated with the Whyalla Sandstone member of the Umberatana Group. Elsewhere on the Stuart Shelf the Whyalla Sandstone is a coarse, well sorted bi-modal sandstone that may have an aeolian origin (Preiss, 1993; Williams, 1998).

No attempt has been made here to document a detailed spatial paragenesis for the THF-hosted mineralisation. However, many of the textures described by (Knutson et al., 1983; Lambert et al., 1984) for Cu in the THF at Mount Gunson and Myall Creek, respectively, were recognised in the Emmie Bluff samples. Iron and Cu sulfides (pyrite, marcasite, chalcopyrite, bornite and chalcocite) occur as thin bedding parallel bands and seams, and fine disseminations in laminated and non-laminated siltstones. Coarse chalcopyrite occurs as clots and rimming grains in coarse (often intraclastic) beds,

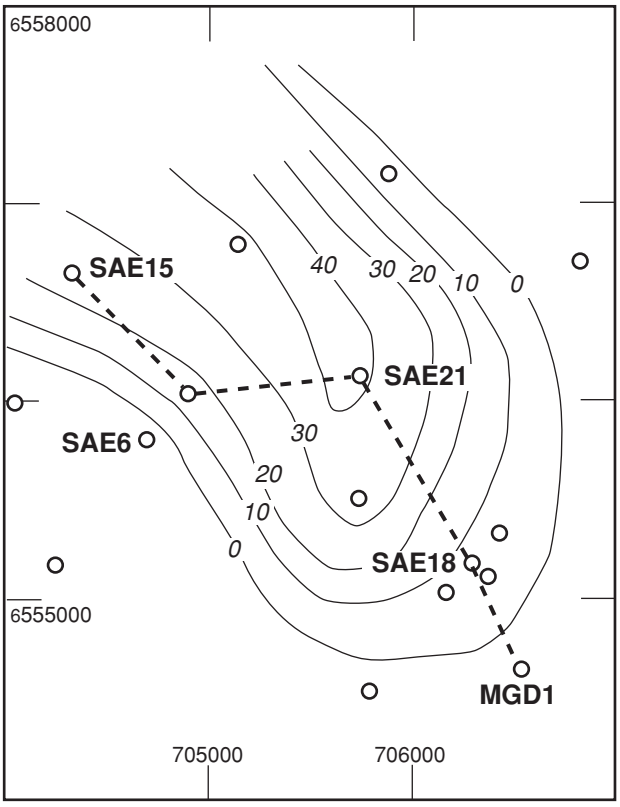

Figure 4
Plan map of the Emmie Bluff area showing drill hole collar locations and thickness contours for the Tapley Hill Formation.

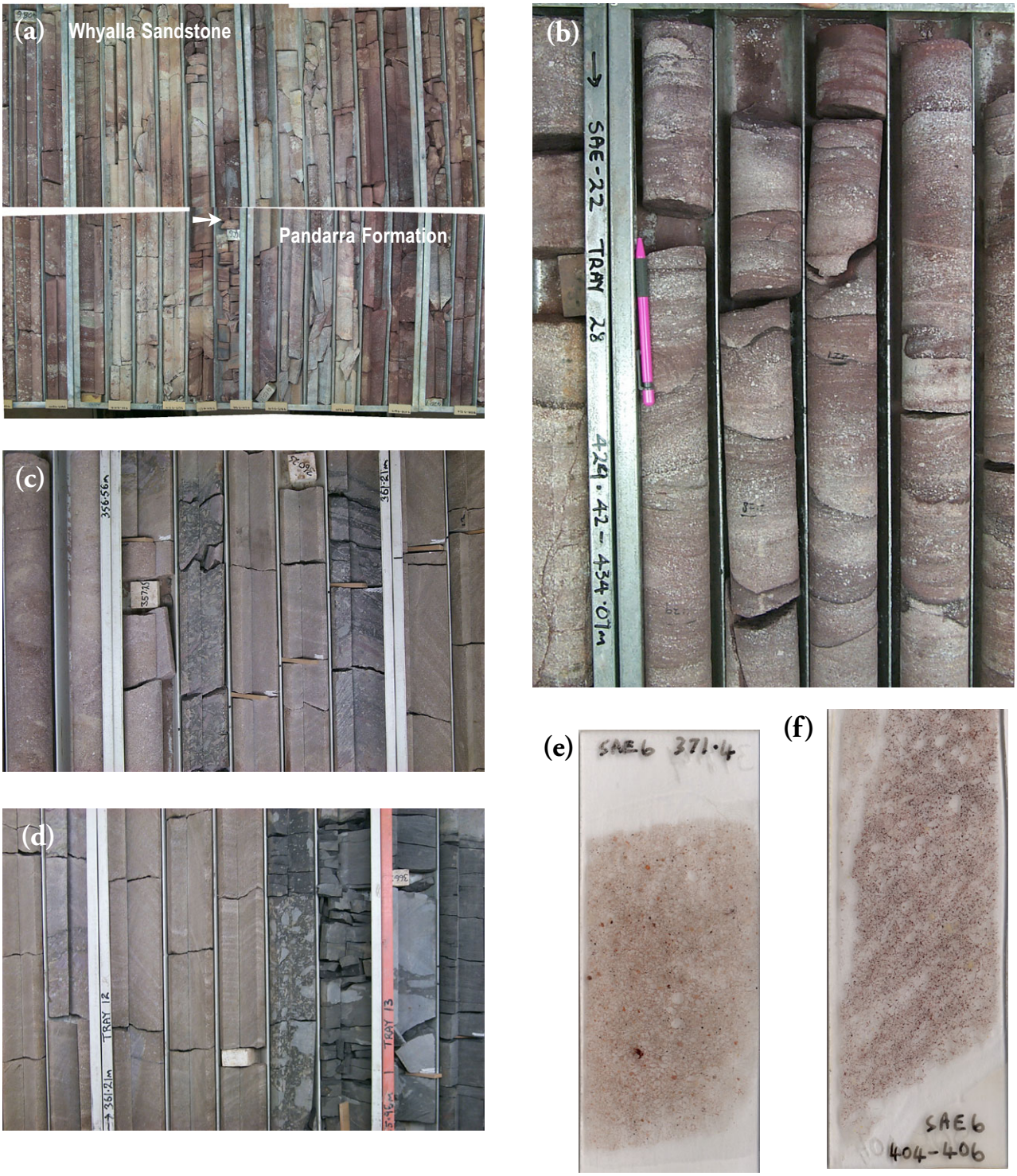

Figure 5
Photographs and photomicrographs of the Pandurra Formation and Whyalla Sandstone.
(a) Core from DDH MGD1 showing the contact between the underlying Pandurra Formation and the Whyalla Sandstone (indicated by arrow at 414.6 m); n.b. intense reddening of the Pandurra Formation at several levels (all core in this figure is HQ core, approximately 45 mm in diameter).
(b) Drill core of Pandurra Formation from DDH SAE 21 showing ferruginous mottles and liesegang bands.
(c) Drill core of Whyalla Sandstone from SAE 15; n.b. coarse beds of (?lag) material derived from underlying Tapley Hill Formation.
(d) Drill core of weakly Cu-mineralised Whyalla Sandstone from SAE 15 close to the contact with the THF.
(e) Scan of a thin section of coarse sandstone from the Whyalla Sandstone in DDH SAE 6.
(f) Scan of a thin section of coarse sandstone from the Pandurra Formation in DDH SAE 6.

and in minor veins (Fig. 6). Visible Cu sulfides are more obvious near top and bottom contacts of the THF with the bounding coarse clastic rocks, and in more permeable-looking lithologies.

Microscopically Cu sulfides replace and/or overgrow framboidal pyrite and marcasite (Fig. 6) and occur associated with euhedral quartz in patchy bedding parallel veinlets (Fig. 6). Occasional grains of clear sphalerite, galena and tetrahedrite were also recognised associated with the Cu sulfide minerals.

Discussion: These textures indicate that Cu introduction into the cover sequence post-dates early diagenesis (timing of Fe sulfide framboid formation), a conclusion reached for the other Stuart Shelf THF-hosted deposits by Knutson et al., (1983) and Lambert et al. (1984). How much later cannot be resolved using textural arguments, but the observed concentration of Cu sulfides near the top and bottom of thicker THF intersections, and the occurrence of Cu sulfides in overlying and underlying clastic rocks can be explained if Cu fluids were introduced into the sequence after substantial burial. Further discussion of the timing of fluid flow is presented below.

A total of 119 samples from a fence of five drill-holes (Fig. 4) were analysed for this study. Four of the drill holes intersected THF with visible Cu mineralisation. In the fifth hole (drilled by Stuart Metals in 1998 just SE of the MIM drill-holes), Tapley Hill Formation is absent and Whyalla Sandstone rest directly on highly ferruginous Pandurra Formation. Figure 7 shows sedimentary graphic logs bracketing the sampled intervals in each of these holes.

All analytical data are presented as a series of Excel worksheets in the Appendix CD to this report, and statistical data for each of the Pandurra Formation, THF and Whyalla Formation samples sets are summarised as boxplots on Figure 8. Selected elements and element ratios are displayed as a series of downhole plots on Figure 9.

Major Elements: From Figure 8 it can be seen that the Pandurra Formation is more Fe-, alumina- and K-rich, and Ca- and Mg-poor than the Whyalla Sandstone. The THF samples contain more alumina, Ca, Mg, and S and have higher ignition losses, than either the Pandurra Formation or the Whyalla Sandstone samples. There is a strong correlation between Ca and Mg in the THF and Whyalla Sandstone samples (Fig. 10), and a strong correlation between K and Al in all samples (Fig. 11). Sodium and Al are less well correlated, except in the Pandurra Formation samples.

Discussion: The major element composition of the Pandurra Formation is consistent with the mature, leached and ferruginous appearence of this unit, and the proximity of the samples collected for this study to the palaeoregolith developed on the top of the PF. The K/Al ratio is consistent with illite or muscovite being the only K-phase in these samples (i.e., no K-feldspar). The low Ca, Mg and relatively low ignition loss indicates that there is little or no carbonate in these samples.

By contrast, elevated Ca, Mg and ignition loss indicates that both the THF and the Whyalla Formation contain significant carbonate, and this carbonate is dolomite (or ferroan dolomite) rather than calcite. Re-calculating whole rock Mn to "MnO_d" (Mn in 100% dolomite — see Large and McGoldrick (1998) for details) produces values of MnO_d between four and six weight percent for the THF samples, and in the thicker sections MnO_d values decrease up section. This result is consistent with dolomite being the major host for Mn in the THF samples. In contrast, although the Whyalla Sandstone samples contain some dolomite, their MnO_d values are highly variable, suggesting that dolomite is not the only Mn host in these samples.

Iron in 100% dolomite (FeO_d) can also be calculated using the MnO_d formula, but substituting FeO_{carb} (Large and McGoldrick, 1998) for MnO. For the thicker THF intersections high FeO_d values broadly correspond to high Zn **and** high Cu, resulting in a 'triple spike' pattern in SAE15 (Fig. 12).

Another way of assessing Fe and Mn enrichment in Proterozoic shales and siltstones is to use the 'Sedex AI' and 'AI3' indices (Large and McGoldrick, 1998; Large et al., 2000). These have been calculated for the THF data and are presented on prospectivity cross-plots developed in a previous AMIRA project (P384A) for northern Australian Palaeoproterozoic sediment-hosted Zn-Pb-Ag deposits (Fig. 13). In isolation, this depiction would suggest that the THF at Emmie Bluff may be quite prospective for stratiform Zn-Pb mineralisation. In particular the MnO_d values are certainly elevated compared to many northern Australian sequences. However, the high MnO_d values may be an artefact of the condensed nature of the THF on the Stuart Shelf, and more 'normal' MnO_d levels may occur elsewhere in the THF. Further work is needed to assess the significance of the elevated Mn in the THF at Emmie Bluff.

The K/Al ratios for the THF and Whyalla Sandstone show more scatter than the Pandurra Formation samples (Fig. 10), but still indicate that illite or muscovite is the dominant K-phase. Some of the scatter to higher K/Al ratios and somewhat higher Na levels may indicate the presence of feldspar in some samples.

Trace Elements

Selected chalcophile trace element data for the THF and Whyalla Sandstone sample sets are presented as a series of box-plots on Figure 14. These data display elevated Cu, Co, Zn and Pb (and probably Ag) in the mineralised samples compared to 'typical' black shales (Vine and Tourtelot, 1970; Wedepohl, 1969, 1970, 1972), but other elements (Ni, As, Bi, Mo, Tl) are not enriched. Furthermore, Cu, and to a lesser extent Co, are 'decoupled' from Zn and Pb (Fig. 9). In the two thickest THF intervals (in SAE15 and SAE21) highest Zn and Pb occurs near the middle of the sampled interval, whereas Cu and Co are highest near the contact of THF with underlying and overlying units. In absolute terms Cu dominates over Zn in the two thinner THF intersection (SAE6 and SAE18 have 9.5 and 6.3 metre weight percent Cu and 4.0 and 1.3 metre weight percent Zn, respectively, compared to 2.2 and 5.7 metre weight percent Cu and 5.5 and 6.7 metre weight percent Zn in SAE15 and SAE21).

In comparison to the ironstone-hosted Cu mineralisation, the mineralised cover sequence rocks contain more Zn, Pb, and Ag, and possibly more Ni and V. Levels of As, Tl and Mo are quite similar in both styles of mineralisation and the ironstone-hosted Cu samples are enriched in Bi and W, and possibly U. Barium in the ironstones and the THF varies over nearly two orders of magnitude, and is independent of Cu in these samples.

Discussion: Although each of the types of Cu mineralisation discussed here have their own characteristic trace element association, this does not preclude a common mineralising fluid. The differences in metal tenor may simply reflect temperature differences and different sulfide precipitation processes for each (a 'single-fluid' model for Emmie Bluff is discussed more fully below).

Formation of the Emmie Bluff copper deposits

The data discussed here do not uniquely constrain the origin of the Cu mineralisation at Emmie Bluff and several alternative scenarios can be considered:

(i) the ironstone Cu and the cover sequences Cu are unrelated and the spatial association is co-incidental
(ii) the ironstone Cu formed earlier than the cover sequence Cu, but was a direct source of Cu for a later fluid that formed the cover sequence mineralisation
iii) the ironstone Cu and the cover sequence Cu formed from during the same fluid flow event during the Neoproterozoic, i.e., there was no Cu in the Emmy Bluff ironstones until Late Neoproterozoic times

The regional scale features (lineaments, faults, 'upwarps', gravity anomalies, Hiltaba Suite ganites) that can be related to the distribution of Cu deposits in Stuart Shelf cover rocks (summarised in Selley, 2000) preclude a coincidental relationship between

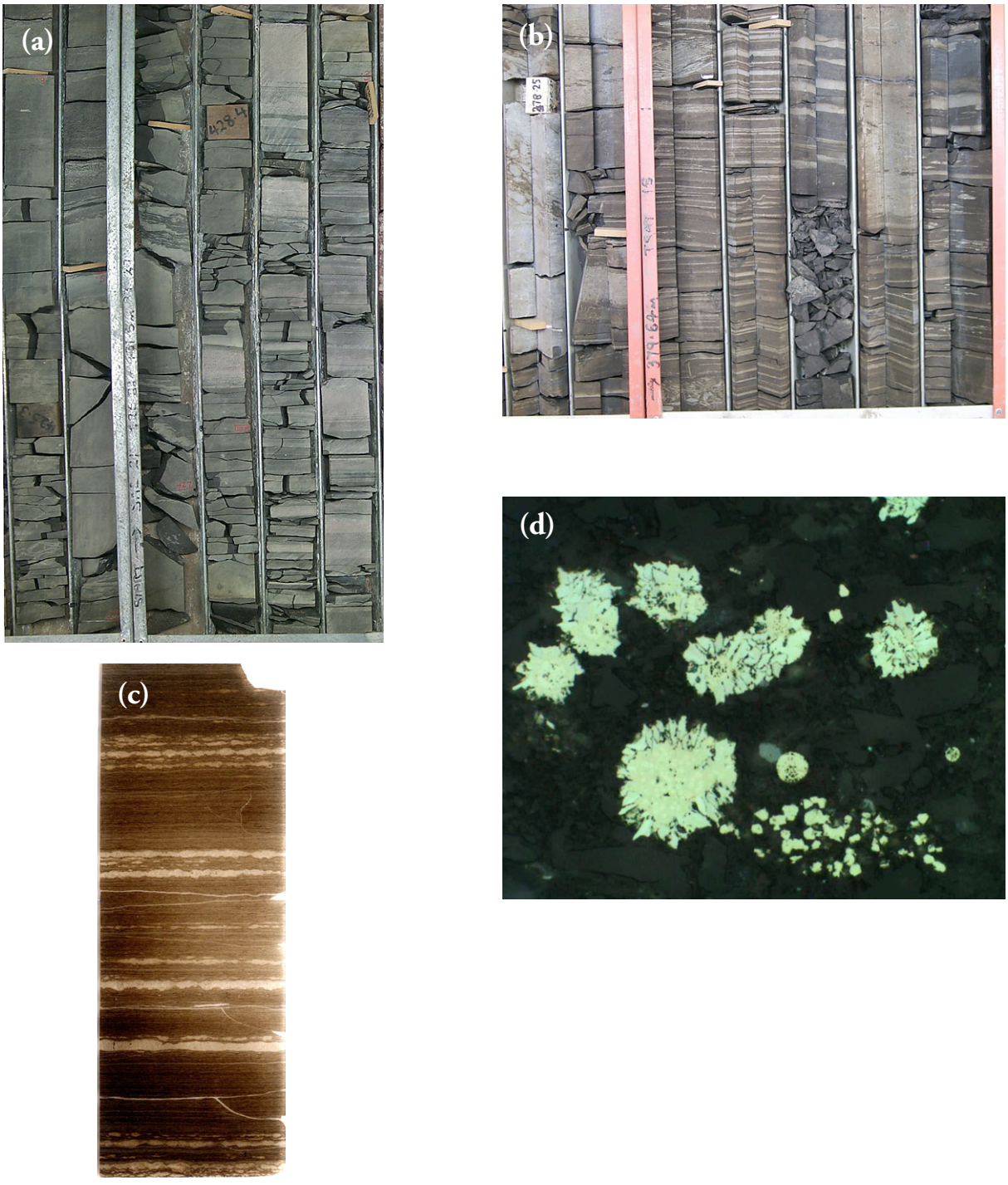

Figure 6
Photographs and photomicrographs of the Tapley Hill Formation rocks and associated mineralisation.
(a) Copper mineralized Tapley Hill Formation siltstones and shales in DDH SAE 21 (HQ core approximately 45mm diameter).
(b) Tapley Hill Formation siltstones, shales , paler dolomitic units, and minor intraclast breccias in DDH SAE 17; this interval is from the middle of the Tapley Hill Formation in this hole, and is low in Cu, but has elevated Zn and Pb.
(c) Scan of a thin section of THF shale/siltstone from SAE 15 (386.6m); paler bands are more carbonate-rich than darker, organic matter-rich silt bands.
(d) Detail from c (reflected light photomicrograph, field of view 200 microns); iron sulfides in silt band – bladed marcasite overgrowths on framboidal pyrite grains.

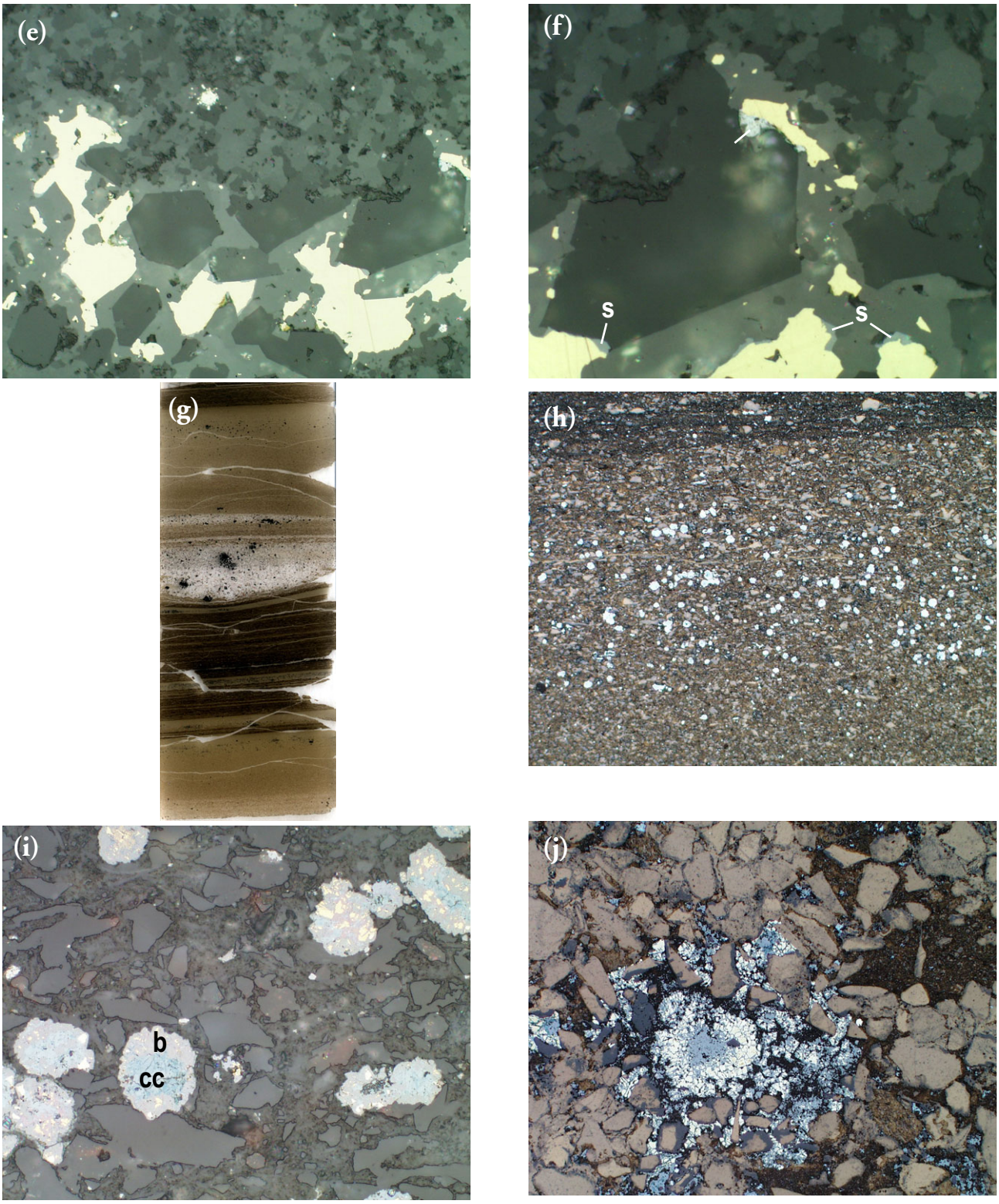

Figure 6 cont.
(e) Detail from (c) (reflected light photomicrograph, field of view 500 microns); chalcopyrite-quartz veinlet in pale silt band.
(f) Detail from (e) (reflected light photomicrograph, field of view 200 microns) revealing sphalerite (s) and galena (g) associated with the chalcopyrite.
(g) Scan of a thin section of strongly Cu-mineralised THF shale/siltsone from SAE 22 (423.6 m); nb. patches of visible Cu sulfides dusting the pale carbonate-rich silt band in the centre of the sample.
(h) Detail from (g) (reflected light photomicrograph, field of view 2mm); bright grains are Cu sulfide minerals (intergrown chalcopyrite, bornite, and chalcocite).
(i) Detail from (h) (reflected light photomicrograph, field of view 500 microns); bornite-b, chalcocite-cc.
(j) Detail from (h) (reflected light photomicrograph, field of view 200 microns); coarse chalcopyrite-bornite-chalcocite within silt/fine sand bed in centre of (g).

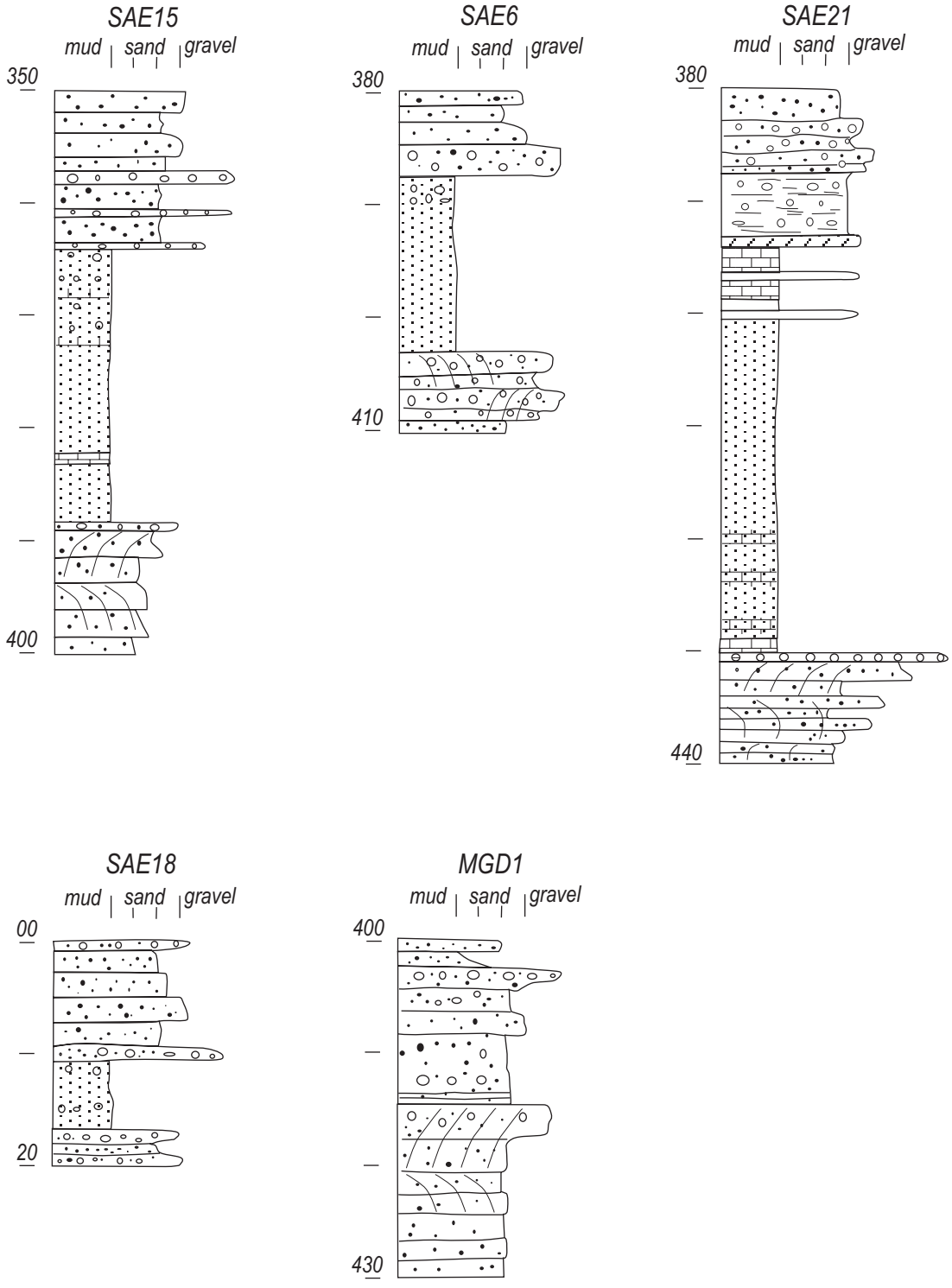

Figure 7
Graphic logs for the sampled interval from drill holes SAE6, SAE15, SAE18, SAE21 and MGD1.

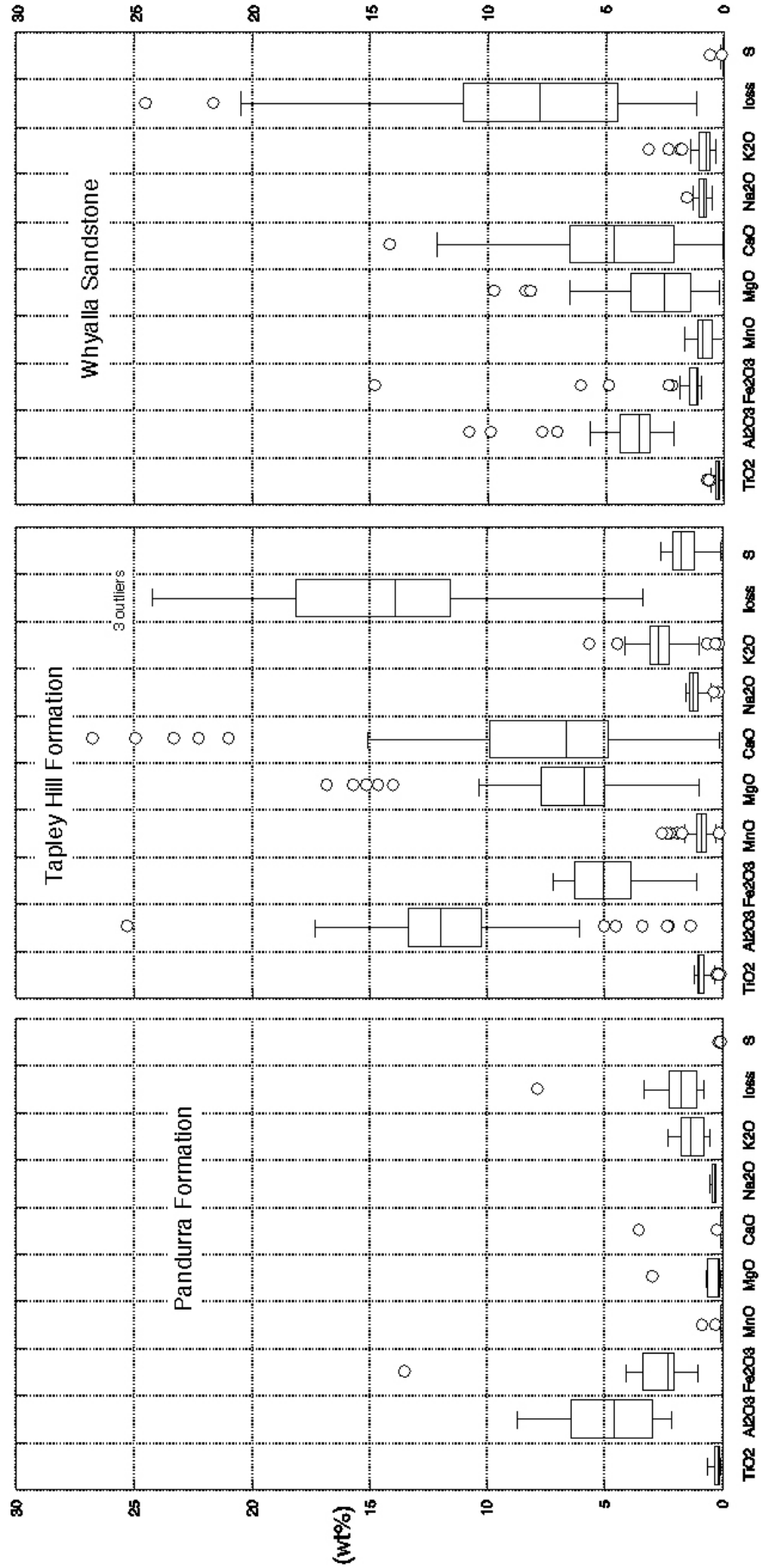

Figure 8
Statistical boxplots for major elements in samples from the Pandurra Formation, Tapley Hill Formation and Whyalla Sandstone; individual boxplots comprise a box enclosing the middle 50% of all data (this defines the interquartile range - IQD), whiskers extending to the highest and lowest data points within 1.5xIQD from the median data point (line in the box) and outliers plotted as individual points.

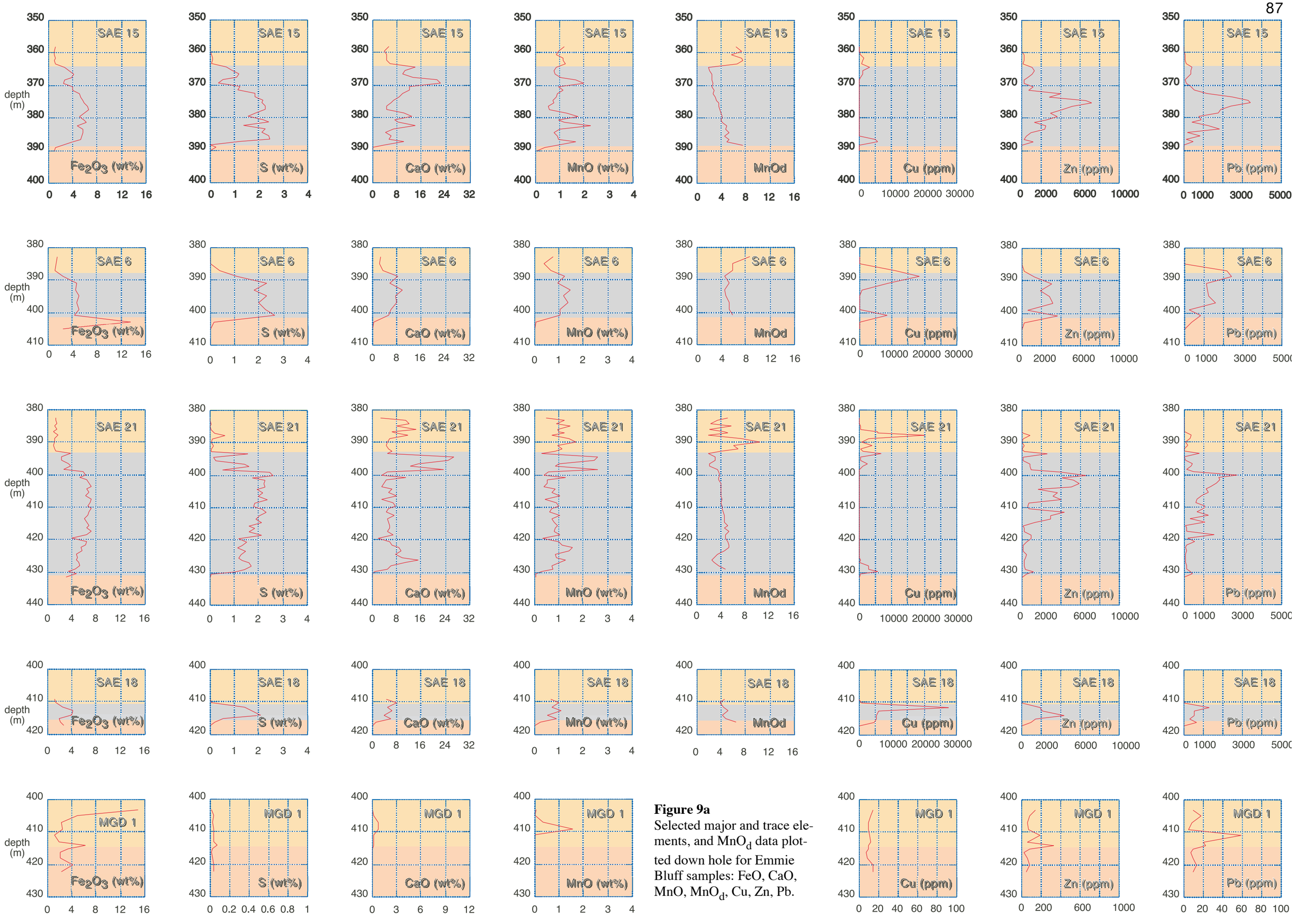

Figure 9a
Selected major and trace elements, and MnO_d data plotted down hole for Emmie Bluff samples: FeO, CaO, MnO, MnO_d, Cu, Zn, Pb.

Figure 9b
Selected major and trace elements, and MnO_d data plotted down hole for Emmie Bluff samples: Co, As, Ni, Bi, V, Tl, Ba.

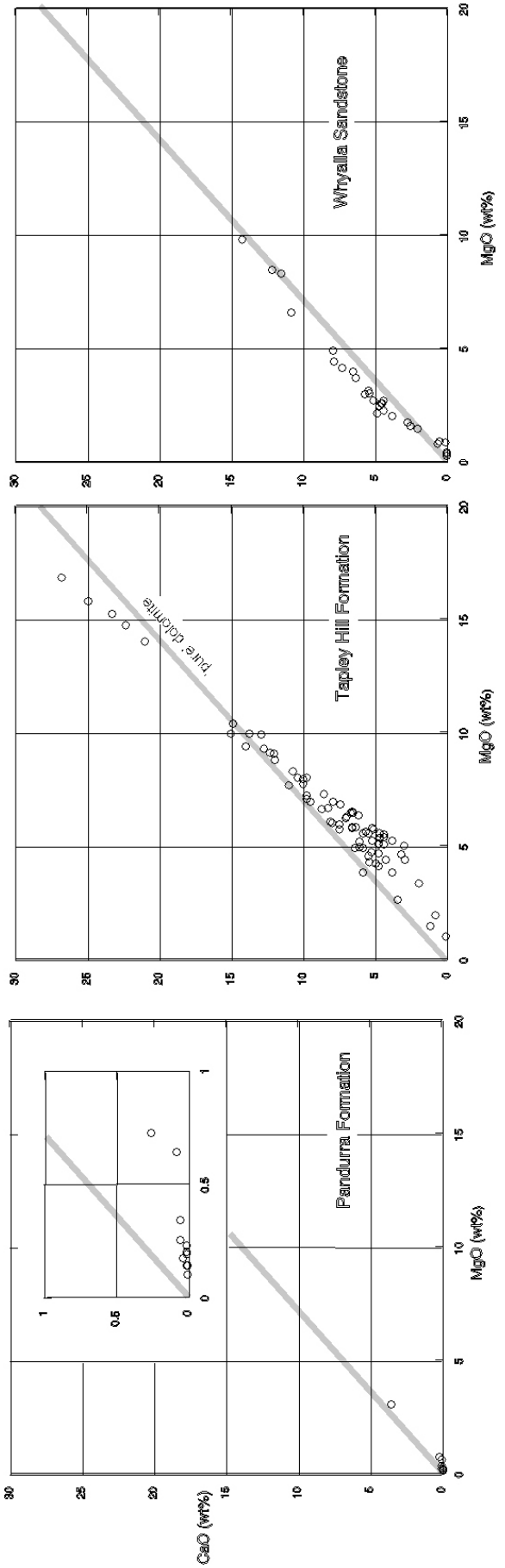

Figure 10
Cross plots of CaO versus MgO for Tapley Hill Formation and Whyalla Sandstone samples.

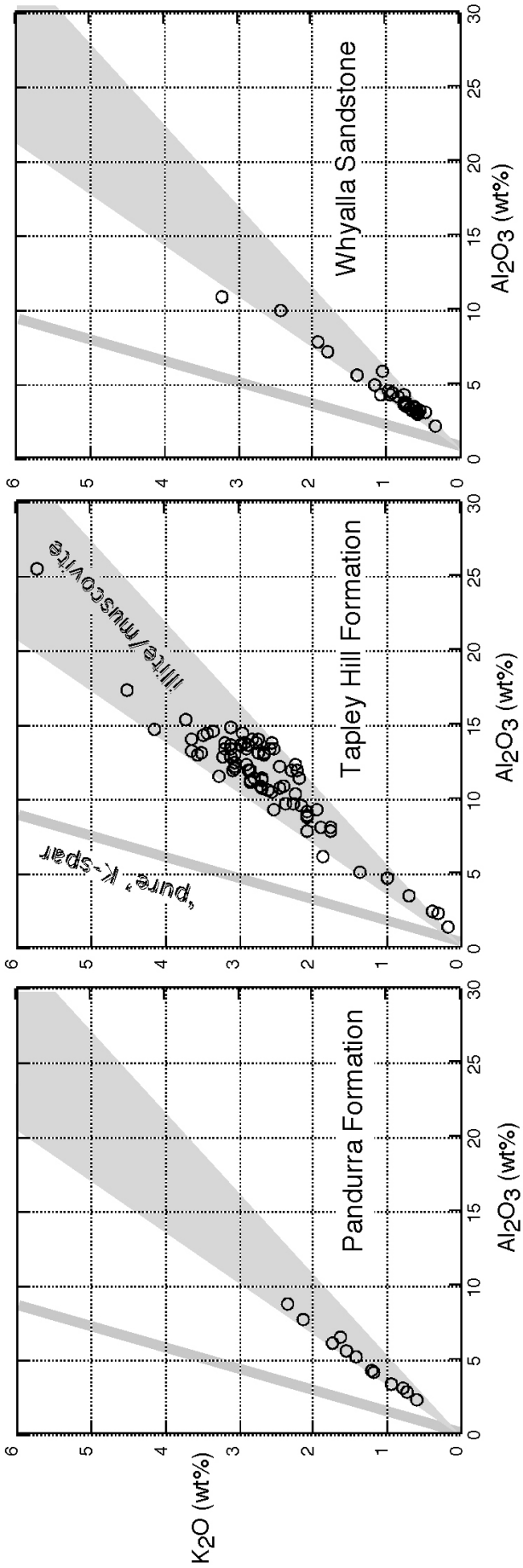

Figure 11
Cross plots of K_2O versus Al_2O_3 for Pandurra Formation, Tapley Hill Formation and Whyalla Sandstone samples.

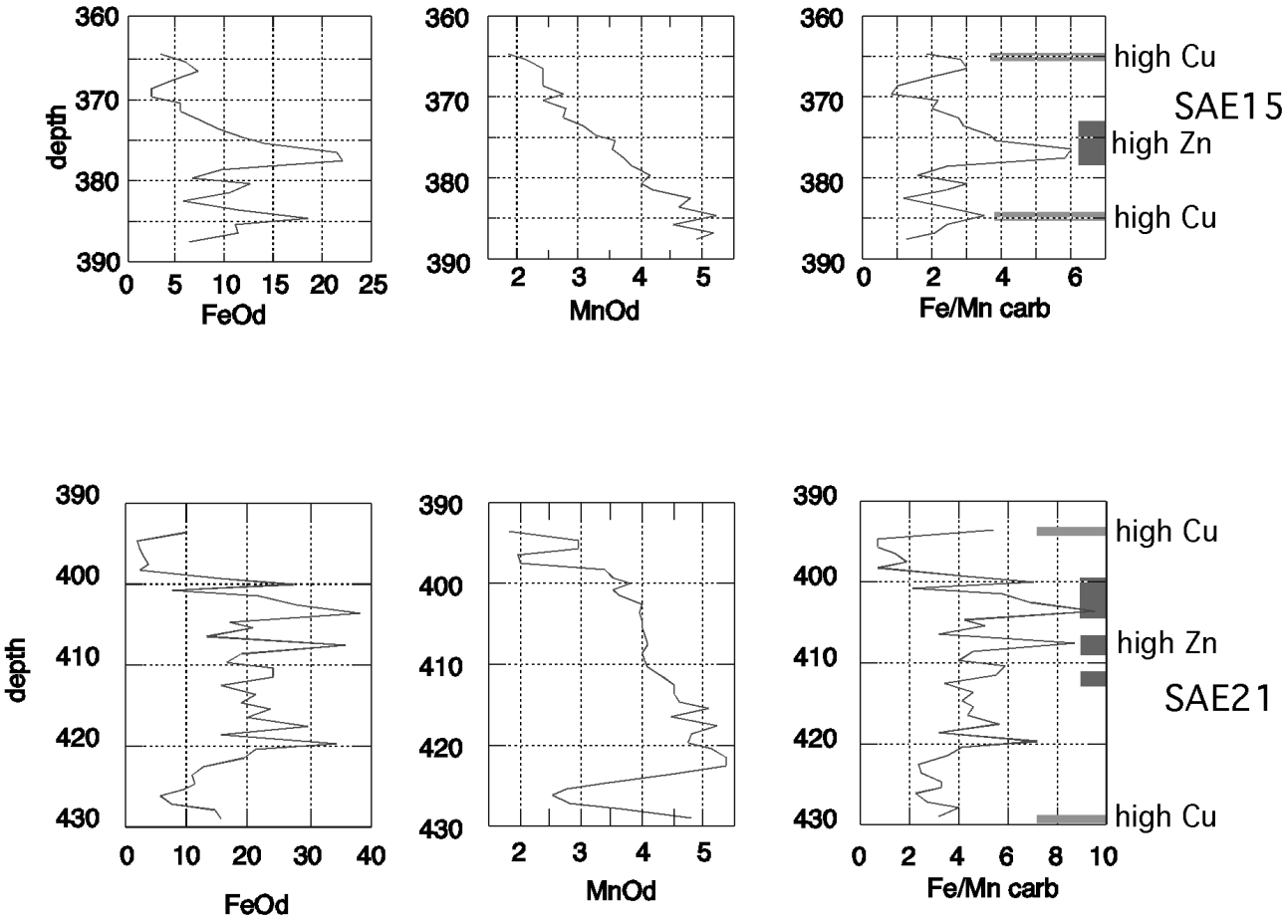

Figure 12
Down hole plots of FeOd, MnOd and Fe/Mncarb for Tapley Hill Formation samples; location of high Cu and high Zn samples is indicated by coloured bars on the Fe/Mncarb plot.

the two mineralisation styles at Emmie Bluff. Regionally, it is not possible to divorce mineralisation in the cover from features in the basement, and the same argument would apply locally at Emmie Bluff. Hence, I would argue there must be a genetic as well as spatial link between the two types of Cu mineralisation, and will now consider each of the alternatives suggested above under the headings 'remobilisation model' and 'single fluid model'.

Remobilisation model

Gow et al. (1994) argued that the ironstone Cu-mineralising fluid at Emmie Bluff was similar in character to the mineralising fluid responsible for the giant Olympic Dam deposit. While there has been no direct dating of the Emmie Bluff ironstone mineralisation, Olympic Dam is thought to have formed at about 1590 Ma (Johnson and Cross, 1995). If the Emmie Bluff ironstone Cu is also Palaeo-proterozoic in age, then this old Cu mineralisation may have contributed metals to cool, oxidized fluids circulating through the cover and basement rocks during late Neoproterozoic times. If these fluids encountered the reducing trap rocks of the THF they would precipitate Cu, Zn and Pb sulfides.

Although this model provides a plausible link between the two ore types, I would argue it has several difficulties. For instance, there is no textural or mineralogical evidence that that the Emmie Bluff ironstone mineralisation has been leached by a cool, oxidized fluid. Such a process might be expected to produce a diverse secondary Cu mineral assemblage. Furthermore, the measured Zn and Pb levels in the ironstones are quite low, and if representative of the levels in the primary ironstone Cu mineralisation, suggest a mass balance problem with obtaining Cu, Pb and Zn for the THF mineralisation from the ironstones. Finally, the remobilsation model requires the fortuitious preservation of Palaeoproterozoic sulfide-hematite-magnetite rock in a near-surface environment for nearly 1000 Ma.

Single fluid model

This model requires a suitable fluid flow regime to have existed on the Stuart Shelf sometime after deposition of the Whyalla Sandstone. Warm to hot, oxidized fluids (the second fluid of Gow et al., 1994) react with magnetite-pyrite 'skarn' rocks at depth to form the ironstone Cu mineralisation, and ascend to shallower levels, cool somewhat, and interact with carbonaceous matter, Fe sulfides and/or Fe-Ti oxides in the THF and precipitate Cu (and Zn-Pb) sulfides (a mechanism proposed for THF Cu mineralisation elsewhere on the Stuart Shelf by Knutson et al. (1983) and Lambert et al. (1984)).

This scenario is compatible with previous modeling of Cu, Zn and Pb solubility in saline, oxidized (defined as $SO_4^{2-} \rightarrow HS^- + H_2S$) fluids. Cooke et al. (2000) indicated that metal solubilites are not greatly affected by temperature changes, but redox changes will have a profound effect. Fluids responsible for the deep Cu mineralisation could cool significantly from the 200 to 400^oC temperatures suggested by Gow et al. (1994), and still transport Cu, Pb and Zn until they encountered the reducing trap of the THF sediments. The solubilities of metals such as Bi and W have not been modelled, but empirically, they probably do have a strong temperature control on their solubility, hence, they were fixed at the higher temperature end of the system.

In this model, broadly speaking, the ore fluid source will either be extrabasinal or intrabasinal, although dense basinal brines may sink and circulate (in part) through basement rocks . Extrabasinal fluids would include magmatic and metamorphic sources, but neither process was particularly active during the late Neoproterozoic development of the Adelaide Fold Belt and Stuart Shelf area. Formation waters (basinal brines) from the lower (evaporitic) parts of the thick Adelaide Fold Belt basin fill are an appealing source for large quantities of saline, oxidized brines. For fluids to circulate from the Adelaide Fold Belt through the Stuart Shelf sequences, hydraulic connectivity would be required, and circulation could not take place during times of low seastand when

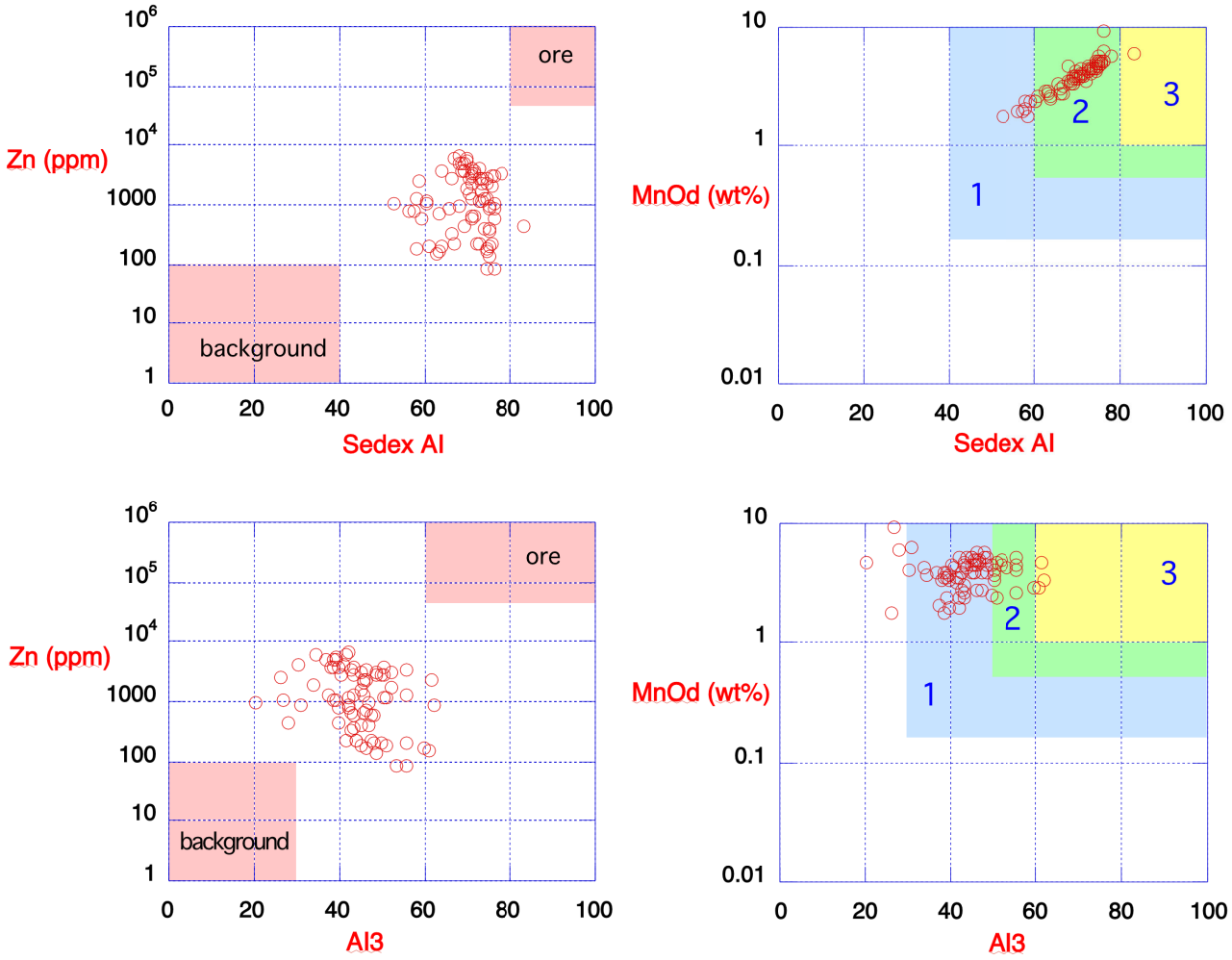

Figure 13
Cross plots of 'Sedex AI', 'AI3', Zn and MnOd for Tapley Hill Formation samples.

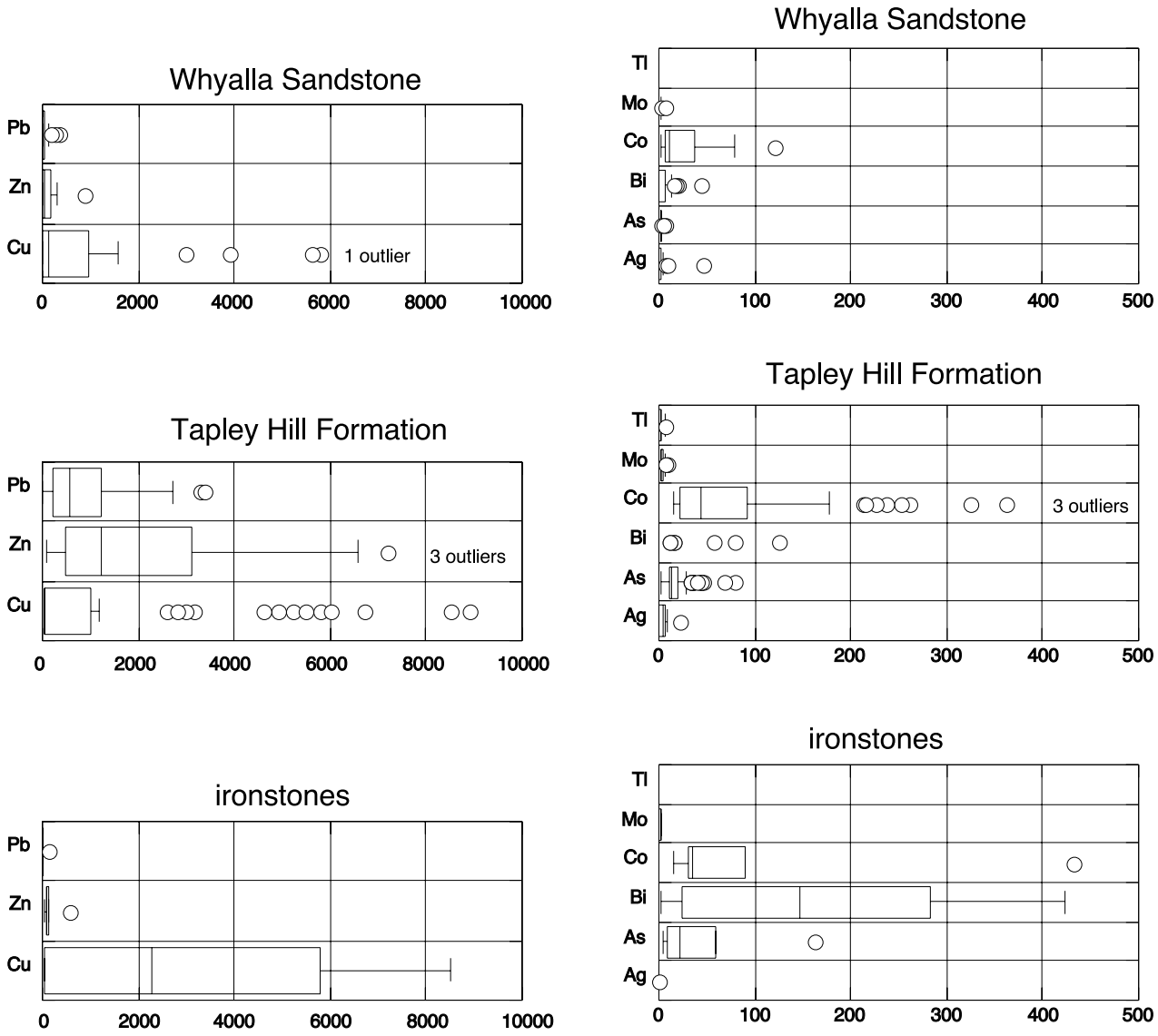

Figure 14
Statistical box plots comparing chalcophile elements from the basement ironstones, Tapley Hill Formation and Whyalla Sandstone samples.

subaerial conditions pertained on the Stuart Shelf (e.g., during Whyalla Sandstone deposition). Hence, such a scenario requires the Emmie Bluff Cu mineralisation (and other THF-hosted Cu deposits on the Stuart Shelf) to post-date the Marinoan glacial event (i.e., Brachina Formation / ABC Quartzite times, or younger – about 600Ma).

It is worth noting that recent work by Foden et al. (2001) indicates the Adelaide Fold Belt experienced a major phase of intrabasinal fluid flow at 586 ± 30 Ma. The same unusual radiogenic Sr isotope signature recognized by Foden et al. (2001) is also present in THF samples from the Stuart Shelf (Lambert et al., 1984) suggesting that these 586 Ma fluids may have circulated to west through the condensed Stuart Shelf sequences.

Concluding remarks: vectors to Cu mineralisation in the Stuart Shelf cover rocks

If the Stuart Shelf Cu deposits were formed during a major fluid flow out of the thick Adelaide Fold Belt sequences at about 600 Ma, then the character and structural grain of the basement rocks to the Stuart Shelf would have exerted a major control on fluid movement through the relatively thin cover sequences. This type of hydrologic control would readily explain empirical association of Cu with major structures recognised in the sub-surface of the Stuart Shelf.

Furthermore, the chemical / alteration effects of this fluid flow are likely to be cryptic and pervasive. Lithogeochemical vectoring at an individual deposit scale may be extremely difficult. Individual deposits are not 'point sources' dispersing ore elements into there immediate vicinity, but rather, they are local redox traps for pervasive, transient 'ore fluids'.

Further work

Several lines of investigation will be followed to complete the work at Emmie Bluff:

- Geochemical data will be obtained from THF samples from elsewhere on the Stuart Shelf, and from the thicker sequences in the Adelaide Fold Belt. This work will focus in particular on Fe, Mn, Zn and Pb (the most promising small-scale vector elements at Emmie Bluff), and on Cu mineralisation at Boorloo Mine (eastern Willouran Ranges).
- In order to complete the characterisation of both types of Cu mineralisation at Emmie Bluff selected samples will be analysed for Au, organic C and rare earth elements.
- Monazite and (possibly) xenotime dating of Emmie Bluff samples will be attempted in the hope of determining direct ages for fluid movements in the cover rocks.
- Fluid flow modeling will be used to assess the viability of large-scale lateral fluid migration from the Adelaide Fold Belt to the Stuart Shelf, and to determine the extent of fluid interaction with the basement rocks.

Acknowledgements

Geological discussions with Stuart Bull and David Selley helped collect my thoughts, but I must take responsibility for the more outrageous flights of fancy presented here. Silver plate service from Brian Logan and staff at the PIRSA core repository is gratefully acknowledged. Dodge and Big Darren dutifully crushed and milled the samples. Katie McGoldrick and Phil Robinson produced 130 excellent quality XRF analyses. June Pongratz turned some of my scribblings into usable diagrams. Gunson Resources are thanked for permission to view and sample MGD1.

References

Cooke, D. R., S. W. Bull, R.R. Large and P.J. McGoldrick (2000). The importance of oxidised brines for the formation of Australian Proterozoic stratiform sediment-hosted Pb-Zn (Sedex) deposits. Economic Geology 95: 1-17.

Cowley, W. M. (1993). Pandurra Formation. in The geology of South Australia, Vol. 1, The Precambrian. J. F. Drexel, W. V. Preiss and A. J. Parker, South Australia department of Mines and Energy: 139-142.

Foden, J., K. Barovich, M. Jane and G. O'Halloran (2001). Sr-isotope evidence for Late Neoproterozoic rifting in the Adelaide Geosyncline at 586 Ma: implications for a Cu ore forming fluid. Precambrian Research 106: 291-308.

Gow, P. A., V. J. Wall, N.H.S. Oliver and R .K. Valenta (1994). Proterozoic iron oxide (Cu-U-Au-REE) deposits: Further evidence of hydrothermal origins. Geology 22: 633-636.

Haynes, D. W., K. C. Cross, R.T. Bills and M.H. Reed (1995). Olympic Dam ore genesis - a fluid-mixing model. Economic Geology & the Bulletin of the Society of Economic Geologists 90: 281-307.

Knutson, J., T. H. Donnelly and D.G. Tonkin (1983). Geochemical constraints on the genesis of copper mineralization in the Mount Gunson area, South Australia. Economic Geology 78: 250-274.

Lambert, I. B., J. Knutson, T. H. Donnelly, H. Etminan and M. Mason (1984). Genesis of copper mineralisation, Myall Creek prospect, South Australia. Mineralium Deposits 19: 266-273.

Large, R. R., S. W. Bull and P.J. McGoldrick (2000). Lithogeochemical halos and geochemical vectors to stratiform sediment hosted Zn-Pb-Ag deposits Part 2. HYC deposit, McArthur River, Northern Territory. Journal of Geochemical Exploration 68: 105-126.

Large, R. R. and P. J. McGoldrick (1998). Lithogeochemical halos and geochemical vectors to stratiform sediment-hosted Zn-Pb-Ag deposits. Part 1: Lady Loretta deposit, Queensland. Journal of Geochemical Exploration 63: 37-56.

Preiss, W. V. (1993). Neoproterozoic. in The geology of South Australia, Vol. 1, The Precambrian. J. F. Drexel, W. V. Preiss and A. J. Parker, South Australia department of Mines and Energy: 171-203.

Selley, David (2000) Geological framework and copper mineralisation in South Australia. AMIRA / ARC Project P544 December 2000 report 42pp.

Vine, J. D. and E. B. Tourtelot (1970). Geochemistry of black shale deposits - a summary report. Economic Geology 65: 253-272.

Wedepohl, K. H., Ed. (1969, 1970, 1972). Handbook of Geochemistry, Springer-Verlag.

Williams, G. E. (1998). Late Neoproterozoic periglacial aeolian sand sheet, Stuart Shelf, South Australia.Australian Journal of Earth Science 45: 733-741.

Stratigraphy and basin geometry at the Chibuluma West copper–cobalt deposit, Zambia

David Selley & Stuart Bull
Centre for Ore Deposit Research, University of Tasmania

Summary

At Chibuluma West, southern margin of the Chambishi "basin", a condensed Lower Roan package was deposited within a series of WNW-trending, asymmetric depocentres. Basin growth was controlled by an array of NNE-dipping growth faults, with probable listric geometry, and a subordinate NNW-trending transfer zone. Tilt-block rotation resulted in uplift of basement-cored blocks, which continued to amplify during sedimentation. Emergence of the transfer zone late during deposition of the Lower Roan, resulted in reworking of basal strata into restricted depocentres and lapping of Upper Roan units directly onto basement. Basin inversion caused further amplification of basement-cored blocks and emplacement within the Lower Roan stratigraphy along mylonitic footwall cut-out thrusts. Roan sub-basins were tightened into WNW-trending synclines, separated by basement inliers.

Introduction and rationale

Chibuluma West is a small, but anomalously high grade sandstone-hosted deposit situated on the southern limb of the Nkana Syncline (Fig. 1). At this position, basal Roan clastic sequences thin progressively onto elevated granitic basement at the southern margin of the Chambishi "basin". The "Ore Shale" facies is absent and host strata have been historically considered to represent an equivalent of the footwall to the Nkana system.

The deposit was selected for focussed research for several reasons:

- The relatively small size of the system allows for a rapid and comprehensive analysis of a number of elements critical to understanding Copperbelt mineralisation: ie. basin analysis, sulfide mineral paragenesis and zonation, style and significance of alteration phases and the effects of basin inversion of sulfide distribution.

- Basement topography and associated thickness variation within the Lower Roan package is pronounced and well documented by Copperbelt geologists. This provides an excellent opportunity to study basin architecture at the time of deposition of the host sequence.

- Initial review of the deposit during the field trip in June this year indicated that structures which bound basement highs were oblique to folds generated as a result of regional shortening. It was envisaged that this relationship would aid discrimination between structural geometry generated during basin growth and basin inversion (a considerably more difficult task within deposits such as Nkana where high strains have blurred these events).

- Cu and Co sulfides show distinct vertical and lateral zonation. Furthermore, there is a direct spatial association of Cu-grade with basement "highs".

- Sulfides are anomalously coarse-grained, allowing examination of mineral paragenesis and distribution directly from drill core.

This report deals specifically with the study of basin geometry as deciphered from thickness and facies variation within the Lower Roan package. An accompanying report presents preliminary results from a mineral paragenesis and sulfur isotope study of the western limit of the ore body (Selley & Cooke, this volume).

Method

Data included in this study were sourced mainly from historical surface and underground drill logs, and cross sections throughout the deposit. We supplemented this dataset with detailed logs of eight surface holes from a section at the western edge of the deposit (390 section) as it appeared to show significant lateral thickness and local facies variation associated with a number of basement "highs". Additional underground mapping was undertaken on the 620 m level, between 367 and 262 sections.

Historical sections were reinterpreted on the basis of our relogging and underground mapping. Plans were produced at 200, 400 and 600 metre levels along with an isopach map of the Lower Roan (see Figs 6–9). Five sections, selected at regular intervals along the strike of the deposit, were restored to the level of basal Upper Roan sedimentation, with the aim of revealing basin architecture at the onset of growth (see Figs 10, 11). Further work is still required to analyse and include structural data recorded from surface drill core and incorporate into level plans and sections.

Stratigraphy

The "mine stratigraphy", based loosely on that of the Nkana system, is largely accepted for the purposes of this report. Basement is represented by quartz-plagioclase-biotite granite (strong saussuritization of feldspar). In terms of the granite's composition, it appears relatively homogenous, however the level of strain varies considerably from undeformed to intensely foliated, with local development of mylonitic quartz-sericite-biotite schist. High strain domains are partitioned within the margins of basement "highs".

The Lower Roan sequence has a maximum thickness of ~200 m and is dominated by coarse to medium grained siliciclastic rocks. From base to top, it comprises a *basal boulder bed* (of variable thickness and extent), overlain successively by *footwall quartzite*, *orebody quartzite*, *hangingwall quartzite* and *hangingwall sandstone*. We were unable to recognise significant facies variation across the upper and lower contacts of the *orebody quartzite* and thus we consider these boundaries to be defined largely by ore-grade. The base of the Upper Roan is defined by the transition to predominantly fine-grained mixed siliciclastic and carbonate-bearing lithotypes. The basal contact of this package is ubiquitously strained, with brecciation or semi-ductile shear fabrics developed at low angle to primary layering.

A conspicuous facies variant occurs locally at the Lower Roan-Upper Roan transition. It involves a highly altered breccia unit, restricted to the western limit of the deposit (although historical logs indicate an undefined breccia at this level at the eastern end of the deposit), and comprises well-rounded to sub-angular clasts set within a relatively fine-grained matrix. Clast types are difficult to establish due to the level of alteration, but appear to have an intrabasinal source (no obvious granite clasts). The origin of the breccia is not clear. It displays textural and compositional similarities to the ?tectonic breccia unit defined by Dave Broughton's work on the Upper Roan-Mwashia contact, however we favour a sedimentary origin on the bases of its restricted distribution but stratabound geometry, well-rounded habit of many of the clasts and its textural contrast to other structures of unequivocal tectonic origin.

Lower Roan Lithotypes

Basal Boulder Bed

A conspicuous breccia unit of probable debris flow origin lies directly on the basement contact in a large number of holes (Figs 2a, 10). Where present in the holes logged from the 390 section, thickness ranges from 1–4 m. We are uncertain as to the maximum thickness attained in other parts of the deposit,

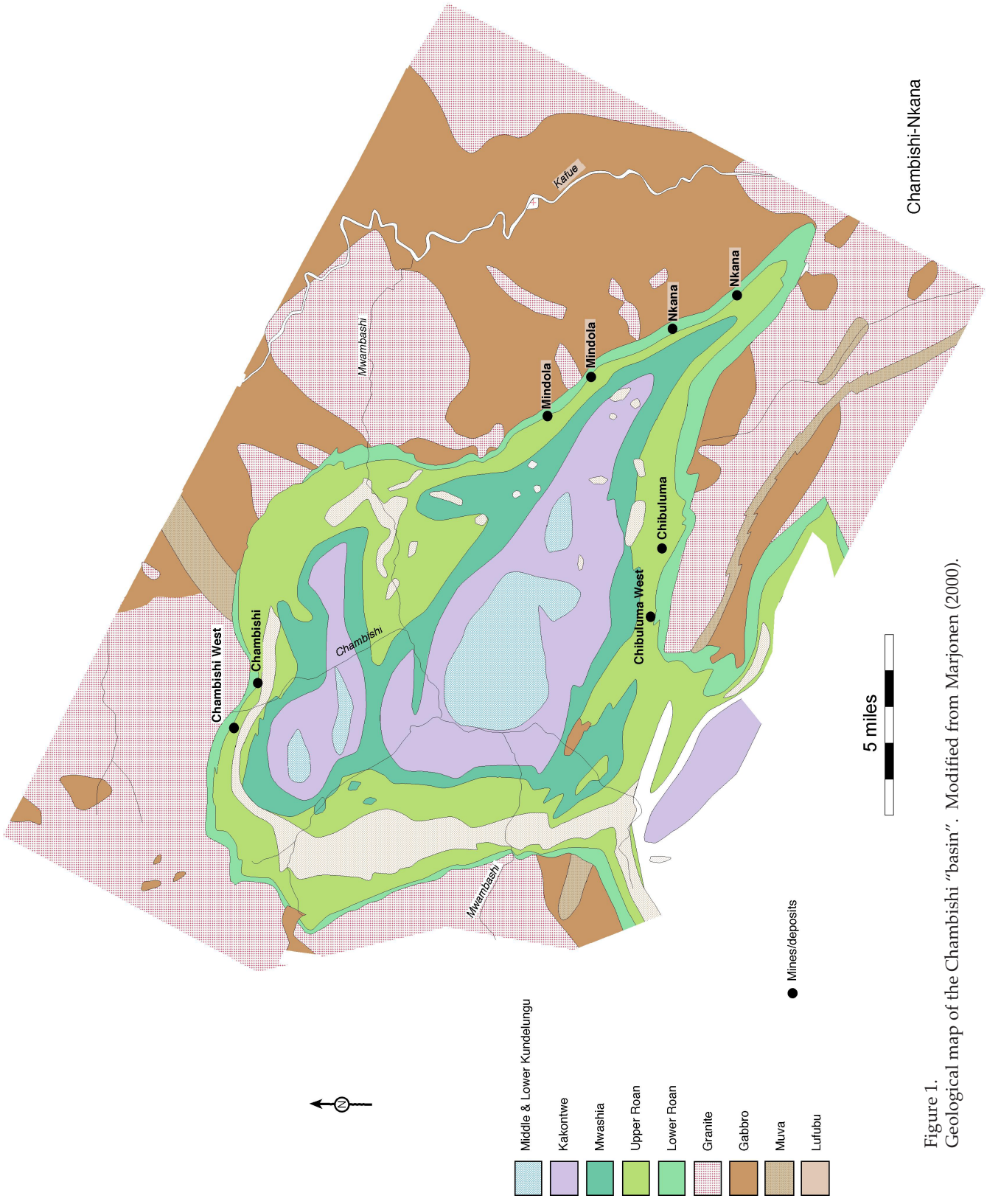

Figure 1.
Geological map of the Chambishi "basin". Modified from Marjonen (2000).

however it is noteworthy that the breccia demonstrates lateral continuity over wide areas, including "pinch-out" positions over several prominent basement "highs" where the remainder of the Lower Roan stratigraphy is highly condensed. This local sheet-like geometry is significant in that it indicates that deposition occurred prior to much of the basin fragmentation that controlled accommodation space higher in the sequence.

Texturally, the breccia is matrix-rich, with a monomictic clast assemblage of biotite granite (texturally and compositionally indistinguishable from basement) set within medium-grained sub-arkosic sand (Fig. 2a). Clasts are rounded to sub-angular and occur up to decimetre proportions. The unit is very similar to a breccia unit(s) at the base of the sequence at Nkana South Orebody.

Footwall Quartzite

The *footwall quartzite* refers to a medium-grained siliciclastic package which underlies the main ore zone. In many holes, primary textures are progressively modified or destroyed upsection by pervasive silicification and/or albitization. In its most pristine form, the sandstone appears relatively clean (minor detrital plagioclase component), moderately sorted, with subangular detrital grains enclosed within a fine, ?originally clay-rich groundmass (presently altered to quartz, calcite, fine biotite and tourmaline needles) (Fig. 2b, c).

Parallel- and cross-stratification is preserved in some cases and becomes most conspicuous where defined by heavy mineral bands (Fig. 2b, c). These are well-developed towards the base of the unit, where they include concentrations of detrital zircon, rutile and tourmaline. Higher in the unit, heavy mineral bands are less pronounced, in part due to pervasive alteration, where relict bands are defined by trails of zircon, recrystallised rutile and biotite, set within an otherwise homogenous mosaic of quartz and albite grains.

Alteration/metamorphic assemblages range from quartz-calcite at the base, with progressive increase of quartz-albite-tremolite-biotite-calcite-chlorite within middle and upper portions of the unit (Fig. 2d). Albite is commonly concentrated within narrow, originally fine-grained seams or heavy mineral bands. Tremolite is similarly concentrated in heavy mineral bands, but also occurs as isolated clots intergrown with albite throughout sandstone beds. It is typically degraded to calcite, phlogopite, biotite and chlorite.

Orebody Quartzite-Hangingwall Quartzite

The *orebody quartzite* is distinguishable from the *footwall quartzite* (and indeed the *hangingwall quartzite*) largely by the presence of sulfides. The rock is still ubiquitously altered to mainly quartz and albite, producing a distinctive "vitreous" appearance (it is commonly referred to in historical logs as "glassy quartzite": Fig. 3a). Textural destruction of primary layering is partly attributable to alteration, however further modification is evidenced by narrow cataclasite seams, generally developed as fracture concentrations and grain-size reduction along original bedding surfaces (Fig. 3b). Heavy mineral bands were less commonly recognised compared to the *footwall quartzite*, but where present, in some cases exhibit a direct spatial association with albitization and sulfide distribution (see Selley & Cooke, this volume). In NS 137, a hole where a fairly intact upper transition from the orebody is preserved, calcite alteration increases upwards into a more "porous" sandstone reminiscent of that near the base of the Lower Roan.

Hangingwall Sandstone

The *hangingwall quartzite* passes upward transitionally into a crudely stratified, poorly sorted, open-framework sandstone (Fig. 4). Subangular to well-rounded grains of quartz, plagioclase and microcline are enclosed within a dark matrix of fine grained calcite, biotite, chlorite and sericite. The matrix component increases upsection to form a gritty siltstone. Individual beds are difficult to establish due to the massive character of the unit, however rare normally graded intervals up to 0.8m thick were recognised.

The unit is considerably less indurated and rheologically weaker than the underlying silicified and albitized succession. Deformation is partitioned into discrete, narrow sericitic shear zones, as opposed to distributed micro-fracturing within lower units.

Upper Breccia Unit

A complete section through the upper breccia unit was recognised in just one hole (NS 115), where it is bounded at both upper and lower contacts by talc-carbonate shear zones. Thickness increases dramatically from 3.5 m in NS 115 to >75 m in the neighbouring hole, NS116 (a distance of roughly 70 m: Figs 7, 10). In both holes, the breccia is overlain by folded and/or brittlely fractured, dark green, chloritic, finely-laminated siltstone.

Internally, the unit appears entirely structureless, with near complete destruction of original textures over much of the interval by a combination of carbonate-talc-biotite-chlorite-albite alteration and shearing. A similar alteration assemblage occurs at the sheared contact of the Lower and Upper Roan in holes where the *upper breccia unit* is absent. Within intervals of relatively low strain a clastic texture is preserved in which sub-rounded to well-rounded clasts are enclosed by a coarse sand-grade matrix (Fig. 5a). Clasts are pervasively albitized, however an original sandstone texture was observed in rare cases. This texture is most clearly defined by relict heavy mineral bands comprising irregular recrystallised grains of rutile and detrital zircon (Fig. 5b). The density of heavy mineral bands in such clasts is compatible with the basal portion of the footwall quartzite. No evidence of a granitic source was recognised, however rare clasts comprising radiating laths of feldspar, quartz, phlogopite and skeletal rutile (possibly after biotite) have textures reminiscent of a coarse-grained mafic rock.

The matrix texture is generally coarser grained than of the clasts (Fig. 5b), with a more complex mineral assemblage of albite, phlogopite, rutile and sparsely distributed zircon. Shear bands within the matrix contain a retrograde assemblage of chlorite and calcite which encloses granulated relicts of the aforementioned mineral assemblage.

The mode of fragmentation is critical to understanding the origin of the breccia unit. In some cases at least, fragmentation has occurred *in situ*, probably via tectonic processes. Such examples include evidence of shearing and progressive cataclastic "erosion" of heavy mineral-rich clasts, leading to concentration of zircon grains within a halo around the clast margins (Fig. 5c). Similarly, fibrous phlogopite was observed to infill fractures or enclose cataclastic tails within and at the termination highly attenuated clasts respectively. In these cases, although there is a clear *modification* of an original clastic texture, it is difficult to prove that cataclasis accounts for the complete fragmentation process. However, this can be demonstrated in rare examples where originally continuous albite bands show progressive denudation at their margins to produce angular breccia zones.

In favour of a sedimentary origin for fragmentation are: (1) the presence of clast types not known from the level of stratigraphy at which the breccia occurs (ie. heavy mineral-rich sandstone), (2) the well-rounded morphology of some clasts (although it could be agued that similar textures are produced via "milling" in a fault zone), (3) the irregular geometry of the unit, characterised by abrupt thickness variation, (4) restriction of the unit to a small, fault-bounded area in the deposit, and (5) the apparently stratabound geometry of the breccia between the *hangingwall sandstone* and Upper Roan chloritic siltstones (lower boundary relationship for NS 116, where core is lost, was deduced from historical drill logs). On these bases, we provisionally interpret a sedimentary origin for the breccia, although textural modification during deformation is clear. The possible presence of coarse-grained mafic clasts, for which the only known source is younger than the Lower Roan (i.e. dolerite intrusive bodies), remains the major drawback for a sedimentary origin. Further work is required to establish the true nature of these enigmatic clasts as well as logging away

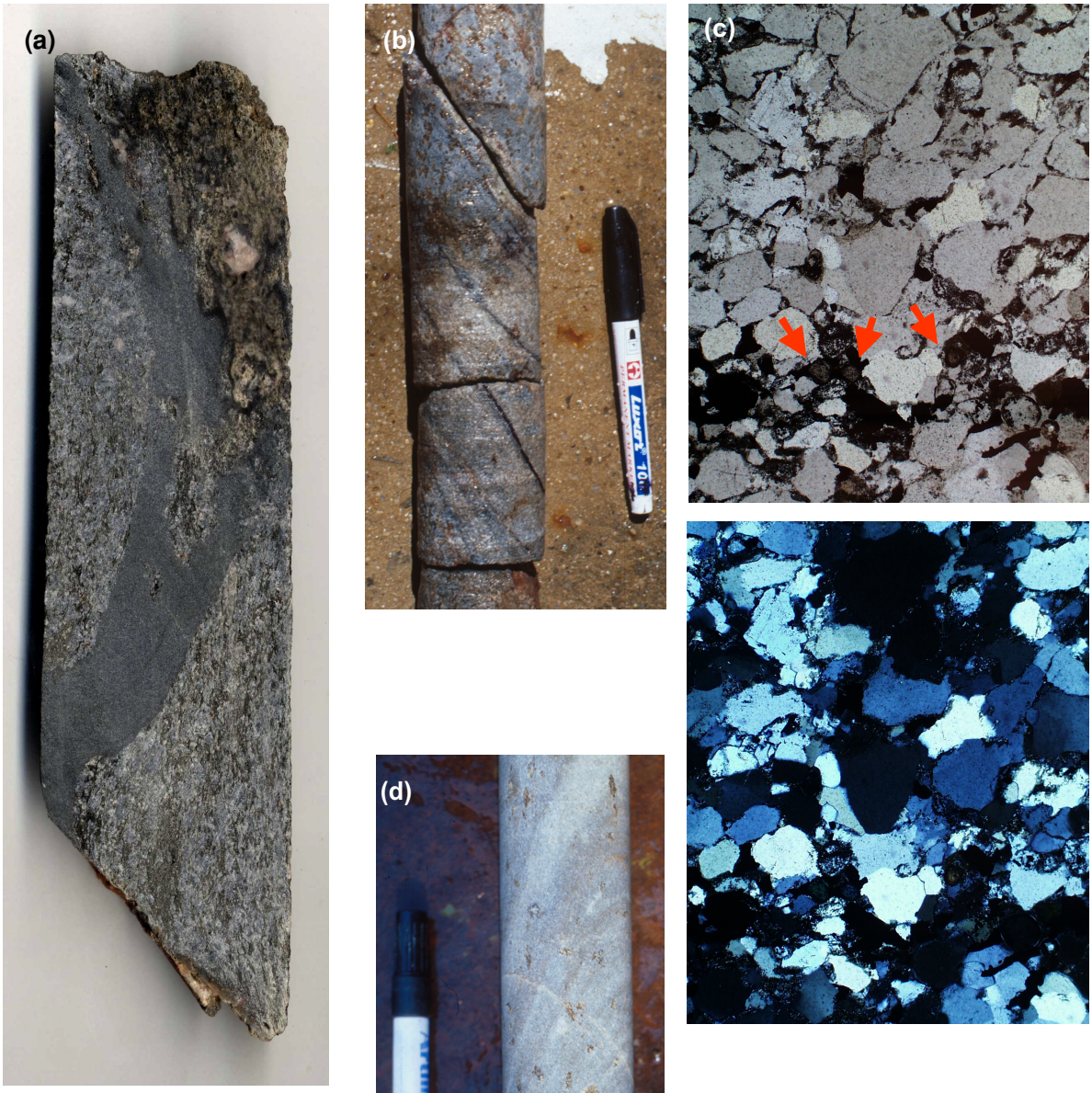

Figure 2. *Basal boulder bed* and *footwall quartzite*.
(a) Basal boulder bed cobble-sized clasts of basement granite floating within sub-arkosic sandstone.
(b) Friable calcitic sub-arkosic sandstone from the base of the *footwall quartzite*. Note distinctive heavy mineral bands and crude cross stratification. Alteration partly destroys these textures at top of core.
(c) Moderately sorted sandstone, with good preservation of original detrital textures. Fine-grained band near base of view is enriched in heavy minerals: arrows indicate detrital zircons. Width of view 2mm.
(d) Strongly silicified and partly albitized *footwall quartzite*. Good preservation of primary banding. Clots of tremolite, largely replaced by calcite and biotite, disseminated throughout.

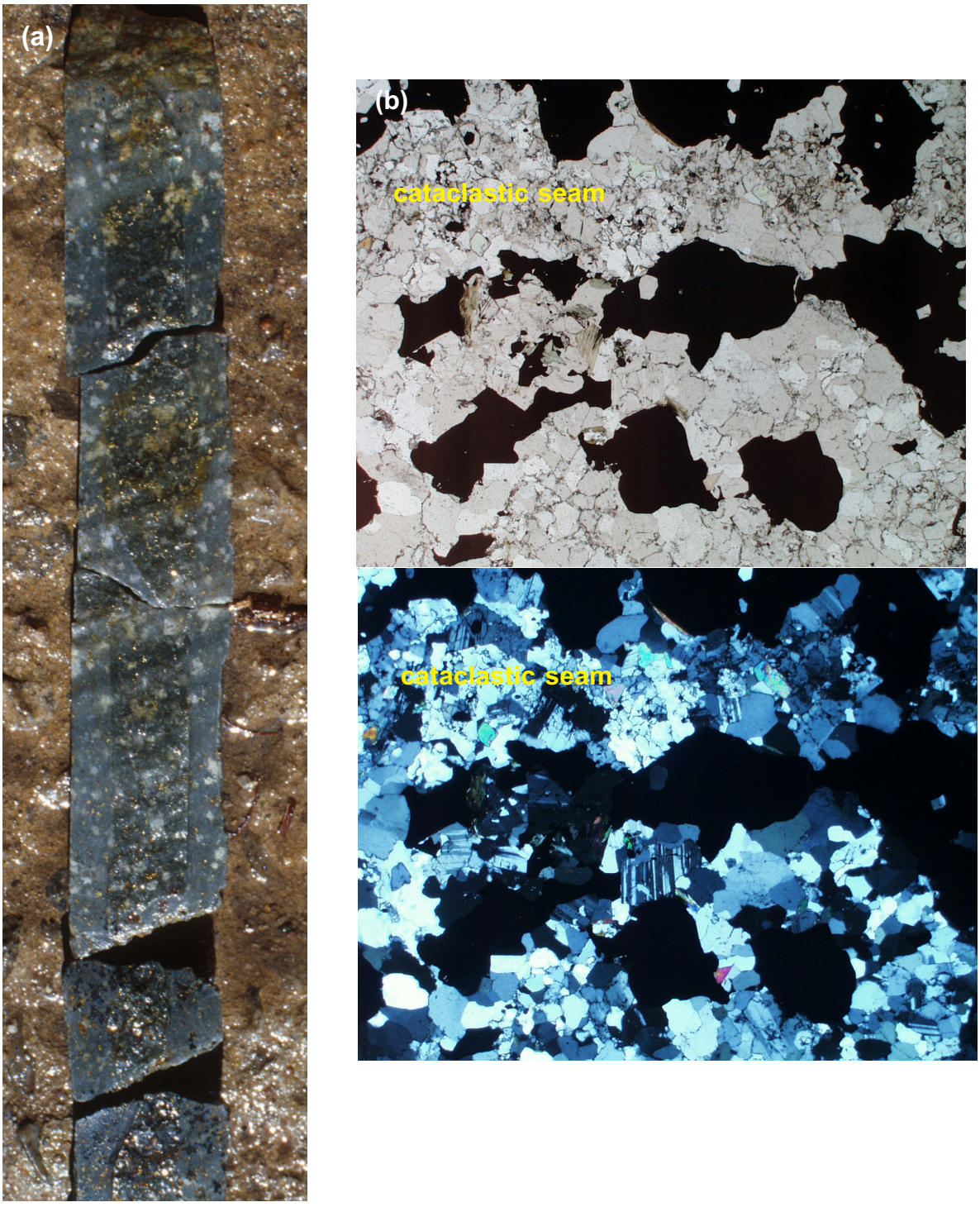

Figure 3
Orebody quartzite
(a) Silicified and albitized banded sandstone, with disseminated sulphides throughout. Pale spots are tremolite.
(b) Banding in thin section defined in part by grain-size reduction along layer-parallel cataclastic seams. Sulphides distributed along margins of seams. Width of view 2mm.

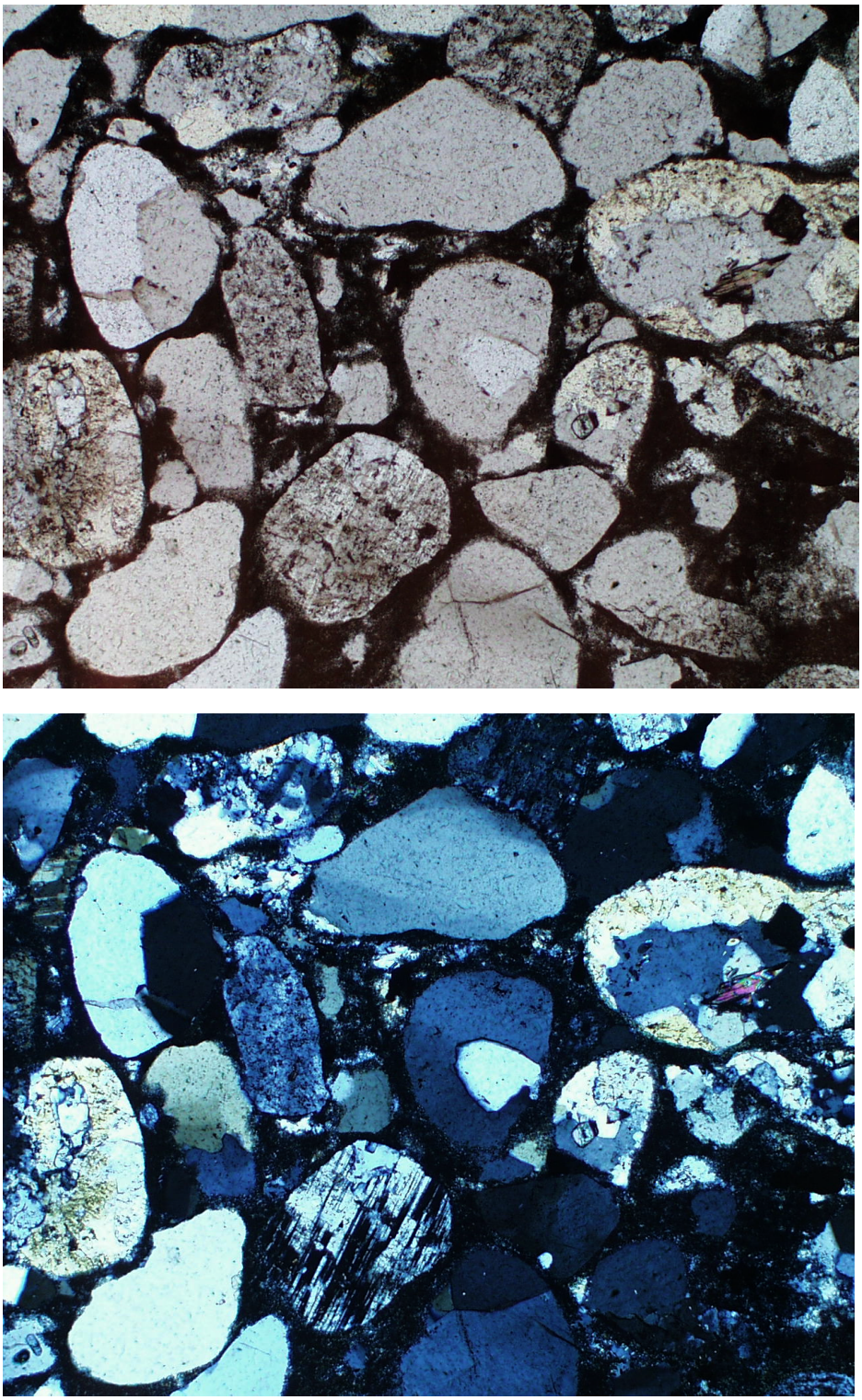

Figure 4
Microphotograph of open framework texture in *hangingwall sandstone*. Excellent preservation of original detrital textures. Quartz and plagioclase, although weakly strained, appear compositionally pristine. Width of view 2mm.

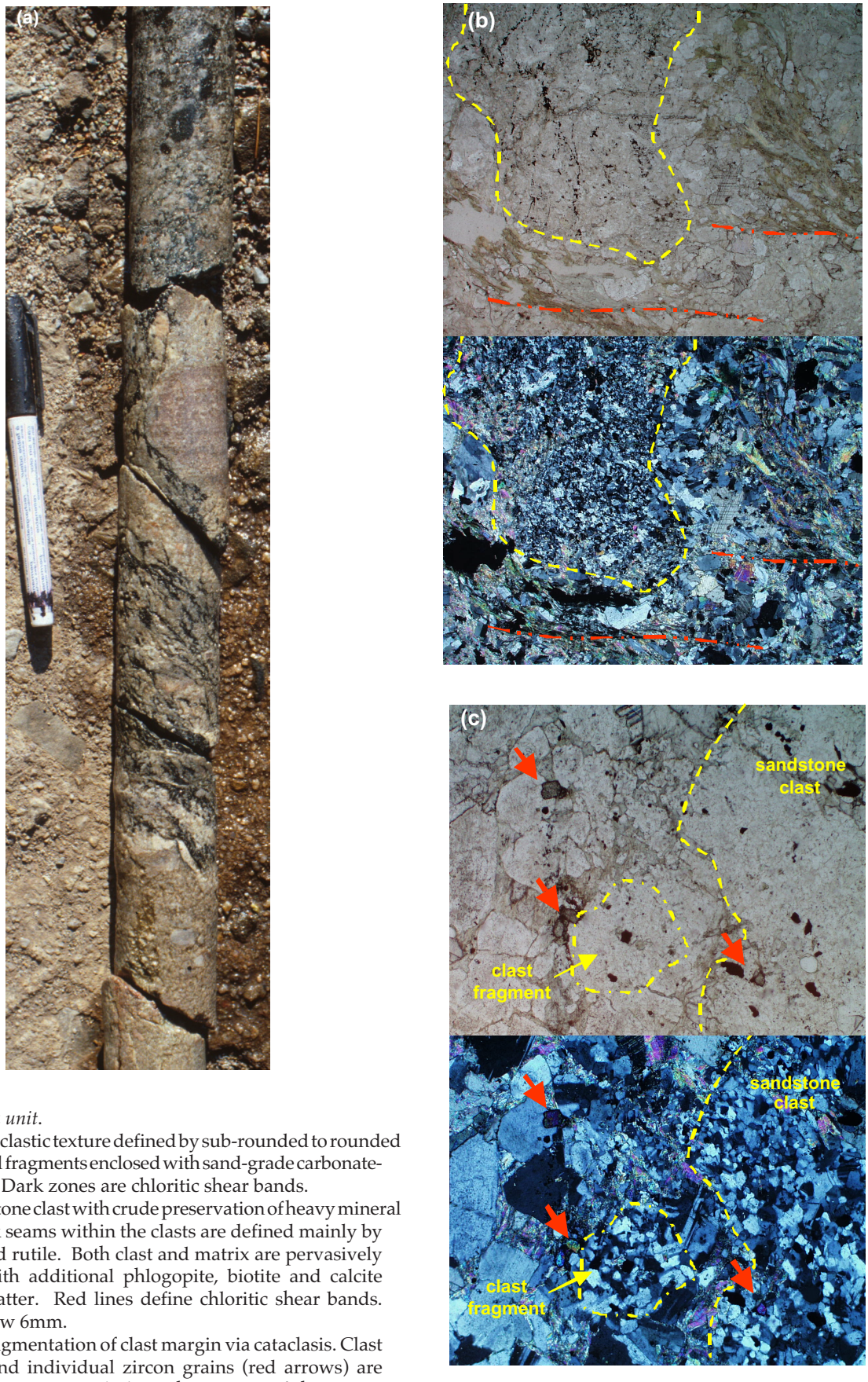

Figure 5
Upper breccia unit.
(a) Crude clastic texture defined by sub-rounded to rounded poorly sorted fragments enclosed with sand-grade carbonate-rich matrix. Dark zones are chloritic shear bands.
(b) Sandstone clast with crude preservation of heavy mineral bands. Dark seams within the clasts are defined mainly by recrystallised rutile. Both clast and matrix are pervasively albitized, with additional phlogopite, biotite and calcite within the latter. Red lines define chloritic shear bands. Width of view 6mm.
(c) In situ fragmentation of clast margin via cataclasis. Clast fragments and individual zircon grains (red arrows) are spalled and concentrated along the margin of the parent clast. Width of view 2mm.

from the 390 section in order to constrain the three-dimensional geometry of the unit.

Structural geometry and basin architecture

Lower Roan strata are contained within the cores of three broadly WNW-striking synclines, separated by fault-bounded inliers of basement (Figs 6, 7, 8, 10). Wavelength of the folds decreases progressively to the western end of the deposit, where they appear to die out against a NNW-striking basement "ridge". At the northeastern end of the deposit, structural geometry simplifies and synclines open up into a broadly northward-dipping ramp (Fig. 10).

An isopach map of Lower Roan strata (Fig. 9) demonstrates coincidence of significant accumulation of sediments with these synclinal closures (maximum ~200 m), although thickness maxima are in some cases offset from the hinges of the folds (Fig. 10). In the northeast of the deposit, isopachs reveal a broadly NNE-thickening wedge, which mirrors the progressive opening of folds in this region. In the central and western parts, thickness maxima occur on the southern limbs of synclines, with progressive thinning against the NNW-trending basement "ridge", where folds die out. This relationship indicates convincingly that the present structural geometry is inherited from original basin topography. That is, the synclines were originally depositional troughs, separated in part at least, by elevated blocks of basement. In this section we consider the possible structural controls on basin development by examining details of the stratigraphic architecture: i.e. contact relationships of the Lower Roan with basement, facies variation and the geometry of the package as a whole.

Two end member scenarios for basin development can be initially considered. In the first of these, depocentres originated as deeply incisive erosional troughs or canyons within basement, into which Lower Roan strata accumulated. Such features had the potential to develop in response to sudden uplift at the onset of basin development, perhaps as a result of footwall block tilting. The present fault-bounded contacts between many of the basement inliers and the Roan package, would thus be attributable to the inversion event. Although this process is geologically viable (indeed we have argued this case for parts of the Adelaide Fold Belt: Selley & Bull, this volume), we consider it unlikely due to relationships between basal Lower Roan strata and the basement "highs". The principal basement element is the WNW-striking axial "ridge" which bisects the deposit along the "orebody zero" and attains a maximum amplitude within the central part (Figs 7, 8, 10). The bulk of the Lower Roan package thins across this feature, however the *basal boulder bed* is shown on historical logs to be preserved at the crest of the "ridge" over much of the central part of the orebody (e.g. section 232 in Fig. 10). This relationship demands that the axial "ridge" was at best an insignificant topographic feature at the onset sedimentation, but subsequently amplified to control sedimentary architecture at higher stratigraphic levels.

The second end member scenario for basin growth involves a structural control on basement uplift and / or basin subsidence. Considering only an extensional environment, basin growth was probably accommodated by either horst-and-graben or half-graben structures, or possibly a combination of the two. Determining which of these structural styles acted as the principal control on basin growth is difficult due to: (1) the relatively wide spacing of drill hole data away from the "zero orebody", (2) the relatively small size of the depocentres (ie. basin growth was not sufficiently advanced to produce thick sequences with distinctive stratigraphic architecture), and (3) modification of original basin geometry and basin-bounding structures arising from inversion. At this stage we have only considered a half graben geometry, in which cross sections were constructed and restored assuming a tilt-block geometry bounded by roughly NNE-dipping growth faults (Figs 10,11).

Several lines of weak evidence have led us to favour a half graben geometry. Firstly, within the central and western parts of the deposit, cross sections and

isopachs of Lower Roan strata reveal a crudely asymmetric stratigraphic architecture, with progressive thickening on the southern sides of depocentres and thinning to the north (Figs 9, 10). Although data are consistent with this modelling, it should be noted that the fairly limited drilling from the cores of the depocentres (ie. synclines) means that isopachs were locally constructed using a deal of "artistic license". The interpreted wedge-shaped depocentres are typical of those developed on progressively rotating basement blocks in a half graben setting. We interpret the southward thickening of stratal wedges to indicate block rotation controlled by NNE-dipping growth faults which truncate strata at the southern margins of the wedges (Figs 10, 11). Providing weak support for this interpretation is the apparent absence of the basal boulder bed on the southern limb of synclines, but preservation on northern limbs in some sections: ie. depositional contact with basement preserved on northern limbs and faulted contacts on southern limbs (e.g. sections 232 & 390 in Fig. 10) . This relationship does not hold for all areas however, with preservation of the basal boulder bed upon the uppermost northern flank of the "axial basement ridge" on sections east of 232 (i.e. central and eastern parts of the deposit). Furthermore, a strongly asymmetric wedge geometry is not developed in all areas, with progressive thinning of stratal packages on both the northern and southern flanks of the "axial basement ridge", particularly within eastern parts of the deposit (e.g. Fig. 9, and section 92 in Fig. 10). Thus the stratigraphic architecture is not everywhere compatible with classical half graben geometry.

The observed thinning of strata on both sides of basement "highs", coupled with preservation of basal stratigraphy on the northern flanks of "highs", is compatible with a compressional setting in which basement topography generates as propagating anticlines during basin growth (e.g. Burbank et al., 1996: Fig. 12). However, recent work on the evolution of rift basins have highlighted the importance of extensional forced folds above blind growth faults, particularly at the onset of extension (Withjack et al., 1990; Schlische, 1995; Hardy and McClay, 1999; Gawthorpe and Leeder, 2000). This geometry occurs in response to the very segmented form of growth faults during initiation of rifting, where structures die out rapidly along strike and significant variation in slip rates occur laterally along fault surfaces. As segments lengthen with progressive extension, the folds can generate due to ductile deformation at the tip of the propagating fault (Gawthorpe and Leeder, op cit.: Fig. 13). Furthermore, transverse folds can generate oblique to the growth fault array along linkage structures or accommodation zones.

We have attempted to reconstruct the basin geometry using extensional forced folds generated above a blind NNE-dipping growth fault along the trace of the "axial basement ridge" (Figs 10, 11). The model is attractive in that is accounts for the inferred amplification of the basement "high" during basin evolution. The fault is interpreted to have breached the surface during sedimentation of middle or upper parts of the Lower Roan, although our restoration requires additional (but localised) gravitational collapse of the forelimb of the fold in order to account for the very shallow bedding cut-out angles. The present exaggerated height-to-width aspect ratio of the "axial basement ridge", combined with the local development of mylonitic shear zones on the southern flank of the "ridge", is interpreted to have resulted from footwall cut outs generated during basin inversion (e.g. sections 232 and 390 in Figs 10, 11).

A possible flaw in the model is shown by the very pronounced wedging of strata onto the footwall of the "axial" growth fault in the restored 232 section (Fig. 11). This could only have been achieved in a half-graben setting by significant block rotation above a shallowly dipping listric master fault further to the south. Even so, the abrupt elevation required of the immediate footwall of the fault may be implausible. At this position, the "axial basement high" appears more like a horst block, and an antithetic, south dipping (?blind) growth fault on the southern side of the ridge may be required.

The highly asymmetric wedge of the upper breccia unit situated at the western edge of the deposit (Figs 10, 11) is tentatively interpreted to record extension along the "axial" growth fault late in Lower Roan sedimentation. The very restricted distribution of this facies indicates rapid, but localised activation of the fault. Again, to account for the extreme thickness variation shown by this unit, a very shallow fault geometry is required. Basal Lower Roan clasts contained within the breccia are interpreted to have been shed from the adjacent NNW-trending ridge which marks the termination of the main depocentre. This structure is interpreted to have formed as a transverse ridge, amplifying late during Lower Roan sedimentation, resulting in erosional stripping of lower units and evidenced by lapping of Upper Roan strata directly onto basement (Figs 7, 8, 10, 11).

Summary and Conclusions

The Lower Roan at Chibuluma West is relatively condensed (maximum of ~200 m thickness) and is conspicuous by its lack of "Ore Shale" facies. Lithotypes are dominated by medium grained sub-arkosic sandstone, with variable matrix component. Sedimentary breccias are interpreted to bound the package locally. Pervasive alteration occurs throughout much of the sequence, the products of which are predominantly albite and quartz, with variable components of calcite, tremolite, phlogopite and talc.

Thickness and facies variation within the Lower Roan package reveal a complex depositional system which progressively narrows from east to west. Within the northeastern part of the deposit, sediments accumulated on a broadly NNE-dipping ramp. The limits of this ramp are unknown, however strata are presumed to thicken progressively northward into the Chambishi "basin" proper. Depocentres become more restricted to the west and are presently preserved as synclinal troughs, separated by thrust-emplaced inliers of basement. The original basin configuration in this area is interpreted to have involved broadly southward deepening accommodation spaces, which terminated against an array of NNE-dipping growth faults. Block rotation association with displacement on ?listric growth faults resulted in progressive uplift of footwall basement-cored blocks (basement "highs") and consequent thinning of the overlying succession. In central and eastern parts of the deposit, the "axial" growth fault is considered to have remained blind at the onset of sedimentation, resulting in thinning of strata on both northern and southern flanks of a extensional forced fold. During late Lower Roan sedimentation, structural activity was most pronounced along the western edge of the depositional system, where a NNW-trending transverse ridge amplified and shed basal Lower Roan detritus into narrow, rapidly subsiding accommodation spaces immediately adjacent to its margin.

The basin evolution outlined above is typical of that developed at the onset of rifting. The schematic block model shown in Figure 14 highlights the fundamental elements of our interpreted basin architecture. With initiation of rifting, sediments accumulated in an array of discontinuous, slowly subsiding depocentres. Sub-basins were bounded by segmented growth faults oriented roughly normal to the far field maximum extensional stress, and secondary transverse linkage structures. Sub-basin geometry evolved with progressive lateral and vertical propagation of fault tips, leading to linking of broader, more deeply subsident accommodation spaces. It is possible that the basin-bounding fault geometry shallows at depth (in contrast to that shown in Fig. 14), such that with accelerated extension, footwall blocks would have been uplifted and thus had the potential to supply intrabasinal- and/or basement-derived debris at higher levels of the stratigraphy.

This study represents the initial stage of analysis of the Chambishi "basin". Continued research of the Nkana system undertaken by Mawson Croaker with be incorporated with further work by ourselves at the Mwambasi and Chambishi deposits (located along the periphery of the "basin"), and of limited drill core from the centre of the "basin", with the aim of developing an evolutionary model for Lower Roan sedimentation.

References

Burbank, D., Meigs, A. & Brozovic, N., 1996. Interactions of growing folds and coeval depositional systems. Basin Research 8: 199-223.

Gawthorpe, R.L. & Leeder, M.R., 2000. Tectono-sedimentary evolution of active extensional basins. Basin Research 12: 195-218.

Hardy, S. & McClay, K., 1999. Kinematic modelling of extensional fault-propagation folds. Journal of Structural Geology 21: 695-702.

Marjonen, R., 2000. Geological map of the Kitwe-Mufulira area. Geological Survey Department, Zambia. 1:100,000 scale map series.

Schlische, R.W., 1995. Geometry and origin of fault-related folds in extensional settings. AAPG Bulletin 79: 1661-1678.

Withjack, M.O., Olson, J. & Peterson, E., 1990. Experimental models of extensional forced folds. AAPG Bulletin 74: 1038-1054.

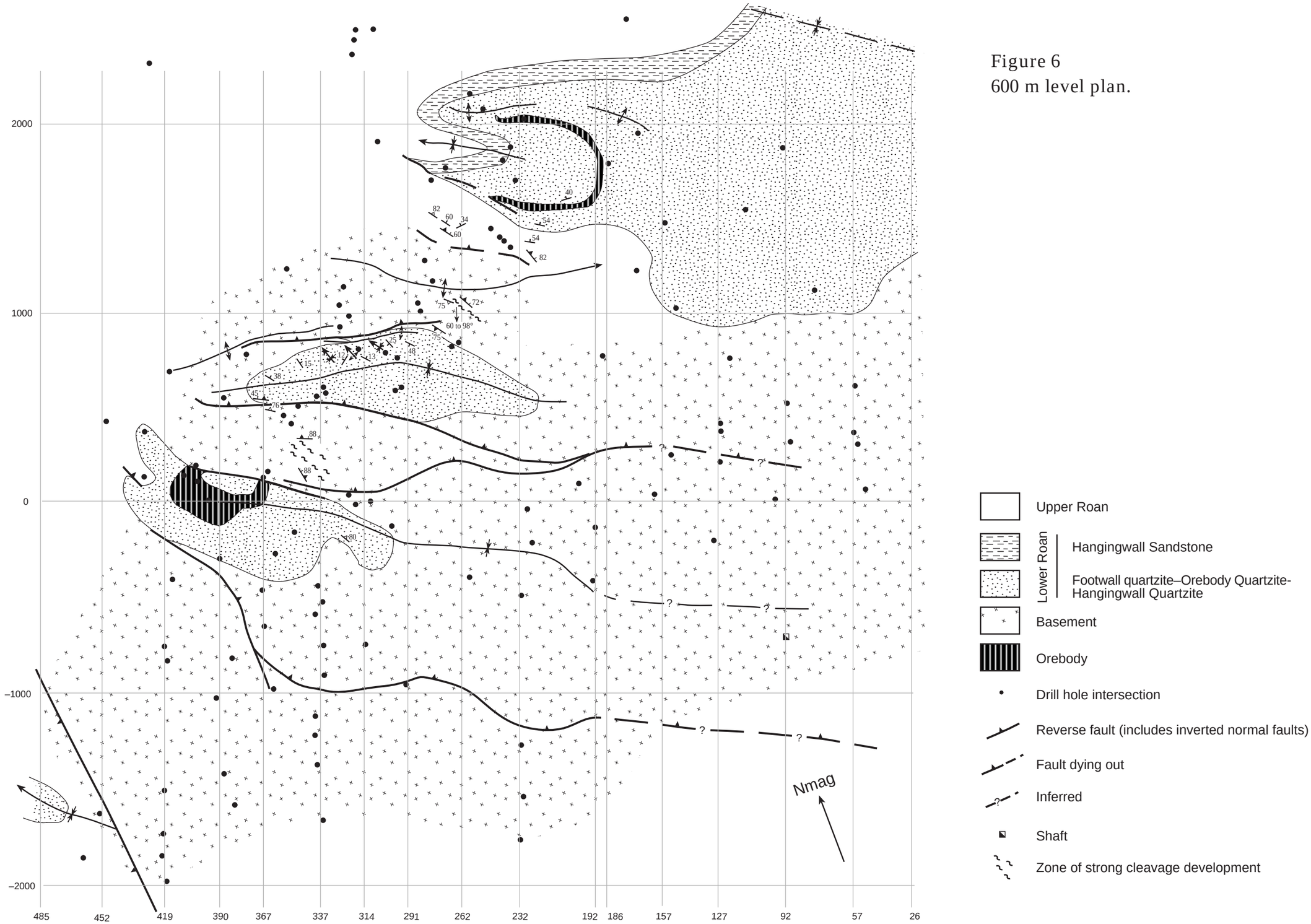

Figure 6
600 m level plan.

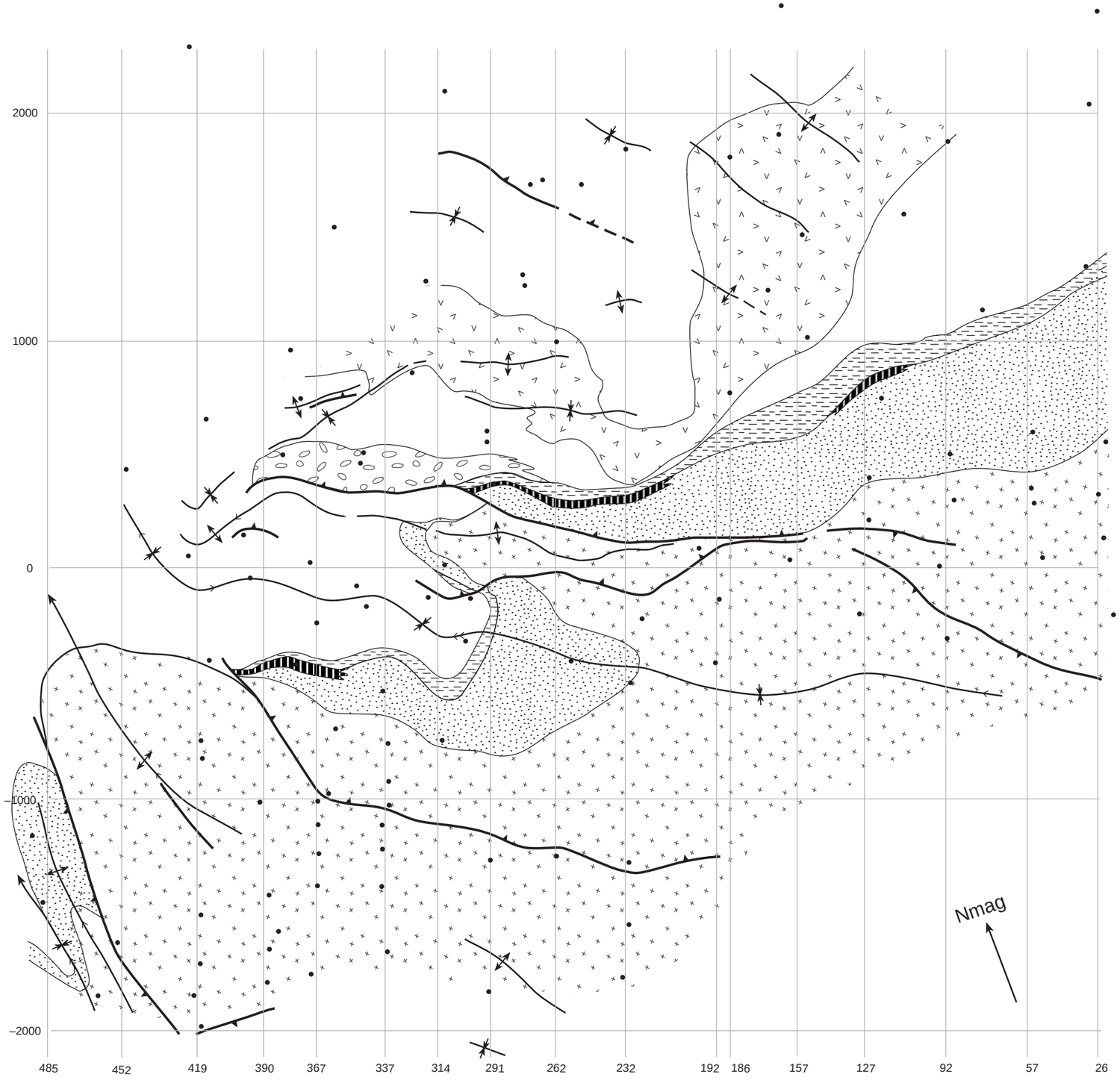

Figure 7
400m level plan.

- Dolerite
- Upper Roan
- Lower Roan
  - Upper breccia unit
  - Hangingwall Sandstone
  - Footwall quartzite–Orebody Quartzite-Hangingwall Quartzite
- Basement
- Orebody
- Drill hole intersection
- Reverse fault (includes inverted normal faults)
- Fault dying out
- Inferred
- Shaft

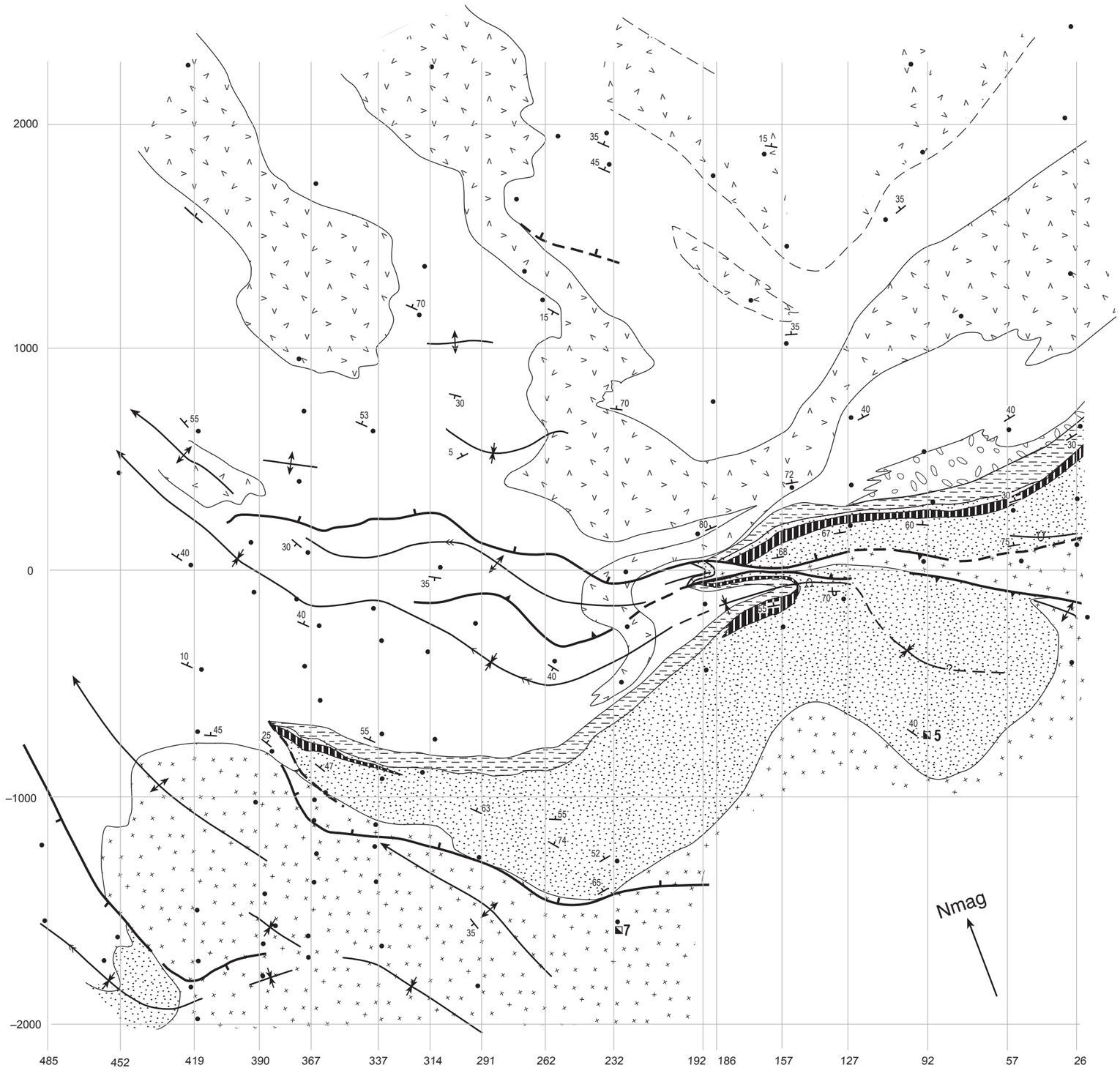

Figure 8
200m level plan.

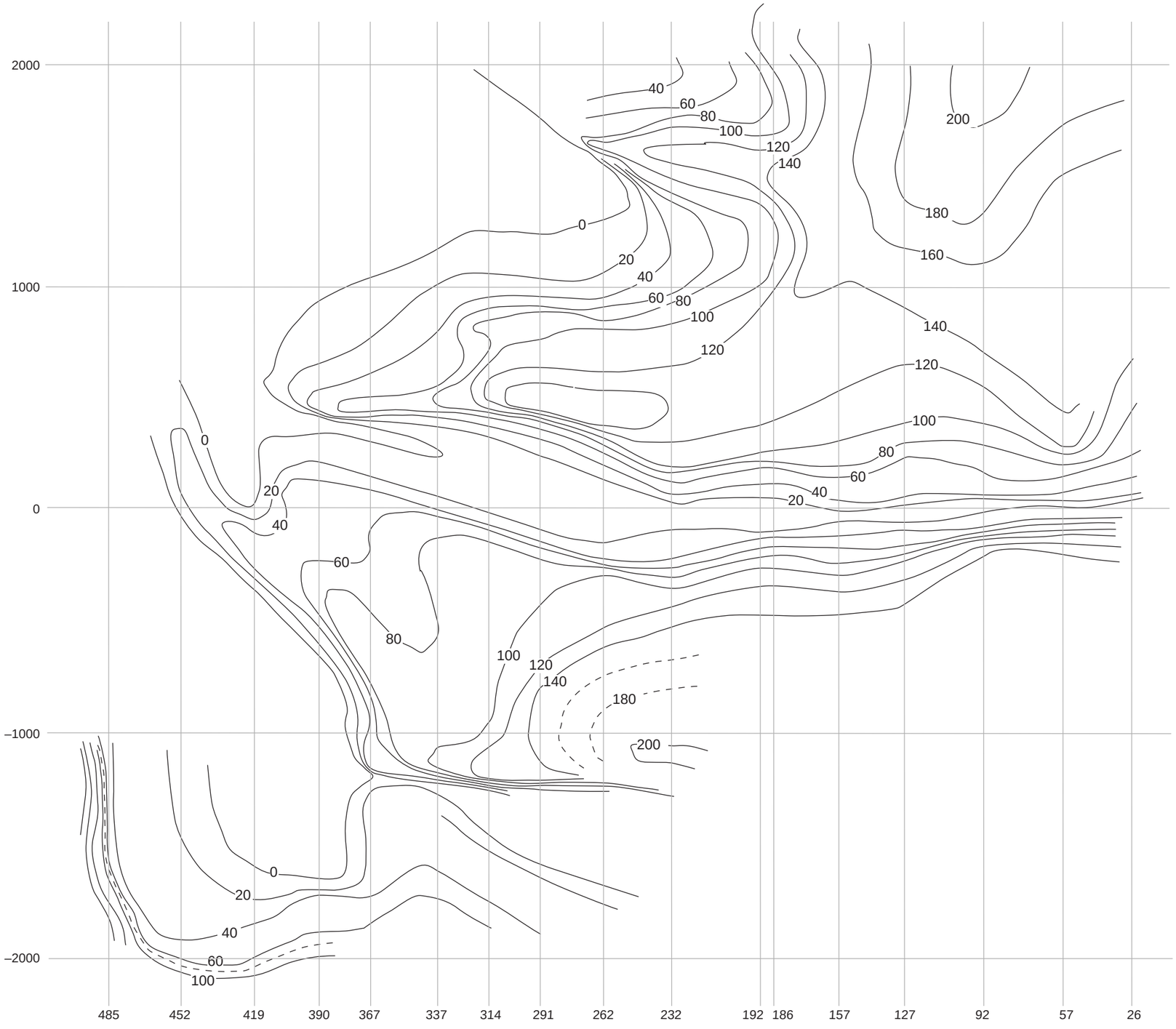

Figure 9
Isopach map of Lower Roan strata.

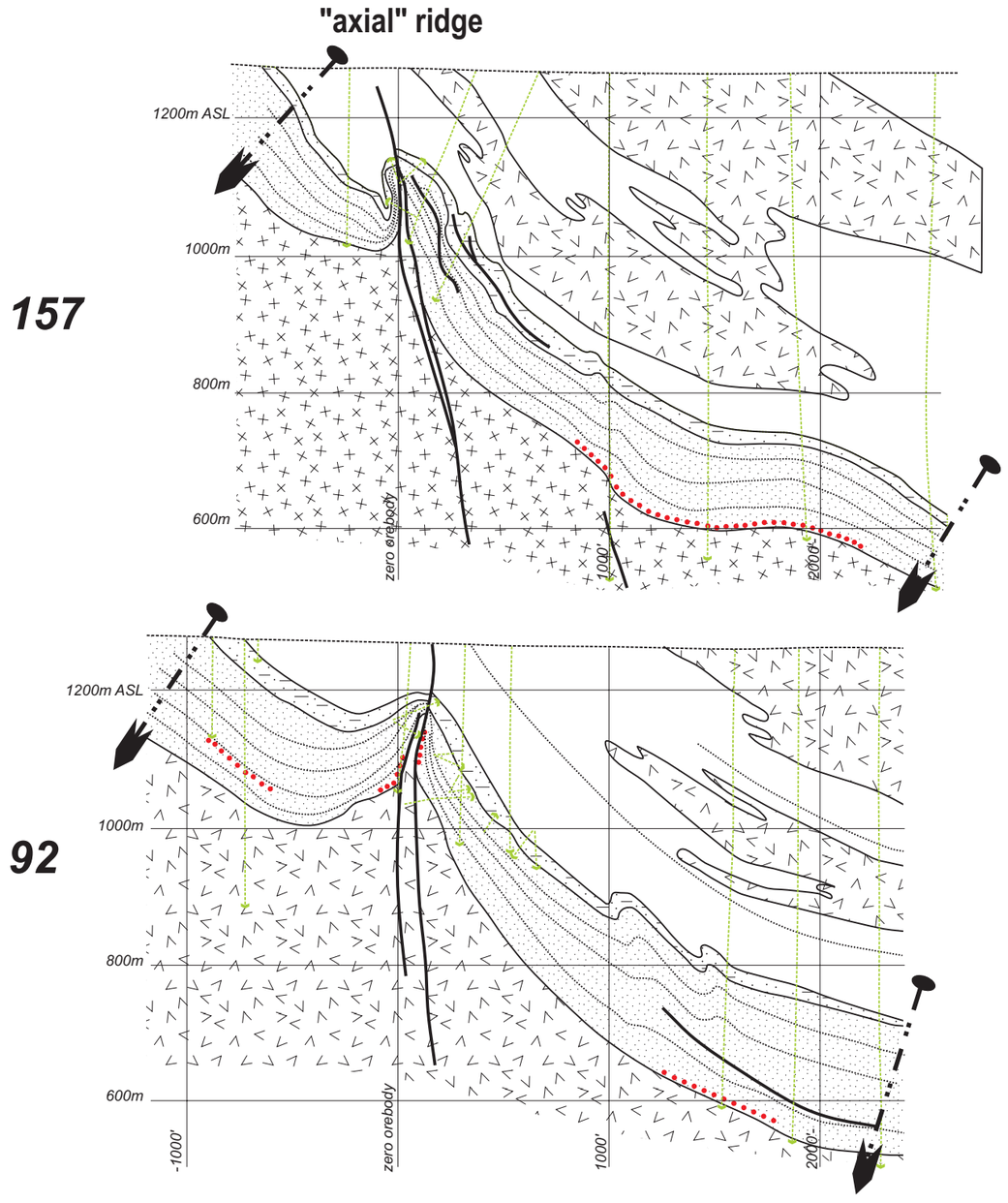

Figure 10
Interpretive, balanced cross sections throughout the deposit. Refer to Figures 6-8 for locations. Section lines increase in value from ESE to WNW.

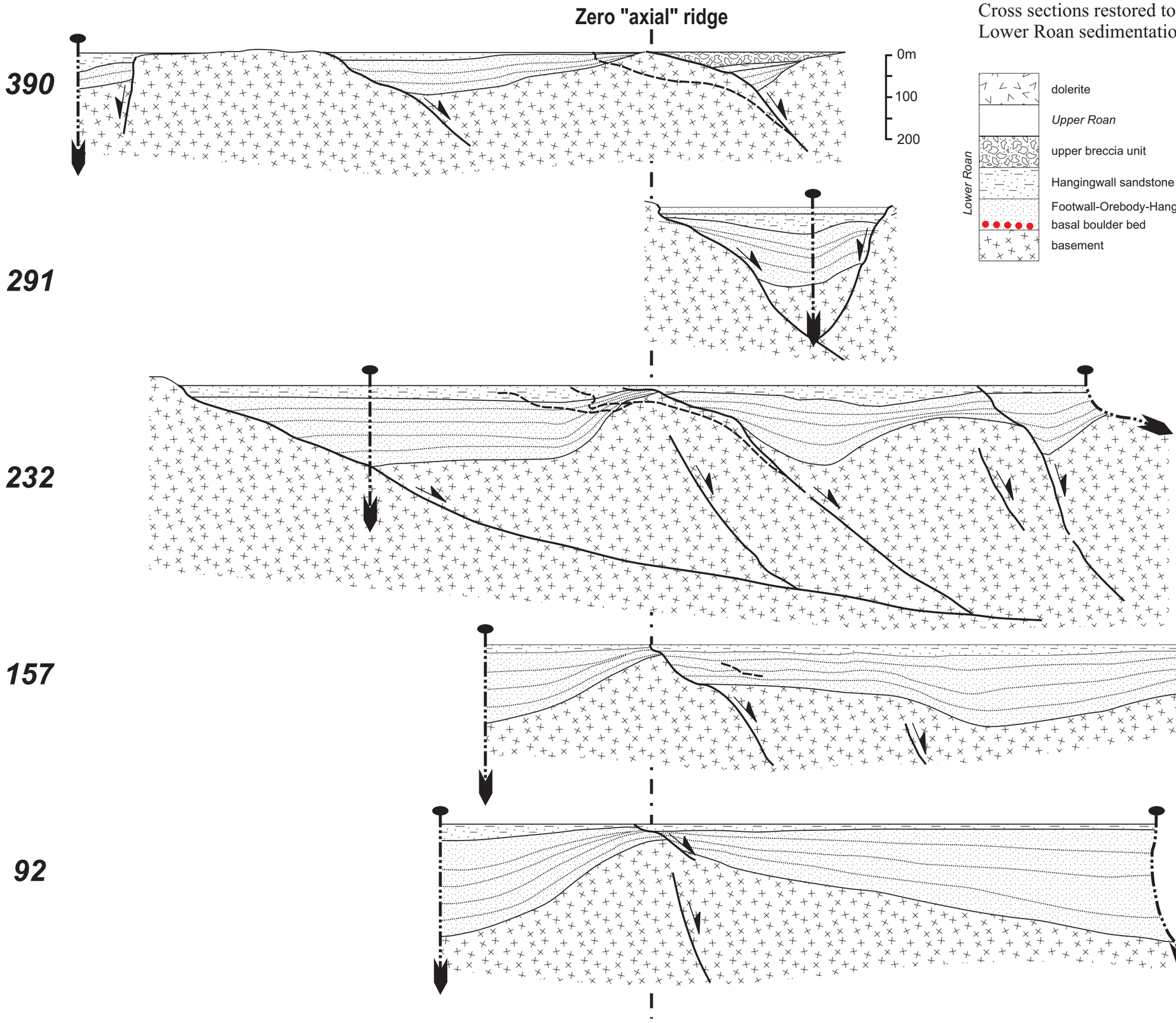

Figure 11
Cross sections restored to the top of Lower Roan sedimentation.

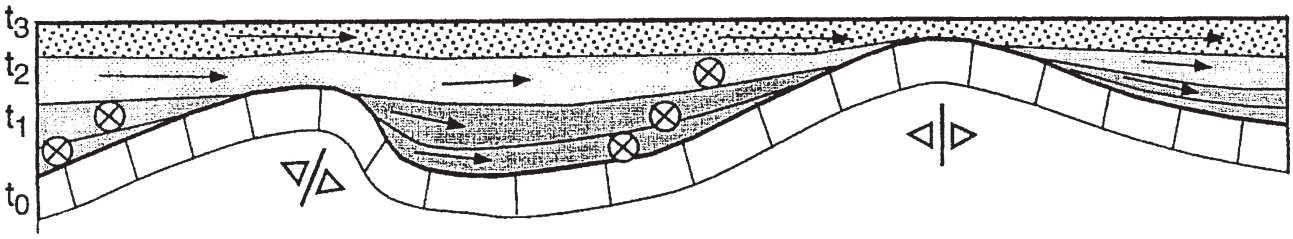

Figure 12.
Conceptual stratigraphic architecture developed in a foreland basin involving basement-cored growth folds. Note symmetrical thinning of lower packages on both flanks of the folds. Unmodified from Burbank et al. (1996).

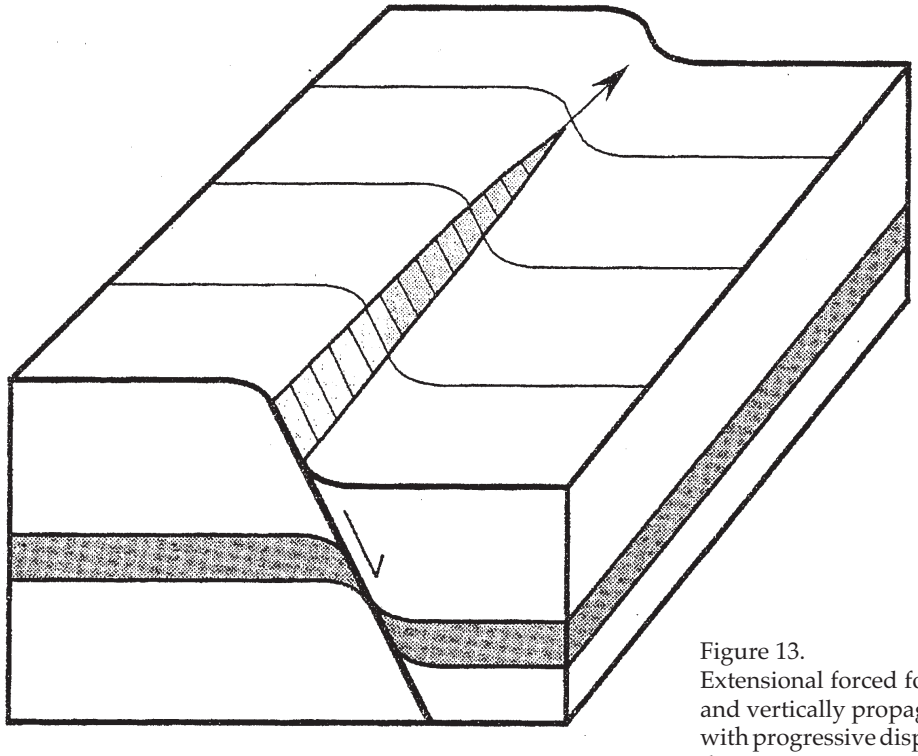

Figure 13.
Extensional forced fold developed at the tip of laterally and vertically propagating growth fault. Fold amplifies with progressive displacement on the "blind" segment of the fault. Unmodified from Schlische (1995).

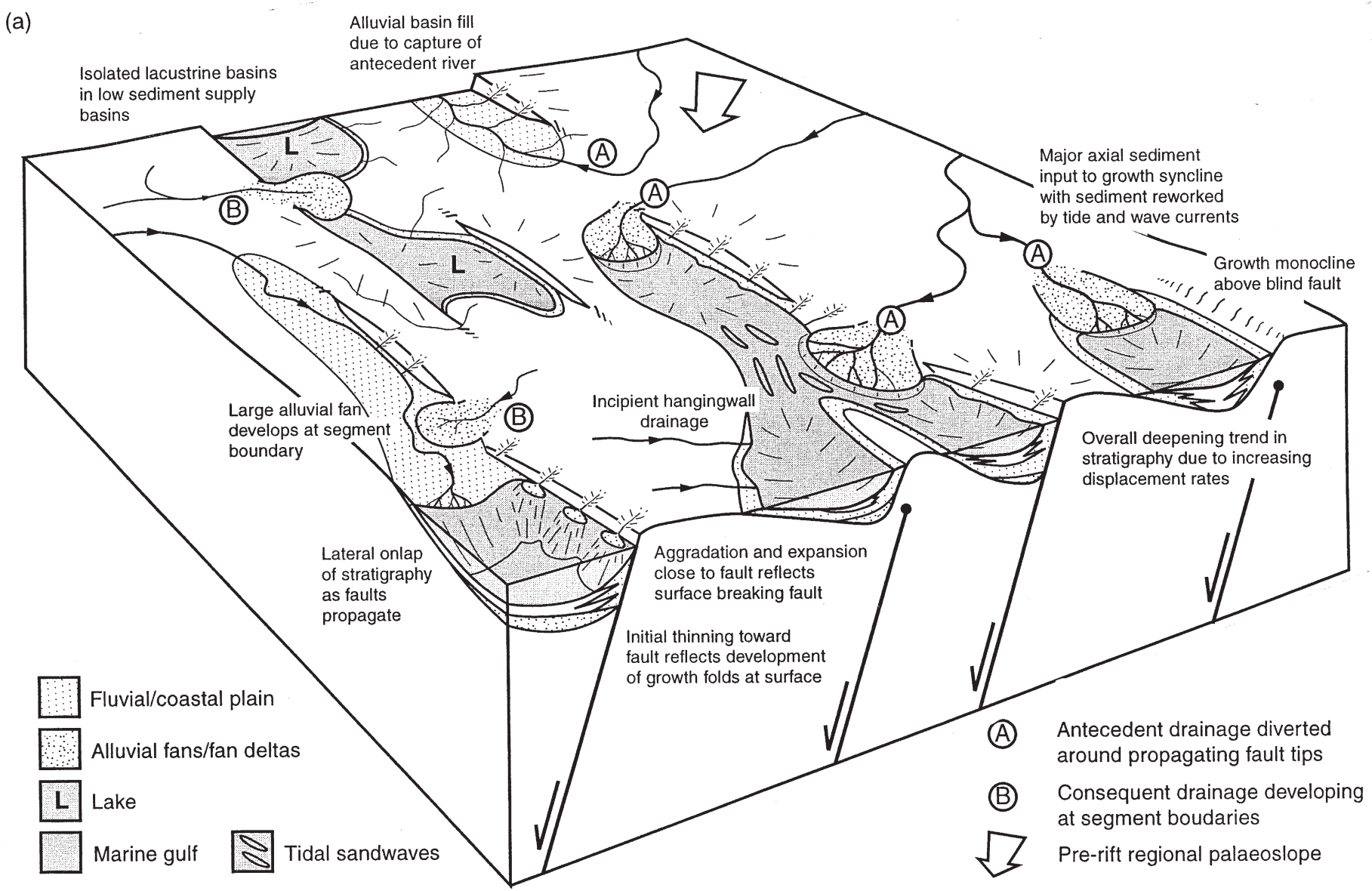

Figure 14
Conceptual model for early basin growth at Chibuluma West. Sub-basins initiate within the hangingwalls of "penetrative" and "blind", disconnected growth fault segments. Note lapping of basal strata onto both limbs of extensional forced folds. Facies associations outlined in this cartoon are not directly relevant to the Chibuluma system. Unmodified from Gawthorpe and Leeder (2000).

Mineral zonation and sulfur isotope systematics of the Chibuluma West copper–cobalt deposit, Zambia

David Selley and David Cooke
Centre for Ore Deposit Research, Univ ersity of Tasmania

Summary

- Sulfide mineral phases are strongly controlled in terms of their distribution by primary layering: stratiform textures are common.
- Highest concentration of sulfides coincide with layer-parallel albitic "flooding zones" and veins.
- Evidence of grain fracturing is common within albite and sulfide-rich domains, implying that structurally-generated secondary permeability provided the means for fluid infiltration.
- Dilation of bedding surfaces potentially occurred during basin inversion, enhanced where thickened Lower Roan packages were juxtaposed at high angles with rigid basement inliers.
- Sulfur isotopic compositions of sulfides are anomalously heavy (+3 to +15‰) with respect to other Copperbelt deposits.
- Sulfides have isotopic compositions that vary stratigraphically through the orebody.
- There is no obvious correlation between metal grades, mineral zonation and sulfur isotopic compositions.
- Bornite-chalcopyrite mineral pairs are not in isotopic equilibrium and cannot be used to determine temperatures of sulfide deposition.
- Although biogenic sulfate reduction has been advocated as an important depositional process at deposits such as Konkola, it is unlikely to have been important at Chibuluma West.
- Grain-scale and stratigraphic heterogeneity of sulfide isotopic compositions preclude a single, homogeneous aqueous source of sulfur for the Chibuluma deposit.

Introduction

This reports documents the mineral zonation, paragenesis and distribution of Cu-Co mineralisation in two diamond drillholes from the Chibuluma West copper deposit, Zambia. Preliminary sulfur isotope analyses have also been conducted on samples from these drillholes to test whether the observed mineral zonation is mirrored by an isotopic zonation pattern, and to evaluate the implications of the isotopic findings for ore transport and deposition at Chibuluma West and other deposits in the copperbelt.

This study has focussed primarily on drillhole NS137, with additional information obtained from NS159. The locations of both drillholes are shown on Figure 1. In these drillholes, mineralisation is hosted primarily in a quartzite unit (*orebody quartzite*) of the Lower Roan, however a thick shear-zone hosted intersection occurs within granitic basement at the base of NS159. The orebody quartzite is overlain by the poorly sorted arkosic hangingwall sandstone.

NS 137 Ore Zone

NS 137 is situated at the western margin of the deposit, near the confluence of an interpreted NNE-dipping growth fault and a NNW-trending basement "ridge". Lower Roan strata thicken southward towards the growth fault, where they are inferred to have a structural contact with uplifted basement (Fig. 1). To the northwest of NS 137, the Lower Roan rapidly thins and ultimately pinches out onto the NNW-trending basement "ridge" (see also Figs 6–10 in Selley & Bull, this volume).

Vertical zonation of Cu-Co grade and mineral phases

Drill core contains a thick intersection of crudely stratabound Cu mineralisation (46' @ 3.4% Cu) with a Co-rich cap (6.5' @ 0.6%Co). These intervals are referred to below as the 'main' and 'upper' ore zones respectively. The upper Co orebody coincides with a narrow Cu-rich zone, but is separated from the main orebody by a 9' thick interval of low grade (>1% Cu) Cu mineralisation. The drill core intersection is highly oblique to layering (~25°), resulting in an exaggerated orebody thickness of 155' (Fig. 2).

Cu-grades exhibit a crudely symmetrical increase from both the lower and upper margins of the main ore zone (Fig. 2). In detail however, grade is spiky, with the best intersection of 3' @ 10.8% Cu occurring just below the middle of the ore zone (i.e. 1300'). This intersection coincides with a slight Co peak, however near the base, Cu-grade has an inverse relationship with that of Co.

Sulfide phases

Sulfide mineral phases also show a distinct vertical zonation (Fig. 2). These data are derived primarily from original company logs and were modified only in rare cases where discrepancies occurred with our own logging. The mineral assemblage is relatively simple: chalcopyrite-bornite-pyrite-carrollite (with minor secondary copper phases and possible hypogene chalcocite). At the broad scale, the distribution of chalcopyrite effectively mimics Cu-grade, with spiky concentrations near the top and base, contrasting with relatively consistent abundances throughout the main ore zone. Bornite is richest towards the middle and lower parts of the main ore zone, where Cu grades are slightly enhanced. Within the upper part, bornite abundance is noticeably more erratic and drops off abruptly at the top of the main ore zone. Pyrite abundances are erratic throughout and exhibit contradictory relationships with Cu-grades. For example, towards the top and base, pyrite is generally enriched at the expense of Cu abundances (although there are some notable exceptions), whereas within the main ore zone, there is with one exception coincidence of pyrite and Cu-grade spikes (Fig. 2). By contrast, the positive relationship of pyrite with Co is crudely systematic, regardless of position within the ore zone.

In detail, the zonal relationship between the various sulfide mineral phases is considerably more complex than outlined above. Repetitive cycles of pyrite + carrollite → pyrite + chalcopyrite + carrollite → chalcopyrite → chalcopyrite + bornite → bornite occur throughout the ore zone (at least six) and exhibit a crude symmetrical distribution about layer-parallel "veins" or alteration flooding zones (discussed further in the following section). This symmetrical vertical zonation is demonstrated in Figure 2 by the relative abundances of pyrite, chalcopyrite and bornite about the high grade interval at 1300'.

Non-sulfide Phases

Within the main ore zone, quartz and albite (together with other minor silicate minerals) have overprinted the original detrital sandstone fabric (Figs 2, 3). This style of alteration extends well into the footwall of the orebody where it becomes quartz-dominant, but is effectively terminated at the top of the main ore zone, where the lithotype passes from a relatively well sorted sub-arkosic sandstone (*Orebody Quartzite*) to a progressively matrix-enriched, poorly sorted arkose (*Hangingwall Sandstone*). Thus, the distribution of quartz and albite appears in part lithologically controlled. Alteration within the *Hangingwall Sandstone* is dominated by calcite (biotite is also enriched at this level), however outliers of quartz and albite occur at 1233' in the form of coarse clots, producing a pseudo-conglomeratic texture.

Additional phases restricted largely to the main ore zone include tremolite, rutile, phlogopite and a very fine-grained translucent mineral with needle habit interpreted as tourmaline. Biotite, calcite and chlorite are locally abundant, and along with phlogopite probably represent an isochemical metamorphic assemblage, with chlorite and calcite forming a late stage retrogressive phase. Tremolite occurs as isolated, coarse-grained clots of radiating sheaves,

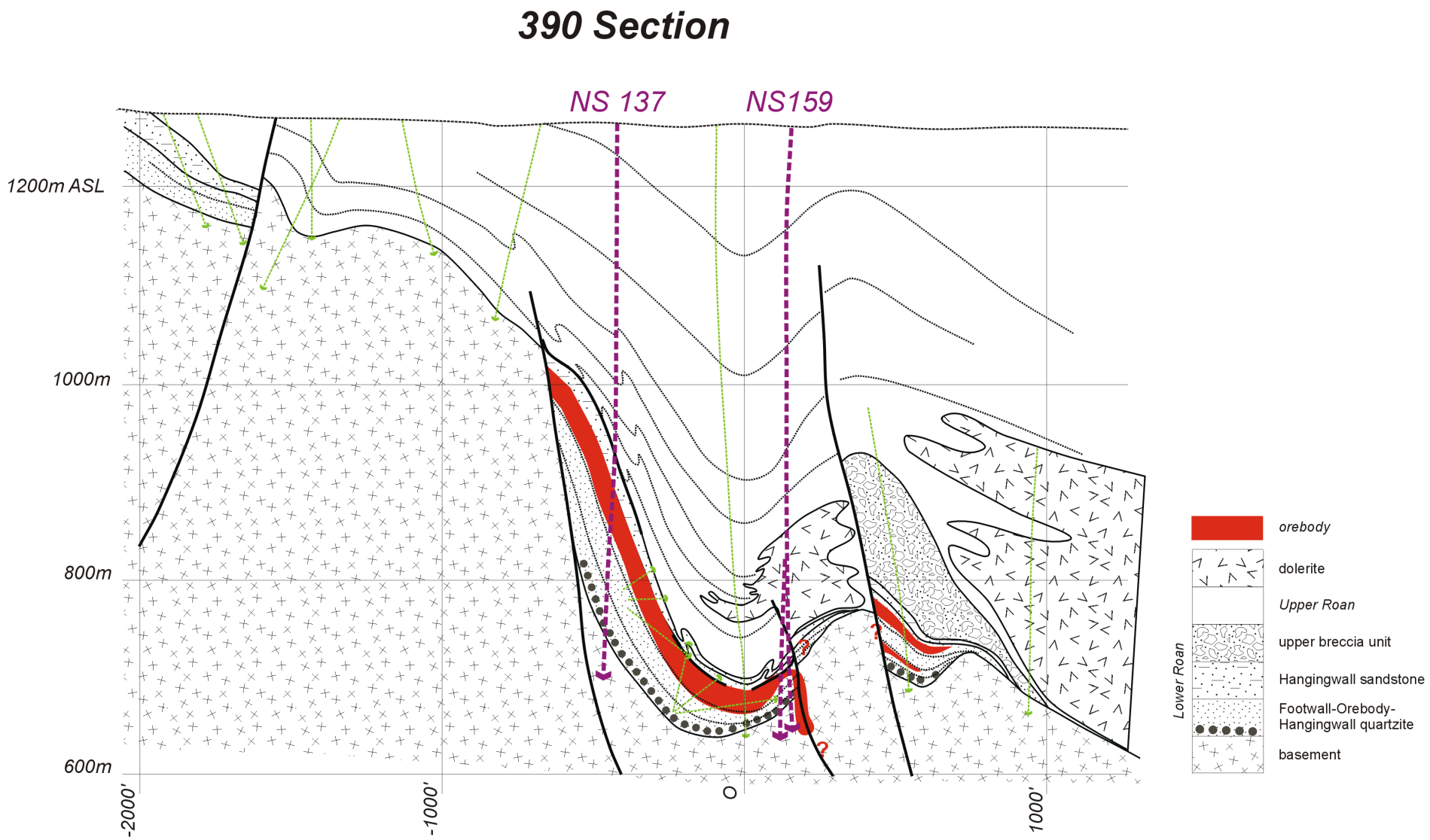

Figure 1
390 section looking WNW and showing drill holes used in this study. Lower Roan strata thickens southward towards interpreted faulted contact with basement inlier. Note lack of Lower Roan strata on crest of basement inlier.

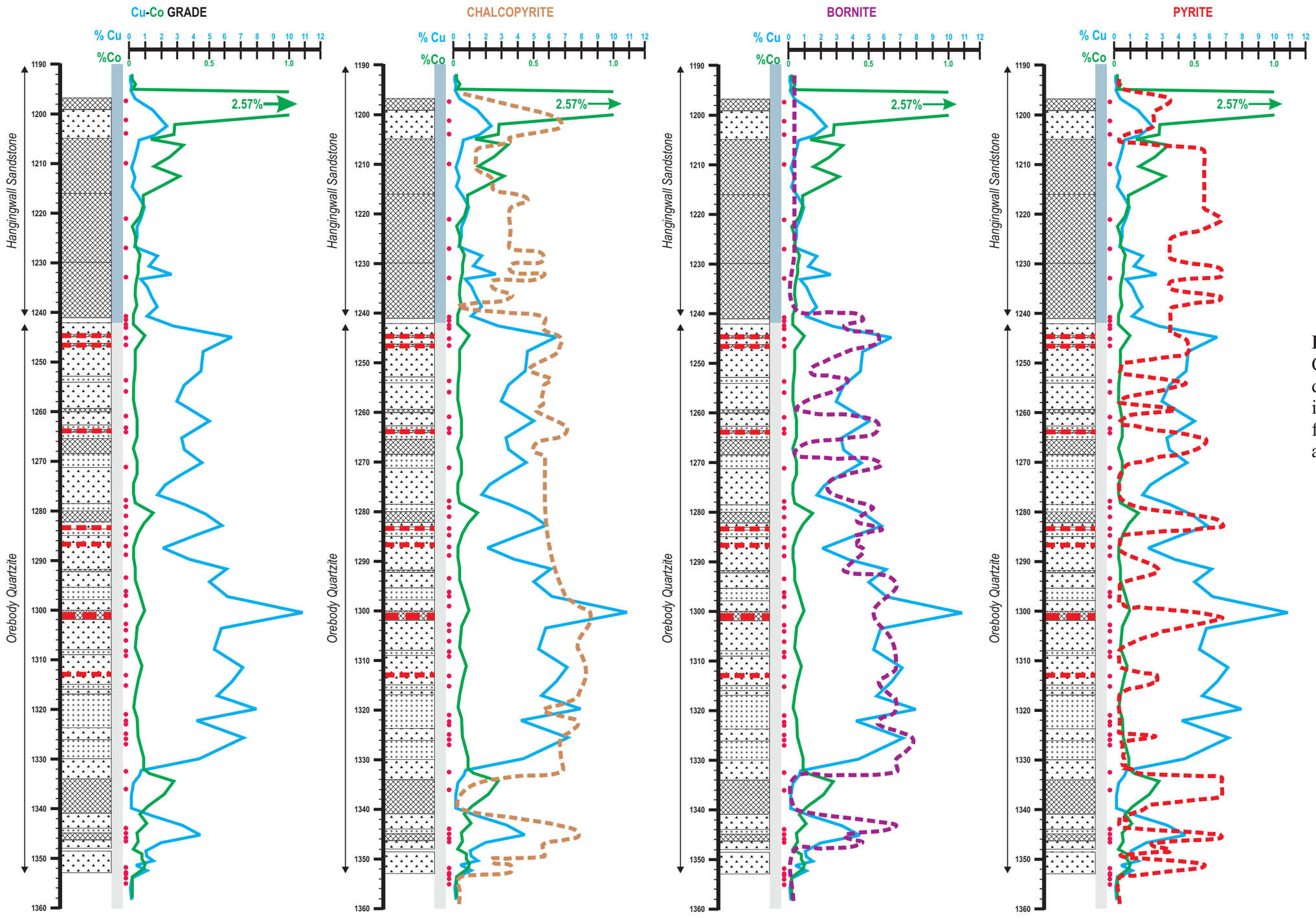

Figure 2
Cu-Co grade and sulfide distribution within mineralised intersection in NS 137. Scale for sulfides abundance is arbitrary.

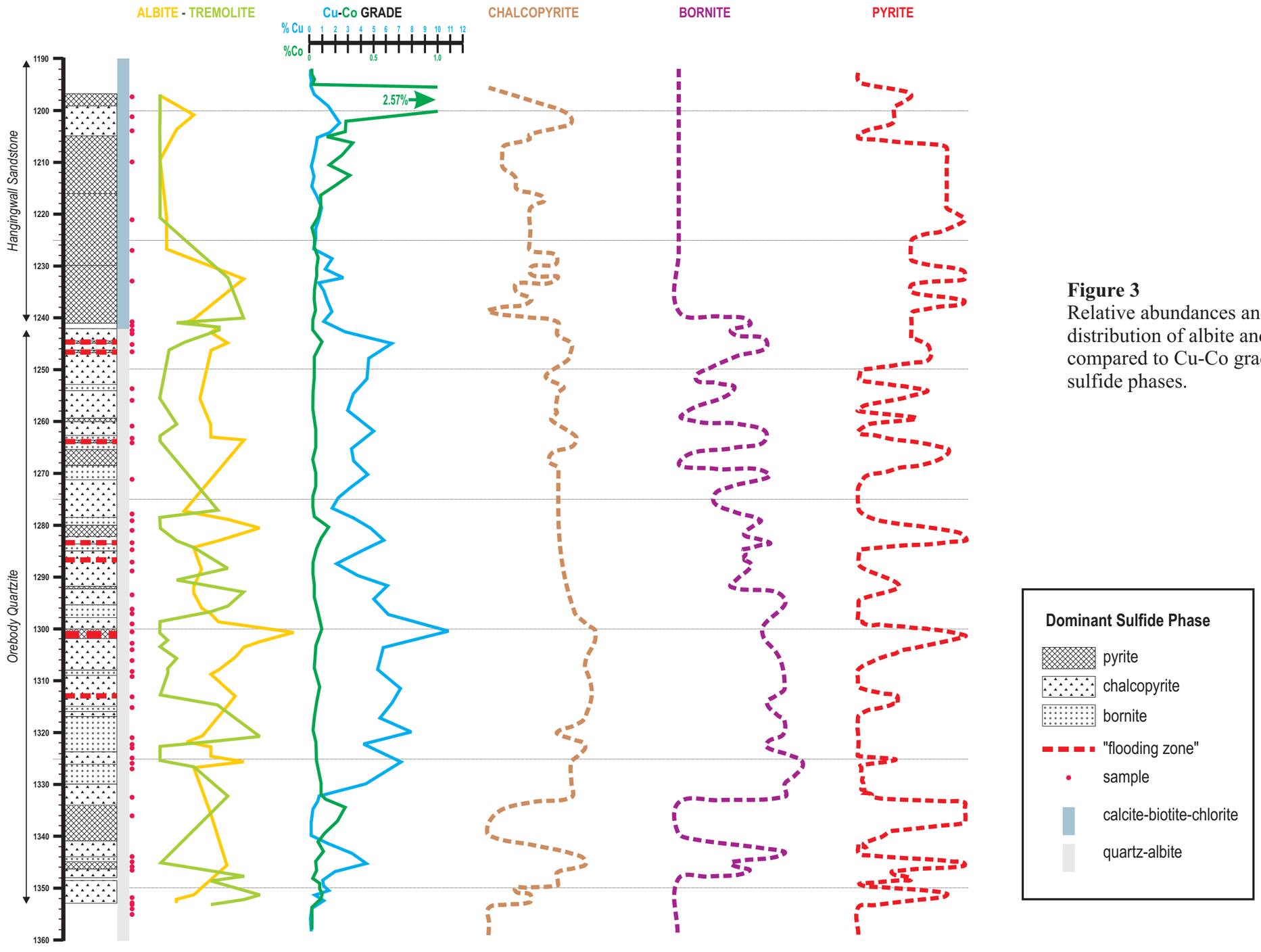

Figure 3
Relative abundances and distribution of albite and tremolite compared to Cu-Co grade and sulfide phases.

concentrated either along relict bedding surfaces or distributed randomly throughout massive sandstone intervals. Although preserved rarely, it is in most cases degraded to phlogopite, calcite, biotite, chlorite and rutile. Tourmaline occurs concentrated within intergranular positions (strongly enhancing original detrital textures), and along fractures within albite.

Vertical zonation of albite and tremolite has been established from thin section and is shown in Figure 3. Tremolite abundances drop off abruptly at the top of the main ore zone, but in a similar fashion to albite, are concentrated within the pseudo-conglomerate layer at 1233'. With the exception of this interval, these two mineral phases exhibit a largely mutually exclusive spatial relationship. Tremolite is concentrated at the peripheries of pronounced albitic spikes at 1346', 1326', 1300', 1280' and a broader albitic domain centred on 1264'. There is also a close relationship between tremolite and albite and both ore grade and sulfide mineral abundances (Fig. 3). Albite peaks display a remarkably consistent positive correlation with those of Cu and to a lesser extent pyrite (the main exception occurring within the upper low grade ore zone). Although elevated Cu-sulfide abundances also coincide with albite peaks, the former show broader peaks which extend both above and below albitic concentrations. This relationship has been confirmed from preliminary examination of thin sections, however the relative distribution shown in Figure 3 may be in part an artefact of sample spacing: i.e. albite abundances were established from closely spaced thin sections, whereas sulfide abundances from company logs were averaged across 3' sampling intervals.

Tremolite, by contrast to albite, concentrates at the peripheries of high grade Cu zones (Fig. 3). There is little evidence of a systematic association with sulfide phase with the exception of a crude negative correlation with pyrite. This relationship breaks down near the base of the hole however, where tremolite and pyrite peaks are broadly coincident. A subtle relationship between tremolite and bornite occurs at the peripheries of the high grade zone centred about 1300', where tremolite peaks coincide with moderate to abrupt negative gradients in bornite content.

Textural characteristics of the ore and mineral paragenesis

Main Ore Zone

A variety of ore textures from the main ore zone in NS 137 are shown in Figure 4. They are immediately distinguishable from those associated with most other Copperbelt deposits by the coarseness of the sulfide phases. Textures range from: (i) disseminated sulfides within structureless sandstone (Fig. 4a, b); (ii) crudely banded sulfides hosted by well-banded sandstone (Fig. 4c); (iii) banded sulfides which mimic primary layering (Fig. 4d); (iv) banded sulfides associated with discrete layer-parallel veins or "flooding zones" (Fig. 4e, f, g); (v) massive sulfides associated with layer-cross cutting veins (Fig. 4h); and (vi) massive sulfide within or at the peripheries of layer-parallel veins (Fig. 4i, j).

Layering within the ore zone

The fundamental control of primary layering on the distribution of sulfides is marked within many of the examples outlined above. Structural reactivation of bedding surfaces is clear in the cases of layer-parallel quartz-albite veins or flooding zones, however where the sulfides are more delicately banded, a structural control is less unequivocal. In thin section, banding is defined by alternating medium grained aggregates of detrital quartz with interstitial secondary albite and quartz, and finer-grained seams. The fine-grained seams are commonly enriched in albite, biotite, detrital zircon, tourmaline and recrystallised rutile and tourmaline (Fig. 5a, b, c). In some cases at least, they were clearly original heavy mineral bands. Tremolite locally exhibits concentration within or immediately adjacent to the seams, where radiating sheaves contain inclusions of zircon and rutile (Fig. 5d).

The internal texture of fine-grained seams is variable. At one end of the spectrum, primary detrital textures of silicate grains appear preserved. This is consistent

with an origin as heavy mineral bands, as coarse quartz (and probably feldspar) grains are expected to have been diluted during the winnowing process. As the component of secondary quartz and albite increases, primary textures are obliterated. The margins of seams become less well defined, and several seams may coalesce to form broader, tabular to irregular fine-grained bands or clots. In such cases, albite in particular is intensely fractured, with fine tourmaline concentrated along fracture surfaces (Fig. 5e–h). Evidence for rotation of grains is very limited, suggesting that displacement along the seams was insignificant. Slip along bedding surfaces appears largely restricted to high grade zones, where the fine grainsize of the seams is clearly attributable to cataclasis imposed upon originally coarse-grained aggregates of albite and quartz. In rare cases, a layer-parallel shear cleavage occurs within the re-crystallised periphery of the seams (Fig. 6a).

Veins and "flooding zones" appear transitional to layer-parallel seams in terms of their textural characteristics. They are distinguished mainly on the bases of their dimensions (up to 5 cm wide) and pervasively destructive alteration. Flooding zones are generally tabular and comprise coarse-grained albite, with subordinate quartz, calcite, biotite and tourmaline (Fig. 6b, c). Fracturing of albite is ubiquitous, however as with many of the seams, there is little evidence of displacement. Selvages of the flooding zones are also texturally destructive, comprising recrystallised coarse-grained quartz with lesser albite. Veins are defined where distinct internal mineral zonation is developed. The best example occurs in the centre of the high grade Cu-interval at 1300.5' (Fig. 4j). Here, the vein consists of a coarse-grained quartz-calcite core, with peripheral albite, largely replaced by massive chalcopyrite. Quartz within the core has a crude fibrous habit and is itself deformed, with ubiquitous undulose extinction and minor grain fracturing. Relict "islands" of albite within the chalcopyrite selvage are enriched in detrital zircon, tourmaline and recrystallised rutile, indicating emplacement along a heavy mineral band (Fig. 6d–f). The margins of the vein comprise cataclastically deformed sandstone, with a minor heavy mineral component.

Sulfide distribution and paragenesis

We have recognised a systematic paragenesis of sulfide phases throughout the main ore zone: ie. pyrite → carrollite → chalcopyrite + bornite. Where pyrite occurs with other sulfide phases, it is generally corroded and forms the nucleus for later sulfide growth. Carrollite, albeit difficult to distinguish from pyrite in many cases, occurs as isolated euhedral crystals, but more commonly forms overgrowths on pyrite (Fig. 7a, b). Chalcopyrite forms anhedral overgrowths on pyrite and carrollite (Fig. 7a), but also occurs as isolated irregular masses in high grade zones. Paragenetic associations between chalcopyrite and bornite are more complicated. In most examples,

Figure 4
(a) Coarse-grained subhedral pyrite hosted within massive sandstone. Sample 1336'.
(b) Coarse-grained subhedral pyrite and carrollite (red arrow), overgrown by irregular chalcopyrite (yellow arrow). Sample 1332'.
(c) Banded sandstone. Dark layers are finer grained and concentrated in albite. Note clots of tremolite a crude alignment of sulfides at peripheries of fine-grained layers. Sample 1289'.
(d) Well banded "stratiform" chalcopyrite ore. Minor pyrite in bottom left hand corner. Sample 1299'.
(e) Banded "stratiform" ore with alternating bands of chalcopyrite and bornite at periphery of wider layer-parallel chalcopyrite-pyrite-albite "flooding zone". Sample 1292'.
(f) Banded "stratiform" ore with symmetrical zonation about sulfide-rich flooding zone. Sample 1306'.
(g) Narrow chalcopyrite-pyrite "flooding zone" with crude symmetrical zonation at its fringes from chalcopyrite + bornite to bornite. Sample 1283.5'.
(h) Chalcopyrite-albite "flooding zone" cross-cutting primary layering. Note zonation at margin of "flooding zone" to chalcopyrite + bornite. Sample 1303'.
(i) Massive banded chalcopyrite-pyrite-albite within selvage of layer-parallel vein. Sample 1346'.
(j) Massive chalcopyrite-pyrite-carrollite-albite (red arrow) at margins of layer-parallel quartz-calcite vein. Sample 1300.5'.


(a)
MM
0
10


(b)
MM
0
10


(c)
0 CM 1


(d)
0 CM 1

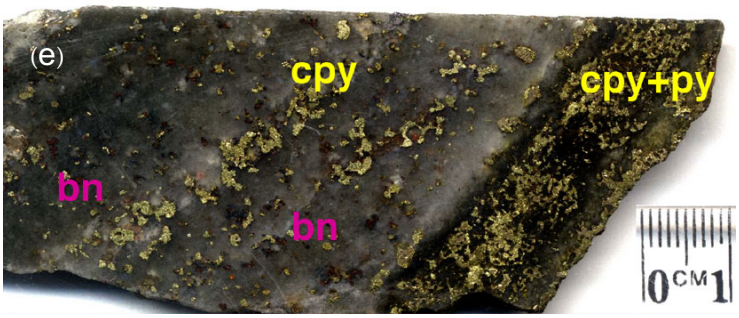
(e)
cpy
cpy+py
bn
bn
0 CM 1

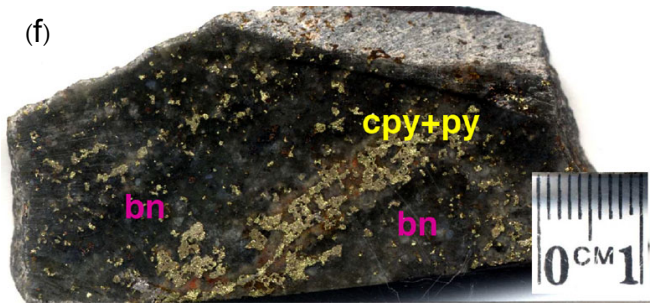
(f)
cpy+py
bn
bn
0 CM 1

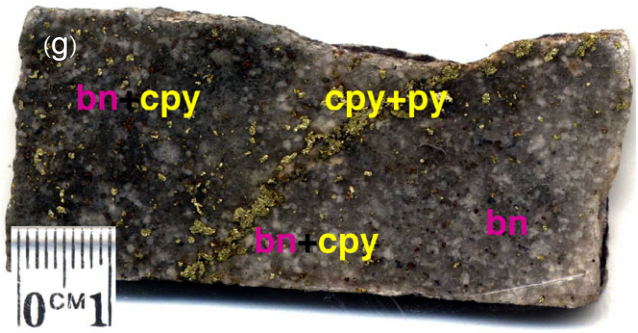
(g)
bn+cpy
cpy+py
bn+cpy
bn
0 CM 1

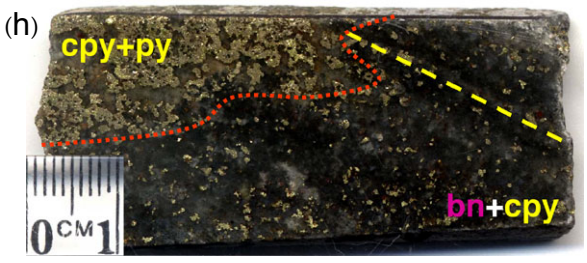
(h)
cpy+py
bn+cpy
0 CM 1


(i)
MM
0
10

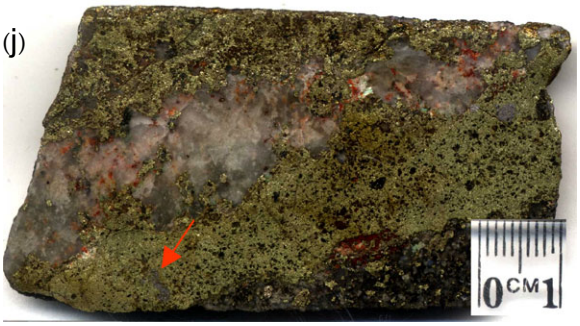
(j)
0 CM 1

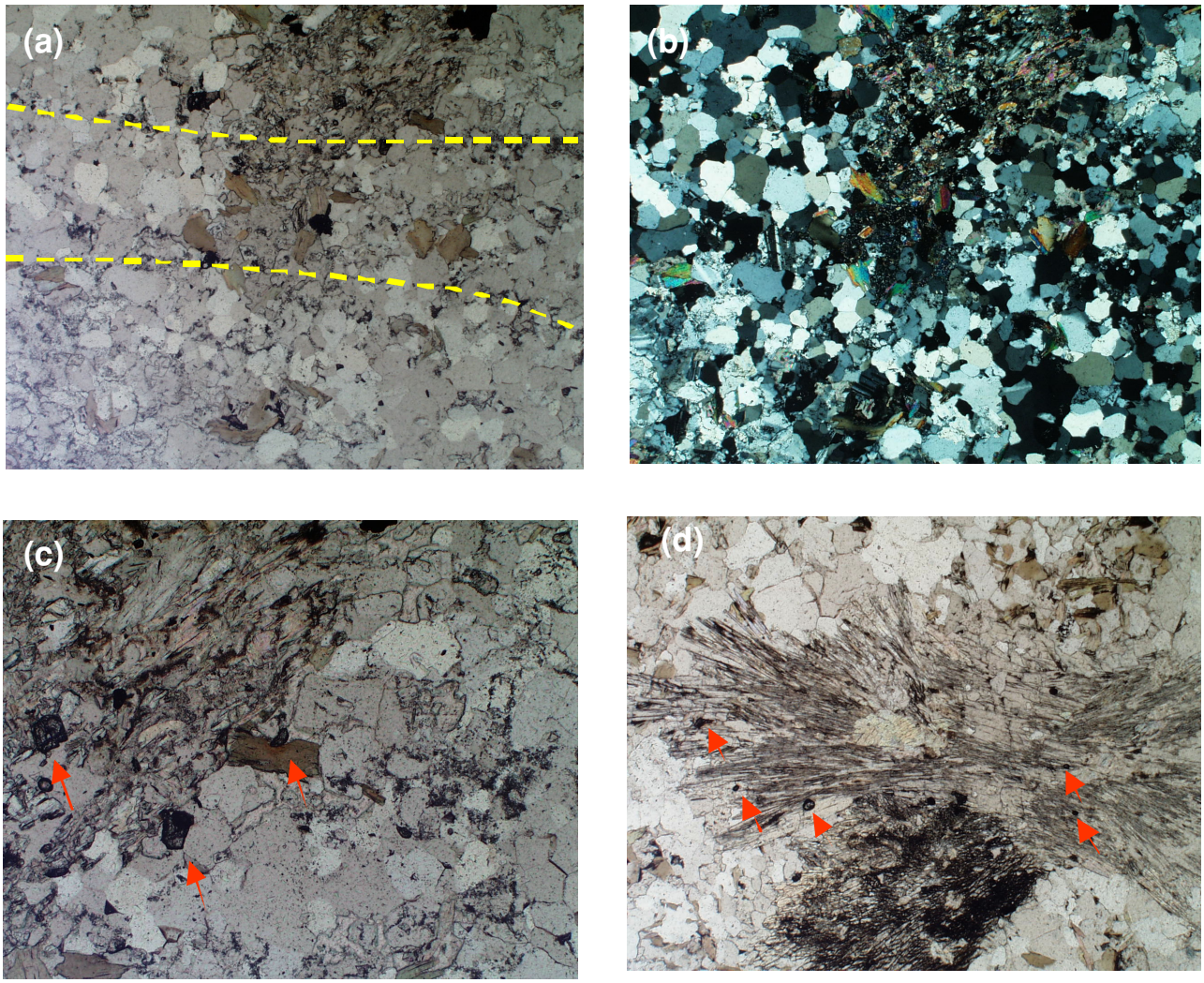

Figure 5
(a & b) Subtle fine-grained layers, with enrichment of albite, biotite and heavy minerals. Tremolite, degraded to phlogopite, calcite and biotite, cross-cuts seam. Width of view 3.75mm. Sample 1332′.
(c) Detail of fine-grained band in (a) showing concentration of detrital zircon (arrows). Width of view 2mm. Sample 1332′.
(d) Radiating sheaves of tremolite containing numerous small zircons (arrows). Width of view 3mm. Sample 1352′.

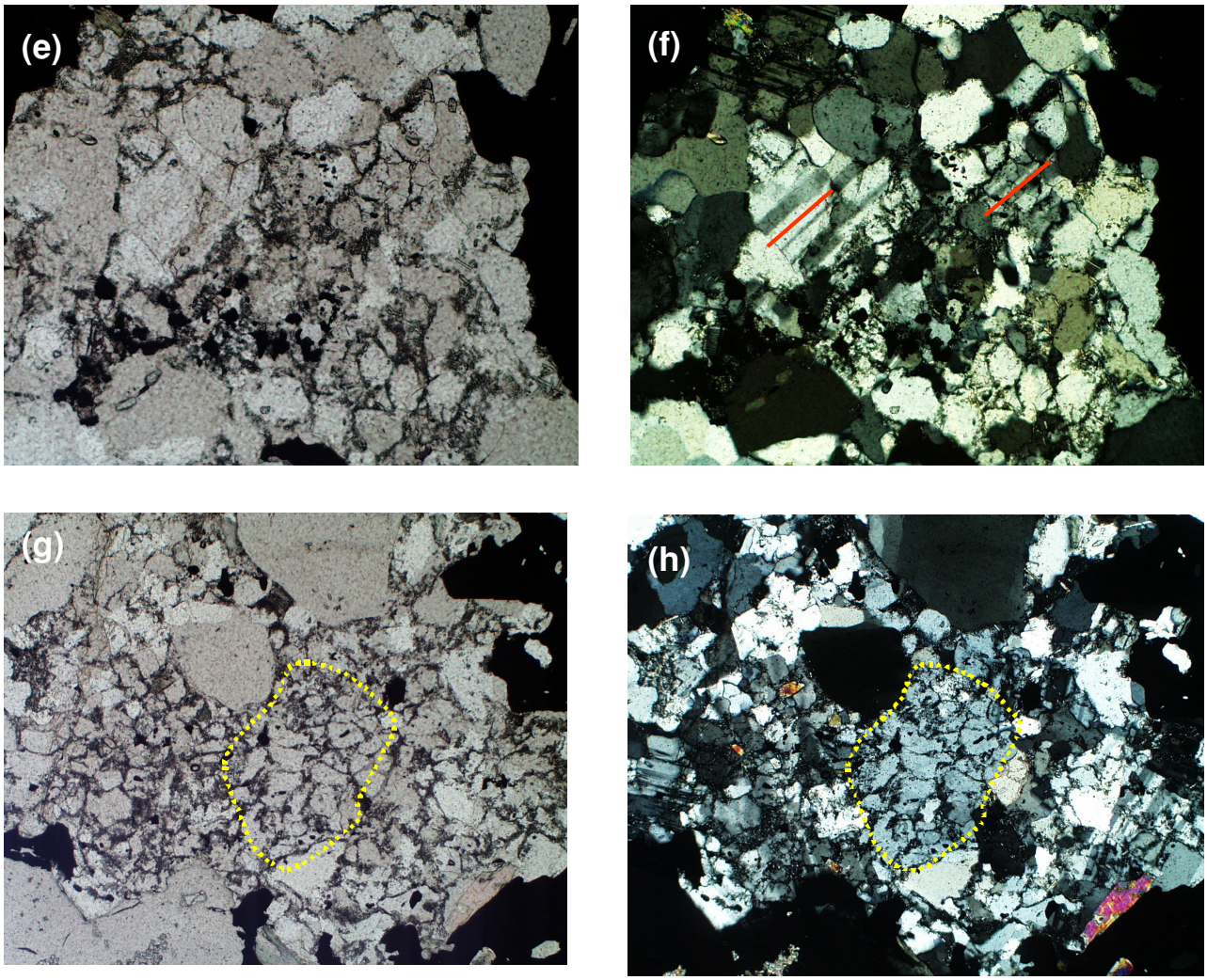

Figure 5 cont.
(e & f) Cataclastically deformed albite grain within layer-parallel seam. Note optical continuity of fragments (red lines on twin planes) and overgrowth by quartz. Width of view 1.25mm. Sample 1303'.
(g & h) Grain-size reduction along layer-parallel seam. Yellow line encloses an aggregate of quartz fragments, all of which show optical continuity, indicating derivation from a single, coarse parent grain. Width of view 2mm. Sample 1303'.

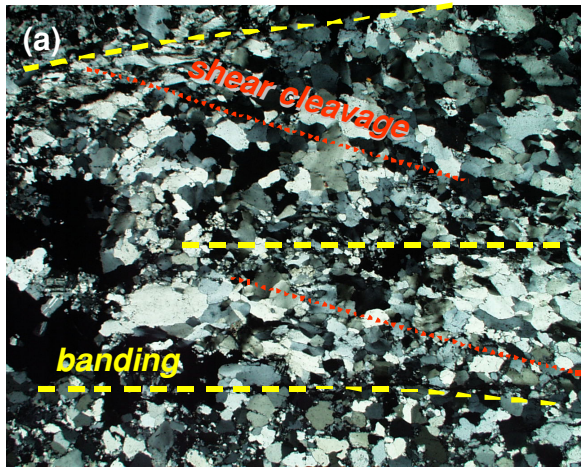

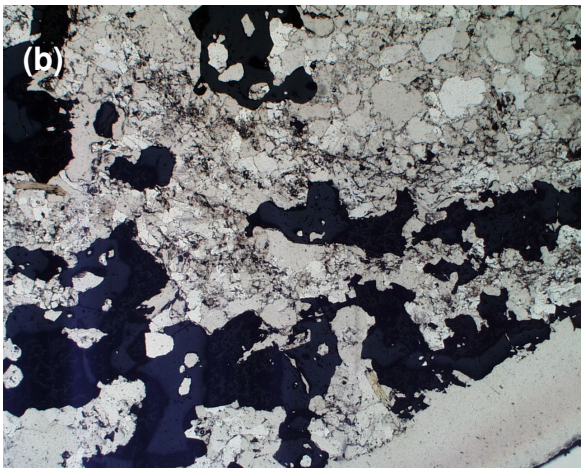

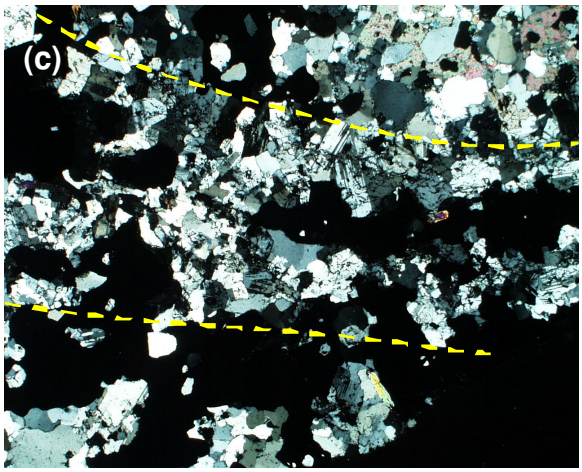

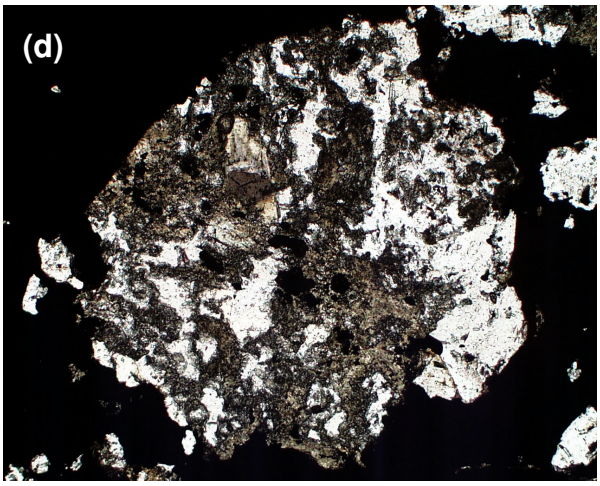

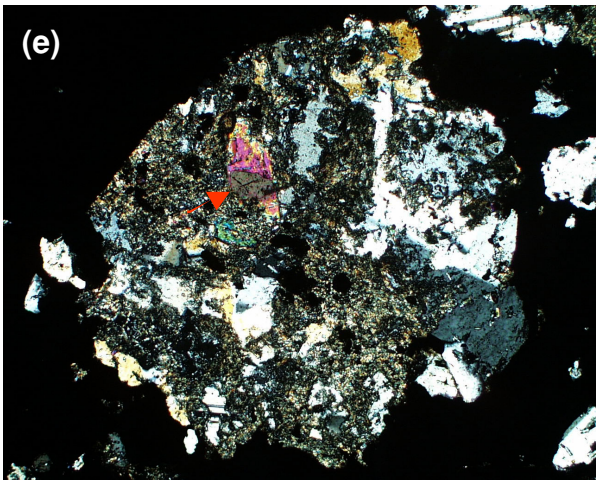

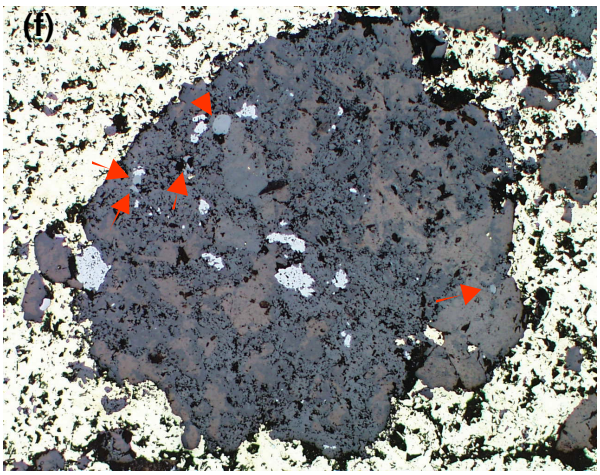

Figure 6
(a) Rare evidence for displacement along bedding surfaces. A locally intense alignment of elongate recrystallised quartz grains is occurs slightly oblique to layering. This fabric is restricted to the immediate peripheries of fine-grained bands. Width of view 6 mm. Sample 1245'.
(b, c) Tabular "flooding zone" comprising albite-chalcopyrite-pyrite, minor quartz and biotite. Note pervasive fracturing of albite grains. Width of view 6 mm. Sample 1306'.
(d-f) Enclave of degraded albite within massive chalcopyrite at selvage of quartz-calcite vein. Albite replaced by calcite, biotite and chlorite. Note anomalously high heavy mineral component: ie detrital tourmaline, arrow in (e); zircon, arrows in (f); recrystallised rutile, lighter grey reflective material within enclave in (f). Width of view 2 mm. Sample 1300.5'.

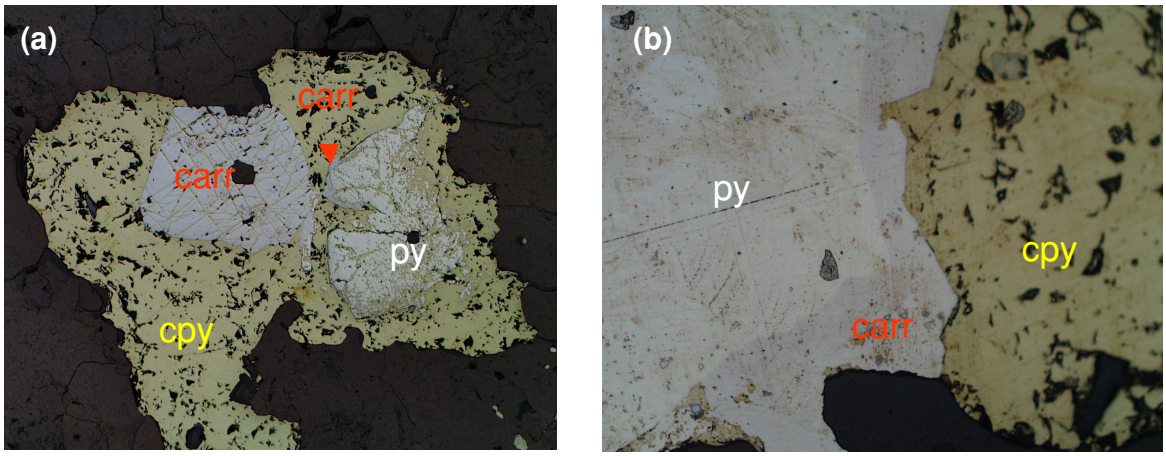

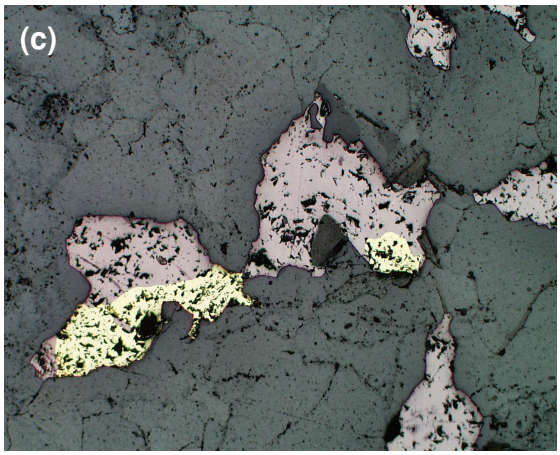

Figure 7
(a) Heavily corroded pyrite, rimmed by carrollite and chalcopyrite. The subhedral carrollite grain on the left is replaced by chalcopyrite along fractures. Width of view 1.6mm. Sample 1352'.
(b) Progressive overgrowth from left to right of pyrite by carrollite which is turn overgrown by chalcopyrite. Width of view 0.5mm. Sample 1352'.
(c) Irregular sulfide grains containing intergrowth of bornite and chalcopyrite. The grains are partly contained within intergranular sites of the sandstone framework. Width of view 2mm. Sample 1327'.
(d, e) Concentration of chalcopyrite and pyrite within narrow albite-quartz flooding zone. Width of view 6mm. Sample 1292'.
(f, g) Intergrowth of bornite and chalcopyrite dispersed throughout framework of medium grained sandstone with good preservation of detrital fabric. Width of view 6mm. Sample 1292'.

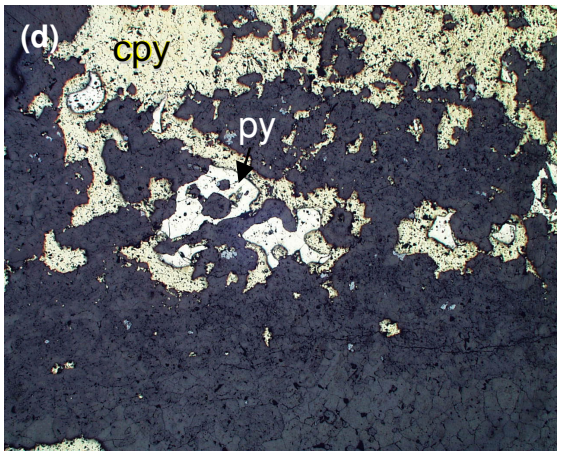

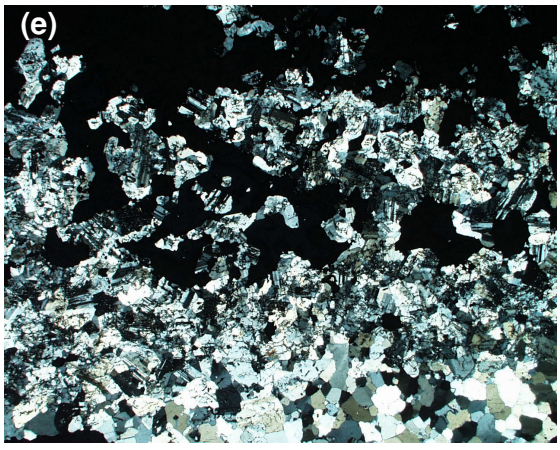

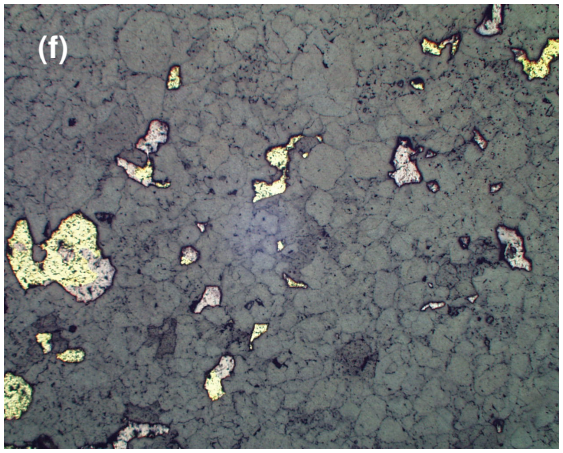

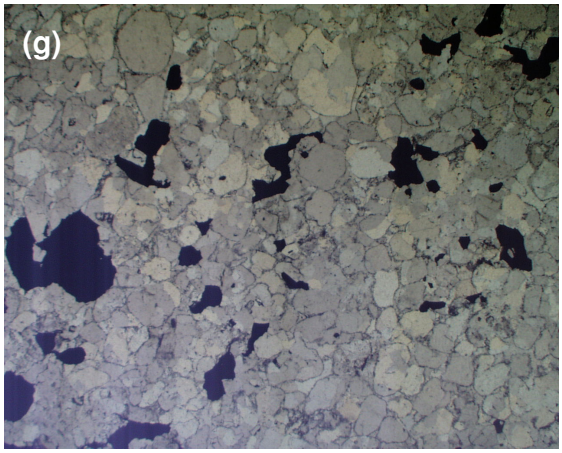

bornite and chalcopyrite appear in textural equilibrium, forming globular grains which generally occupy intergranular spaced between detrital quartz and/or secondary albite grains (Fig. 7c). Rarely, however, bornite is concentrated at the margins of chalcopyrite grains and demonstrate a crude overprinting relationship.

Zonation of sulfide phases is commonly pronounced both at the large scale (as demonstrated in the previous sections) and the meso-scale. At the finest scale, chalcopyrite ± pyrite and bornite ± chalcopyrite form sub-cm rhythmic layer-parallel alternations such as shown in Figure 4e. In these zones, chalcopyrite rich domains coincide with narrow albite-quartz flooding seams (Fig. 7d, e), whereas detrital textures are better preserved within more disseminated bornite-rich domains (Fig. 7f, g). Broader mineral zonation occurs about major flooding zones and veins. In Figure 4f & g, albitic flooding zones are bounded by a crude symmetrical zonation from chalcopyrite + pyrite + carrollite → chalcopyrite →bornite + chalcopyrite over a distance of 2 cm. The density of sulfide mineral decreases outward from the core of the flooding zones. Within the highest grade part of the ore zone (centred on 1300': Fig. 2) a 3' thick interval (true thickness) consists of a dense array of veins and flooding zones. The sulfide mineral assemblage throughout this interval is dominated by chalcopyrite and pyrite, with subordinate carrollite. Bornite is very sparsely distributed within the interval, but becomes the dominant mineral phase above 1298' and below 1308'.

Although a spatial association of sulfides and albite occur at all scales, from individual grains of chalcopyrite or pyrite enclosing albite to the broad coincidence of these phases at the scale of the entire orebody, temporal relationships are unclear. This is primarily due to the irregular habit of the Cu-sulfide grains and the consequent difficulty in distinguishing intergrowth from overgrowth relationships with albite. That Cu-sulfides display symmetrical zonation about albitic veins and flooding zones, provides evidence for a coeval relationship. In detail however, Cu-sulfides almost always enclose irregular relict albite grains, possibly indicating an overgrowth relationship. It is thus possible that the fluids from which albite and Cu-sulfides were precipitated shared a common pathway, but changed composition with time.

The relationship between ?metamorphic biotite and Cu-sulfides is similarly unclear. There is commonly an increased abundance of biotite with chalcopyrite in particular, however definitive intergrowth textures were not seen. Biotite generally occurs along the outer margins of sulfides, indicating growth was either coeval with, or post-dated sulfide precipitation.

Upper Ore Zone

Mineralisation within the upper ore zone is predominantly controlled by quartz-calcite veins oriented at relatively high angles to layering. Detrital assemblages are enclosed within a groundmass replaced largely by calcite, biotite and chlorite. Transition from the lower albite-quartz zone is abrupt and defined by progressive replacement of intergranular albite by calcite, with gross preservation of original layering (Figs 8, 9a, b). Immediately above the transition, the primary lithotype changes to an effectively undeformed matrix-rich sandstone. Rare quartz-albite clots occur at 1233', producing a pseudo-conglomeratic texture (Fig. 8b) and coinciding with a slight elevation of Cu-grade (Fig. 3). Sulfides within this zone include pyrite and minor chalcopyrite, contained largely within or at the peripheries of quartz-albite clots (Fig. 9c). Those which occur within the framework of the sandstone occupy intergranular positions between detrital quartz and feldspar (Figs 8b, 9d, e). Matrices of mineralised framework domains are distinguishable from unmineralised domains by the presence of calcite and biotite intergrown with the sulfides.

Vein density increases within the upper Co-Cu rich zone (1205–1197'), with pyrite and chalcopyrite concentrated within the selvages of cross-cutting pink calcite veins (Fig. 8c). The Co-peak coincides with a zone of dense quartz-calcite veins containing largely

pyrite + carrollite, with minor chalcopyrite and very rare bornite (Fig. 8d). Sulfide paragenesis is broadly comparable with that of the main ore body, however carrollite and pyrite boundaries are considerably more complicated, indicating potential intergrowth of the two phases.

Summary

In terms of their distribution, sulfide phases within the main orebody are strongly controlled by primary layering. At scales or sub-cm to 1m, symmetrical mineral zonation occurs about layer-parallel to slightly layer-oblique fracture seams, flooding zones and veins. The cores of these layer-parallel domains are concentrated in pyrite-chalcopyrite-carrollite and pass outward through zones of chalcopyrite to chalcopyrite and bornite.

Albite shows a strong spatial (and possibly temporal) relationship with sulfides at all scales. It is concentrated within bedding-parallel seams, fracture seams, flooding zones and veins, but also occurs within intervening domains, either interstitially or as overgrowths on detrital grains. Albite coincides with high grade Cu-zones and its distribution is thought to define sites of infiltration of the Cu-bearing fluid. The common association of albitic zones and detrital heavy mineral phases, indicates that heavy mineral bands provided favourable sites of fluid movement.

Tremolite shows a mutually exclusive spatial association with albite and concentrates at the limits of high grade Cu-mineralisation. It is likely to represent mineral growth at the upper and lower peripheries of the fluid systems.

Fluid pathways appear predominantly fracture controlled, although passive dissolution of intergranular material is likely to have provided secondary permeability within intervening, coarser-grained layers as well as low strain heavy mineral bands. The latter mechanism is likely to account for the domains of intergranular sulfide precipitation within the upper orebody. Despite the locally high density of grain fracturing, there is little evidence for significant displacement along bedding surfaces. We envisage that bedding surfaces became dilatant during inversion, in response to buttressing of thickened Lower Roan strata against uplifted basement blocks (see Selley & Bull, this volume). Heavy mineral bands potentially acted as sites of rheological weakness during dilation. The abrupt upper contact of the main ore zone may also be a function of rheology: ie transition from relatively clean, closed framework sandstone to matrix-rich sandstone and gritty siltstone.

The association of Cu-sulfides and heavy mineral bands is a common phenomenon with Copperbelt deposits. Heavy minerals, in particular ilmenite, may provide the localised reductant required to precipitate copper. In support of this interpretation is the observation that detrital Fe-Ti oxides are not preserved: i.e. rutile is ubiquitously recrystallised. However, mobile hydrocarbons cannot be discounted as another potential reductant at this stage.

Sulfur Isotopes

Sulfur isotope analyses of pyrite, chalcopyrite and bornite from Chibuluma have been undertaken to:

- test whether the observed vertical mineralogical zonation at Chibuluma is matched by zonation of the sulfur isotopic compositions of sulfide minerals,
- evaluate whether sulfur isotope compositions in combination with textural analysis can provide insights into sulfur sources and metal deposition mechanisms both at Chibuluma and elsewhere in the copper belt.
- establish whether sulfide mineral pairs from Chibuluma can be used to determine the temperatures of sulfide deposition using sulfur isotope geothermometry.

Previous work

In their comparative study of sulfur isotope compositions from a number of Central African

copper deposits, Dechow and Jensen (1965) analysed 17 composite sulfide samples from Chibuluma (Figs 10, 11). They obtained results ranging from +6.3 to +16.1‰. At Chibuluma, lighter isotopic compositions were found to characterise the central pyrite zone and the centre of the orebody (+6.3 to +12.7‰). The sulfides most enriched in ^{34}S were found to occur on the western limits of the deposit (+10.2 to +16.2‰). The eastern limits were also enriched in ^{34}S relative to the central zone (+12.5 to +14.2‰). Dechow and Jensen (1965) found that sulfides from Chibuluma have the heaviest average sulfur isotopic compositions of any of the 'stratiform' copper deposits that they studied from the Lufulian arc (Fig. 10). They also noted that Chibuluma and other deposits on the western side of the arc are characterised by ^{34}S-enrichment, whereas those on the east are enriched in ^{32}S.

Sweeney et al. (1996) undertook a detailed stable isotope study of the Konkola system, where they found that chalcopyrite and carollite had $\delta^{34}S$ values of –7.0 to +1.2‰ (Fig. 12). These compositions were attributed to bacterial reduction of seawater sulfate. A correlation was demonstrated between sulfide isotopic compositions and the stratigraphic position of the sample (Fig. 13). Sweeney et al. (1996) attributed the light isotopic compositions to rocks associated with marine transgressions, and heavy compositions to marine regressions. No evidence was found for metamorphic re-equilibration of sulfur isotope compositions. Instead, an early diagenetic timing of sulfate reduction and ore deposition was advocated, and stratigraphic variations in sulfur isotopic compositions were attributed to sedimentological variations in the host sequence (transgression vs regression).

Methodology

In the current study, the sulfur isotopic compositions of sulfide minerals have been analysed by laser ablation at the University of Tasmania using the procedure outlined in Huston et al. (1995). Results are expressed in the standard δ (‰) notation relative to the Canon Diablo Troilite (CDT). Where possible, two grains were analysed of each hypogene sulfide phase (pyrite, chalcopyrite, bornite). Although carrollite was present in several samples, it was not analysed, as no laser ablation fractionation factor has been determined for this mineral due to the lack of a suitable standard. Analytical precision (1σ) was between 0.007 and 0.058‰. All results are listed in Table 1.

Results

Sulfide grains from a total of eight samples have been analysed for their sulfur isotopic compositions. Six of these samples were taken from drillhole NS137 (Orebody quartzite and hangingwall sandstone; Figs 1, 2), one from NS159D1 (mylonitic granite basement; Fig. 1) and one from NS159D2 (hangingwall tremolite-quartz rock; Fig. 1). Analyses of the sulfur isotopic compositions of 39 individual sulfide grains yielded the following results (Table 1):

- Pyrite: +6.56 to +14.78 ‰ (n = 16)
- Chalcopyrite: +3.47 to +14.45 ‰ (n = 17)
- Bornite: +9.91 to +13.03 ‰ (n = 6)

Figure 13 illustrates that the total range of isotopic compositions analysed during this study (+3.47 to +14.78‰) are consistent with the data obtained from composite sulfide samples analysed by Dechow and Jensen (1965). Note, however, that we have obtained Dechow and Jensen's entire spread of isotopic compositions from one vertical section through the orebody (NS137: Table 1). This contrasts with Dechow and Jensen's (1965) claim that the heavy sulfur occurs on the western margin of the deposit, and light sulfur in the core of the system.

Significant compositional variations were detected between grains of the same mineral in any given sample. Isotopic compositions varied from 0.4‰ to 5.4‰ for any given pair of mineral analyses (Table 1).

Spatial variations in isotopic compositions

Figures 15 and 16 show the sulfur isotopic compositions of sulfides from drillhole NS137 as a function of drillhole depth. Even though sulfides from only six samples have been analysed from this drillhole,

Table 1
Laser ablation sulfur isotopic analyses of sulfide grains from Chibuluma. PY(CP) indicates that some chalcopyrite was ablated in addition to the pyrite grain.

Drillhole	Depth (ft)	Analysis	Material	$\delta^{34}S$	error	Lithology
NS137	1233	1A	pyrite	14.44	0.021	Hangingwall Sandstone
NS137	1233	1B	pyrite	14.78	0.013	Hangingwall Sandstone
NS137	1233	2A	chalcopyrite	10.85	0.015	Hangingwall Sandstone
NS137	1233	2B	chalcopyrite	11.61	0.030	Hangingwall Sandstone
NS137	1292	1A	pyrite	11.81	0.047	Orebody quartzite
NS137	1292	1B	chalcopyrite	10.92	0.014	Orebody quartzite
NS137	1292	2A	pyrite	12.39	0.013	Orebody quartzite
NS137	1292	2B	chalcopyrite	10.26	0.015	Orebody quartzite
NS137	1299	1A	bornite	10.39	0.013	Orebody quartzite
NS137	1299	1B	chalcopyrite	9.03	0.038	Orebody quartzite
NS137	1299	1C	pyrite	9.98	0.020	Orebody quartzite
NS137	1299	2A	pyrite	13.84	0.006	Orebody quartzite
NS137	1299	2B	chalcopyrite	14.45	0.046	Orebody quartzite
NS137	1299	2C	bornite	11.27	0.028	Orebody quartzite
NS137	1304	3A	bornite	13.03	0.012	Orebody quartzite
NS137	1304	3B	chalcopyrite	13.49	0.012	Orebody quartzite
NS137	1304	4A	bornite	9.91	0.040	Orebody quartzite
NS137	1304	2A	pyrite	11.91	0.007	Orebody quartzite
NS137	1304	4B	chalcopyrite	12.77	0.008	Orebody quartzite
NS137	1304	2B	pyrite	14.03	0.017	Orebody quartzite
NS137	1308	1A	bornite	11.64	0.012	Orebody quartzite
NS137	1308	1B	chalcopyrite	13.29	0.012	Orebody quartzite
NS137	1308	1C	pyrite	13.53	0.012	Orebody quartzite
NS137	1308	2A	bornite	12.16	0.025	Orebody quartzite
NS137	1308	2B	pyrite	14.24	0.009	Orebody quartzite
NS137	1308	2C	chalcopyrite	11.76	0.021	Orebody quartzite
NS137	1346	1A	pyrite	6.56	0.007	Orebody quartzite
NS137	1346	1C	pyrite	7.09	0.007	Orebody quartzite
NS137	1346	1D	chalcopyrite	3.47	0.019	Orebody quartzite
NS137	1346	2A	chalcopyrite	5.72	0.008	Orebody quartzite
NS159-D1	1944	1A	PY(CP)	11.70	0.020	Mylonitic granite (basement)
NS159-D1	1944	2A	chalcopyrite	12.04	0.014	Mylonitic granite (basement)
NS159-D1	1944	3A	chalcopyrite	12.56	0.017	Mylonitic granite (basement)
NS159-D1	1944	3B	chalcopyrite	12.12	0.016	Mylonitic granite (basement)
NS159-D2	1809	1A	chalcopyrite	9.48	0.048	Hangingwall Sandstone
NS159-D2	1809	1B	chalcopyrite	7.10	0.057	Hangingwall Sandstone
NS159-D2	1809	2A	pyrite	13.06	0.011	Hangingwall Sandstone
NS159-D2	1809	2B	pyrite	12.10	0.011	Hangingwall Sandstone
NS159-D2	1809	3A	pyrite	12.58	0.020	Hangingwall Sandstone

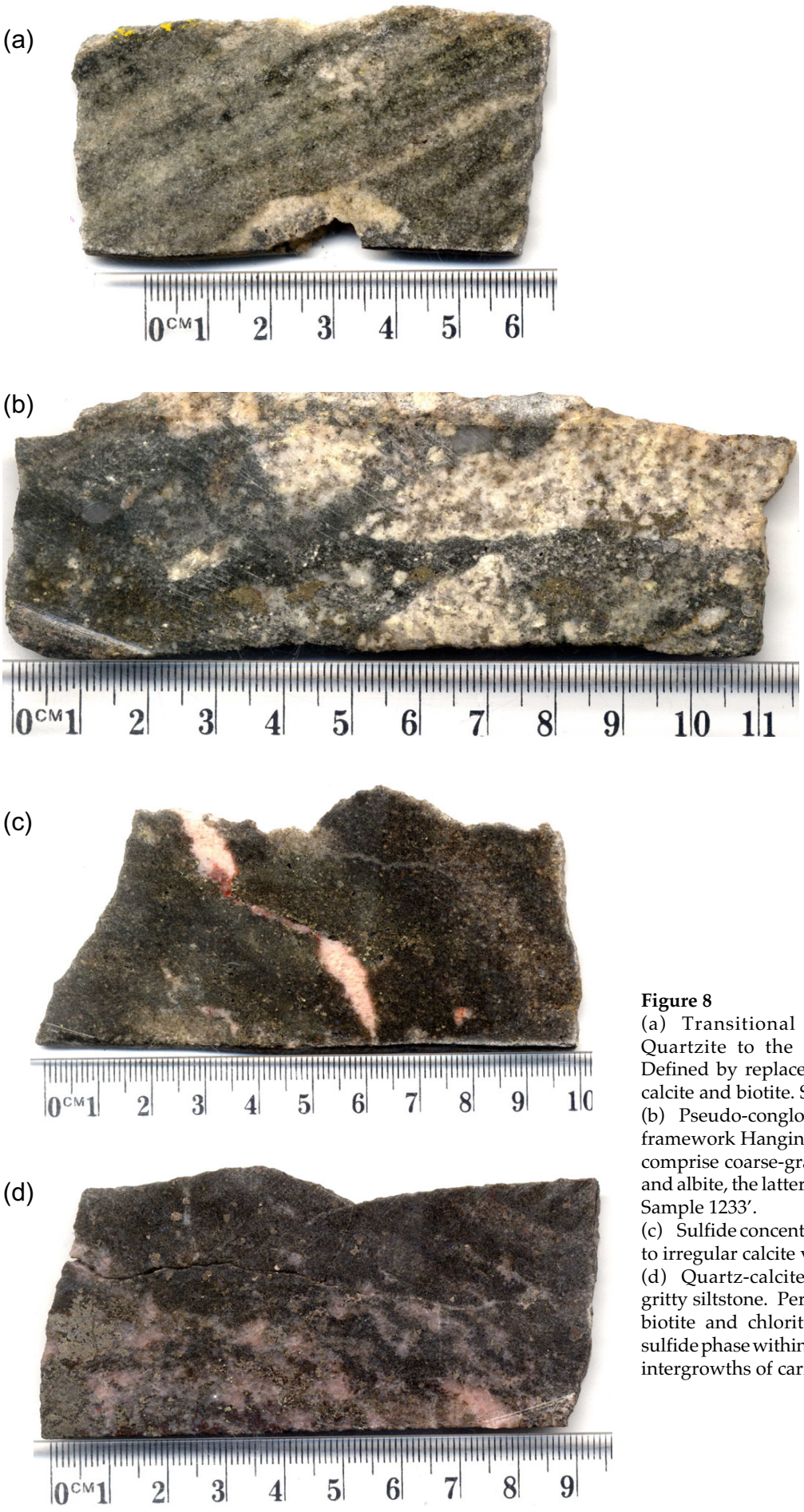

Figure 8
(a) Transitional zone from the Orebody Quartzite to the Hangingwall Sandstone. Defined by replacement of albitic cement by calcite and biotite. Sample 1241′.
(b) Pseudo-conglomerate texture within open framework Hangingwall Sandstone. "Clasts" comprise coarse-grained aggregates of quartz and albite, the latter largely replaced by calcite. Sample 1233′.
(c) Sulfide concentrated within narrow selvage to irregular calcite vein. Sample 1210′.
(d) Quartz-calcite vein within fine-grained gritty siltstone. Pervasive alteration to calcite, biotite and chlorite. The abundant silvery sulfide phase within the vein comprises delicate intergrowths of carrollite and pyrite.

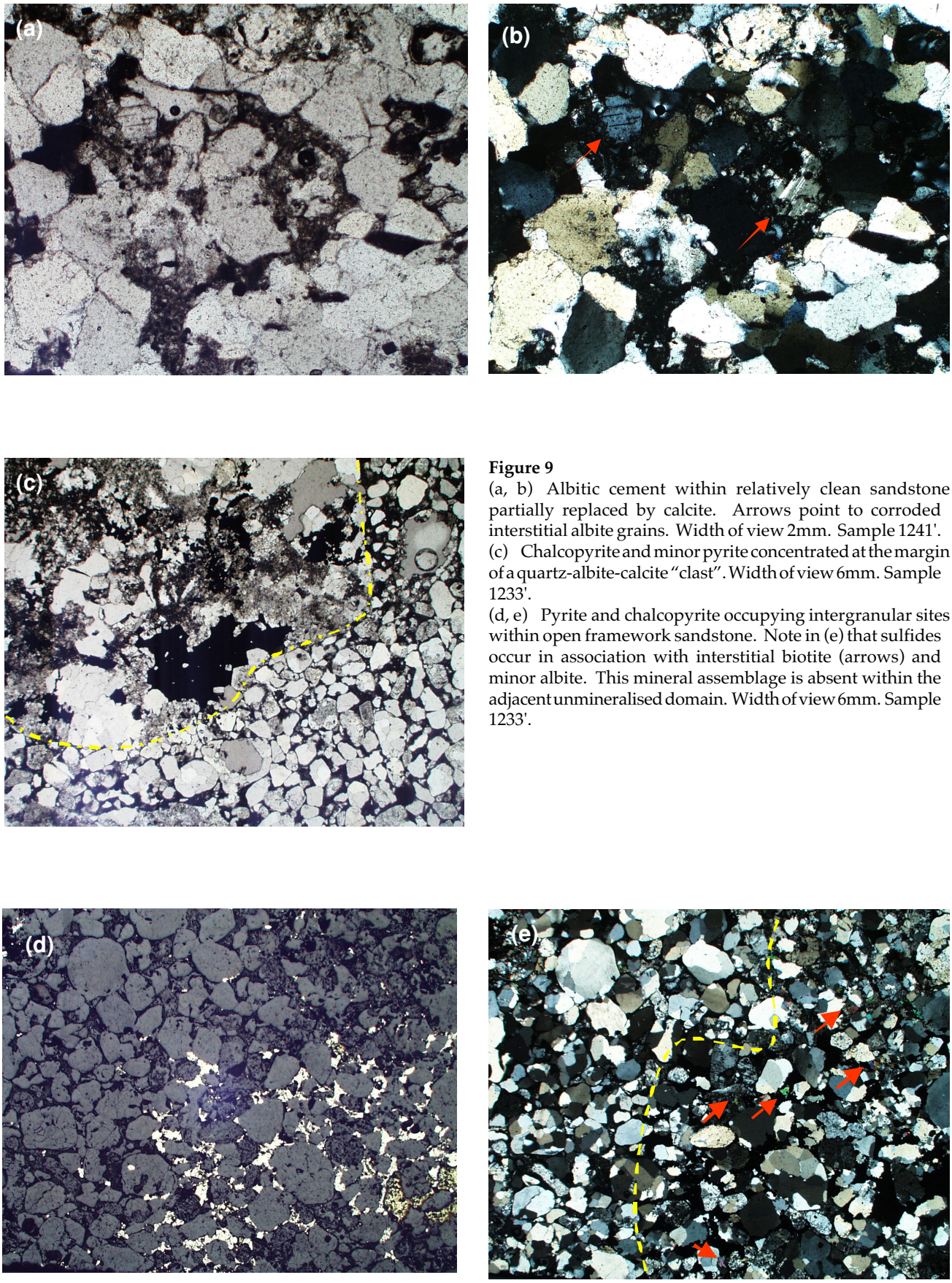

Figure 9
(a, b) Albitic cement within relatively clean sandstone partially replaced by calcite. Arrows point to corroded interstitial albite grains. Width of view 2mm. Sample 1241'.
(c) Chalcopyrite and minor pyrite concentrated at the margin of a quartz-albite-calcite "clast". Width of view 6mm. Sample 1233'.
(d, e) Pyrite and chalcopyrite occupying intergranular sites within open framework sandstone. Note in (e) that sulfides occur in association with interstitial biotite (arrows) and minor albite. This mineral assemblage is absent within the adjacent unmineralised domain. Width of view 6mm. Sample 1233'.

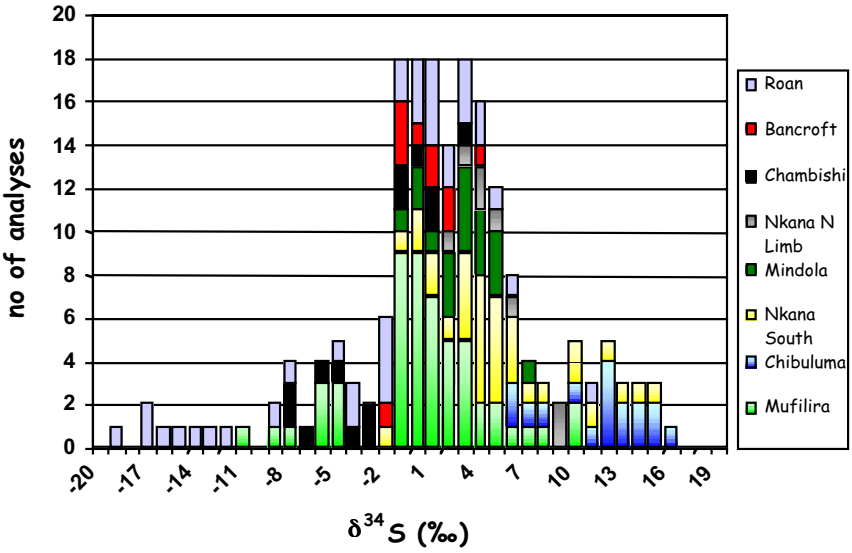

Figure 10
Histogram showing results of sulfur isotope analyses for the Copperbelt mineral deposits by Dechow and Jensen (1965). No. of analyses: Roan – 36; Bancroft (Konkola) – 10; Chambishi – 14; Nkana N Limb – 8; Mindola – 18; Nkana South – 34; Chibuluma – 17; Mufilira – 53.

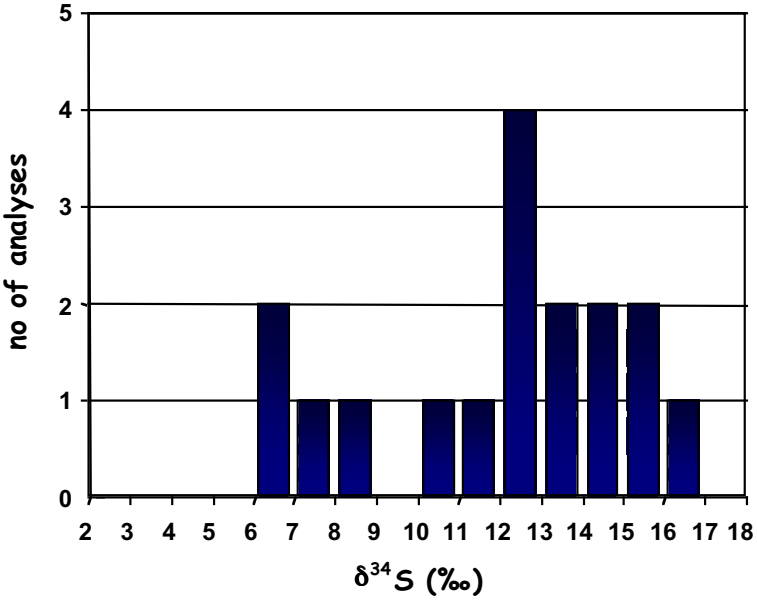

Figure 11
Histogram showing results of 17 analyses of sulfur isotopic compositions from Chibuluma by Dechow and Jensen (1965).

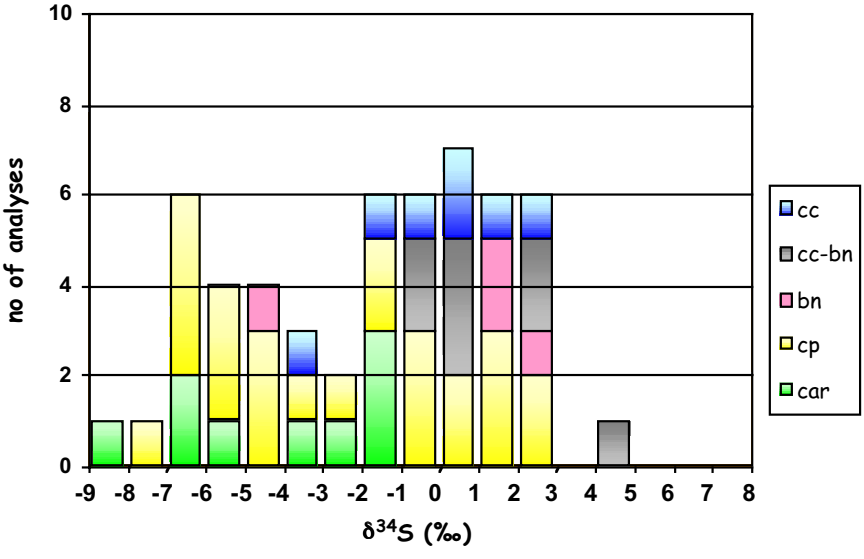

Figure 12
Histogram showing results of sulfur isotopic analyses of sulfide minerals from Konkola by Sweeney et al. (1986) and Dechow and Jensen (1965). Abbreviations: cc – chalcocite; cc-bn: chalcocite-bornite intergrowths; bn – bornite; cp – chalcopyrite; car – carrollite.

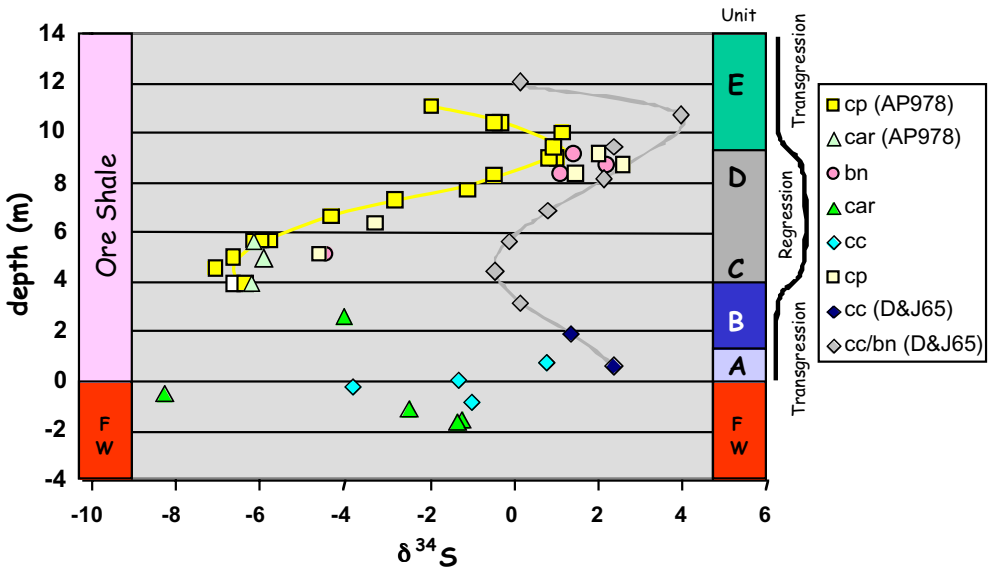

Figure 13
Sulfur isotopic compositions of sulfide minerals from Konkola plotted as a function of depth relative to the footwall – ore shale contact (modified after Sweeney et al., 1986). Samples from drillhole AP978 show systematic variations in their isotopic compositions with respect to depth, which Sweeney et al. (1986) attributed to early diagenetic introduction of sulfate, with rocks deposited during marine transgression events associated with increasingly lower $\delta^{34}S$ values. The chalcocite-bornite data from Dechow and Jensen (1965) show similar stratigraphic variations, although at higher $\delta^{34}S$ values, which Sweeney et al. (1986) attributed to the different mineral species analysed (cp vs cc-bn).

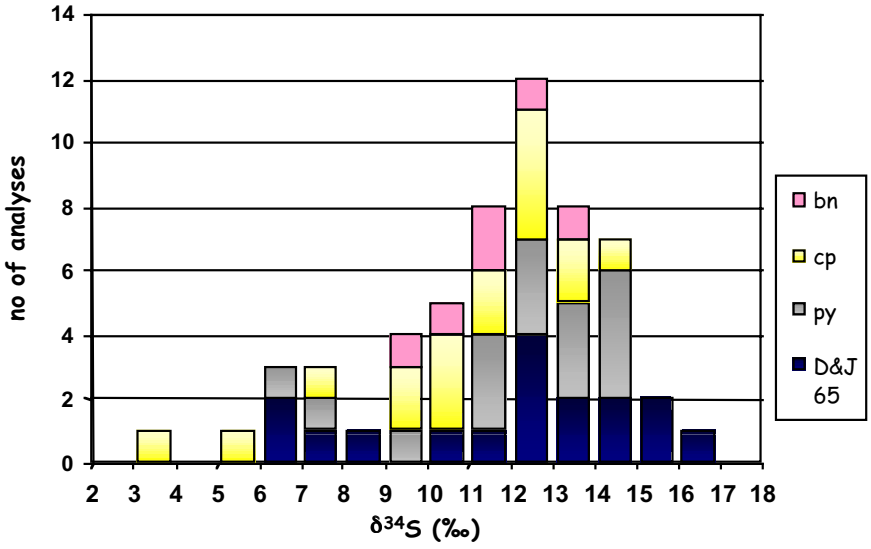

Figure 14
Histogram showing results of sulfur isotopic compositions of 39 pyrite, chalcopyrite and bornite grains from Chibuluma (this study), together with the 17 analyses from Chibuluma by Dechow and Jensen (1965).

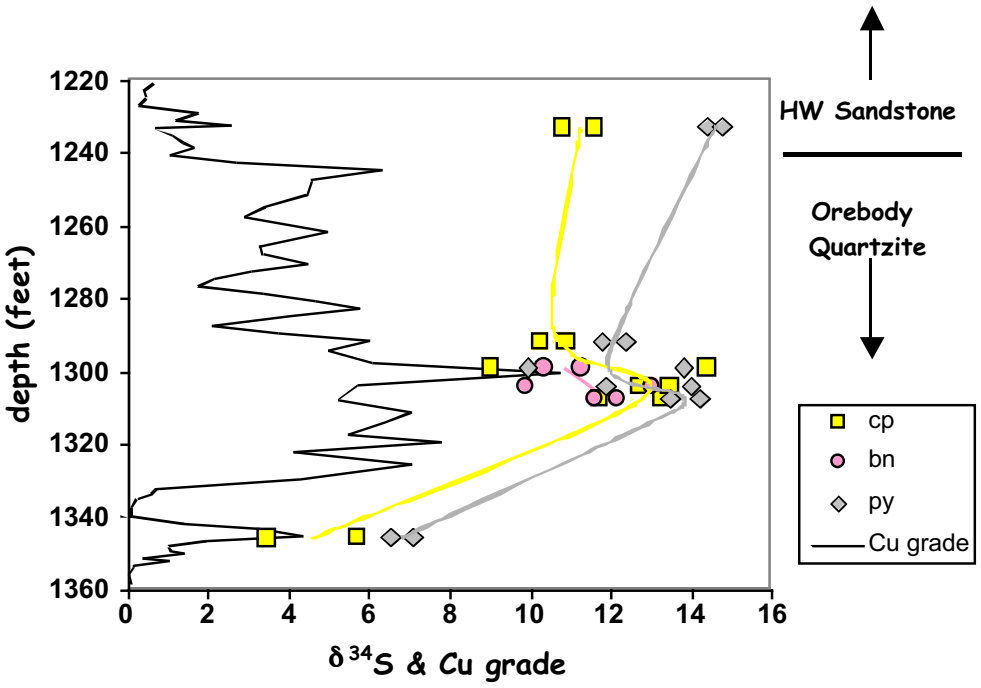

Sulfur isotopic compositions of all sulfide grains analysed from drillhole NS137 plotted as a function of drillhole depth. The solid lines have been plotted using average values for sulfide ^{34}S from each sample

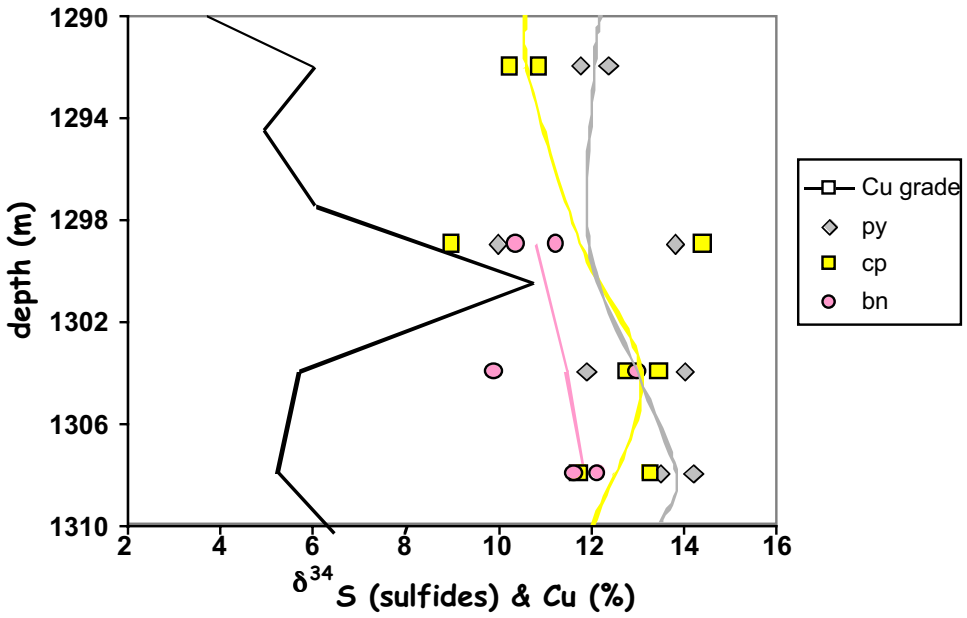

Figure 16
Sulfur isotopic compositions of sulfide minerals for the 20 ft high grade interval from drillhole NS137 plotted as a function of drillhole depth. Also plotted are copper grades based on 2-4 ft composite samples. Assay values are plotted at the mid-point of any given composite sample

there are apparent variations in sulfur isotopic compositions with respect to depth similar to that documented from Konkola by Sweeney et al. (1986; Fig. 13). Furthermore, the Chibuluma stratigraphic isotopic variations are recorded by pyrite, chalcopyrite and bornite (Fig. 16), even though there is paragenetic evidence for pyrite replacement by chalcopyrite (e.g., Fig. 7a). This is interpreted to indicate a local stratigraphic control on sulfide isotopic compositions, rather than introduction of externally sourced, isotopically homogenous aqueous sulfur during the copper mineralising event.

The trend of increasing ^{34}S content of sulfide minerals upwards through the host stratigraphy in NS137 (Fig. 15) is comparable to other Copperbelt deposits studied by Cunningham (1986) and reported by Annels (1989; Fig. 17). The upwards increase in $\delta^{34}S$ values at Chambishi, Chambisi S, Pitanda and Mwambashi B were attributed to a single infusion of metalliferous fluids at each system, with sulfides deposited at progressively later times higher in the stratigraphy, thus accounting for progressive depletion of ^{32}S in the residual brine with time (i.e. closed system behaviour; Annels, 1989). However, such a model does not explain the ^{34}S-enriched sulfides in the basement at Chibuluma (Table 1).

Relationship to copper grade

There appears to be no direct correlation between copper grades and sulfur isotopic compositions at Chibuluma (Figs 15, 16). The sulfides most enriched in ^{32}S occur at 1346 ft in the bottom of the Orebody Quartzite in NS137, and correlate with a moderate grade zone (1.9–4.4 % Cu). At 1233', the hangingwall sandstone contains sulfides enriched in ^{34}S which are associated with a low grade intersection (0.7–2.5% Cu; Fig. 15). The 20' intersection that contains the highest copper grades (3.7 to 10.7% Cu) is associated with sulfide minerals that have $\delta^{34}S$ values ranging between +9.0 and +14.5‰, with no obvious systematic variations (Fig. 16). Poor correlations exist between between the sulfur isotopic data and Cu grades, which may relate to:

- The sampling methodology (1–4' bulk composite assay samples which include all sulfide paragenetic stages, compared with single grain laser ablation samples with heterogenous isotopic compositions)
- The controls on grade distribution not being the same as the controls on sulfur isotopic compositions within individual sulfide grains

Geothermometry

The sulfur isotopic compositions of chalcopyrite-bornite mineral pairs were used in an attempt to calculate temperatures of sulfide deposition (Table 2). Although the two minerals appear to be in textural equilibrium, they are clearly not in isotopic equilibrium, based on the large spread of calculated temperatures (180–920˚C). Consequently, these data cannot be used to determine the temperature of sulfide deposition at Chibuluma.

Table 2
Apparent temperatures of sulfide deposition calculated for chalcopyrite-bornite pairs from Chibuluma. Isotopic compositions of individual grains are listed in Table 1. Temperatures of formation could not be calculated for two samples, because the $\delta^{34}S$ values for chalcopyrite were lower than that of the co-existing bornite grain.

Drillhole	Depth	Analysis No.	Temperature (°C)
NS137	1299	1A…B	–
NS137	1299	2B…C	179.5
NS137	1304	3A…B	919.5
NS137	1304	4A…B	203.7
NS137	1308	1A…B	354.5
NS137	1308	2A…C	–

Discussion

Sulfur isotopic compositions in drillhole NS137 at Chibuluma West vary as a function of the host stratigraphy, and are highly variable, ranging from +3.5 to +14.8‰. Sulfides in the mylonitic granite basement intersected in drillhole NS159-D1 have similar isotopic compositions (+11.7 to +12.6‰). The sample from the base of the orebody quartzite in NS137 has anomalously low $\delta^{34}S$ values (+3.5 to +7.1‰) compared to all other samples analysed in this study.

On the basis of sulfur isotopic compositions, Sweeney et al. (1986) argued that early diagenetic biogenic reduction of seawater sulfate was a critical process in the formation of sulfide mineralisation at Konkola. The lack of sulfate minerals at Konkola prevented them from determining the $\delta^{34}S$ fluid value, although they noted that sulfate at Mufilira has an isotopic composition of 17‰, which is comparable to the late Proterozoic seawater sulfate composition of 18.9 + 0.8‰ estimated by Veizer et al. (1980). Dechow and Jensen (1965) also argued for biogenic sulfate reduction as an important process in the Copperbelt, although they also advocated subsequent modification by metamorphism.

Chibuluma West does not contain any sulfate minerals, which means that the sulfur isotopic composition of the mineralising fluid cannot be estimated. If the isotopic composition of Late Proterozoic aqueous sulfate in the Copperbelt was approximately 17‰, as argued by Sweeney et al. (1986), then biogenic sulfate reduction is unlikely to have been the source of H_2S at Chibuluma. Hitzman et al. (2000) noted that anhydrite had isotopic values of +20.5 to +22.6‰ at Chambishi, with values in the Copperbelt ranging from +11 to +23‰. Even with the heaviest $\delta^{34}S$ sulfate compositions reported by Hitzman (2000), it is unlikely that biogenic sulfate reduction was important at Chibuluma, given the anomalously high $\delta^{34}S$ values of the sulfides (ave. 11.4‰) compared to other Zambian copper deposits. Thermochemical sulfate reduction, or decomposition of organic matter to generate H_2S gas may be viable alternatives, or some other more complicated combination of processes may have been relevant to the Chibuluma West system.

Does the fact that sulfides at Chibuluma West have anomalously heavy sulfur isotopic compositions (Fig. 10) imply that ore at Chibuluma West formed via different processes compared to Konkola and other deposits of the Copperbelt (e.g., thermochemical vs biogenic sulfate reduction; syn-tectonic vs diagenetic, etc.)? The only deposit with comparable sulfur isotopic compositions is Nkana South (Fig. 10), which is also strongly deformed. Is it possible that different types of sulfur reservoirs were available at the trap sites in the various deposits (sour gas, pre-existing sulfides, aqueous sulfate, or anhydrite as pore-space filling)? Did Chibuluma form at a different time and/or from waters with distinctly different $^{34}S_{sulfate}$ compositions compared to deposits such as Konkola? Has deformation and metamorphism superimposed a second isotopic composition over the original diagenetic sulfides in the host sequence at Chibuluma? If so, why are the sulfides so heterogeneous in their compositions at the hand-sample scale? Further work is required to resolve these issues in order to help us understand both the origins of the Zambian copper ores, and to establish the implications for copper exploration in other sedimentary basins. Specifically, more details of the sulfur and carbon isotopic variations stratigraphically through and spatially along the ore horizon, coupled with studies of the stable isotopic systematics of sulfides and carbonates in stratigraphically equivalent portions of the host basin, should help to resolve these questions.

References

Annels, A. E. 1989. Ore genesis in the Zambian Copperbelt, with particular reference to the northern sector of the Chamishi Basin. In: Boyle, R.W., Brown, A.C., Jefferson, C.W., Jowett, E.C., and Kirkham, R.V., eds., Sediment-hosted stratiform copper deposits: Geological association of Canada, Special Paper 36, p. 427-452.

Cunningham, M.J., 1986. Copper-cobalt mineralisation in the northern portion of the Chambishi Basin, Zambia. Unpublished PhD research report, University College, Cardiff.

Dechow, E., and Jensen, M.L., 1965. Sulfur isotopes of some Central African sulfide deposits. Economic Geology, 60, 894-941.

Hitzman, M., 2000. Powerpoint presentation.
In: Sediment-hosted copper deposits shortcourse volume, Centre for Ore Deposit Research, University of Tasmania, p. MH1 – MH14.

Sweeney, M., Turner, P. and Vaughan, D.J., 1986. Stable isotope and geochemical studies of the role of early diagenesis in ore formation, Konkola Basin, Zambian Copper Belt. Economic Geology, 81, 1838-1852.

Veizer, J., Holser, W.T., and Wilgus, C.K., 1980. Correlation of $^{13}C/^{12}C$ and $^{34}S/^{32}S$ secular variations. Geochimica et Cosmochimica Acta, 44, 579-587.

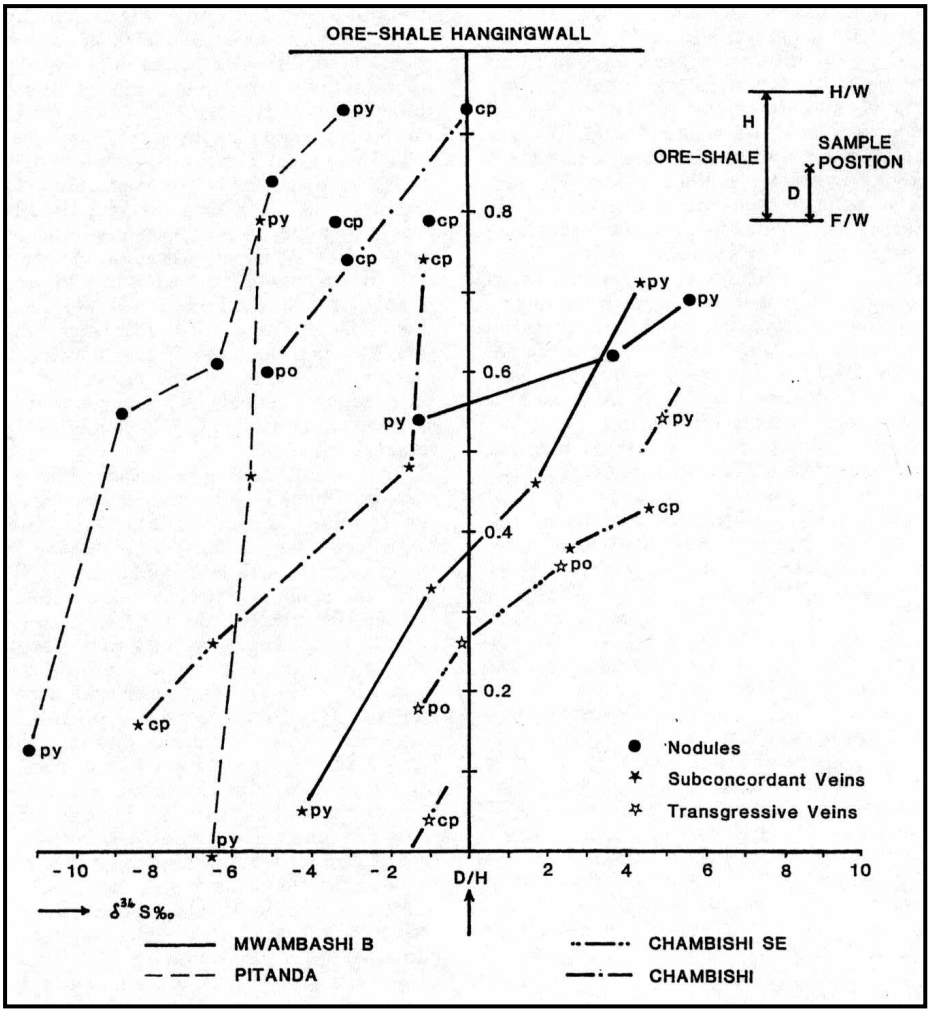

Figure 17
Variations in the sulfur isotopic compositions of sulfides in the ore shale from selected deposits in the Chamibishi basin. Data from Cunningham (1986). Diagram reproduced from Annels (1989).

Structural setting and paragenesis of the Mufulira copper deposit, Zambia

Robert J. Scott
Centre for Ore Deposit Research, University of Tasmania

Introduction

The Mufulira deposit, discovered in 1923 by Guy Bell and James Moir (Gunning, 1961) is the largest of the Copperbelt deposits NE of the Kafue anticline (Fig. 1). Unlike the predominantly shale-hosted deposits SW of the Kafue anticline those to the NE are primarily hosted by arkose and quartzite within the Lower Roan Group (Fleischer, 1976; Evans, 1980). Copper sulfides at Mufulira are largely strata bound, but occur within 21 distinct lithological horizons. All but three of these occur within the 30–80 m thick Ore Formation which consists of variably carbonaceous and argillaceous quartzite and arkose, interbedded with lesser shale and dolomite (Brandt et al., 1961; Fleischer et al., 1976). The Ore Formation generally overlies planar to cross-stratified quartzite and arkose termed the Footwall Formation. This in turn overlies the Palaeoproterozoic basement of Lufubu Schist and granite. A 70 m thick sequence of quartzite and argillaceous quartzite termed the Hanging Wall Formation overlies the Ore Formation, and is itself overlain by predominantly dolomitic sediments of the Upper Roan (Brandt et al., 1961).

The Footwall Formation at Mufulira ranges from 0 to 180 m thick. Thickness variations reflect an original irregular basin topography, of broad shallow basins separated by relatively narrow "palaeo-highs" (Brandt et al., 1961). However, the present topography of the basal unconformity reflects substantial modification during basin inversion. Deformation was commonly localised along the margins of original palaeo-highs (Annels, 1979), such that the present pinnacle-like basement protrusions (Fig. 2) are much narrower and more pronounced than the original palaeo-highs and should not be interpreted as original topographic features.

Nonetheless sedimentary successions with the Footwall Formation can not be correlated from one "basin" to the next, indicating the palaeo-highs controlled initial patterns of sediment dispersal in the Lower Roan Group. The irregular basin topography was largely filled in by the Footwall Formation and the Ore Formation and stratigraphically higher units are *relatively* uniform in thickness and continuous across the tops of the palaeo-highs (Fig. 2, Brandt et al., 1961). The Ore Formation directly overlies basement on some of the palaeo-highs, although nowhere do these protrude into it, suggesting an episode of peneplanation may have preceded deposition of the Ore Formation (Fleischer et al., 1976).

Although no longer prominent topographic features, Brandt et al. (1961) argued the basement highs may have had an ongoing (albeit subtle) influence on facies development during deposition of the Ore Formation. These workers proposed differential compaction of the underlying Footwall Formation across the irregular basement topography resulted in the development of three main depressions above the major palaeo-valleys — the Western, Central and Eastern basins, and that these controlled facies distribution during accumulation of the Ore Formation (Brandt et al., 1961). Of these, the Eastern Basin has the thickest accumulation of ore-bearing sediments. However in detail, isopach maps indicate

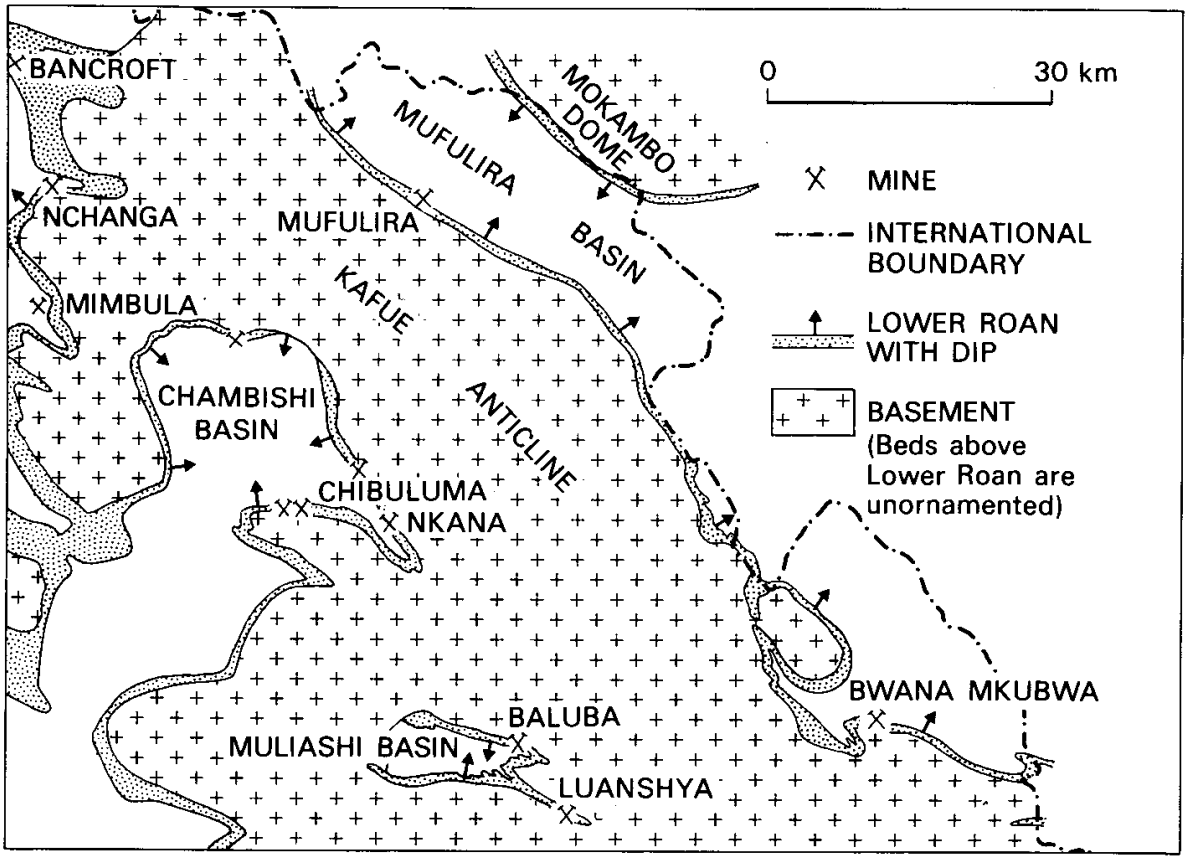

Figure 1.
Simplified map of the Zambian Copperbelt, showing the location of the Mufulira deposit on the NE flank of the Kafue Anticline. (From Evans, 1980, modified from Fleischer et al., 1976).

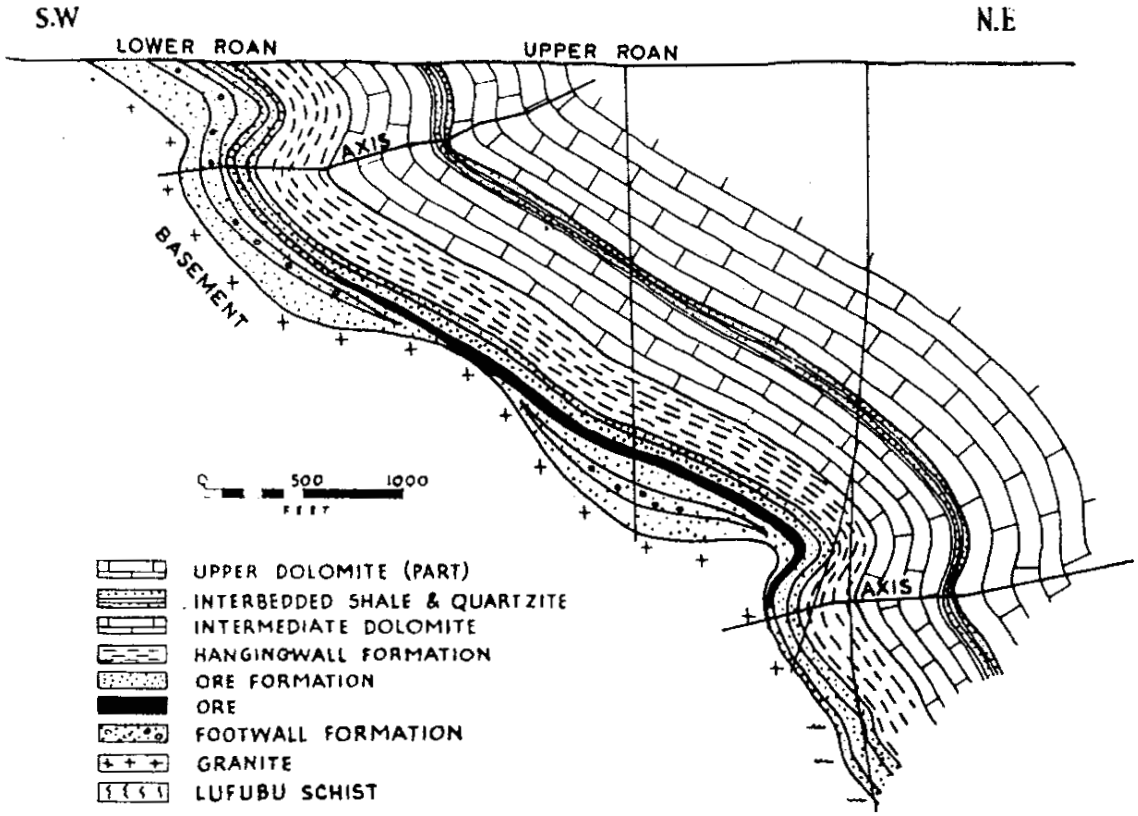

Figure 2
Section along the 55/56 (Imperial) mining block boundary (3087m E, metric mine grid). Only the lowermost C-Orebody is developed in this area. Note the thickness variations in the Footwall Formation do not correspond with the present topography of the lower-most "basement high". The stratigraphic interval that hosts the C-orebody onlaps the basement down dip of the "basement hill", indicating that the original basement high was a much broader low-amplitude feature, and the pinnacle-like basement protrusion is largely an artefact of younger deformation localised along the margin of the original high.

that while the C-, B- and A-orebodies are approximately confined to the regions between major basement ridges, there is little correspondence between their thickness and that of the underlying Footwall Formation (Annels, 1979).

Nonetheless, the location of basement highs, in particular, appears to have had some influence on copper mineralisation. The lowermost C-Orebody quartzite of the Ore Formation is lower-grade and pyritic where it straddles basement highs, while the surrounding flanks host some of the richest copper mineralisation (Fleischer et al., 1976). The grade and distribution of the uppermost A-Orebody quartzite also appears controlled to some extent by the location of the basement highs (Annels, 1979; Mwape Makwaza, pers. comm., 2001). Clearly the origin evolution of the basement topography is of interest both in terms of understanding controls on early basin development (facies patterns, stratigraphic thickness variations) and sulfide zonation patterns within the Ore Formation. It also appears to have had a fundamental role in localising subsequent deformation at Mufulira (e.g. Annels, 1979).

Most workers have favoured syngenetic and/or diagenetic models for formation of the Mufulira deposits (e.g. van Eden, 1974). Binda (1975) and Fleischer et al. (1976) argued at least some of the sulfides were detrital in origin. However, metal zonation patterns and the generally accepted antipathetic relationship between copper sulfides and early diagenetic anhydrite within the Ore Formation (e.g. Fleischer et al., 1976), suggests sulfate reduction was a key process leading to the precipitation of copper sulfides from metal-chloride rich brines during diagenesis (Annels, 1979).

The primary objectives of this report are to:

- Briefly review mine geology and previous models for copper mineralisation at Mufulira
- Characterise mineralogical, textural and microstructural features of the Ore Formation (particularly the major mineralised horizons)
- Determine mineralogical zonation patterns (sulfide/gangue) within the Ore Formation
- Evaluate the extent and significance of internal deformation within the Lower Roan (Footwall and Ore Formation) and basement (Lufubu Schist) rocks
- Determine the origin and significance of the present basement topography, the nature of the basement contact, and its significance (or otherwise) in regard to the distribution and metal zonation within the ore horizons.

This analysis based on review of existing published work on Mufulira together with observations and samples collected during three underground visits (1140 and 1240 Levels) to Mufulira. The areas visited underground were in the Eastern Basin, and adjacent to basement highs of Lufubu Schist. Analysis of the palaeo-topography of the basin also involved extraction of data from mine sections in the central-western portion of the mine (between 2600 and 4000mE, Fig. 3). Because direct observations and sampling were restricted to a limited area of the mine, many critical geological relations and larger-scale facies variations, that have been used by previous authors to support models for basin development and copper mineralisation, were not observed and thus can not be fully assessed. Accordingly this report attempts to identify aspects of basin development and mineralisation that support or conflict with previous deposit models, but does not constitute a thorough evaluation of these models.

Deposit setting

The deposit is situated NE of the Kafue Anticline on the SW limb of the Mufulira syncline (Mufulira Basin, Fig. 1). At Mufulira the mine sequence generally dips 45°NE (Fig. 2). Copper mineralisation within the Ore Formation is best developed in three main strata-bound horizons of massive to poorly stratified, argillaceous and locally carbonaceous quartzite and arkose (termed the A-, B- and C-orebodies; Table 1). The three main orebodies get smaller and higher grade up sequence (Table 1; Fleischer et al., 1976). The stratigraphically lowest, C-Orebody, is the largest (lateral dimensions 8 x 8 km) while the strati-

graphically highest, A-Orebody, is the smallest (Fig. 3). In long-section the outline of the A-Orebody is almost entirely enveloped by that of the B-Orebody which is in turn enveloped by that of the C-Orebody (Fig. 3). The mineralised horizons are generally < 5–10 m thick although the C-Orebody is locally over 20 m thick (Brandt et al., 1976). The entire mineralised package varies from 30–80 m thick (Fleischer et al., 1976). As of 30 November 2000, the total ore reserves (A, B and C-orebodies) at Mufulira were: 25.3 Mt @ 3.0% Cu (with a total resource 41.5 Mt @ 3.0% Cu).

The main ore horizons are separated by barren to sporadically mineralised intervals 10–20 m wide (inter-B/C and inter-A/B beds). Particularly in the east of the mine ("Eastern basin") inter-orebody beds reach economic grade and are mined locally (Brandt et al., 1961). Generally, other than sulfide content there are not necessarily marked lithological differences between mineralised and unmineralised strata comprising the Ore Formation (Fleischer et al., 1976).

Except for pyritic zones within the C-orebody (i.e. above palaeo-hills), economic fringes of the orebodies are not related to basement topography, nor do they correspond to the lateral limits of the host rocks (Brandt et al., 1961). Although the host sequences thin towards the orebody fringes, in general there are no associated lateral facies changes that could account for the lack of sulfides (Brandt et al., 1961).

Metal distribution and zonation

Copper sulfides are irregularly to pervasively disseminated throughout the host arenites. Lesser carbonate ± quartz vein-hosted mineralisation occurs locally, particularly within the C-Orebody where it directly overlies basement. In these areas vein-hosted mineralisation may extend several to tens of metres into the underlying basement (Brandt et al., 1961). Hanging wall cut-offs in Cu-grade are generally sharp for each of the three orebodies, and at least for the C- and B-orebodies correspond to a change from arenite to a package consisting of dolomite or "calcareous mudstone" and shale (Fleischer et al., 1976). Locally the basal portion of the Lower Dolomite which overlies the B-Orebody hosts patchy and largely fracture-controlled chalcopyrite (Annels, 1979), but is barren elsewhere (Mwape Makwaza, pers. comm., 2001).

Table 1
Copper distribution within the Ore Formation at Mufulira (Brandt et al., 1961; Fleischer et al., 1976; Annels, 1979)

Unit	Lithology	Thickness	Mineralisation
A-Orebody	Argillaceous feldspathic quartzite, black carbonaceous quartzite ("greywacke"). Minor pebble to boulder conglomerate locally.	Av.: 6.1 m Max.: 13.7 m	4.5–5.5% Cu, disseminated Cc and Bn at upper levels, Cpy + Bn ± (?)Cc at depth
B-Orebody	Argillaceous and locally feldspathic quartzite, black carbonaceous quartzite ("greywacke")	Av.: 7.6 m Max.: 15.2 m	3.5–4.5% Cu, dominantly disseminated Bn, Cpy increases towards the fringes
C-Orebody	Argillaceous (sericitic) and locally feldspathic fine to medium grained quartzite, black carbonaceous quartzite ("greywacke")	Av.: 13.7 m Max.: 22.7 m	2.5–3.5% Cu, disseminated and lesser quartz + carbonate vein-hosted Cpy >> Bn, except at fringes

Complex vertical and lateral primary sulfide zonation have been recognised at Mufulira. Chalcocite is primarily developed in the upper levels of the mine. While some primary chalcocite may be present (Brandt et al., 1961) most is interpreted to be supergene in origin (van Eden, 1974; Fleischer et al., 1976). In contrast to shale-hosted deposits on the eastern limb of the Kafue antiform, cobalt is negligible at Mufulira (Fleischer et al., 1976).

Both the iron content and grade of the C-Orebody increase inwards from the orebody fringes towards the carbonaceous greywacke (Annels, 1979). Chalcopyrite is dominant sulfide in the greywacke but bornite increases and becomes dominant towards the fringes (van Eden, 1974; Annels, 1979). Fleischer et al. (1976) report a slightly different zonation for the C-Orebody, particularly with respect to the position of underlying basement highs. The C-Orebody is markedly pyritic where it straddles granitic basement highs and the Footwall Formation is thin or absent (Brandt et al., 1961; van Eden, 1974; Fleischer et al., 1976). On the flanks of the highs there is a complex transition through chalcopyrite- to bornite-rich zones. Further into the "basin interior" bornite gives way to chalcopyrite, then pyrite and finally barren "dirty" argillaceous arenites. It is not known whether pyritic zones adjacent to the highs are genetically-related to those around the fringes of the orebody (Fleischer et al., 1976).

In the B-Orebody, bornite is dominant in both the greywacke and argillaceous quartzite, although chalcopyrite increases towards the fringes (Fleischer et al., 1976; Annels, 1979). At upper levels of the mine (above 580 m Level) chalcocite is dominant sulfide in the A-orebody giving way to bornite in the fringes (Annels, 1979). Although most of the chalcocite is likely to be secondary, it persists to depths beyond the zone of likely secondary enrichment (Brandt et al., 1961). Nonetheless, at depth the sulfides in the A-orebody are chiefly bornite and chalcopyrite, with the latter generally dominant.

This study

Nature of the basement contact

The origin and significance of basin topography at Mufulira (i.e. the basal contact of the Lower Roan succession) was approached in two ways. Firstly by direct observations and sampling along the contact in the vicinity of a "palaeo-high" of Lufubu Schist on the 1140' and 1240' Levels in the mine. Secondly by extracting stratigraphic thickness data from mine sections to produce detailed restored isopach maps for the Footwall Formation and C-Orebody. The isopach maps enable the effects of subsequent folding and faulting to be removed and delineate basement topography at Ore Formation time. However, in this section only observations relating to the nature of the basement contact in the areas visited underground are presented. The origin, significance and evolution of the basin floor topography is discussed later in the report.

Despite representing a time gap of up to 1000 m.y., in the absence of a basal conglomerate, previous workers have noted the exact position of the basement contact is remarkably difficult to pinpoint, particularly where the footwall sequence is massive and the Lufubu rocks lack a well developed schistosity (Brandt et al., 1961; Fleischer et al., 1976). This was certainly the case in the areas visited underground, where both the C-Orebody and Footwall Formation were relatively massive (non-stratified) where in contact with non-foliated Lufubu Schist in the basement (Fig. 4a, b). In this area, the Lufubu Schist has a similar grainsize to the overlying sediments but is slightly darker (Fig. 4a, b) and primarily composed of fine to medium grained mica (Fig. 4c, d). It is not truly schistose but typically consists of a felted mass of white mica with lesser finer-grained interstitial quartz and biotite (Fig. 4c, d). The decussate micro-texture of the larger white mica laths is interpreted to reflect mica growth and recrystallisation under greenschist facies metamorphic conditions, with little if any associated grain-scale deformation. Locally the characteristic cross-hatch pattern of the coarser-grained micas is seen to

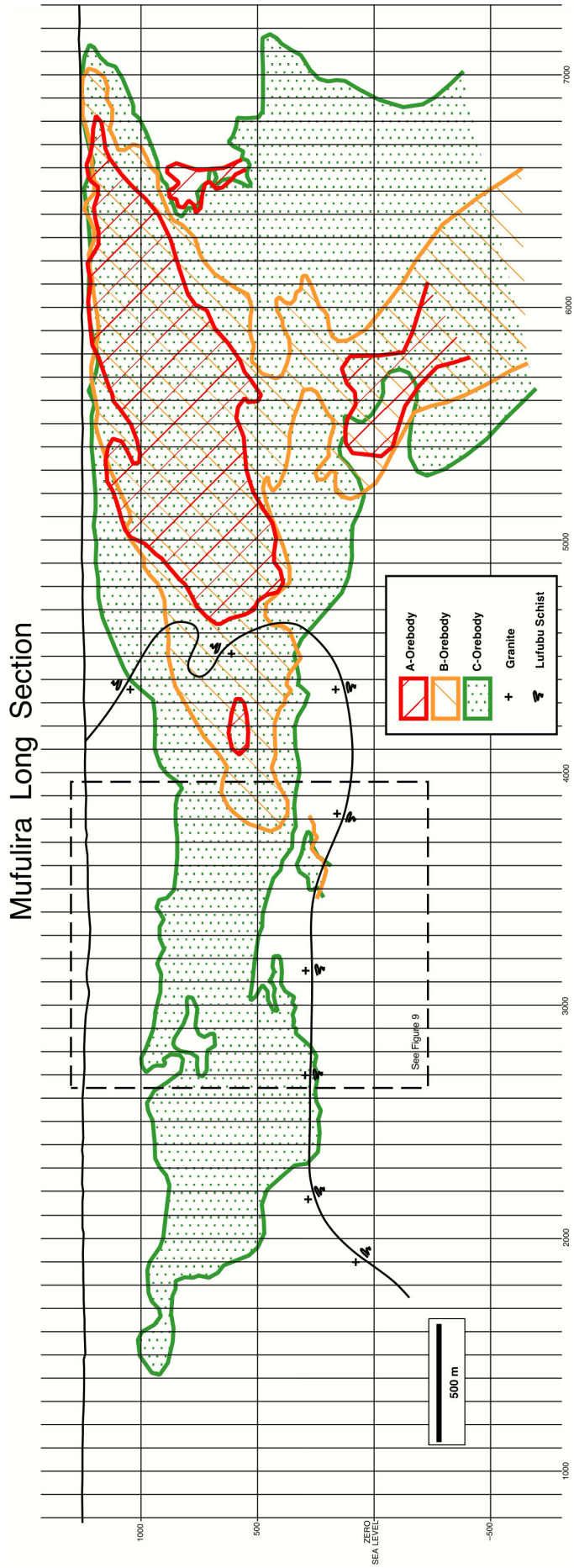

Figure 3.
Long-section through the Mufulira Mine showing the extents of the A- (stratigraphically highest), B- and C- (stratigraphically lowest) orebodies and the approximate distribution of granite and Lufubu Schist within the basement.

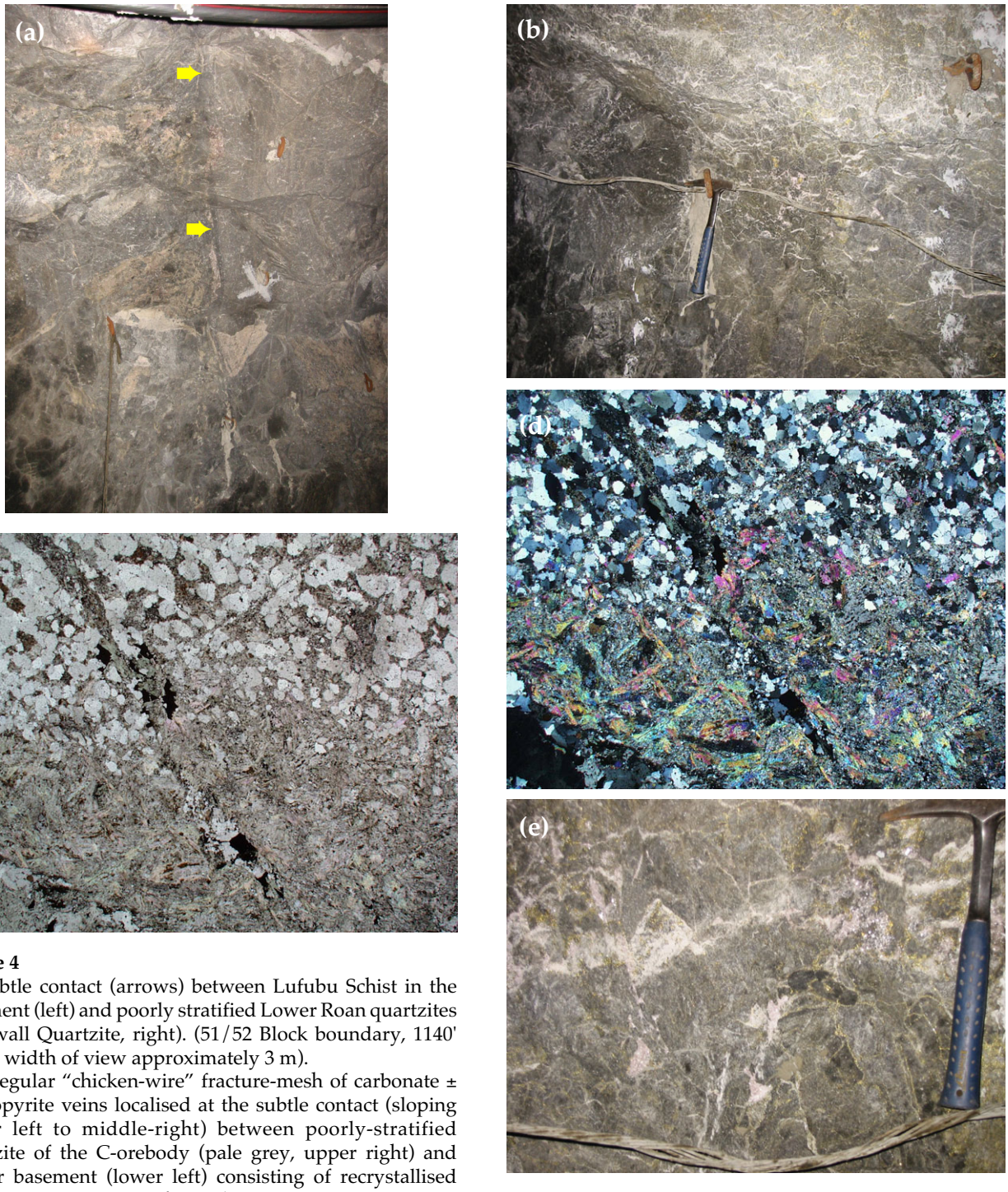

Figure 4
(a) Subtle contact (arrows) between Lufubu Schist in the basement (left) and poorly stratified Lower Roan quartzites (Footwall Quartzite, right). (51/52 Block boundary, 1140' Level, width of view approximately 3 m).
(b) Irregular "chicken-wire" fracture-mesh of carbonate ± chalcopyrite veins localised at the subtle contact (sloping upper left to middle-right) between poorly-stratified quartzite of the C-orebody (pale grey, upper right) and darker basement (lower left) consisting of recrystallised white mica + quartz "schist". (Basement contact, mining block 53P5, 1140' Level, hammer for scale)
(c, d) Transmitted light photomicrographs, in PPL and XPL, respectively, showing the sharp contact between Lufubu "Schist" (bottom) and Lower Roan quartzites (C-Orebody). Although largely recrystallised, original detrital quartz grain shapes are well preserved where grains are at least partially surrounded by interstitial biotite + white mica + carbonate (after original detrital feldspar and interstitial clays?). Despite the generally darker colour of the basement rocks they appear no richer in biotite than the overlying Katangan rocks. Nor is the Lufubu Schist in this area truly schistose and actually consists of a felted mass of white mica with minor interstitial quartz and biotite. The decussate micro-texture of white mica in the basement rocks is interpreted to reflect mica growth and recrystallisation during a greenschist facies metamorphism, with little if any associated deformation. At least locally the characteristic cross-hatch pattern of the micas reflects the dominant orientations of former cleavage-parallel and microlithon (crenulated) micas defining a once well developed crenulated mica fabric. (Sample MUF-12, Basement contact, mining block 53P5, 1140' Level, width of view 8 mm).
(e) Dark, chalcopyrite-rimmed basement clasts (centre-right) within extensively veined C-Orebody quartzite, just above basement contact (mining block 53P3, 1140' Level, hammer for scale).

reflect the dominant orientations of former cleavage-parallel and oblique microlithon micas defining once well developed S_2(?) and crenulated S_1(?) tectonic fabrics, respectively. Neither of these foliations was sufficiently well preserved to form a measurable fabric in underground exposures. Except for minor fracturing locally, in this part of the mine the Lufubu Schist *appears* massive and structureless. Fleischer et al. (1976) interpreted the Lufubu schist at Mufulira to have been derived from a felsic igneous protolith as bedding has not been observed.

Because of difficulties in accurately delineating the basement contact and the poorly to unstratified nature of the overlying sediments, the angular relationship between basal contact and bedding in the Lower Roan is difficult to determine with confidence. Such information is critical to interpreting the true nature of the basal contact (fault, unconformity, or both) as well as helping to constrain the development of basin topography relative to sedimentation (see *Basement topography: interpretation and significance*). Nonetheless, a few general comments about the nature of the basement contact in the areas visited can be made.

- No intensification of either ductile or cataclastic fabrics towards the contact were observed in either the basement or Lower Roan. Although poorly preserved, relict tectonic fabrics in the basement appear largely oblique to the contact. Accordingly there is no evidence to support significant faulting or shearing along the basement contact in the areas visited.
- Locally the tops of palaeo-highs (i.e. C-Orebody directly overlies basement) are marked by extensive development of small carbonate + quartz + chalcopyrite veins in both the basal C-Orebody and the underlying few metres of basement. Locally the vein arrays form fracture meshes with a distinctive ~hexagonal "chicken-wire" geometry. The wider purely extensional segments are consistently at a low-angle to the inferred basement contact and linked by high-angle shear veins (Fig. 4b). Overall the vein arrays indicate dilation normal to bedding. Accordingly if these developed prior to significant folding of the Katangan sequence, the vein arrays imply development of supralithostatic fluid pressures during a regime of bulk horizontal shortening.
- Rare preservation of apparently locally-derived basement clasts within the immediately overlying sediments (Fig. 4e) supports the interpretation that the basal contact is an unconformity. In the absence of any clear evidence to the contrary bedding in the Lower Roan is interpreted to be either subparallel to the basement contact or onlaps palaeo-highs at low-angle.

Figure 4c and d show an interpreted contact between the basement and argillaceous quartzite at the base of the C-Orebody in thin section (Sample MUF-12). Rounded detrital quartz grains outlined by the recrystallised matrix micas (sericite + biotite) in the quartzite are readily apparent in plane polarised light (PPL, Fig. 4c) although internally these grains show moderate degrees of recrystallisation (Fig. 4d). The fine grained micaceous matrix of the quartzite appears similar in composition and is texturally identical to finer-grained domains within in the adjacent Lufubu Schist (Fig. 4c, d). Indeed, difficulty in delineating the exact position of the basement contact has been attributed to local derivation of detritus within the Lower Roan, such that the composition of the sediments is similar to the underlying basement (Mwape Makwaza, pers. comm., 2001). However, with the exception of small clasts of Lufubu Schist locally incorporated into the overlying sediments (e.g. Fig. 4e), the quartz-rich ± feldspathic sediments that comprise the bulk of the Lower Roan succession in this area were clearly not derived from the immediately underlying basement. The Lufubu Schist contains minor interstitial quartz and little to no feldspar, and both are finer grained than much of the detritus comprising the Lower Roan sediments (Fig. 4c, d). Fine grained (?)weathered micas derived from the Lufubu Schist may have been incorporated into the matrix of the argillaceous sandstones, however coarser-grained detrital white mica is a relatively minor constituent of the Lower Roan sandstones examined so far. The compositions

of the Lower Roan sediments in this area are more consistent with derivation largely from basement granitic intrusions located less than a kilometre to the west (on restored plans), which apparently formed low basin-bounding hills during the initial stages of Roan sedimentation (e.g. Brandt et al., 1961; van Eden, 1974).

A striking feature of the basement contact illustrated in Figure 4c and d, is the degree of textural preservation in the basement. It is possible, and in fact likely, that the decussate texture of white micas in the basement reflects grain growth during metamorphism *following* deposition of the Katangan sequence. However, development of this texture requires the originally crenulated (± schistose) basement fabric to have been at least moderately well preserved prior to metamorphism. Thus despite a difference in age of ~1000 m.y., basement rocks in this area could not have been deeply weathered prior to deposition of the Katangan sequence. Although limited regolith development (~60 cm) along the basement contact has been reported elsewhere at Mufulira (Brandt et al., 1961), the admittedly limited observations of the present study suggest rapid basin development following an episode of erosion that exposed relatively fresh rock within the basement.

Characteristics of mineralised horizons

Primary sedimentary textures in all of the Ore Formation samples examined in this study have been variably modified by the effects of alteration, metamorphism, and deformation. Although the extent of recrystallisation and destruction of primary textures and mineral assemblages is highly variable both laterally and stratigraphically, in general detrital quartz is more extensively recrystallised in "cleaner" sandstones (containing less interstitial mica and or carbonaceous material) (Fig. 5). In more carbonaceous (e.g. Sample MUF-23, Fig. 6) or argillaceous (e.g. MUF-23, Fig. 7a–d) sandstones it is likely that other mineral phases within the matrix effectively "pinned" external quartz grain boundaries such that detrital grain shapes are better preserved, even though individual grains may have recrystallised internally (e.g. Fig. 4c, d). In one sample (MUF-23) from a high-grade portion of the A-Orebody sedimentary textures within the host sandstone are comparatively well preserved and detrital quartz shows only minor internal deformation or recrystallisation (Fig. 6). Carbonaceous(?) coatings rim both original rounded detrital grains and later (?)early diagenetic quartz overgrowths (Fig. 6), suggesting the carbon was not deposited with the sediment but introduced (as a hydrocarbon?) during diagenesis (e.g. Annels, 1979).

In the cleaner (matrix-poor) sandstones quartz typically displays minor to moderate internal recrystallisation, as well as extensive dissolution and/or grain boundary migration at original grain edges. The result is a tightly interlocking fabric of polygonal to anhedral grains (Fig. 5a, b). Except where destroyed during diagenesis or subsequent hydrothermal alteration, detrital feldspars commonly preserve original grain shapes and early diagenetic feldspar overgrowths, much better than adjacent quartz (Fig. 5c, d). There is no relationship between sulfide content and the degree of recrystallisation suggesting sulfides were probably introduced prior to significant compaction.

Besides quartz, feldspar and sulfides the other constituents of arenites from the Ore Formation are (Figs 5–8) anhydrite, carbonate (probably predominantly dolomite), white mica (detrital muscovite plus sericite and coarser-grained white mica of metamorphic origin), biotite (metamorphic), chlorite (metamorphic) locally as well as minor to locally significant tourmaline (both detrital and secondary), zircon (detrital) and rutile (secondary, and commonly associated with copper sulfides). The relative proportions and habits of these minerals vary significantly but for the most part non-systematically through the sequence. However the following seemingly consistent features were noted:

- there is an inverse relationship between anhydride and sulfide abundance within the arenites (see also van Eden, 1974; Fleischer et al., 1976, Annels, 1979)

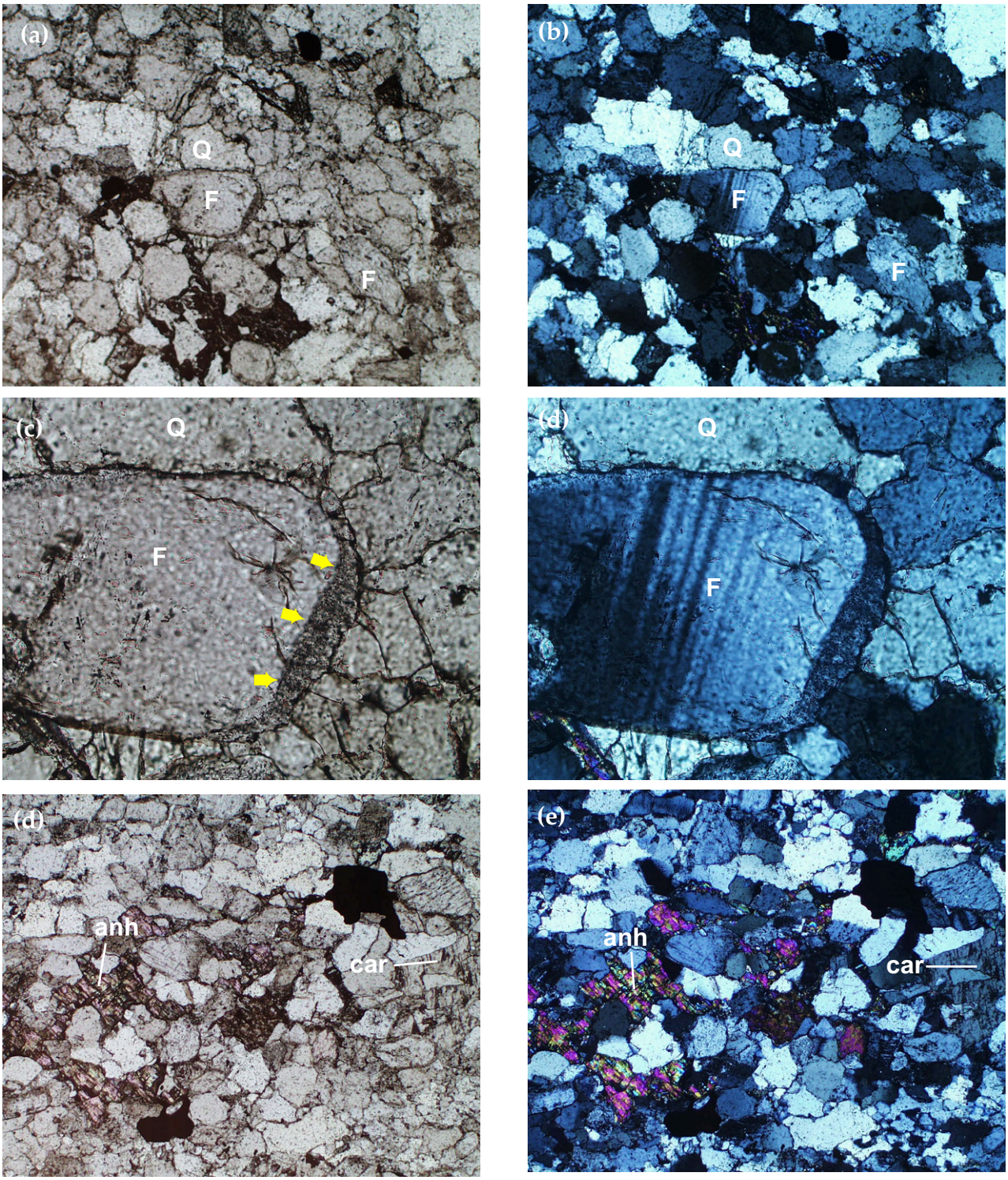

Figure 5
(a , b) Transmitted light photomicrographs, in PPL and XPL, respectively, showing recrystallised grain mosaics after original detrital quartz (Q) and feldspar (F). Feldspar shows greater preservation of originally rounded grain shapes. (Sample MUF-1, Footwall quartzite to A-Orebody, mining block 53/54 boundary, 1140' Level, width of view 2 mm).
(c, d) Transmitted light photomicrographs, in PPL and XPL, respectively, showing detail from a). Narrow, optically-discontinuous early diagenetic(?) feldspar overgrowth (arrows) on detrital plagioclase (F) truncated by dissolution seam developed during compaction at an interpreted high-stress grain contact with quartz (Q) (width of view 500 μm).
(e, f) Transmitted light photomicrographs, in PPL and XPL, respectively, showing typical textural association of anhydrite (anh) and carbonate (car). Both form small interstitial to larger poikilitic grains encasing detrital quartz and feldspar grains. Carbonate crystals generally have rhombic shape (euhedral), whereas anhydrite is more commonly sub- to anhedral. Carbonate and anhydrite grains encase the mutually interpenetrating quartz – feldspar grain aggregates indicating they formed after during or after development of the strong compaction fabric in the arkose. (Sample MUF-1, Footwall quartzite to A-orebody, mining block 53/54 boundary, 1140' Level, width of view 2 mm).

- anhydrite and carbonate occur together in the B-Orebody, Lower Dolomite and A-orebody, but only carbonate was observed in the C-Orebody
- chlorite (as selvedges to quartz + carbonate veins, and rimming carbonate and chalcopyrite grains) and secondary tourmaline appear restricted to the lower-most C-Orebody and Lufubu Schist
- biotite is a minor to abundant interstitial phase in the A-orebody and the base of the C-Orebody, where it abuts basement, but is largely absent elsewhere.

To some extent the distribution and particularly the habit of anhydrite and carbonate appear to reflect the degree of compaction and dissolution/recrystallisation, and thus the argillaceous component of the arenites. In matrix-rich argillaceous arenites anhydrite and carbonate generally occur as smaller interstitial grains (i.e. between framework grains). In "clean" well-compacted arenites anhydrite and carbonate form larger optically-continuous, poikilitic grains that envelop a number of detrital grains. Because the larger carbonate and anhydrite grains encase the mutually interpenetrating quartz–feldspar grain aggregates they must have formed during or after development of the strong compaction fabric in the arkose. Accordingly the contrast in habit is interpreted to reflect migration and recrystallisation of early diagenetic interstitial carbonate and anhydrite during compaction (± deformation/metamorphism).

Sulfides

In samples examined in this study, copper sulfides occur as ragged anhedral interstitial grains and irregular masses of probable replacive habit that are irregularly disseminated throughout the host arenites or less commonly as vein- and fracture-fill. Textural relations for bornite and chalcopyrite are generally similar, and where the two minerals occur together intergrowth textures imply coeval precipitation. However bornite is absent or subordinate to chalcopyrite where sulfides occur as fracture- or vein-fill (independent of stratigraphic level). Fracture-fill sulfides are best developed within semi-massive carbonate at the base of the Lower Dolomite (immediately above the B-Orebody). Carbonate + quartz + chalcopyrite veins are best developed at the base of the C-Orebody where it directly abuts Lufubu Schist over palaeo-highs (Fig. 4b, e). Mineralised veins in these areas extend for at least several meters into the basement.

To some extent the habit of the sulfides reflects the degree of compaction within the host layers. In the more recrystallised sediments sulfide–silicate grain boundaries are significantly modified by grain-scale dissolution and recrystallisation. The primary disseminated nature of the ores is generally well preserved, suggesting they were introduced before development of the tightly interlocking quartz ± feldspar grain textures in the host arenites. However while a pre- to syn-diagenetic origin is favoured, in general it is not possible to tell whether sulfides represent deformed and recrystallised detrital grains (e.g. van Eden, 1974; Fleischer et al., 1976), filled interstitial pore-spaces, or preferentially replaced specific detrital or early diagenetic mineral phases.

Less recrystallised samples provide a clearer indication of the timing of copper mineralisation. In the high-grade A-Orebody sample (MUF-23) bornite and chalcopyrite primarily form irregular (pore) space-fillings around detrital grains. Importantly, the copper minerals appear to largely post-date early (?)diagenetic overgrowths on detrital quartz ± feldspar grains (Fig. 6), but are finely disseminated through some diagenetically-altered (now sericite) feldspar grains (Fig. 6b, c). Locally sulfides are preferentially partitioned into cleaner (matrix-poor) thin arenite layers. The grainsize and distribution of the sulfides indicates they were not deposited in hydrodynamic equilibrium with the silicates. Rather this suggests copper introduction occurred early in the compaction history of the host sediments and was strongly controlled by layer porosity and permeability.

Several samples of the C-Orebody are markedly pyrite-rich (it is the dominant sulfide in the rocks), consistent with its proximity to a basement high in the areas sampled (e.g. Brandt et al., 1961; van Eden,

1974; Fleischer et al., 1976). Pyrite occurs as fine anhedral to euhedral interstitial grains (Fig. 7e). In one sample (MUF-22) from the base of the orebody adjacent to a basement high, subordinate chalcopyrite both rims and is intergrown (in apparent textural equilibrium) with pyrite along grain margins (Fig. 7f). These relations indicate chalcopyrite largely post-dates but does not replace pyrite. Contrasting relations were observed in sample MUF-9 (both stratigraphically higher in the C-Orebody, and further from the "apex" of the basement high). In this sample chalcopyrite is preferentially developed along a carbonate alteration front within a thin pyrite-rich sandstone layer. Here chalcopyrite appears to partially replace the earlier pyrite.

Locally copper sulfides are preferentially developed in thin heavy mineral-rich layers, along bedding or ripple / dune foresets (see Fig. 8a). Such features have been interpreted to indicate detrital sulfide deposition in a high-energy environment (Fleischer et al., 1976). During the present study copper sulfide enrichment along heavy mineral-rich layers was observed in the immediate footwall of the A-Orebody, and here a detrital origin for the sulfide can be readily dismissed. Heavy mineral bands up to several millimetres wide are defined by high detrital zircon and tourmaline concentrations (Fig. 8b). Patchy rutile + bornite + chalcopyrite is developed along the layers, apparently filling original pore-space as well as replacing some primary phases (Fig. 8b). Rutile is interpreted to reflect the breakdown of detrital FeTi-oxides (ilmenite, titano-magnetite) concentrated within the heavy mineral layers, with some or all of the liberated iron incorporated in the formation of bornite and chalcopyrite. Subhedral to euhedral crystals of chalcopyrite either nucleated or form partial to complete overgrowths of many of the zircon grains (Fig. 8c–f). Some zircons also contain chalcopyrite inclusions along now healed intragranular fractures and dissolution zones (Fig. 8c–f). Fine inclusions of chalcopyrite along growth zones in zircon probably reflect later deposition within areas affected by (?)earlier preferential dissolution of specific growth zones, rather than incorporation during growth of the zoned zircon rims. However some zircons have distinctive (?)diagenetic overgrowths with pyramidal form interpreted as xenotime (Fig. 8e, f). The similar euhedral form and local intergrowth of chalcopyrite and xenotime overgrowths suggest they are broadly coeval, and represent ideal material for dating studies to constrain the age of copper mineralisation at Mufulira.

Basement topography: interpretation and significance

Deposition of the Ore Formation at Mufulira apparently occurred once the original irregular basin topography was filled in by deposition of the Footwall Formation, and thus coincided with a change from small restricted basins, to a more extensive basin, whose limits were apparently well outside the Mufulira area. The irregular basin topography and relative stratigraphic position of the "ore horizon(s)" is broadly similar to many other Copperbelt deposits where the footwall succession (underlying the ore horizon) is relatively thin (e.g. Chibuluma, Nkana, Nchanga). The suggestion that deposition of the host-package to the copper mineralisation coincided with a major change in the internal basin geometry raises questions in regard to the extent to which evolving basin topography may have influenced copper mineralisation, and if so how and why? A critical step towards answering these questions is to address the origin of the early basin topography and the extent to which the distribution, grade and thickness of mineralised horizons reflects the distribution of basement highs and lows (e.g Brandt et al., 1961, Fleischer et al., 1976, c.f. Annels, 1979).

The shallow basins filled by the Footwall Formation at Mufulira are separated by roughly linear basement highs and vary from approximately symmetric (deepest in the middle) to markedly asymmetric (deepest near or adjacent to a basin margin). The major basement "ridge" trends Mine E (approximately SE on restored plans). Subordinate ridges extend either SW, S or SE from the main ridge (e.g. Fig. 9) and divide the Mufulira deposit into three major basins:- the western, central and eastern basins

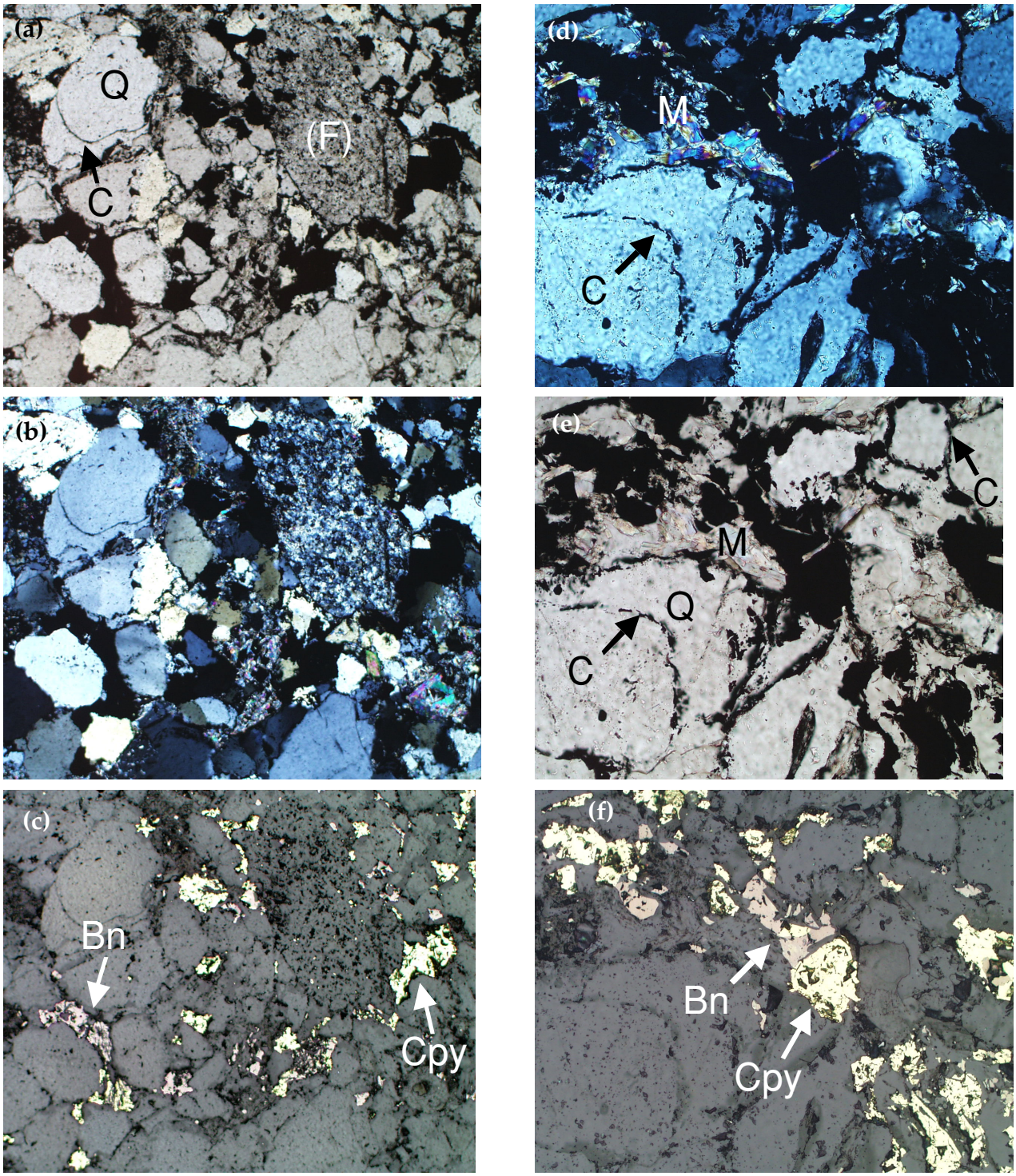

Figure 6
(a–c) Photomicrographs in transmitted PPL, XPL and reflected PPL, respectively, of high-grade A-Orebody arkosic sandstone, with abundant interstitial chalcopyrite (Cpy) and bornite (Bn). Original rounded quartz (Q) grains show minor recrystallisation at grain boundaries but appear internally undeformed (optically continuous). Note optically continuous quartz overgrowth on rounded detrital grain (top left). Original feldspar (F) grain is almost completely overprinted by fine-grained sericite and minor chalcopyrite. Non-reflective fine-grained dark material along grain boundaries is interpreted to be carbonaceous material.(Sample MUF-23, A-Orebody, mining block 54P5, 1240' Level, width of view 2mm)
(d–e) Photomicrographs in transmitted PPL, XPL and reflected PPL, respectively, of high-grade A-Orebody arkosic sandstone. Fine-grained non-reflective opaques that rim detrital grains and overgrowths are interpreted to carbonaceous material (C), after hydrocarbons introduced during diagenesis. Note fine-grained white mica (M) locally intergrown with sulfides (Sample MUF-23, width of view 500 μm).

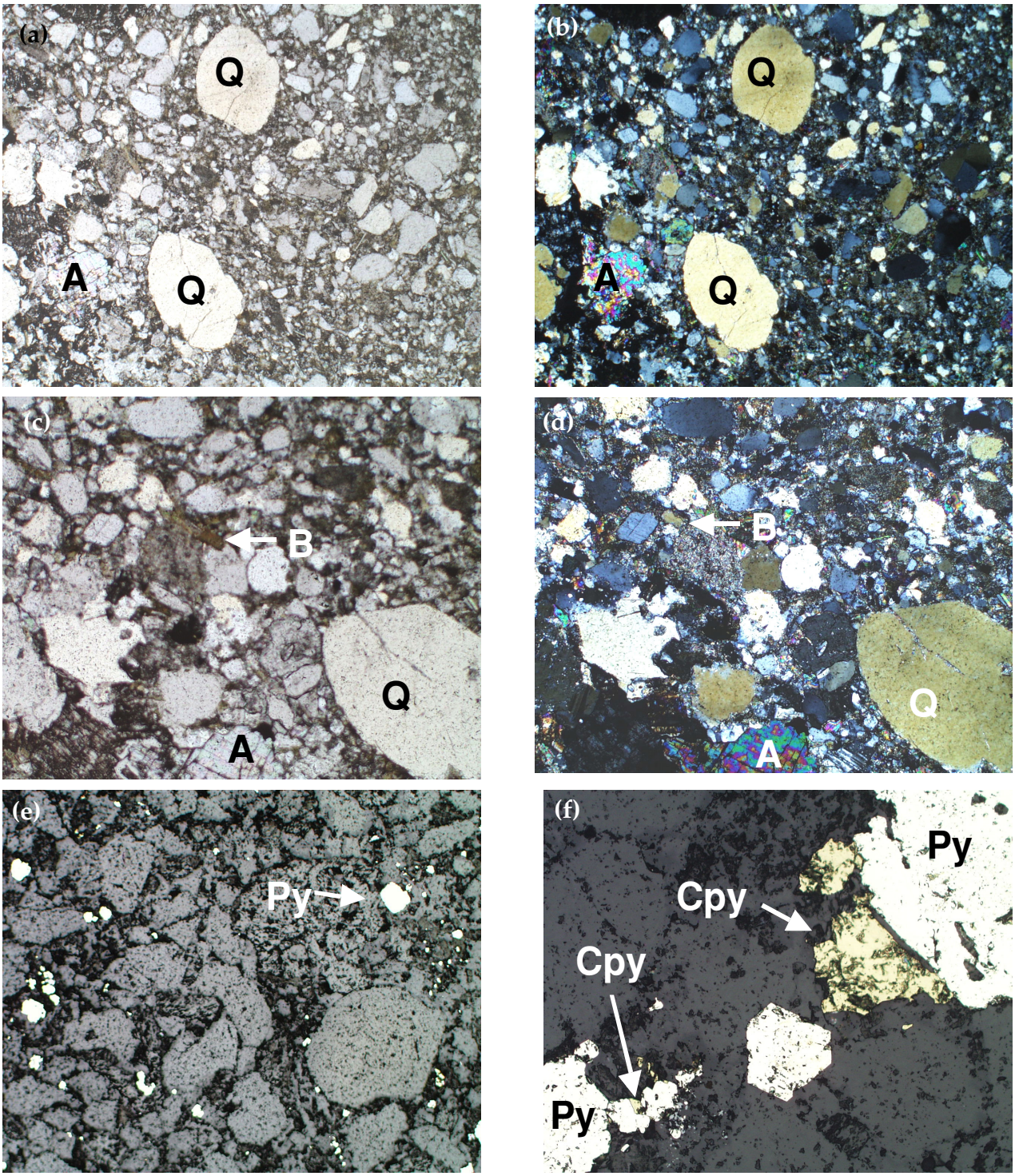

Figure 7
(a, b) Photomicrographs in transmitted PPL and XPL, respectively showing excellent preservation of sedimentary textures within poorly-sorted, matrix-rich arkosic sandstone on the unmineralised margins of (and stratigraphically equivalent to) the A-Orebody. Detrital quartz (Q) grains are well preserved although some feldspars are largely sericitised. Note patchy development of (?)diagenetic anhydrite (A). (Sample MUF-21, A-Orebody horizon, mining block 57/58, 1240' Level, width of view 4 mm).
(c, d) Photomicrographs in transmitted PPL and XPL, respectively showing detail from a) and b). Note development of secondary biotite (B) throughout matrix. (width of view 2 mm).
(e) Reflected PPL photomicrograph of pyritic C-Orebody sandstone. Anhedral to euhedral pyrite (Py) is disseminated throughout the matrix (Sample MUF-22, A-Orebody horizon, mining block 53/54, 1240' Level, width of view 4 mm).
(f) Reflected PPL photomicrograph showing chalcopyrite (Cpy) as late-stage intergrowths or overgrowths on pyrite (Py) in C-Orebody sandstone (Sample MUF-22, width of view 500 μm).

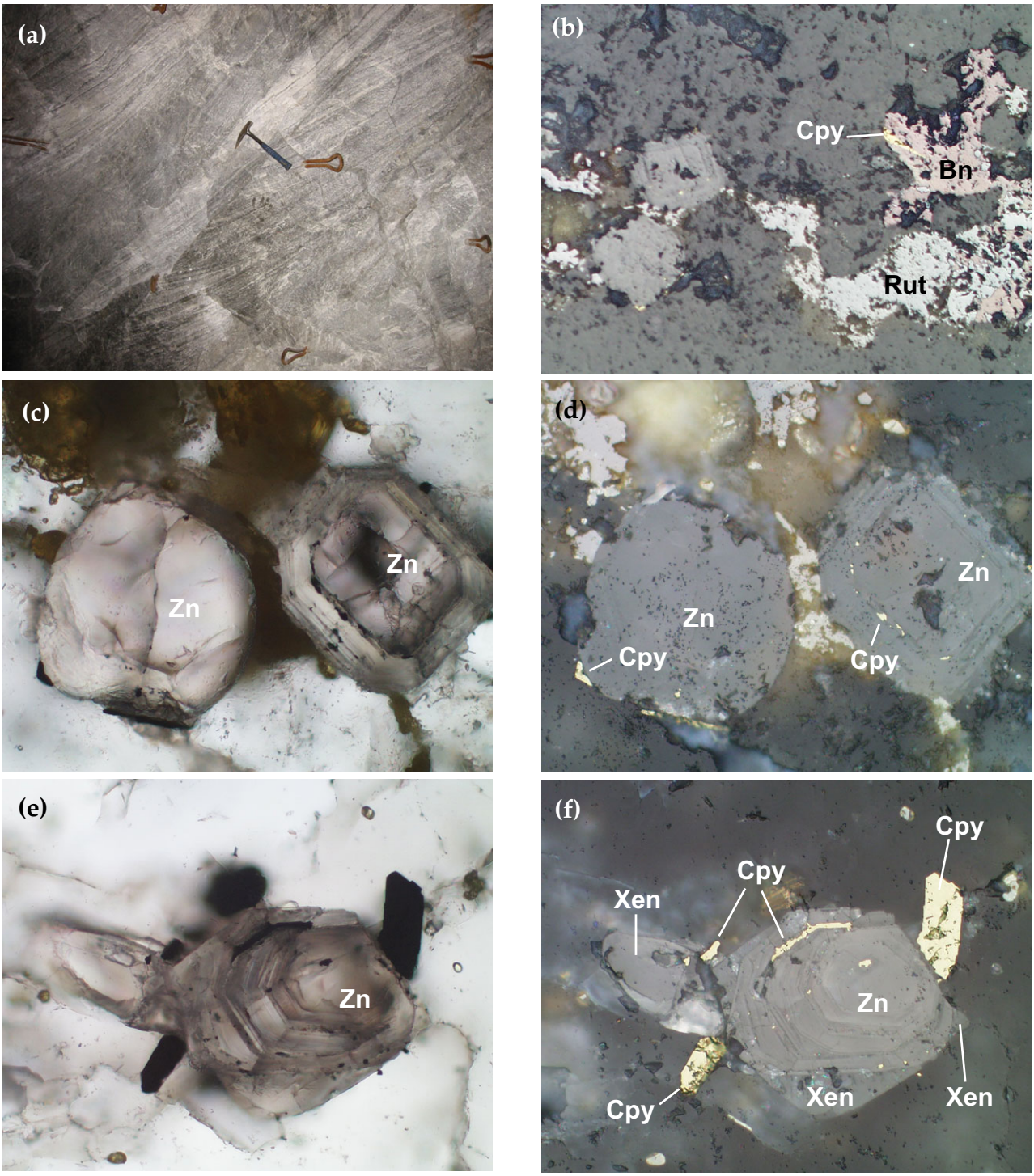

Figure 8
(a) Cross-stratified Footwall Quartzite (below C-orebody). Note alternating dark and light, heavy mineral-rich and -poor layers.
(b) Reflected PPL photomicrograph showing selective rutile (Rut) and copper sulfide (Bornite (Bn) > Chalcopyrite (Cpy)) development along heavy mineral band in Footwall quartzite to A-Orebody (Sample MUF-4, Footwall quartzite to A-Orebody, mining block 53P5, 1140' Level, width of view 500 μm).
(c, d) Transmitted and reflected PPL photomicrographs, respectively showing detail from heavy mineral band in b). Zoned and unzoned zircon crystals (Zn) contain chalcopyrite (Cpy) inclusions along now healed intragranular fractures and dissolution zones. Fine inclusions of chalcopyrite rimming unzoned euhedral zircon core, probably reflect deposition within preferentially dissolved growth zones, rather than sulfide grains incorporated during later development of the zoned zircon rim. (width of view 200 μm).
(e, f) Transmitted and reflected PPL photomicrographs, of zoned zircon crystal (Zn) with inclusions and overgrowths of chalcopyrite (Cpy). As in the previous example, chalcopyrite within the zircon grain is ascribed to later deposition along now healed intragranular fractures and dissolution zones. However (?)diagenetic overgrowths with pyramidal form are interpreted as xenotime (Xen). The similar euhedral form and local intergrowth of chalcopyrite and xenotime overgrowths suggest they formed at the same time. Accordingly dating xenotime overgrowths in this and similar samples has the potential to constrain the age of copper mineralisation at Mufulira. (Sample MUF-4, Footwall quartzite to A-Orebody, mining block 53P5, 1140' Level, width of view 200 μm).

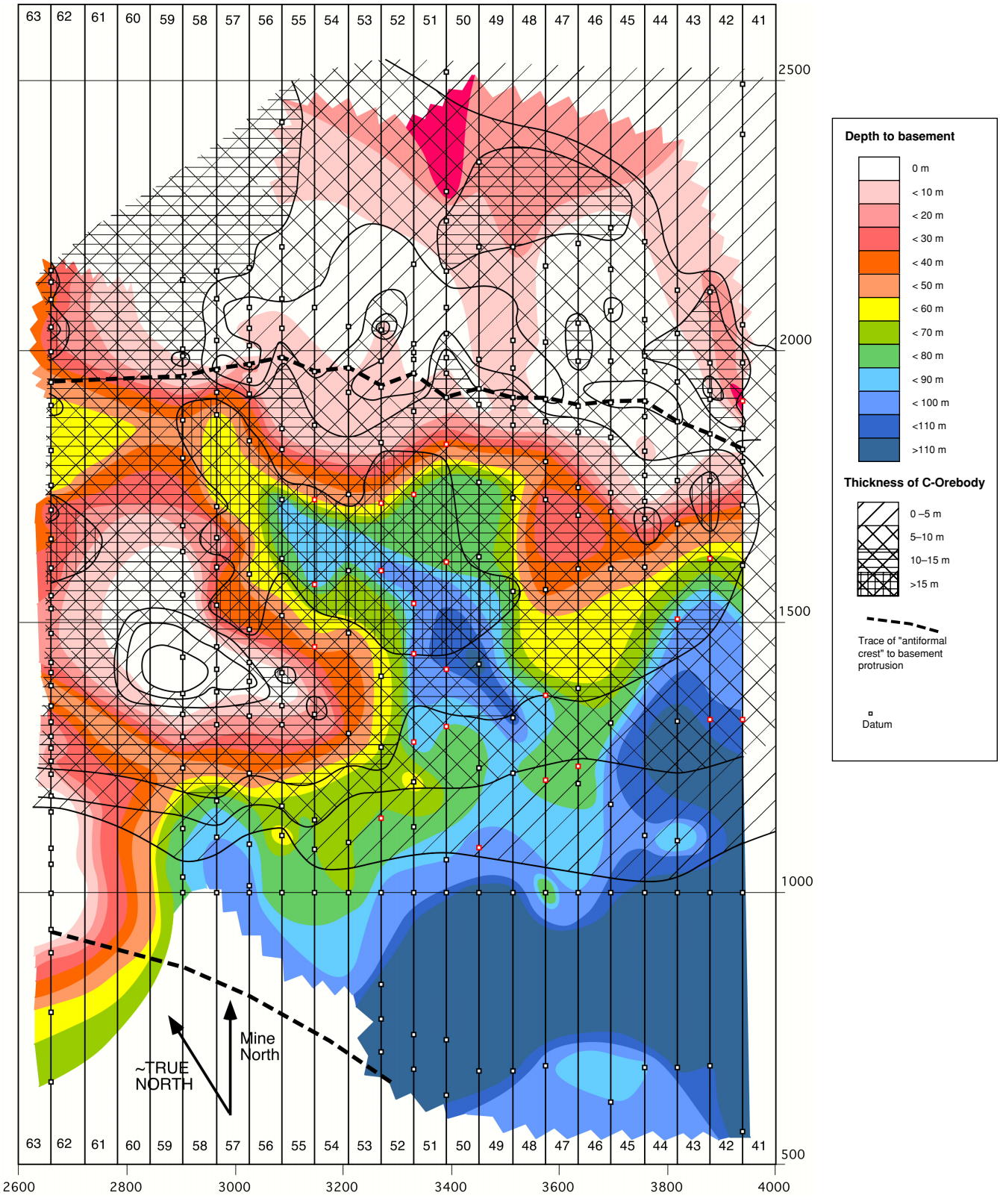

Figure 9
Isopach maps for the C-Orebody and Footwall Formation (showing depth below C-Orebody or stratigraphic equivalent) between 2600 and 4000m E (metric mine grid). Maps were produced by measuring true thicknesses of the Footwall and C-Orebody from mine plans (along section lines indicated), using the base of the C-Orebody as a datum. Data were unfolded and restored to horizontal. Although the C-Orebody is largely continuous across the irregular basement topography, thickness variations closely reflect those in the underlying Footwall Formation.

(van Eden, 1974; Fleischer et al., 1976; Annels, 1979). Mine sections (e.g. Fig. 2) suggest the (original) NE basin margin was steeper than that to the SW.

There are three end-member possibilities for development of the basement topography: (1) it entirely predates deposition of the Lower Roan, (2) its development was roughly synchronous with deposition of the Footwall Formation ("palaeo-valleys" are half graben formed during deposition of the Footwall Formation), or (3) it reflects an episode extensional faulting and tilting and subsequent peneplanation (c.f Fleischer et al., 1976) following deposition of the Footwall Formation, but prior to deposition of the Ore Formation. Although the irregular basin palaeo-topography is or may be structurally-controlled in each case, it should be possible to chose between the three possibilities from the nature of the basal contact of the Lower Roan. If option (1) is correct, the basal contact should be an unconformity everywhere. While some margins to palaeo-highs may be remnant fault scarps, the Lower Roan should everywhere be in depositional contact with the basement, unless faulting continued during it deposition of the overlying sequence. Palaeo-highs and ridges should have influenced sediment dispersal patterns throughout deposition of the Footwall Formation. Inability to correlate (in detail) units in the Footwall Formation between the three main basins certainly supports the existence of the basement highs as significant topographic features during deposition.

However, the apparent basin asymmetry, the roughly linear nature of intervening highs and the fact that maximum height of the "palaeo-hills" nowhere exceeds the thickness of the intervening Footwall Formation are all consistent with the development of basement topography during deposition of the Footwall sequence (option 2, above). In this scenario basement highs represent horst blocks, or perhaps more likely given the apparent asymmetry of the basins, the upturned edges of tilt blocks bounding a series of half graben. The exact nature of the basal contact of the Lower Roan and stratigraphic patterns within the Footwall Formation would depend on whether (and when) normal faults breached the basin floor, and if so the relative rates of faulting and sedimentation. For example, if sedimentation rates were always faster than the creation of accommodation space by faulting, uplifted basement blocks may have rarely breached the basin floor, and thus would not have formed significant palaeo-highs that influenced patterns of sediment dispersal. If faults did breach the basin floor, and up-thrown (or tilted) basement blocks formed topographic barriers that restricted patterns of sediment dispersal, continual erosion of the fault scarps would mean that even at "fault-bounded" margins of the basin, the basal contact of the Footwall Formation could be in part an unconformity.

The final option for the origin of the basement topography, as the result of faulting following deposition of the Footwall Formation, appears the least likely of the three. In this scenario, the contact between basement and the Footwall Formation must be partly faulted, and the Footwall Formation should be separated from the overlying Ore Formation by an angular unconformity, as the latter is continuous across the tops of the basement highs. Furthermore the present "basement highs" would have had no influence on initial patterns of sediment dispersal. As this was not the case, and there is no evidence for a significant unconformity separating the Footwall and Ore formations, the basement highs must have formed during or prior to deposition of the Footwall Formation.

Based on the findings of previous workers and observations from this study it is not possible to fully discriminate between the prior existence of the irregular basin topography or its development during deposition of the Footwall Formation. No evidence for significant faulting at the basement–Lower Roan contact was found in this study, although this alone does not mean basement topography entirely predates deposition of the Footwall Formation. However, elsewhere at Mufulira, relations are more consistent with active development of the basement topography during deposition of the Footwall

Formation. In the area immediately west of 4500 m E, between the 580 and 810 m levels (Fig. 3) Annels (1979) reported numerous shear zones in the basement granite which are parallel the dominant NW–SE topographic trend, and originally dipped at 55° to the southwest. Although the shear zones are best developed in the basement, some propagated into the overlying Footwall Formation and may extend as far as the C-Orebody (Annels, 1979).

The subsequent localisation of contractional strain along some margins of the basement highs (Fig. 9) is also consistent with the reactivation of earlier basin-bounding faults. Ground conditions in the basement at Mufulira are commonly poor directly below the pronounced pinnacle-like basement protrusions (A.K. Singh, pers. comm., 2001). Although, it is not clear whether the increased intensity of fracturing in the basement along the margins of some basement highs is entirely due to the younger deformation, the fact that such ground conditions are restricted to regions beneath "highs", strongly suggests fracturing (and possibly the highs themselves) post-date the initial basin topography. It seems unlikely that the presently least cohesive basement rocks should have formed erosion-resistant basement highs, prior to deposition of the Footwall Formation.

Figure 9 shows the thicknesses of both the C-Orebody and Footwall Formation for the central basin at Mufulira, between 2600 and 4000m E (metric mine grid). Maps were produced by measuring true thicknesses of the Footwall and C-Orebody from mine plans (along section lines indicated), using the base of the C-Orebody as a datum. Data were unfolded and restored to horizontal. Although the C-Orebody is largely continuous across the irregular basement topography, thickness variations closely reflect those in the underlying Footwall Formation, suggesting continued minor subsidence on basin bounding faults at this time. However, there is no evidence these faults breached the basin floor.

Overall geologic relations in the Lower Roan are interpreted to be most consistent with deposition of the Footwall Formation into actively forming half graben. As no unit within the Footwall Formation can be correlated between the various sub-basins, it is likely significant relief existed prior to the onset of Katangan sedimentation, and that this was maintained by faulting until just prior to deposition of the Ore Formation when rates of subsidence on at least the sub-basin bounding faults slowed. Whether extensional faulting ceased during deposition of the Ore Formation, or became localised along faults away from the immediate area of the Mufulira deposit is unclear. However, given the thickness of the Katangan sequence overlying the relatively thin Footwall Formation, ongoing fault-related subsidence is favoured.

Genetic model for copper mineralisation at Mufulira

A key issue with regard to mineralisation models at Mufulira is the origin of the carbonaceous arenites (1-2% C as graphite, "greywackes" in the local mine terminology) that are major hosts to the ores (Annels, 1979). The greywackes occur within what has been interpreted as the deepest portions of the three sub-basins (Brandt et al., 1961). In the Eastern basin, three greywackes are centrally located with respect to the orebodies; coinciding with their thickest and/or highest grade portions (van Eden, 1974; Fleischer et al. 1976; Annels, 1979). Fleischer et al. (1976) considered the greywackes to be entirely of sedimentary origin, deposited at a late-stage during accumulation of each of the three main sedimentary intervals that host significant copper mineralisation. In contrast Annels (1979) proposed the carbonaceous arenite (greywacke) formed as a result of hydrocarbon migration into minor domal to antiformal flexures (culminations formed during incipient folding), capped by impermeable horizons within the Lower Roan succession. Reaction between the hydrocarbons and early diagenetic anhydrite resulted in inorganic reduction of sulfur which in turn precipitated copper sulfides from metal chloride-rich brines (Annels, 1979). However at the local scale there is either no relationship (Annels, 1979) and perhaps even an inverse relationship (Fleischer et al., 1976) between copper grade and carbon content.

Annels (1979) noted sedimentary characteristics of the greywackes are identical to laterally adjacent strata (i.e. massive greywacke passes laterally into massive argillaceous quartzite, while well stratified intervals can be traced right through carbonaceous areas, cf. Garlick, 1969). Other features such as interstitial sericite content, degree of compaction and sedimentary parameters such as grainsize, degree of sorting and rounding are also identical between argillaceous quartzites and greywackes (Annels, 1979). Annels (1979) interpreted mineralogical differences such as anhydrite and feldspar content to reflect diagenesis with more intense alteration (feldspar and anhydrite destruction) of the carbonaceous rocks (greywacke) compared to the surrounding argillaceous quartzites. Other features apparently suggest the carbon content of the greywackes was due to impregnation of existing sediments. Cut-offs in carbon content are abrupt and locally transgress stratigraphy, and the greywackes are best developed at the top of each ore horizon, directly beneath (interpreted) less permeable "caprocks" (Annels, 1979).

Although of a fairly limited nature, observations in the present study support introduction of both copper and carbonaceous material during diagenesis and the genetic model of Annels (1979). No evidence to support a detrital origin for the sulfides has been identified (c.f. van Eden, 1974; Fleischer et al., 1976). Preferential development of copper sulfides within original heavy mineral bands, is here interpreted to reflect either the enhanced permeability or favourable chemical micro-environment within these layers, as sulfides are demonstrably secondary (Fig. 8). If the identification of fine-grained carbonaceous material in the high-grade A-Orebody sample proves correct, it appears initial introduction of carbonaceous material (presumably as a hydrocarbon) predates copper introduction and occurred early in diagenesis as it rims both original detrital grains and later (?)early diagenetic overgrowths. The gross distribution of the copper sulfides also support introduction during diagenesis, well before development of the tightly interlocking intergranular textures (compaction ± deformation) typical of the "clean" arenites at Mufulira. The apparent inverse relationship between anhydride and copper sulfide within the Ore Formation, noted by many previous workers, is confirmed by the present study and strongly supports local sulphate reduction as a means of precipitating the copper sulphides from metal-chloride rich brines (Annels, 1979).

Although evidence presented here supports Annels (1979) model of diagenetic sulphate reduction by hydrocarbons, the nature of the trap that facilitated hydrocarbon impregnation of the ore horizons remains enigmatic. Annels (1979) envisaged hydrocarbons migrated into structural culminations (domal or antiformal flexures) formed during incipient folding. He considered hydrocarbon trapping to have resulted from the generally less permeable nature of the overlying rocks, coupled with fracture development along the crests of the culminations, allowing limited vertical migration of the hydrocarbons (and later metal-rich brines) to form the stacked orebodies.

As yet there is no clear evidence to support the inferred patterns of hydrocarbon and fluid migration. However, it is clear that if Annels (1979) "vertical leakage theory" is to be viable, the culminations must have been extremely low amplitude in order to explain both the stratigraphic confinement and large areal extent of strata-bound copper mineralisation (e.g. C-Orebody: <15 m x 8 km x 8 km). Such low-amplitude folding could be equally well caused by minor tilting and fault-related subsidence during basin development, as by contractional folding during later basin inversion. The progressive decrease in size but increase in grade of the stratigraphically higher orebodies at Mufulira could be the result of several factors. In the simplest model, the hanging wall of the C-Orebody represents the main aquaclude for both migrating hydrocarbons and metal-bearing brines. Only locally did fluids breach this and subsequent barriers to flow contributing to the smaller areal extent of the higher orebodies. The

higher grade of the stratigraphically higher deposits may be explained by more efficient fluid focussing and physically smaller trap sites at higher structural levels. The relative timing of copper mineralisation in the C- B and A-orebodies is unknown. However if the orebodies get younger up sequence the corresponding decrease in area and increase in grade of the stratigraphically higher orebodies could reflect progressive amplification of the structural culminations during mineralisation.

Acknowledgements

This study benefited greatly from the assistance and support provided by A. K. Singh, Jackson Mulili, Mwape Makwaza and Obino Mwila (Mopani Copper Mines PLC, Mufulira Mine). Useful discussions with CODES colleagues, particularly Dave Selley, have contributed significantly to my understanding of the Mufulira system.

References

Annels, A. E., 1979, Mufulira greywackes and their associated sulphides, IMM Transactions/Section B, v. 88, p. B15–B23.

Binda, P. L., 1975, Detrital grains in the late Precambrian B greywacke of Mufulira, Zambia: Mineralium Deposita, v. 10, p. 101–107.

Brandt, R.T., Burton, C.C.J, Maree, S.C. and Woakes, M. E., 1961, Mufulira: *in* Mendelsohn F. (ed.), Geology of the Northern Rhodesian Copperbelt, McDonald, London, p. 411–461.

Evans, A. M., 1980, An Introduction to Ore Geology: Blackwell, 231 pp.

Fleischer, V. D., Garlic, W. G. and Haldane, R., 1976, Geology of the Zambian Copperbelt – Konkola and Musoshi: *in* Wolf, K.H. (ed.), Handbook of Strata-bound and Stratiform Deposits: II. Regional Studies and Specific Deposits, v. 6, p.244–249.

Garlick, W. G., 1969, Special features and sedimentary facies of stratiform sulphide deposits in arenites: in James, C. H. (ed.) Sedimentary Ores Ancient and Modern (revised), Leicester, University, Proceedings 15th Inter-University Geological Congress, Leicester, p.107–169.

Gunning, H. C., 1961, The Early Years: *in* Mendelsohn F. (ed.), Geology of the Northern Rhodesian Copperbelt, McDonald, London, p. 3–10.

van Eden, J. G., 1974, Deposition and diagenetic environment related to sulfide mineralisation, Mufulira, Zambia: Economic Geology, v. 69, p. 59–79.

Character, paragenesis and zonation of the copper ores at Konkola (Kirilabomwe), Zambia

R. J. Scott and N. Pollington
Centre for Ore Deposit Research, University of Tasmania

Summary

Copper ores at Konkola contain chalcopyrite, bornite and chalcocite, both finely disseminated throughout the Ore Shale (although some what concentrated within thin sandstone interbeds), and within thin, generally fibrous, bedding-parallel veins and lenticular aggregates. The latter are interpreted to reflect minor remobilisation and concentration of the disseminated ores during deformation at greenschist facies conditions. Deformation was minor and restricted to minor dilation and shear within or along specific layers, and did not affect the bulk of the Ore Shale. A strong bedding parallel compaction fabric is the only pervasive fabric recognised. Both primary and secondary chalcocite can be recognised on textural grounds. Hypogene chalcocite occurs as intergrowths in apparent textural equilibrium with bornite in disseminated ores in the middle of the Ore Shale. Secondary (supergene) chalcocite partially to completely replaces primary copper sulfides primarily within the upper and lower 2–3 m of the Ore Shale. Secondary chalcocite is invariably associated with haematite. A later phase of supergene oxidization concentrated at the very top and bottom of the Ore Shale has altered supergene chalcocite to malachite and cuprite. Initial sulfide introduction to form the disseminated ores was prior to the development of the strong compaction fabric, most likely early during diagenesis. We find no evidence to support structurally-controlled epigenetic origin for the ores. Although minor remobilisation and local enrichment of the copper ores occurred during localised layer-parallel dilation and shearing (probably during regional folding), this is on such a small-scale that "structural up-grading" of the ores is negligible in this area.

Introduction

Konkola copper ores are hosted by a sequence up to 12 m thick of thinly bedded, finely laminated arkosic meta-siltstone, fine-grained meta-sandstone, and lesser shale, known as the Ore Shale. Copper sulfides within the Ore Shale are extremely fine-grained and disseminated throughout the host rock. Higher concentrations of generally coarser grained sulfides also occur in thin bedding-parallel bands, lenticular aggregates and veins. Although at Konkola the Ore Shale is folded about the Kirila Bomwe antiform, the extremely fine-grained nature of the sulfides and the host rocks, together with the excellent preservation of the fine-scale sedimentary layering suggests the original character of the ores was not *significantly affected* by deformation and metamorphism (Sweeney and Binda, 1989). Accordingly Konkola represents one of the best deposits in which to investigate the primary origin of the copper deposits.

The purposes of this report are two-fold:

(1) to evaluate evidence for and the nature, extent and significance of internal deformation within the Ore Shale, with a view to assessing both the evidence for
   (i) structurally-controlled epigenetic mineralisation, and
   (ii) structural upgrading of existing ores (e.g. Hitzman, 1998).

(2) to determine the mineralogy, distribution and character of the ore, and specifically the
(i) textural character and relative ages (paragenesis) of the various ore minerals
(ii) lateral and/or vertical zonation within the Ore Shale, and
(iii) relative timing and nature of processes responsible for the original introduction (± remobilisation) of copper into these rocks.

Zonation patterns of both ore and gangue minerals within the Ore Shale are critical to developing and evaluating models for copper deposition. However it is important to identify and distinguish primary metal zonation from that which is the result of subsequent modification by metamorphic or supergene processes. Of particular importance is the question of whether chalcocite is (1) part of the primary assemblage, (2) is a late-stage "hypogene" mineral after chalcopyrite and/or bornite, (3) whether it is the result of supergene alteration of primary chalcopyrite and bornite, or (4) has multiple origins. If some or all of the chalcocite forms part of the hypogene assemblage it can be used, along with coexisting (coeval) mineral assemblages to constrain conditions of sulfide deposition. Accordingly techniques for identifying distinguishing different generations of chalcocite (and all other ore minerals) are essential if patterns of primary mineral zonation are to be correctly identified and interpreted.

This report is based largely on the initial petrographic examination of 18 polished thin sections from 14 samples collected during three visits to the Konkola Mine (No. 1 and No. 3 Shafts). Further, more detailed SEM, electron microprobe and laser-ablation ICPMS studies are planned for 2002, and will be reported at a later date.

Stratigraphic setting/deposit geology

The Konkola deposit is located in the northwestern end of the Zambian Copperbelt and straddles the Zambian/Congolese border (Fig. 1). Historically the deposit has been divided at the border and on the Congolese side it is known as Musoshi. The copper deposits are hosted within the first significant interval of fine-grained sediments (i.e. the Ore Shale) within the Lower Roan Group, which predominantly consists of coarse siliciclastics (Fig. 2). Sediments were deposited within an interpreted basin between the Konkola Dome in the northwest and the Kirila Bomwe Dome in the southeast (Fig. 1; Fleischer et al., 1976). The zone of copper enrichment within the Ore Shale is essentially continuous across the central saddle between the two domes. This study is concerned with mineralisation at the Konkola Mine (No. 1 and 3 Shafts) adjacent to the Kirila Bomwe Dome.

The Konkola Deposit has been mined from three shafts. Shafts 1 and 3 are still in production whereas Shaft 2, in the Konkola North (Konkola Dome) area, was only developed for a short period before closing. In 1988 the deposit had in combined total production and resource about 685 Mt at 3.1% Cu with a further 100 Mt at 4.33% Cu in the Konkola Deeps prospect. At Konkola, the footwall sequence (Mindola Clastics) underlying the Ore Shale is up to 1000 m thick. It consists of a lower sequence (Bancroft) of grossly upward fining boulder to pebble conglomerate, quartzite and argillaceous sandstone, and an upper sequence (Kafue Arenites) of conglomerate and argillaceous to arkosic sandstone (Sweeney and Binda, 1989). At Konkola Mine, the Ore Shale is divided into 5 sub-members, termed Units A–E which have a typical combined thickness of 10–12 m (Table 1). Economic mineralisation is predominantly hosted by Units B and C. Overlying the Ore Shale Member is the Nchanga Quartzite, known locally as the Hanging Wall Quartzite. In the north the contact is marked by the Konkola Member, an oxidised pebbly conglomerate. Up to 300 m of interbedded arkose, silt and grit, known as the Shale with Grit, gradationally overlies the Nchanga Quartzite (Fig. 2).

At Konkola, the Ore Shale is folded around the large-scale, open, gently WNW-plunging Kirila Bomwe anticline (Fig. 1), and a number of smaller parasitic folds developed in both the western limb and nose of this structure. Underground observations and samples discussed here are from both the "North

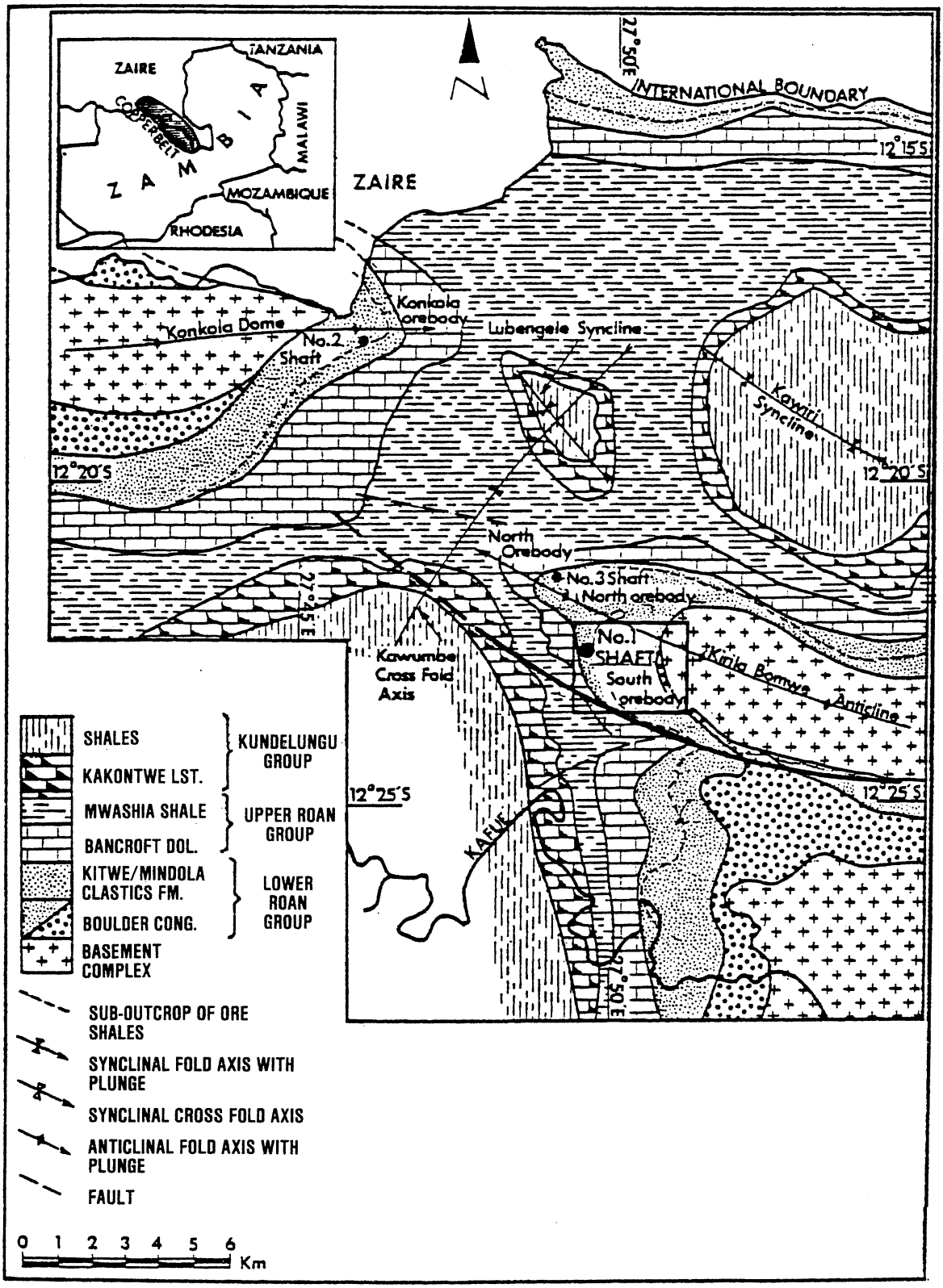

Figure 1
Geology of the Konkola mine area. From Sweeney and Binda (1989)

Table 1.
Subdivision of the Ore Shale at Konkola

Unit	Thickness	Host Rock	Mineralisation
Unit A	0.6 – 1 m	Finely inter-laminated grey siltstone and pink/brown carbonate	Erratic oxide mineralisation and chalcocite in streaks or laminae parallel to bedding (~1.5% Cu).
Unit B	1.4 – 2 m	Grey to yellow/brown, relatively massive sandy siltstone	Uniformly disseminated fine-grained chalcocite, chalcopyrite and bornite (~5.5% Cu).
Unit C	0.9 – 2 m	Finely laminated grey siltstone with common calcareous horizons up to 4 cm thick	Chalcopyrite, bornite and chalcocite as fine disseminations, bedding parallel veins and lenticles (3–6% Cu).
Unit D	1 – 1.8 m	Dark grey laminated siliceous siltstone, minor calcareous horizons	Similar to Unit C but more erratically distributed, sulfide lenticles more common (2.4% Cu).
Unit E	0.6 – 1.5 m	Micaceous dark grey siltstone interbedded with brown feldspathic sandstone	Highly erratic chalcocite and minor oxide mineralisation (1.3% Cu).

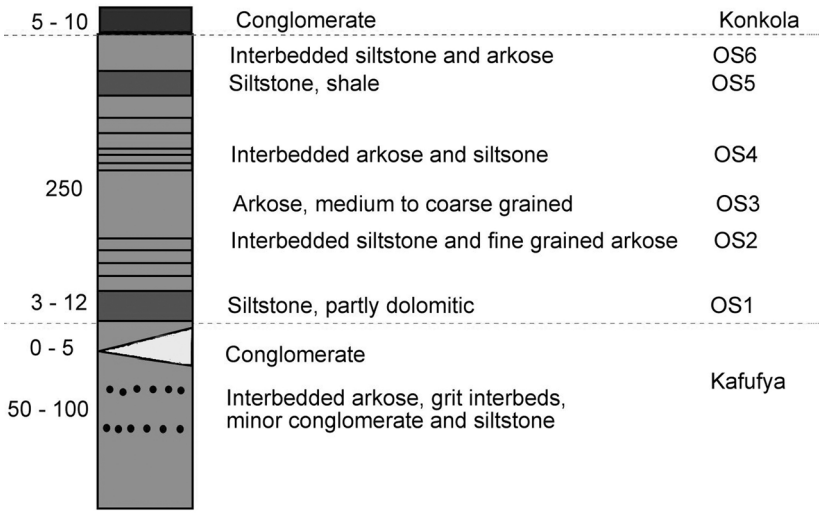

Figure 2
Lower Roan stratigraphy in the Konkola Mine area.

Orebody" (No. 3 Shaft) in the nose and on the north limb of the Kirila Bomwe anticline and the "South Orebody" (No. 1 Shaft) on the west limb of the fold (Fig. 1). The west limb of the Kirila Bomwe anticline is moderate to steeply W-dipping while the north limb dips at <35–40° N at upper levels and steepens to greater than 60° below the 300 m level.

Internal deformation and character of the Ore Shale

Apart from minor broad gentle folds and flexures of bedding (related to the main Kirila Bomwe anticline), in the areas visited as part of this study the Ore Shale is very weakly deformed (e.g. Fig. 3a) and internal deformation is subtle, localised and generally minor. Rare asymmetric open to isoclinal folds enveloped by planar bedding surfaces (i.e. "intrafolial" folds) are developed locally, particularly within or where carbonate layers are well developed (e.g. Units C, D ± E; Fig. 3b, c). Broadly strata-bound, highly-irregular partly disaggregated small-scale late-stage disharmonic folds and minor shears are essentially restricted to Units A and E, at the top and bottom of the Ore Shale respectively. These structures overprint the earlier open to isoclinal folds (e.g. Fig. 3b), but do not significantly effect the more consistently oriented strata above and below units A and E. The style of the deformation coupled with the fact that it appears restricted to the horizons which show the greatest levels of "late" supergene oxidation suggests these processes may be coupled. Accordingly, folding and shearing are interpreted to reflect localised slumping caused by partial dissolution of the rock in these horizons.

Compositional and textural variations throughout the Ore Shale are relatively minor. In general the lower portion (e.g. Unit B) is not as well stratified as the remainder of the unit, and carbonate bands are largely restricted to Unit C and to a lesser extent Units D and E (Table 1, Fig. 3a, b). In the areas sampled the Ore Shale predominantly consists of thinly interbedded siltstone and lesser fine- to medium-grained sandstone, and shale. Sandstone layers are generally less than a few millimeters thick and consist of detrital quartz, feldspar (microcline + albite) and white mica (Fig. 4a, b). Minor interstitial biotite, carbonate and rutile are interpreted to reflect greenschist facies metamorphism of original clay minerals. Siltstone layers have the same mineralogy, but are more matrix-rich, containing a greater proportion of fine-grained secondary biotite, white mica, carbonate ± rutile (Fig. 4a, b). Although many detrital grains (particularly feldspar and white mica) and textures are moderately well preserved, detrital quartz is typically significantly modified by dissolution and recrystallisation, particularly in matrix-poor sandstone layers. As a result, original sandstone layers now consist of tightly interlocking aggregates of irregular to polygonal quartz and feldspar grains.

Narrow bedding-parallel carbonate bands (Figs 3a, b, 5a) are well developed in Unit C and D of the Ore Shale. These layers contain minor to abundant quartz and feldspar, that appears to be, at least in part, detrital in origin. However, there is no direct evidence to support a detrital origin for the carbonate. While grossly bedding-parallel, "carbonate fronts" are commonly gradational (Fig. 5a) and transgress bedding locally. Carbonate grains within these layers are generally elongate, with a strong preferred orientation oblique, but at variable angles, to bedding. The grain shapes are most consistent with either *in situ* growth or recrystallisation during deformation. The morphology and distribution of carbonate grains could simply reflect deformation and minor dispersal (during metamorphism) from an originally carbonate-rich clastic. However as no detrital features are preserved carbonate introduction during diagenesis or subsequent hydrothermal alteration are equally plausible. If the latter is the case, the grossly strataform nature of the bands presumably reflects preferential percolation of carbonate-rich fluids along (?)thicker, more permeable sandstone layers.

Detrital white micas within the Ore Shale are often partially overgrown by biotite but have a distinctive appearance (aspect ratios >15:1, and maximum dimension proportional to the grainsize of the host

layer) and strong bedding-parallel alignment in siltstone and shale layers (Fig. 4a, b). Alignment of detrital micas in sandstone layers is generally more irregular, reflecting the greater influence of other framework grains on their orientation. Fine-grained interstitial and matrix micas (predominantly biotite) are more equant and blocky or irregular in outline. In general they lack a preferred orientation or evidence of significant internal deformation. The only pervasive fabric developed within the Ore Shale is the strong bedding-parallel compaction fabric defined by detrital white micas (Fig. 4a, b) and sutured quartz grain boundaries within sandstone layers.

In contrast, carbonate layers are typically characterised by subtle to well developed fabrics oblique to bedding. These are most apparent where defined by elongate blebs of copper sulfides (Fig. 5). Other constituents of these layers (especially carbonate and secondary micas: biotite ± white mica) may exhibit similar alignment, but sulfide grains are typically up to an order of magnitude larger than other minerals (Fig. 5b–d). The fabric appears to be primarily a lineation rather than a foliation, but locally it is axial planar to small, asymmetric, open to isoclinal strata-bound folds within the carbonate layers (Fig. 3c). The fabric is morphologically, geometrically and compositionally similar, and in part transitional to, bedding-parallel "fibrous" copper sulfide ± carbonate ± quartz ± biotite ± feldspar veins and asymmetric lenticular aggregates (e.g. compare Figs 4c–f , 5b–d). Significantly, these and the bedding parallel fibrous veins and lenticles (described below) are the only components of the Ore Shale that developed (deformation) fabrics oblique to bedding.

Microstructural character and distribution of ore minerals

Copper ores at Konkola are irregularly distributed throughout the host sequence. There are three main textural associations: (1) disseminated fine to very fine grained sulfides (Figs 4a, b, 5a), (2) fine to medium grained, typically elongate sulfides in narrow bedding-parallel veins and lenticular aggregates (Figs 4c–f, 5a), and (3) as fine- to medium-grained equant to markedly elongate irregular grains in pale carbonate bands and adjacent haloes (Fig. 5).

Particularly in the upper part of the Ore Shale (e.g. Sweeney and Binda, 1989) disseminated copper sulfides are commonly coarser grained and more abundant in beds of originally coarser-grained detritus. The range in grainsize of the ore minerals is similar to that of detrital grains comprising the host layer (Fig. 4a, b). In coarser-grained layers (medium to fine-grained sandstone) sulfide grains <1 mm in diameter, can compose up to 30 % of individual thin layers. However, sulfide abundance in beds of similar grainsize and thickness is highly variable overall. Generally minor but ubiquitous recrystallisation of detrital material indicates it is unlikely the observed grain contacts between sulfides and the host silicates are identical those formed at the time of copper introduction. Nonetheless, the fact that grainsize and abundance of the disseminated ores reflects the original grainsize of the host layers, strongly suggests textural relations were not substantially modified by deformation and metamorphism (see also Sweeney and Binda, 1989).

In contrast, the numerous small, fibrous bedding-parallel sulfide-bearing veinlets and lenticles within Units C and D of the Ore Shale are interpreted as evidence of at least limited remobilisation of copper minerals during deformation and metamorphism. Similarly sulfides within the thin carbonate layers form elongate grains and blebs that are moderately to strongly aligned and significantly larger than the grainsize of the host (Fig. 5b–d). The elongate chalcopyrite ± bornite grains are intergrown with carbonate ± quartz ± biotite ± feldspar within the veins, lenticular blebs and carbonate layers (Figs 4c–f, 5a–d), suggesting they formed at peak metamorphic conditions. The orientation of sulfide "fibres" and elongate blebs is highly variable and ranges from 90° to <20° to bedding. Commonly there are significant variations in "fibre" orientation over small distances within individual veins or carbonate layers.

The geometric and compositional similarities between

Figure 3
(a) Well stratified, medium- to thinly-bedded siltstone, sandstone and pale carbonate layers within weakly to undeformed Unit C of the Ore Shale. Note secondary chalcocite (silver) + cuprite (red) in thin band immediately to the right of the point of the pick head.

(b) Irregular tight to isoclinal recumbent ("intrafolial") folds in Unit E of the Ore Shale. Recumbent folds are overprinted by upright disharmonic folds.

(c) small asymmetric fold within carbonate band, Unit C, Ore Shale. Note alignment of elongate sulfides parallel to the axial plane of the fold within carbonate layer.

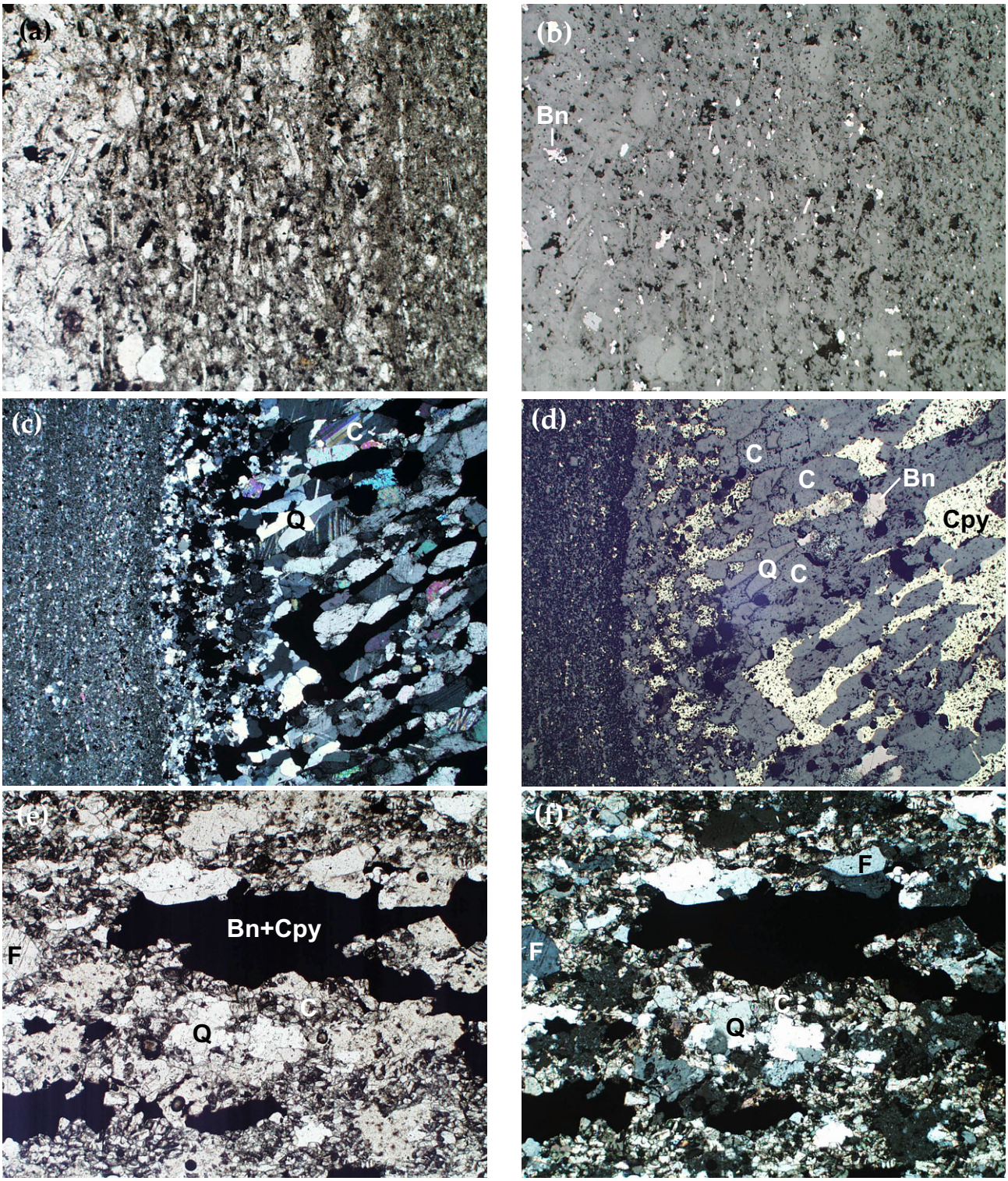

Figure 4
Ore textures. Abbreviations are: Q = quartz, F = feldspar, B = biotite, C = carbonate, Cpy = chalcopyrite, Bn = bornite
(a and b) Photomicrographs transmitted and reflected PPL, respectively. Well stratified sandstone, siltstone and shale (L to R) within Ore Shale (Unit C). Note strong bedding-parallel (vertical in figure) alignment of detrital white micas in siltstone layer. Grainsize of copper sulfides is similar to that of the host layer. (Unit C, Sample K3-2, width of view: 2 mm).

(c and d) Photomicrographs transmitted XPL and reflected PPL, respectively. Bedding parallel (vertical in figure) fibrous carbonate + chalcopyrite + bornite + quartz vein. Ore Shale (Unit C). (Sample K3-2, width of view: 2 mm).

(e and f) Photomicrographs in transmitted PPL and XPL, respectively. Elongate chalcopyrite + bornite grains within carbonate + quartz + feldspar vein. Note silicates are elongate parallel to the sulfides while the (?)recrystallised carbonate crystals appear more randomly oriented, and an order of magnitude smaller than the other minerals in the vein. Ore Shale (Unit C). (Sample K3-2, width of view 2 mm).

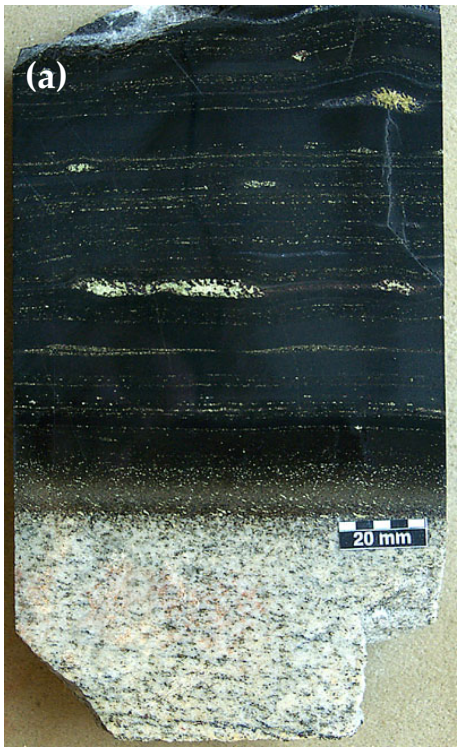

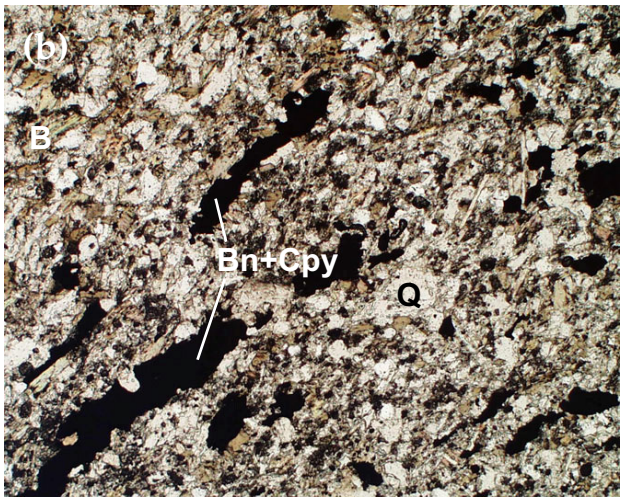

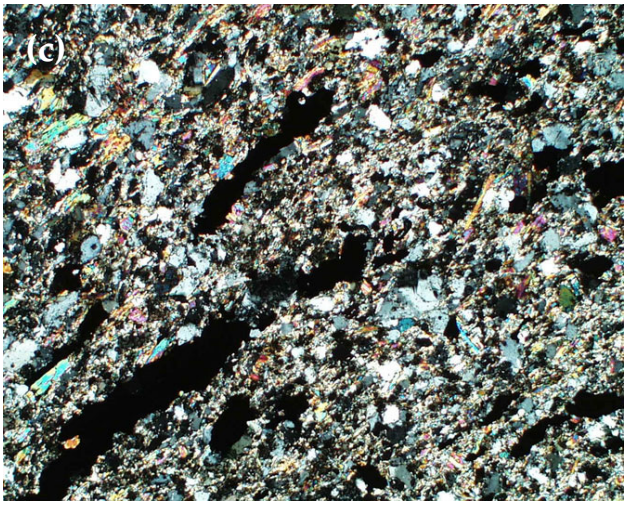

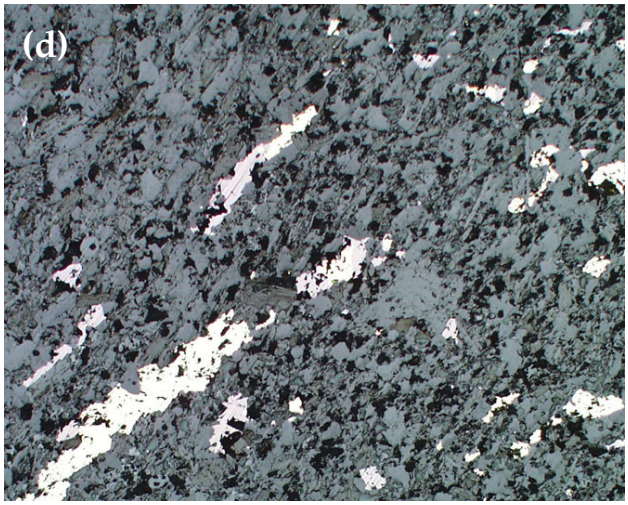

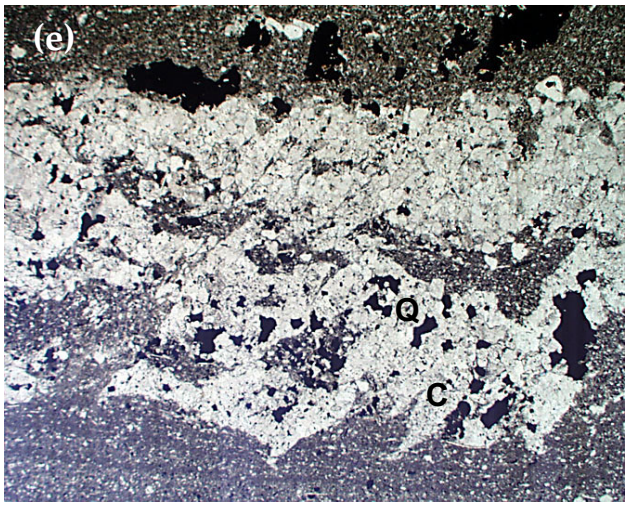

Figure 5
Deformation and remobilisation of primary disseminated ores. Abbreviations are: Q = quartz, F = feldspar, B = biotite, C = carbonate, Cpy = chalcopyrite, Bn = bornite

(a). Bedding-parallel carbonate band and asymmetric fibrous sulfide lenticles in Unit C of the Ore Shale. Note alignment of fine chalcopyrite needles oblique to bedding within the 1 cm band immediately above the carbonate band. The paler colour of this band compared to the overlying siltstone reflects fine-grained disseminated carbonate + chalcopyrite (Sample K3-3, Unit C).

(b to d) Photomicrographs in transmitted PPL and XPL, and reflected PPL, respectively. Detail from pale band above carbonate layer in (a). Note well developed alignment of secondary mica (biotite + white mica) parallel to sulfide grains, but oblique to bedding. Relict detrital micas subparallel to bedding (subvertical in photomicrograph) are apparent at centre left. (Sample K3-3c, Unit D, width of view: 1.6 mm).

(e) Photomicrograph in transmitted PPL showing disaggregation of siltstone layer due to irregular dilation at high-angle to bedding. Light coloured coarser grained material is a mixture of quartz + carbonate vein fill and detrital quartz and feldspar within an original sandy layer. (Sample RS-K-4e, Unit C, width of view: 8 mm).

carbonate layers with elongate blebby sulfides and the bedding-parallel fibre veins suggest distributed grain-scale dilation at moderate to high-angles to bedding, within relatively porous beds (rather than localised dilation across bedding parallel fractures to form veins) may have been an important process in their formation. Evidence for such a processes is preserved locally as layers consisting of irregularly disaggregated detrital grains (original sandstone layer) and siltstone fragments (originally adjacent layer) separated by hydrothermal quartz and carbonate (Fig. 5e). However the variation in orientation of the elongate sulfide blebs with respect to bedding, and their geometric relationship to asymmetric strata-bound folds, suggests elongation was at least in part due to flattening during localised layer-parallel shear.

Ore mineralogy and paragenesis

In the areas sampled chalcopyrite ($CuFeS_2$), bornite (Cu_5FeS_4) and chalcocite (Cu_2S) are the major copper ores present. The dominant sulfide assemblage throughout most of the Ore Shale is chalcopyrite + bornite, although relative proportions differ significantly (e.g. from >95% to <5% chalcopyrite) within individual units, and no systematic zonation was observed. On textural grounds, two generations of chalcocite can be recognised. The most abundant is interpreted as secondary, resulting from the apparently *in situ* replacement of primary bornite and chalcopyrite. Secondary chalcocite occurrences range from (1) partial replacement bornite and chalcopyrite, generally rimming or along internal fractures within grains (Fig. 6c, d), to (2) forming entire grains, with chalcocite the only copper sulfide present in a sample (Fig. 6e). Secondary chalcocite is intimately associated with fine-grained specular haematite (Fig. 6c, d), and more rarely the bismuth sulfasalt, wittichenite (Cu_3BiS_3). The subtle blue-grey mottling of some of the chalcocite (obscured by tarnishing within a few days of polishing) is characteristic of the low temperature djurlite ($Cu_{1.96}S$, stable at T < 100°C, D. Clark, pers. comm., 2001).

"Primary" (hypogene) chalcocite is not associated with haematite and occurs in apparent textural equilibrium with bornite (common graphic intergrowths) ± carrollite ($Cu(Co, Ni)_2S_4$) (Fig. 6a). Bornite intergrown with hypogene chalcocite tarnishes rapidly after polishing (i.e. within a few days) to pale purple-brown (in reflected light) and is visually distinct from the bronze to orange-brown bornite which occurs in textural equilibrium with chalcopyrite (Fig. 6a, b). Hypogene chalcocite is best developed where chalcopyrite is rare or absent. However, in some samples, adjacent texturally-similar grains of bornite are inter-grown with either hypogene chalcocite or chalcopyrite (Fig. 6b). At the scale of petrographic observation, the three are never observed in the same grain. In our sample suite hypogene chalcocite was only observed to be intergrown with bornite in the disseminated ores, and never with sulfides in the bedding-parallel veins and lenticles (although one sample, K3-4, has ambiguous bornite–chalcocite textural relations within a fibrous veins, and may contradict this assertion).

Secondary chalcocite is best developed in the upper and lower parts of the Ore Shale; specifically Units A ± B, at the base and Units E ± D at the top, where it is the dominant or only copper sulfide present. Its distribution throughout the central portion of the Ore Shale is variable. If present, it typically occurs as partial replacements of hypogene chalcopyrite and bornite (along grain rims and internal fractures) or as complete replacements within narrow bands and seams (e.g. Fig. 3a). Chalcopyrite and bornite are replaced to similar extents by chalcocite (no preference to replace one mineral over the other, as indicated by the uniform widths of chalcocite rims that cross chalcopyrite-bornite phase boundaries in individual grains). Minor covellite (CuS) after bornite (particularly as small "blooms" along grain edges and contacts with chalcopyrite), is also common, and best developed where secondary chalcocite development is advanced but not complete.

The distribution, grainsize and textural relations of the secondary chalcocite are identical to the hypogene

sulfides suggesting *in situ* replacement of these ores, with limited copper mobility. Similarly, iron liberated from chalcopyrite and bornite during conversion to chalcocite appears to have been largely immobile. In chalcopyrite + bornite grains partially altered to chalcocite, secondary haematite occurs as irregular aggregates of small grains, often with a distinctive bladed or needle-like form, reflecting preferential replacement (nucleating on and / or pseudomorphing) lenticular, bladed or flame-like segregations of bornite within the chalcopyrite (Fig. 6c, d). In grains completely altered to chalcocite, the liberated iron forms distinctive inclusion-rich haematite rims around the larger sulfide grains (Fig. 6e) or occurs as patchy haematite alteration of the matrix around smaller grains. While conversion of chalcopyrite and bornite to chalcocite is favoured by interaction with acidic fluids, the limited mobility of iron (more soluble in acidic fluids) and preservation of the biotite-white-mica assemblage in the matrix (i.e. not altered to clays) suggests the supergene fluid was either near-neutral or rapidly neutralised by reaction with the copper sulfides.

A further phase of supergene alteration of the copper sulfides suggesting more oxidizing conditions is particularly well developed at the base, and to a lesser extent, the top of the Ore Shale (A and E horizons, respectively). Here secondary chalcocite is partially to completely replaced by malachite ($Cu_2(OH)_2CO_3$; Fig. 6f–h). Remnant textural features from the earlier supergene alteration are locally preserved within zones of strong secondary oxidation and malachite development. For example the haematite rim on the malachite grain illustrated in Figures 6f–h, probably reflects iron liberated from bornite + chalcopyrite during conversion to chalcocite (c.f. Fig. 6e). Again, the apparently limited mobility of iron during supergene oxidation suggests interaction with carbonate-rich, near-neutral fluids. Lesser manganiferous "wad" (MnO_2) and cuprite (Cu_2O) are commonly developed in association with malachite.

Figure 6
Paragenetic stages recognised within the Konkola ores. Abbreviations are as follows: Cpy = chalcopyrite, Bn = bornite, Cc = chalcocite, Hem = haematite, Mal = malachite.

a) Interpreted primary graphic intergrowth of bornite (purple) and chalcocite (silver grey) within disseminated ore. Small pale pink prismatic crystal intergrown with copper sulfides at left is probably carrollite. (Sample K1-1, reflected PPL, width of view 500 μm).

b) Adjacent grains of orange- to purple-brown bornite intergrown with chalcopyrite and purple bornite intergrown with chalcocite. Both are constituents of the disseminated ore (Sample K1-1, reflected PPL, width of view 200 μm).

c) Secondary chalcocite (bright silver) rimming chalcopyrite–bornite grain in bedding-parallel vein. The irregular bornite flames and exsolutions in chalcopyrite are partially replaced by bladed haematite aggregates (steel grey). (Unit D, Sample K3-3c, reflected PPL, width of view 200 μm).

d) Same field of view as (c), with crossed-polars to emphasise characteristic red internal reflections of haematite. (Unit D, Sample K3-3c, reflected XPL, width of view 200 μm).

e) Specular haematite rim around secondary (supergene) chalcocite grain in bedding-parallel sulfide lenticle. Chalcocite is interpreted to replace primary chalcopyrite + bornite, with liberated iron forming the haematite rim. (Unit D, Sample RS-K-6, reflected PPL, width of view 2 μm).

f) Partial replacement of supergene chalcocite by malachite. Note preservation of haematite rim formed in prior supergene alteration of chalcopyrite + bornite. (Unit A, Sample K3-1, transmitted PPL, width of view 8 μm).

g) Same field of view as (f), in reflected light emphasising contrasting reflectance of chalcocite and haematite. (Unit A, Sample K3-1, reflected PPL, width of view 8 μm).

h) Detail from (f) and (g) illustrating distinctive red internal reflections of haematite rimming partially replaced chalcocite grain (Unit A, Sample K3-1, reflected XPL, width of view 200 μm).

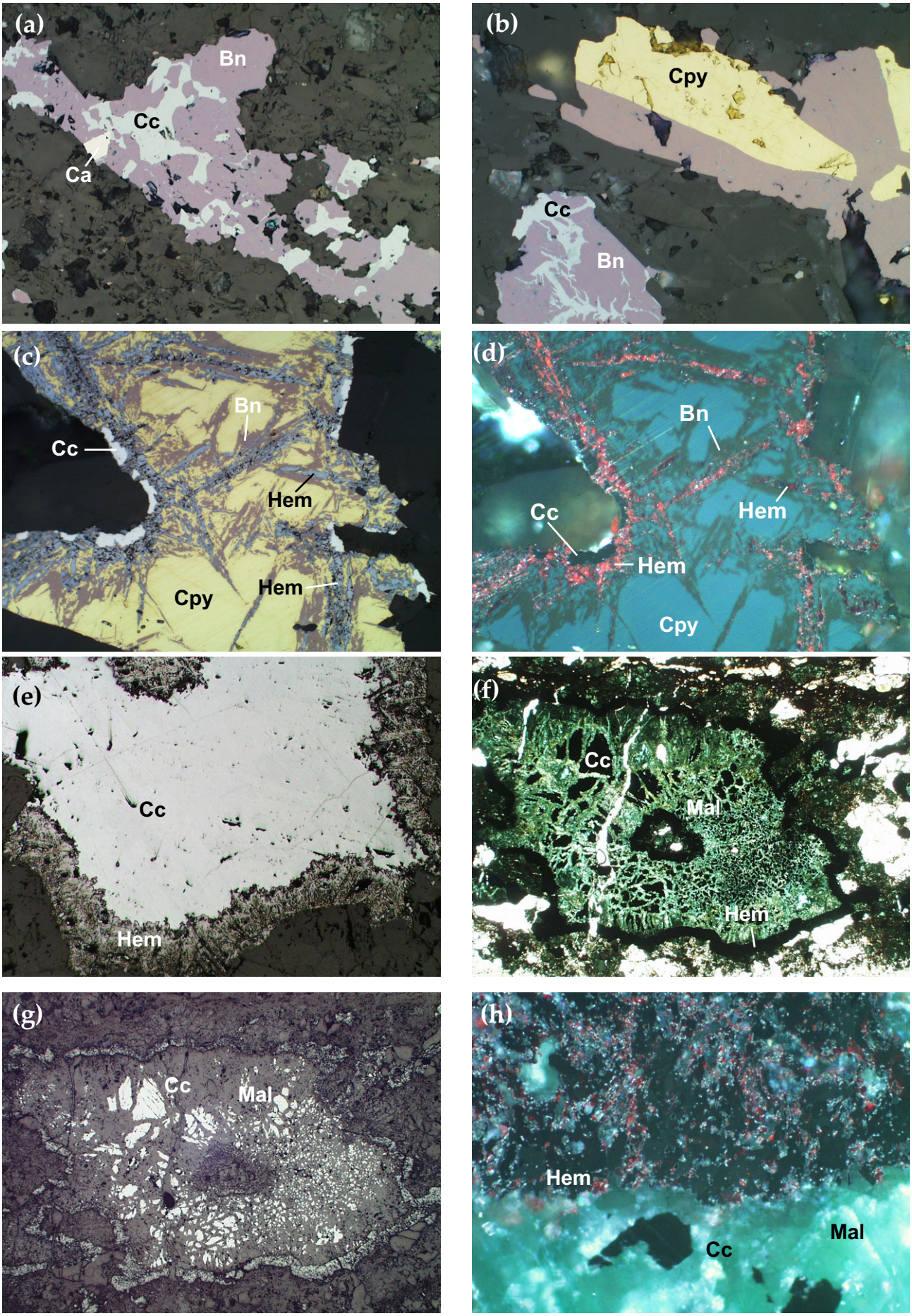
(a)
Bn
Cc
Ca
(b)
Cpy
Cc
Bn
(c)
Bn
Cc
Hem
Cpy
Hem
(d)
Bn
Cc
Hem
Hem
Cpy
(e)
Cc
Hem
(f)
Cc
Mal
Hem
(g)
Cc
Mal
(h)
Hem
Mal
Cc

Discussion

There is no evidence that copper sulfides at Konkola were detrital. There is no obvious grainsize sorting in individual layers, and the scattered occurrence of relatively dense copper sulfides with similar variations in grainsize as the host layers indicates the sulfides were not deposited in hydrodynamic equilibrium with the silicates (Sweeney and Binda, 1989). Rather the distribution and variation in grainsize of the disseminated ores is most consistent with replacement of detrital phases or precursor diagenetic mineral(s) or with the in-filling of primary or secondary porosity early during the burial history of the host succession. The greater concentration of sulfides in sandstone layers suggests porosity of individual layers after initial compaction, but prior to lithification, was a major control on ore fluid access. The present low apparent porosity of sandstone layers, suggests copper sulfides were already present prior to significant compaction (i.e. before significant dissolution and recrystallisation lead to the development of interlocking grain mosaics).

Although the grainsize and distribution of the copper ores does not appear to have been significantly effected by metamorphism to lower greenschist facies, the extent to which sulfide compositions and/or internal textural relations were modified by metamorphism is unclear (c.f. Sweeney and Binda, 1989). Textural and phase relations herein termed "primary" or "hypogene" may (at least in part) reflect those at the time of copper introduction. However, these relations could equally well reflect syn-metamorphic re-equilibration. Furthermore, our identification of a "primary sulfide assemblage" does not exclude the possibility this assemblage actually encompasses multiple temporally-distinct phases. Here we have used phrases such as "primary sulfide assemblage" and "hypogene assemblage" to describe the earliest recognisable sulfides which, on textural grounds, appear to have been introduced (or modified) at the same time.

Although locally complicated, Sweeney and Binda (1989) considered the overall paragenetic sequence of sulfide development at Konkola to be pyrite–carrollite–chalcopyrite–bornite–chalcocite. However detailed petrographic evidence to support the sequential development of all of these minerals was not presented. They argued mineralisation occurred during diagenesis and resulted from bacterial reduction of interstitial and nodular sulfate (anhydrite) within the Ore Shale early during the burial history of the rocks. While we concur that copper introduction most likely occurred during diagenesis, some details of the ore paragenesis are unclear to us. Neither our study or that of Sweeney and Binda (1989) identified anhydrite within the Ore Shale. Sweeney and Binda (1989) argued its former existence and importance to ore formation based on the presence of trace amounts of calcium sulfate within some of the lenticular carbonate. In our sample suite, pyrite is also very rare, and where present, timing with respect to copper sulfides is unclear. Nonetheless, the occurrence of rare copper sulfide grains with square outlines suggests pyrite was once more abundant and completely replaced by copper sulfides.

Based on our present observations, at least four distinct phases in the paragenetic development of the copper ores at Konkola can be recognised. The earliest comprises the bulk of the ore consists of finely disseminated copper sulfides interpreted to be of diagenetic origin (as described above). The next stage is interpreted to have been synchronous with deformation and greenschist facies metamorphism, and involved coarsening and attenuation of sulfides in carbonate-altered layers and development of "fibrous" bedding-parallel sulfide-bearing veins and lenticles. Collectively these two stages comprise what we have described as the hypogene ore. Development of secondary (supergene) chalcocite as partial to complete replacements of chalcopyrite and bornite, particularly at the top and bottom of the Ore Shale represents the next paragenetic stage. The final stage involved local supergene oxidation of the ores (again

concentrated at the top and bottom of the Ore Shale) to form malachite ± cuprite.

While direct overprinting criteria enable the last two stages to be readily distinguished, we have no direct overprinting criteria to indicate the finely-disseminated sulfides and coarser-grained "carbonate layer/vein-hosted" sulfides are of different age. As noted above disseminated ores may have re-equilibrated *in situ* during metamorphism, which could account for the internal textural similarities of both ore types. In contrast, Sweeney and Binda (1989) interpreted carbonate + sulfide (± minor quartz, feldspar) lenticles to reflect replacement of original anhydrite nodules during diagenesis and thus have formed at the same time as the disseminated ores. The presence of euhedral and fibrous crystals within the lenticles was explained by creation of open space due to the volume reduction accompanying the replacement of anhydrite by carbonate (Sweeney and Binda, 1989).

Textural features and mineralogy of the bedding-parallel veins and lenticles are more consistent with the development of these features during deformation and greenschist facies metamorphism. Depletion of very fine-grained disseminated sulfides around the coarser grained sulfide blebs and fibrous veins and lenticles suggests the latter were formed by remobilisation of the originally surrounding finely-disseminated ores. Both the shape of the lenticles and the orientation of the elongate mineral grains (fibres) within have consistent asymmetry along and across a number of layers (Fig. 5a). This is most consistent with development during (limited) dilation and shear along bedding, rather than the more random space fillings envisaged by Sweeney and Binda (1989). Furthermore the morphology and asymmetry (with respect to bedding) of elongate sulfide grains in the carbonate-rich bands and is identical to that within the lenticles, and replacement of anhydrite does not appear to be a feasible explanation for the more extensive carbonate bands. Finally, the local occurrence of biotite intergrown with, and parallel to, elongate sulfides within lenticles and carbonate-altered bands indicates they developed under greenschist facies metamorphic conditions.

Carbonates from the Ore Shale exhibit a significant range in $\delta^{13}C$ (–20.7 to –9 PDB ‰) at similar values of $\delta^{18}O$ (–16 to –14 PDB ‰), clearly distinct from values for carbonates in the underlying footwall sequence (Sweeney and Binda, 1989). The latter are enriched in Na and Sr and interpreted to be of marine origin. In contrast, Sweeney and Binda (1989) interpreted Ore Shale carbonates to have precipitated from meteoric-dominated ground-waters early during in diagenesis. Significantly, carbon- and oxygen-isotope values for carbonate from bedding-parallel lenticles envelop values for carbonate bands, a fact interpreted by Sweeney and Binda (1989) to support a common diagenetic origin for the carbonate in both cases. On mineralogical, textural and microstructural grounds we favour development of the bedding-parallel veins and lenticles during deformation at greenschist facies metamorphic conditions. Accordingly we contend that either all of the carbonate was introduced during metamorphism or carbon and oxygen isotopes do not allow discrimination of metamorphic and diagenetic carbonate.

The primary (disseminated ore) assemblage includes bornite that is intergrown (in apparent textural equilibrium) with both chalcocite and chalcopyrite. However as chalcocite and chalcopyrite do not precipitate under the same physio-chemical conditions, the proximity and textural similarity of bornite + chalcopyrite and bornite + chalcocite grains is problematic. This suggests either (i) the "hypogene" ore consists of at least two temporally distinct assemblages deposited under different physio-chemical conditions, or (ii) that marked grain-scale chemical gradients controlled patterns of copper sulfide precipitation/recrystallisation. Though seemingly unlikely, such small-scale chemical gradients could perhaps result from differences in the composition of minerals adjacent to or replaced by the depositing sulfides. It is perhaps significant that the hypogene chalcocite + bornite assemblage

appears restricted to the disseminated sulfides and does occur in the veins and lenticles, where bornite, if present, is intergrown with chalcopyrite. This could be interpreted as evidence that the hypogene bornite-chalcocite assemblage and current textural relations are in fact diagenetic in origin and were not substantially modified by greenschist facies metamorphism.

Although the elongate sulfide grains in and adjacent to carbonate layers are commonly at a high-angle to bedding, and locally axial planar to folds (Fig. 3c), this does not constitute a pervasive fabric (cleavage) in the rock. It is only present in either the carbonate layers or the bedding-parallel veins and lenticles. Elsewhere only the layer-parallel compaction fabric, principally defined by strongly aligned detrital white micas and sutured grain boundaries in quartz. Significantly the oblique fabric in carbonaceous layers may be partly defined by strongly-aligned biotite (randomly oriented elsewhere). These apparently disparate observations can only be rationalised if the oblique fabric are the result of localised dilation and shear along bedding planes or weaker (i.e. carbonate-rich) horizons. Accordingly deformation (which may have involved isoclinal folding locally (Fig. 3b), was largely restricted to relatively narrow individual (bedding-parallel) horizons.

On textural grounds we favour initial sulfide introduction prior to the development of the strong compaction fabric, and find no evidence to support structurally-controlled epigenetic origin for the ores. Layer-parallel shearing is interpreted to caused minor remobilisation and enrichment of the copper ores, but did so on such a small scale that "structural up-grading" of the ores is negligible (c.f. Hitzman, 1998).

Acknowledgements

We gratefully acknowledge the assistance of Davey Mubuta, Charles Sihole, Gotson Siame and John Waters (Konkola Copper Mines) for organising underground and drill core access and assistance with sampling. Darryl Clark's (CODES) help in the interpretation of textural and mineralogical relations within the ores was invaluable.

References

Fleischer, V. D., Garlick, W. G. and Haldane, R., 1976, Geology of the Zambian Copperbelt – Konkola and Musoshi: in Wolf, K.H. ed., Handbook of Strata-bound and Stratiform Deposits: II. Regional Studies and Specific Deposits, v. 6, p.244–249.

Hitzman, M.W., 1998, Petrographic studies of "ore shale" from the Zambian Copperbelt - implications for models of ore formation (abs.): Geological Society of America Program with Abstracts, v. 30, p. A-19.

Sweeney, M. A. and Binda, P. L., 1989, The role of diagenesis in the formation of the Konkola Cu-Co Orebody of the Zambian Copperbelt, in Boyle et al eds., Sediment-hosted Stratiform Copper Deposits: Geological Association of Canada, Special Paper 36, p.499–518.

Sedimentology, mineral paragenesis and geochemistry of the Konkola North Copper deposit, Zambia

Nicky Pollington
Centre for Ore Deposit Research, University of Tasmania

Summary

The Konkola North deposit in the North Western end of the Zambian Copperbelt contains 290 Mt @ 2.5% Cu and 26 Mt @ 0.13%Co (Avmin internal report). The deposit is hosted by fine grained silts (the Ore Shale Member) which wraps around the SW tip of the Konkola Dome. The economic mineralisation includes both surface oxides and deep sulphides which have been shown to be continuous through the central "saddle" area through to the currently working Konkola Mine (Fleischer, Garlick and Haldane, 1976). Past work by company geologist show that the mineralisation in the deposit is zoned according to mineral type and grades. The southern limb of the dome hosts mostly chalcopyrite, the eastern limb is dominated by chalcocite. Cobalt is only evident in the south eastern end of the deposit (Fig. 1). To the west of the main deposit is dominated by pyrite and rare Cu minerals.

As part of the P544 Amira project, this PhD research will provide a detailed study of the deposit in order to give insight on the sedimentology, mineral paragenesis and geochemistry of what is arguably the most pristine deposit in the copper belt (i.e. least affected by later metamorphism and alteration).

Aims

The overall aims of this study are to elucidate the sedimentology, mineral paragenesis and geochemistry of the Konkola North deposit. In order to do this a number of specific aims have been defined.

- Document the sedimentology of the host sequence at Konkola North and interpret them using modern facies analysis techniques. An important part of this will be to develop a more contempary understanding of the environment of deposition of the host lithologies to ore.

- Understand the sulphide mineral paragenesis and zoning, with particular reference to chalcocite. Determine criteria for distinguishing hypogene and supergene chalcocite.

- Better understand the controls on Cobalt mineralisation throughout the deposit.

- Document the effects of post sedimentary processes at Konkola North. These include diagenetic, hydrothermal and metamorphic, and also in the porous and permeable units, the effects of deep circulating groundwaters.

- Make an assessment of source of Cu/Co bearing fluids and the chemical processes responsible for sulphide deposition, and the environment required for sulphide precipitation, in particular why mineralisation is confined to the Ore Shale 1 member and is not present in other reduced lithologies.

Methods

Exploration in this area has occurred over a number of years and targeted different aspects of the deposit. Early drilling covered the shallow oxides following the nose of the Konkola Dome. This material was deeply weathered at the time of drilling and has deteriorated further since then so will not be of much use for sedimentary studies. Therefore this core will only be used for mineral studies and comparative studies for the mineral paragenesis.

Majority of the work for this study will be carried out on the most recent drilling programme which was completed in 1998. During this campaign about 50,000 m of core was drilled throughout the deposit, mostly exploring the deeper sulphide resource indicated from drilling between 1970 and 1980.

In order to document the sedimentology of the host sequence detailed sedimentary logging is required. The host sequence for this area includes the Upper Roan from the local marker bed – the Konkola Member in the hangingwall, through the Nchanga Formation, to as deep into the footwall as drilling allows – generally only 20 – 30ms into the Lower Roan, a generalized section is shown in Fig. 2. A number of fences have been defined to investigate all the possible environments of deposition (Fig.1). These include the east and south limb of the dome and across the basin to the south east where the deposit is cut off by company boundaries and becomes the Konkola Mine area. The macro scale facies analysis techniques will be complemented by detailed microscopic petrographic studies.

Investigating the mineral zoning will also require detailed logging of a number of fences of holes throughout the deposit. Therefore the fences have also been designed to cover the different mineral zones. That is, chalcocite in the east limb, chalcopyrite in south limb, cobalt in the far south east and pyrite in the far west of the deposit (Fig.1). This work will emphasise on detailed fine logging and extensive sampling of the mineralised sequence. Thin section petrography of the sulphides and detailed textural studies to determine sulphide paragenesis and will address the chalcocite questions. Once a paragenetic framework has been developed from textural studies LA-ICPMS will be used to measure trace elements in the sulphides.

Assay data from Avmin includes Cu, Co, Fe, Mn and S and these will be interpreted along with some additional whole rock geochemistry and LA-ICPMS.

During logging the effects of post depositional processes will also be examined. Samples will be taken specifically for their varying alteration assemblages observed. Detailed petrographic work will be carried out on these samples and some whole rock geochemistry will be done to determine overall changes in rock chemistry. Comparison with samples from Konkola Mine will also be made.

If appropriate, later in the project geochemical modeling of fluids and the chemistry responsible for the mineral deposition will be carried out.

Work completed to date

Emphasis for the first field season was on logging core and extensive sampling in order to address the sedimentology, mineral paragenesis and alteration aspects of the research.

Since commencing in July 2001 one field season has been completed. All work for this season was carried out on the most recent drilling available which was stored at the Chambishi Metals process plant site, some distance from the actual site of the Konkola North field area. Information from the Avmin geologists indicated very little outcrop existed in the field area and none of which related to the sequence being studied for this project. Also access to the Number 2 shaft which is located within the deposit was not available for this season but is tentatively planned for the next field season if logistics allow. So all emphasis for this season was put on detailed logging of a number of fences throughout the deposit.

Twenty-five holes were logged which covered three fences through the deposit. The Eastern Limb of the Konkola Dome which is mineralised by predominantly chalcocite. The Southern limb, which has more varied mineralisation but is dominanted by Chalcopyrite. The third fence covers from the southern chalcopyrite zone through to the most South Easterly drilling done on the property which has some higher cobalt grades. Focus for the season included sedimentological logging of the host sequence and detailed observation of sulphide distribution and zoning. To assist with sulphide zoning studies a number of holes were logged and photographed in finer detail.

A number of holes from the very weathered surface mineralisation around the dome were also logged although due to the intense weathering of the surrounding rocks only the mineralized zones were logged and sampled.

During logging, five holes were identified from different zones of mineralisation and splits of remaining crush from the sampling during exploration were taken of the mineralized area and 3–5 m into the footwall and hangingwall. Also approximately 300 samples were taken throughout the logged holes for mineral identification, sedimentary texture investigations, alteration texture and mineralogy and detailed sulphide mineralogy studies.

Objectives for 2002

- Drafting and interpretation of the sedimentological logging done during 2001 in order to understand the environment of deposition and what has affected the sediments since deposition.

- A number of samples were taken in order to investigate sedimentary features and mineral textures in the sediment groups observed. Thin sections of a large number of these samples will be cut and detailed petrography performed in order to carry out these investigations. At least 50 sections will be cut and described before the next field season.

- Also approximately 50 polished sections from the varying mineralised zones will be prepared and paragenetic sequences established for the sulphide mineralisation. These polished sections will be instrumental in determining the styles of mineralisation and which are supergene and which are hypogene. Techniques used will be determined by the grain size constraints of the mineralised zones. Predominantly textural work will be completed and a pilot LA-ICPMS study will be undertaken.

- Another three months of field work in Zambia will be carried out in 2002. During this time 2–3 fences of holes will be logged; one in the far West of the deposit which is reported to be pyrite-rich with minimal Cu mineralisation and another in the South East to study the Co distribution. Also observations in the North and South extensions of the mineralisation - Konkola and Musoshi. Given ideal circumstances, a trip underground at Number 2 shaft will also be carried out. The shaft was sunk in 1954 and Cu was produced for about a year, however due to low copper prices the mine was closed down. Thus an underground trip is not a definite as it is not a working mine and trips down the shaft are not made regularly.

References

Guart C., 1998, Lateral and vertical variation of lithology and mineralisation of the "Ore Shale"(OS1) in the Konkola North area, Zambian Copperbelt and constraints on the controlling factors, AVMIN internal report.

Fleischer V.D., Garlick W.G. and Haldane R., Geology of the Zambian Copperbelt – Konkola and Musoshi, in Wolf K.H. ed., Handbook of Strata-bound and Stratiform Deposits: II. Regional Studies and Specific Deposits; v6, Cu, Zn, Pb and Ag Deposits, p.244-249.

Konkola copper/cobalt deposit summary

Nicky Pollington
Centre for Ore Deposit Research, University of Tasmania

Regional Setting

The Konkola deposit is located in the North Western end of the Zambian Copperbelt and straddles the Zambian/Congolese border (Fig. 1). Historically the deposit has been divided at the border and on the Congolese side it is known as Musoshi. This review will only cover the Zambian portion.

The mineralisation occurs within the sediments of the Lower Roan Group which are generally coarse siliciclastics. These clastics form a basin between the Konkola Dome in the North West and the Kirilabomwe Dome in the South East (Fleischer, Garlick and Haldane, 1976). Mineralisation has been shown to be continuous between the shallower zones nearer the domes and through the central "Saddle" as it was termed during exploration.

Host Rocks

The deposit is hosted by the Lower Roan Group (Fig. 2) which comprises the footwall Mindola Clastics which can be up to 1000 m thick and is a fining upward sequence of polymict boulder conglomerate and arkoses deposited in an alluvial fan setting.

It is overlain by the rarely mineralised Kafue Arenites, which can be divided into three clastic units. The Porous Conglomerate with rounded to subangular boulders of quartzite, quartz, aplite and porphyry. The Footwall Sandstone a medium to coarse grained sandstone with minor argillite bands. The Footwall Conglomerate which is interbedded with arkosic and argillaceous lenses.

Unconformably overlying these is the Ore Body Member which can be broken into five submembers, Units A–E, which have a combined thickness of commonly 10–12 m. Table 1 provides descriptions of each unit and associated sulphide distributions. Economic mineralisation is predominantly hosted by Unit B.

Overlying the Ore Shale Member is the Nchanga Quartzite, also known as the Hangingwall Quartzite. In the north the contact is marked by a pebbly, oxidised conglomerate, the Konkola Member. A thick sequence, up to 300 m, of interbedded arkose, silt and grit, known as the Shale with Grit, gradationally overlies the Nchanga Quartzite.

Size and Grade

The Konkola Deposit has been mined from three shafts. Numbers 1 and 3 are still in production and number 2, which is in the Konkola North, area was only developed for a short period before closing. In 1988 the deposit had in combined total production and resource about 685 million tonnes at 3.1% Copper plus another 100 million tonnes at 4.33% Copper in the Konkola Deeps prospect.

Mineralisation

The majority of the mineralisation is hosted by the Ore Body Member, which varies in true thickness between 3–15m. The footwall and hangingwall transition to >1% Cu is very abrupt, the hangingwall

Table 1
Description of Ore Shale 1 divisions (after Sweeney and Binda, 1989).

	Thickness	Host Rock	Mineralisation
Unit A	0.6–1 m	Finely interlaminated grey siltstone and pink/brown carbonate	Erratic mineralisation ~1.5% Cu as oxide or Cc in streaks or laminae parallel to bedding
Unit B	1.4–2 m	Grey to yellow/brown, relatively massive sandy siltstone	Fairly uniform mineralisation ~5.5% Cpy finely disseminated
Unit C	0.9–2 m	Finely laminated grey siltstone and calcareous horizons	3–6% Cu as fine disseminations, sulphidite bands and lenticles
Unit D	1–1.8 m	dark grey siliceous siltstone, thinly laminated	Similar to Unit C but more erratically distributed
Unit E	0.6–1.5 m	Micaceous dark grey siltstone interbedded with a feldspathic sandstone	Highly erratic mineralisation — 1.3% as minor oxide minerals

more so and occurring over just a few centimetres. Mineralisation occurs as fine disseminations generally assuming the grain size of the host, and as slightly coarser grains along bedding boundaries, in thin veinlets/stringers and bedding parallel lensoids (Guart, 1998). Minerals present include: chalcocite, chalcopyrite, bornite, digenite, covellite, pyrite and carollite in order of abundance. Also, the non sulphide minerals present include: malachite, pseudo-malachite, chrysocolla, cuprite, azurite and native copper (Guart, 1998).

References

Sweeney M.A. and Binda P.L., 1989, The role of diagenesis in the formation of the Konkola Cu-Co Orebody of the Zambian Copperbelt, in Boyle et al eds., Sediment-hosted Stratiform Copper Deposits: Geological Association of Canada, Special Paper 36, p.499 – 518.

Guart C., 1998, Lateral and vertical variation of lithology and mineralisation of the "Ore Shale"(OS1) in the Konkola North area, Zambian Copperbelt and constraints on the controlling factors, AVMIN internal report.

Fleischer V.D., Garlick W.G. and Haldane R., Geology of the Zambian Copperbelt – Konkola and Musoshi, in Wolf K.H. ed., Handbook of Strata-bound and Stratiform Deposits: II. Regional Studies and Specific Deposits; v6, Cu, Zn, Pb and Ag Deposits, p.244-249.

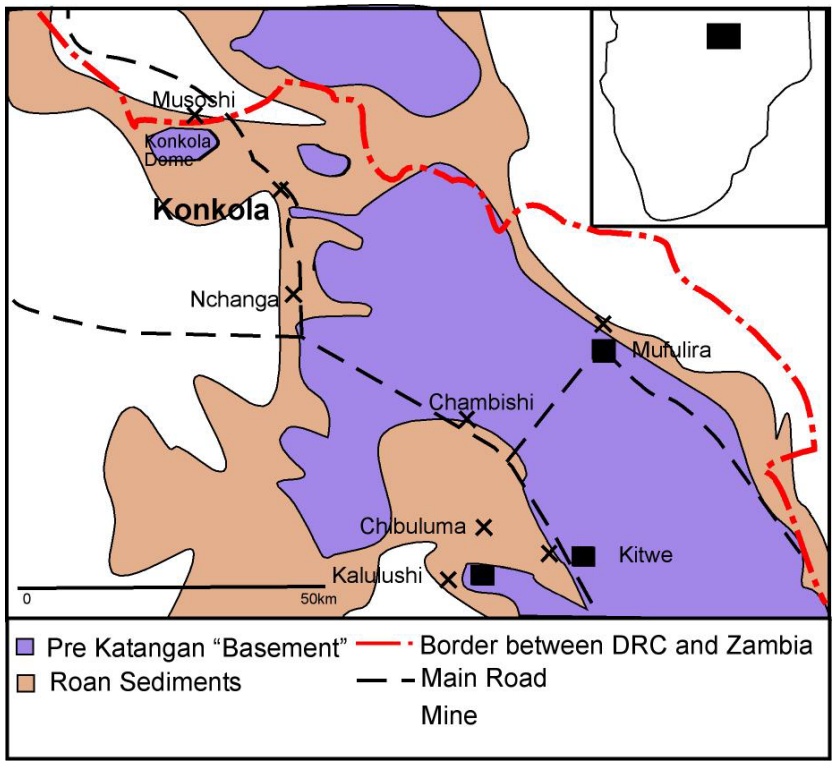

Figure 1
Generalised geology and Konkola location map.

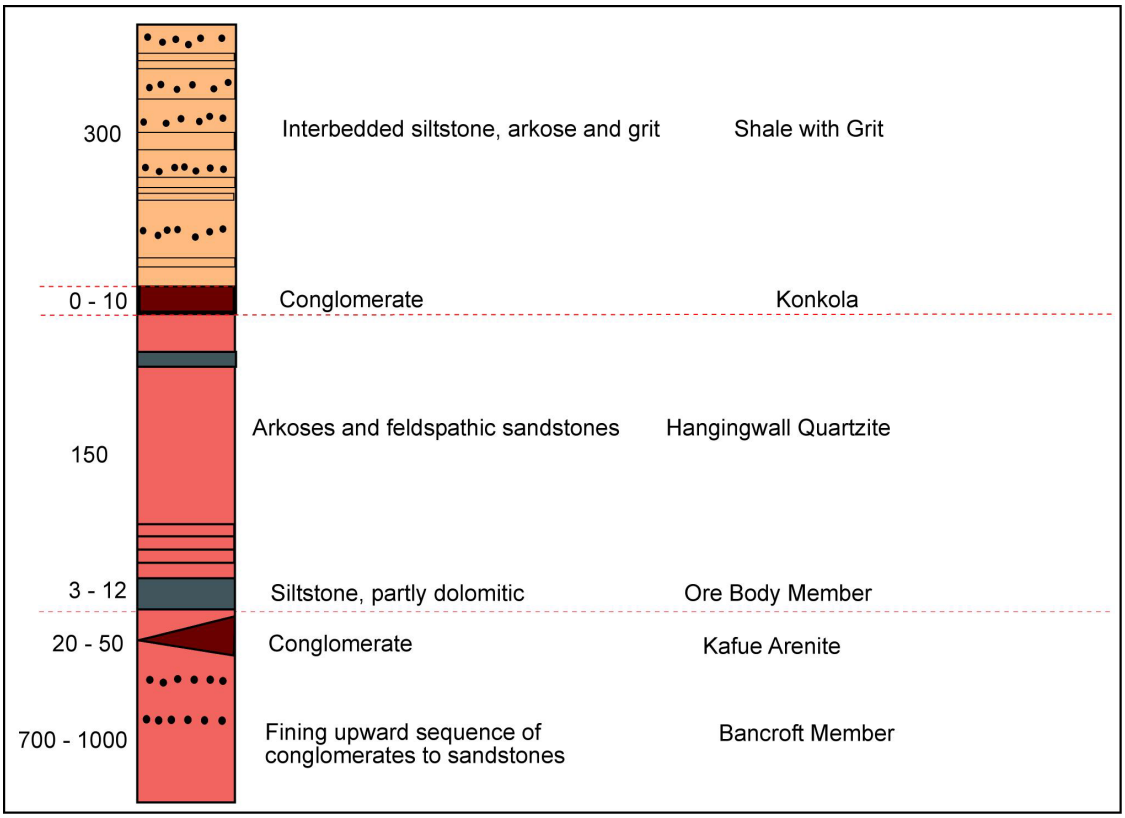

Figure 2
Generalised stratigraphy (after Avmin internal report)

PhD project: Geology and genesis of the Nkana deposit, Zambia

Mawson Croaker
Centre for Ore Deposit Research, University of Tasmania

Project aims

This PhD has been incorporated within the framework of the AMIRA P544 Proterozoic Sediment-Hosted Copper Deposits. The project studies the Neoproterozoic Lower Roan Sequence along the Nkana-Mindola (NM) mineralised system of the Zambian Copperbelt (Fig. 1). The NM mineralised system was targeted as (1) deformation intensity varies within the system, (2) lateral and vertical facies variations within the mineralised horizon appear to occur along the 17 km strike length and (3) copper mineral assemblages change along the strike of the orebody.

The principal objective of this study will be:
To constrain the genesis of copper mineralisation at NM by investigating stratigraphic, sedimentological, structural, petrological and geochemical aspects of the Neoproterozoic mineralised system.

Specific aims of this project are to:

- Document the local stratigraphy and establish the sedimentary architecture of the Lower Roan package at NM and within the Chambishi Basin by undertaking core logging, underground mapping, petrology and geochemistry.
- Determine the local deformation history of the NM system, particularly investigating the relationship with basement and possible controlling mineralising conduits through detailed underground mapping of high and low strain zones, core logging and petrological studies.
- Use petrological and geochemical methods to document the spatial and temporal relationships of the copper assemblages between the four shafts at NM.
- Document the nature and timing of metamorphic and hydrothermal processes that have affected the Lower Roan rocks at specific localities using structural, geochemical and isotopic information.
- The synthesis of results from each specific aim to develop a stratigraphic-structural-geochemical model of the NM system and to place this within the Pan African tectonic framework of the Zambian Copperbelt and central-southern Africa.

Work to date

Work on the Nkana-Mindola PhD project began in August 2001. Eight weeks of fieldwork were completed during August and September 2001. Field work focused on core logging of new diamond drillholes from South Orebody (SOB) and Mindola, underground mapping at SOB and Mindola and compiling old mine data including assays results and logs of old diamond core where possible. Considerable time was spent during the field season assessing access to underground areas of interest and investigating availability of old diamond drill core.

Sedimentology and lithology

Clemmey (1976), Mopani and First Quantum geologists, and field evidence collected in 2001 clearly indicate significant sedimentological and lithological differences between the northern Mindola Orebody

and the SOB (Figure 2). The recognition of sedimentary facies from field evidence is obsured by greenshcist facies metamorphism. Primary sedimentary textures are well preserved outside high strained zones, however original sedimentary mineralogical assemblages and grain textures are commonly overprinted by metamorphism and alteration. A further discussion of the metamorphism and alteration of the NM system is outlined below.

At Mindola the main ore horizon is a carbonate-siliciclastic sequence while at SOB ore is hosted within a black, graphitic pyritic shale. No petrographic examinations have been undertaken to date on samples from either Mindola or SOB. A brief description of lithologies/sedimentology collated from current field investigations and work by Clemmey (1976) is given in Figure 2.

Structure

The NM system is situated within the north westerly plunging Nkana Synclinorium in the Chambishi Basin. SOB Shaft and to a lesser extent Central shaft occur towards the keel of Nkana Synclinorium, demonstrated by the intense deformation at each orebody, whereas Mindola Shaft occupies the relatively undeformed moderate to steep dipping northeastern limb of the Nkana Synclinorium.

Detailed underground mapping in 2001 focused on the lower levels at SOB where the current Mopani Nkana Synclinorium Drilling Program is being undertaken. Sponsors visited this area during the June 2001 AMF-AMIRA Copperbelt fieldtrip. Preliminary fieldwork and interpretations suggest the structure is dominated by early tight to isoclinal, NW and SSE plunging folds with extensive axial plane shearing possibly the result of progressive deformation (Figs 3, 4). Later NNW to NE thrusts have been identified cutting the straitigraphy and a possible late more open fold event is interpreted from plans for the Central Shaft area, however field work is still needed to assess this confirm this fold phase.

Alteration – Metamorphism

One significant lithological difference between the South Orebody and Mindola is the degree of alteration-metamorphism of the Lower Roan Sequence, particularly in areas of intense deformation. For the purpose of this report the term alteration is used to describe significant modifications of mineral assemblages which on the basis of field allow cannot be attributed primary textural or compositional variations.

Alteration has been noted by previous workers including Richards (1965) and Annels (1974), however the significance and possible relationship to mineralisation has only recently been highlighted by First-Quantum and Mopani geologists working on results of the Nkana Synclinorium Project. Recognition of the alteration underground is often difficult, however from drillcore mineral assemblage changes on the scale of 10 cm's are recognised and initial work suggests some alteration mineral assemblages have a close relationship to structure and certain stratigraphic boundaries. No petrological examinations have been undertaken to date to further identify the alteration.

Biotite and anhydrite flooding zones are common at SOB and Central Shafts. However finer, less well-defined and recognizable mineral assemblages, commonly associated with mineralised zones, have been identified in the field by First-Quantum and Mopani geologists and during this study. Preliminary evidence from comparing alteration lithology to copper and cobalt mineralisation distribution indicates a direct relationship between the dolomitic alteration and high cobalt grades. The relationship of alteration to structure is yet to be determined.

Possible alteration/metamorphic mineral assemblages identified in the Lower Roan Sequence (Basal Quartzite, Footwall Sandstone and Ore Shale) from field evidence include:
Calcite-mica, anhydrite-mica-quartz, anhydrite-mica, calcite-blue-amphibole-mica, calcite-mica-anhydrite, calcite-mica-tremolite, dolomite-mica, dolomite-mica-

tremolite, dolomite-mica-anhydrite, calcite-blue amphibole-mica, feldspar-quartz-mica and feldspar-quartz-anhydrite-mica, altered carbonate-calc phyllite.

Initial whole rock and trace geochemical data of samples from NS009 have been received, however at the time of writing no interpretation of the results had been undertaken. Preliminary results will be presented during the Feburary 2002 AMIRA progress meeting.

Future work

Over the next six to twelve months several keys areas of investigation will be followed.

Before the 2002 field season:

1. A complete review of the literature surrounding the Copperbelt, focused mainly at the Chambishi Basin.
2. Compilation of detailed stratigraphic logs, one each for SOB and Mindola Shaft, before fieldwork commences in 2002. These sedimentological sections will be based upon field data, petrological data and data from previous publications.
3. Compilation of field data from the 2001 field season with the aim to produce preliminary geological maps and sections for the Nkana Synclinorium Project (NSP) area before the 2002 field season. This will involve assessing and using current Mopani geological plans where appropriate. Due to the large volume of new drillcore data from the NSP and the complexity of underground workings and geology, it is envisage Vulcan™ will be used to build and better visualise a geological model for the region. This model will then help focus future fieldwork in the area and be used in combination with petrological investigations to constrain Cu mineral assemblages, alteration zones and relationship to structure.
4. Detailed petrological examinations to ascertain the alteration assemblages before the 2002 field season with the intention to relate these back to structure, copper mineralisation distribution and whole geochemical analyses. This work will build on field base observations of First Quantum-Mopani geologists and this study.
5. A visit to South Australia will be undertaken before commencement of fieldwork 2002.

2002 fieldwork

A substantial field season will be undertaken during 2002. Currently work will be focused in several areas:

1. Sedimentological logging underground and from drillcore beyond highly strained zones for SOB, Central, Mindola and North Shafts to further define both vertical and lateral facies variations.
2. Structural mapping at Central Shaft focused around the zero anticline-syncline structure along with follow-up logging of new drillcore.
3. Detailed copper mineral assemblage logging of key holes from each shaft to accurately define vertical copper mineralisation assemblage.
4. Possible underground mapping and drillcore logging associated with the Kitwe Barren Gap.

An interesting and quite appropriate quote relating to field work in Zambia from Clemmey (1976) might be a good way to conclude this report.

> "Special problems are inherent in any underground study, especially one of a sedimentological nature. The advantages of three dimensional exposure are offset by ; the selective nature of mine development and drilling; the logistics of gaining access and even moving a few metres underground when this involves changing levels, the ephemeral nature of most exposure; a hostile working environment caused by a combination of heat, light, and excessive noise; the restrictive access period (blasting) and finally the compulsive tendency that mining engineers have for whitewashing any bare rock!"

Nkana deposit summary

Mawson Croaker
Centre for Ore Deposit Research, University of Tasmania

Regional setting

The Nkana-Mindola (NM) line of deposits is hosted within the Neoproterozoic Ore Formation part of the Lower Roan Group. The NM deposits occur on the southern flank of the Kafue Anticline within the Chambishi Basin. The mining area is immediately west of the city of Kitwe, some 285 km north of the Zambian capital, Lusaka.

Size and grade

Production occurs from four shafts along the NM system. Mining commenced on the NM system in 1932 with preprodution reserves estimated at 312 Mt @ 2.81 % Cu and to date approximately 6 million tones of copper has been mined. Currently underground mining is continuous from approximately 500 feet to 5000 feet. Total ore resources (measured and indicated) as at 30 November 2000 were calculated at approximately 186.5 Mt @ 2.28 Cu and 0.12% Co.

Mineralisation

Economic copper mineralisation at Nkana is associated with the NE limb of the north westerly plunging Nkana synclinorium. Mineralisation is predominately confined to the Ore Formation and the upper most portion footwall clastics. The Nkana-Mindola desposits are divided into two main mineralised systems, separated by the 1.2 km wide Kitwe Barren Gap. The 6.1km strike length tightly folded black, graphitic pyritic shales at South Orebody and the carbonate-siliciclastic sequence at Central Shaft host chalcopyrite and chalcopyrite-bornite style mineralisation respectively. To the north of the Kitwe Barren Gap the steeply dipping, 6.4 km strike length Mindola desposit, hosted within a carbonate-siliciclastic sequence, is dominated by bornite-chalcopyrite style mineralisation. Cobalt occurs as carrollite and cobaltiferious pyrite. Oxide copper mineralisation in the form of malachite, chrysocolla, native copper, cuprite and libenthenite is restricted to the upper levels of the orebodies.

Provisional stratigraphic comparison of three Cu mineralised basins; the Zambian Copperbelt, the Polish Kupferschiefer and the Adelaide Fold Belt

Stuart Bull, David Selley, David Cooke, Wallace Mackay, Ross Large and Peter McGoldrick

Centre for Ore Deposit Research, University of Tasmania

Summary

A stratigraphic comparison of the Cu mineralised Zambian Copperbelt (ZCB), Polish Permian and Adelaide Fold Belt (AFB) has highlighted some striking similarities and marked differences. In terms of the stratigraphic position of the main mineralisation, the ZCB and Polish systems are similar, in that ore is focused around a relatively thin reduced shale that immediately overlies the basal clastic 'rift' succession. In the essentially undeformed Polish deposits, it seems clear that this configuration allowed trapping of Cu in the reduced shales, that was sourced by syn-diagenetic brine convection in the sandstone aquifers (and the basement?). In this type of system, the evaporite units concentrated in the hangingwall acted as part of a regional seal to contain the brine convection, but they would also been susceptible to dissolution in areas of fluid upflow, thereby contributing to the overall salinity of the system.

In contrast, the stratigraphy of the AFB is both much thicker and more complex, comprising four major basin phases. The stratigraphic element equivalent to the mineralised level in other systems, the basal Callana Group certainly hosts Cu, but is largely covered by younger basin phases. In many areas where it is exposed, it occurs as dismembered stratigraphy that defines diapiric breccias. Because of this association, the diapirs are generally attributed to salt tectonism sourced from major evaporitic units in the Callana Group. This situation of wholesale evaporite migration, and the Polish system where the evaporitic units are essentially in situ, provide end members for understanding the ZCB, where the role of evaporites in basin development and Cu metallogeny is still unclear.

The AFB deposits usually compared to the ZCB and Kupferschiefer systems, those of the Tapley Hill Formation where it transgresses the Stuart Shelf, are part of the third basin phase. As a result, in the basin depocentres, this reduced stratigraphic package is insulated from the basal Callana Group, where early (syn-diagenetic) concentration of Cu from rift clastics and volcanics (and basement?) would have been most efficient, by an intervening basin phase. The Stuart Shelf deposits on the basin fringe more likely represent lateral, rather than convective fluid flow, which could have occurred at various times in the basin history, including compaction generated dewatering and periods of active basin growth and inversion.

Introduction

During the field meeting in Zambia in June this year, the industry sponsor group responses were used to identify a series of major questions that need to be addressed during the current study. Now that work is well underway in both the Zambian Copper Belt and Adelaide Fold Belt, it is an opportune time to compare what we know and think from our initial work in these basins. The ultimate aim of this process is to list the testable hypotheses that are forming the framework for the basin studies section of the project. The discussion below also incorporates ideas that arose from a trip to the Polish Kupferschiefer undertaken by some members of the research team in August this year. Although there are no plans to

work on this system in the current project, underground visits to two of the mines highlighted the Kupferschiefer's importance in understanding sediment-hosted Cu systems.

Zambian Copperbelt (ZCB)

It is clear from our initial studies in the ZCB that a comprehensive regional basin framework is going to be difficult to achieve. This is due to:

(1) the relatively small area of exposure of a presumably much larger basin;
(2) the lack of outcrop around the Kafue Anticline from which to collect the necessary detailed sedimentological (e.g. facies geometry, lateral variation etc.) and structural (e.g. kinematic) data;
(3) the unavailability of regional geophysical datasets which would to some extent overcome these problems.

The degree of metasomatism, deformation and metamorphism are additional complicating factors. The approach taken to date has been to commence the collection of what regional data can be obtained from the available stratigraphic drilling, and to focus more detailed studies on the available mines, where underground and/or surface workings and more abundant drilling information exist.

In spite of the above limitations, a broad picture of the stratigraphy of the ZCB around the Kafue Anticline is beginning to emerge. In general, it can be considered in terms of three elements (Fig. 1). A basal clastic succession of quartzite and arkose of variable thickness (lower Roan), is abruptly overlain by relatively thin but laterally persistent finer-grained deposits of either carbonaceous siltstone or correlative carbonates (Ore Shale and equivalents). These are in turn overlain by a diverse package of coarse- and fine-grained clastics and carbonates (hanging wall sequence, upper Roan and lower Kundelungu). Primary evaporite textures in the form of nodular anhydrite are preserved from around the level of the Ore Shale and equivalents, but are most abundant in the overlying succession, as "secondary" anhydrite cements, vughs and veins which presumably represent remobilised evaporitic material.

The genetic interpretation of the origin of the Cu and Co mineralisation is complicated by the same factors that hinder broader basin analysis, however some general observations on this issue can also be made. The bulk of the mineralisation is stratabound, and concentrated around the contact between the lower clastic succession and the ore shale and equivalents. A substantial proportion of the mineralisation is hosted in the footwall sandstone. In terms of the arguments regarding a diagenetic versus syn-deformational timing for the mineralisation, it is clear that much of the Cu and Co now resides in structurally controlled sites. However, a significant amount also occurs as disseminations within fine-grained, reduced ore shale (e.g. the Konkola system; Pollington and Scott, this volume) that is not obviously structurally controlled.

It should be noted that there is a potential problem in making direct comparisons between the stratigraphic setting of the ZCB and that of the other Cu mineralized systems considered here. It is likely that the Kafue Anticline area, the only region where the stratigraphy of the ZCB can currently be studied, is only a small window into a basin that originally had a much larger aerial extent. Although some data is available from the DRC to the north, doubt has recently been cast on published stratigraphic comparisons with this succession (Wendorf, 2001). As a result, there are two possible scenarios for the Katanga Supergroup. It is assumed above that what you see is what you get, and the Roan is the basal phase of sedimentation of the Katangan system. However, it is always possible, due to the limitations of available outcrop, that the Roan is a later basin phase transgressing the shoulder of a much larger system, the way the Umberatana, the third main basin phase of the Adelaide Fold Belt, transgresses the Stuart Shelf (see below).

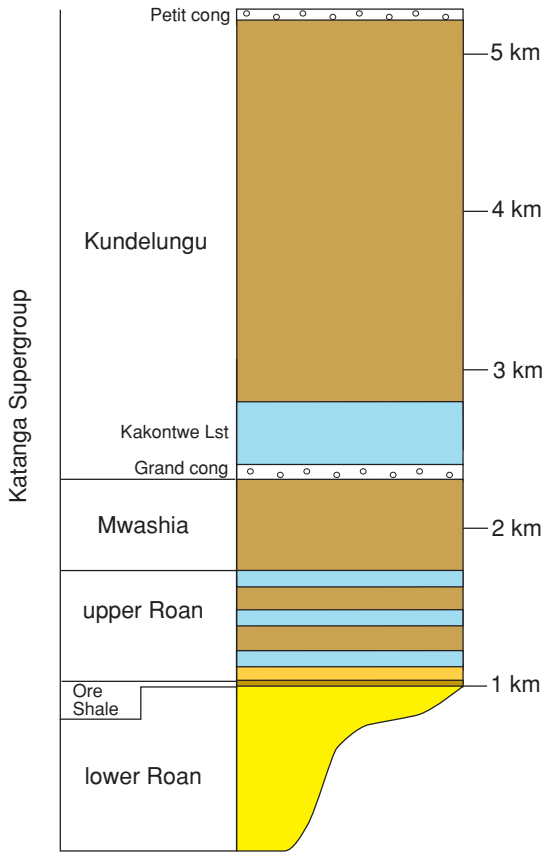

Figure 1
Schematic stratigraphic column of the lower part of the Katangan Supergroup in the Kafue Anticline area; yellow = clastics, brown = siltstones / shales, blue = carbonates, pebble fill = glacials.

Polish Kupferschiefer

In general terms, the Permian stratigraphy of the Polish Cu system is similar to that of the ZCB (Fig. 2) in that it comprises a basal clastic sequence of variable thickness (Rotliegendes), which in this case includes substantial bimodal volcanic units; overlain by a thin organic rich shale (Kupferschiefer) with carbonate correlates; overlain by a carbonate- and evaporite-dominated succession (Zechstein). The broad distribution of the mineralisation is also analogous, in that it is stratabound and concentrated at the level of the base of the Kupferschiefer, with substantial deposits occurring entirely within the underlying sandstones (e.g. the Lubin mine).

The significance of the Polish system for our work in Zambia, is that the Permian host sedimentary succession is essentially intact and undeformed, allowing the Cu to be placed in a basin context. Current genetic models are that the mineralisation is syn-diagenetic (e.g. Jowett, 1986). In summary, these models invoke leaching of metals during diagenetic convective migration of oxidised brines through the permeable basal sandstones (and volcanics), and reduction-induced metal deposition around the base

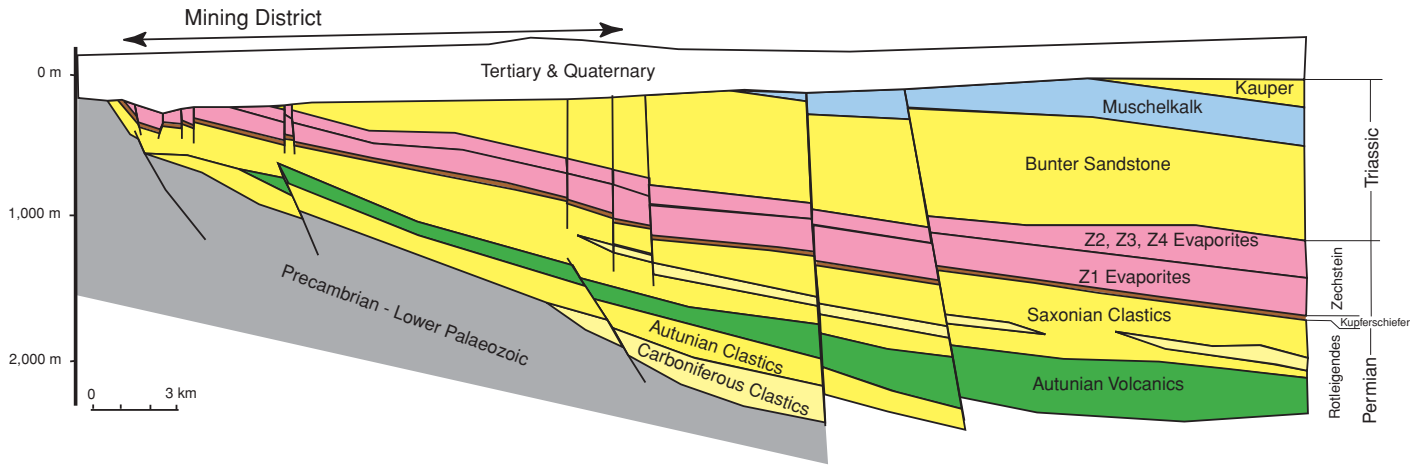

Figure 2.
Geological cross-section through the Polish Kupferschiefer district (veritcal exaggeration x5 (modified after Wodzicki & Piestrzynski, 1994); yellow = clastics, blue = carbonates, green = mafic volcanics, pink = evaporitic unit, brown = siltstone / shale.

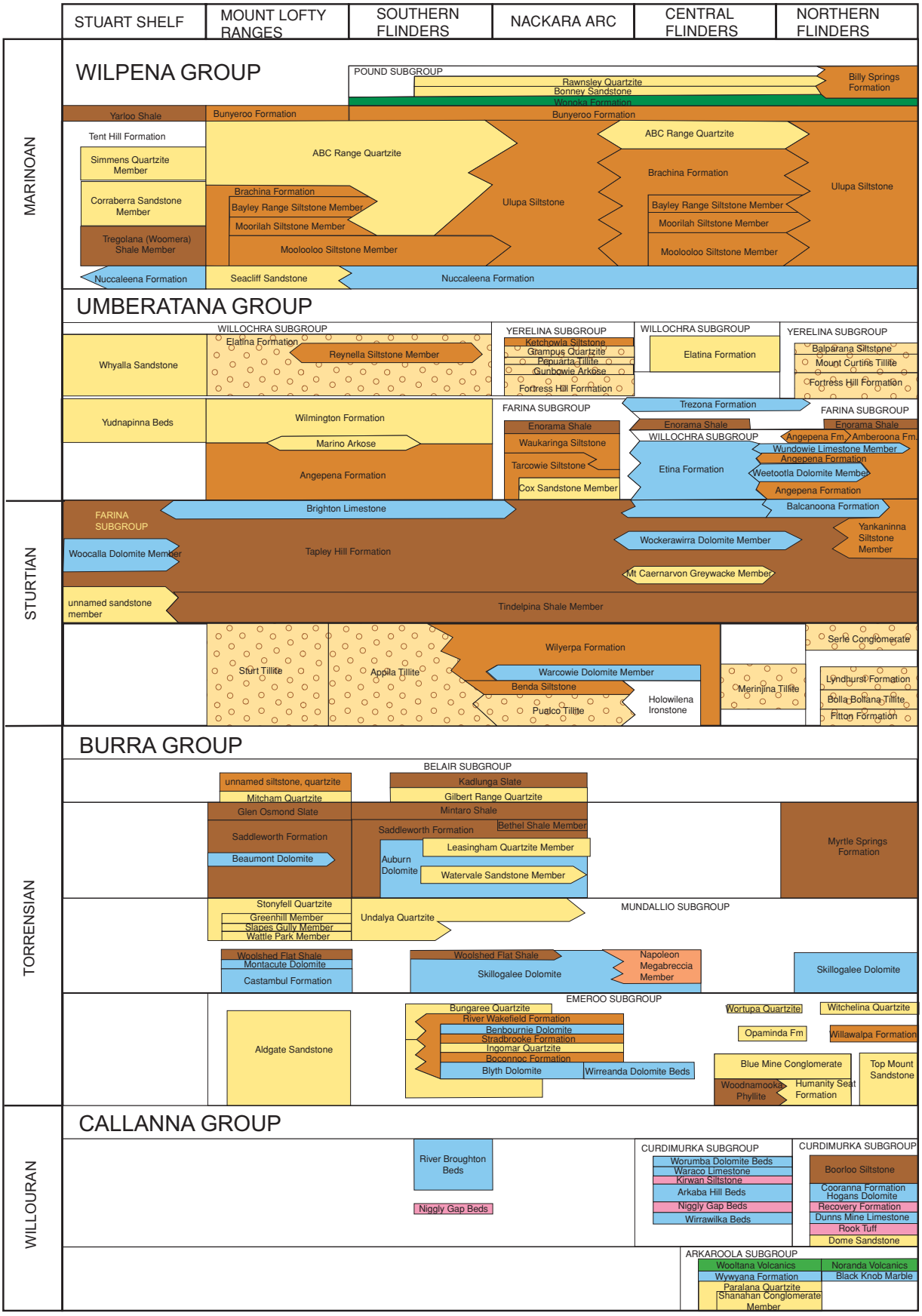

Figure 3
Stratigraphy of the Adelaide Fold Belt (modified after Preiss, 1993); yellow = clastics, blue = carbonates, green = mafic volcanics, pink = evaporitic unit, light/dark brown = siltstone/shale, pebble fill = glacial deposits.

of the organic-rich Kupferschiefer, which acts as a regional seal. At first glance, the Zechstein evaporites, which are still in their primary position in the hanging wall, are relegated to a passive role as part of the regional seal. However, where the Kupferschiefer was thin or absent, the convecting brine could potentially have come into contact with the evaporites, resulting in dissolution and increase in the overall salinity of the system (e.g. Warren, 1997).

Adelaide Fold Belt (AFB)

The stratigraphy of the AFB is markedly different to that of both the ZCB as we currently understand it, and to the Polish Permian. The basin succession is considerably thicker and has a more complex history (Fig. 3). This is reflected in the basin fill, which comprises four stacked depositional cycles (broadly represented by the Callana, Burra, Umberatana and Wilpena Groups), separated by disconformities/unconformities. In addition, in marked contrast to the Polish system in particular, there has been extensive salt tectonics in the form of wholesale migration of evaporites, as evidenced by extensive diapiric breccias (e.g. Preiss, 1987).

In terms of position within a developing basin, the stratigraphic equivalent of the main mineralized level in the Polish and Zambian systems in the AFB would be the basal basin phase, the Callana Group (Fig. 4). This unit certainly has similarities to these successions, comprising fault controlled clastics, carbonates and mafic volcanics, overlain by a carbonaceous siltstone unit (Boorloo Siltstone and equivalents). However, it is difficult to asses the regional palaeogeography and distribution of mineralisation within this basin phase in detail, because it is largely covered by younger sedimentary cycles (fig. 4) and coherent exposure is restricted to small inliers. Dismembered stratigraphic elements of this succession are a major constituent in diapiric breccias, which has led to the general inference that it was the source of the thick evaporites that drove salt tectonism (e.g. Preiss, 1987). Minor Cu mineralisation is present in the Callana Group, some of which is hosted in dolomite and some in carbonaceous siltstone, and many of the other small Cu shows are spatially associated with the diapiric breccias that are dominated by dismembered Callana Group stratigraphy (Preiss, 1987; Selley and Bull, this volume).

One further factor that needs to be considered is the nature of the basement to the AFB. The Mesoproterozoic Hiltaba suite of granites are an important element of the basement to the AFB. One of the two constituent granite series, the Roxby Downs-type, are spatially associated with the Olympic Dam deposit. It is well documented that these granites are enriched in radiogenic elements and produce anomalously high heat flow that in places has persisted to the present (Neumann et al., in press). Heat anomalies associated with these units could therefore have been an important factor in determining fluid flow patterns and hence Cu metallogeny of the Neoproterozoic system (Selley, 2000).

Discussion

The general observations outlined above have implications for the relationship between basin history and Cu mineralisation. The youngest and best preserved large-scale Cu system is the Kupferschiefer. In this case, extensive convection of brines in the basal sandstones and volcanics is possible in current syn-diagenetic models for mineralisation, because primary permeability and porosity can still be present. Provisional observations made during our brief visit to Poland earlier this year, indicate an absence of penetrative fabrics that could host structurally controlled Cu, supporting a diagenetic timing for the mineralisation in this case.

Convective circulation in sandstone aquifers is currently the focus of investigations at CODES as part of the ongoing studies of fluid flow and Zn mineralisation in the McArthur Basin (e.g. Garven et al., in press; Yang et al., 2001). These studies indicate that convection works well where a thick clastic succession is overlain by a relatively impermeable barrier. In this type of system, Cu could precipitate

where ascending oxidised brines infiltrated and were reduced by organic-rich cap rocks. Due to the low rates of fluid flow expected in the relatively low permeability host shales, this process would be facilitated by sustained basin-scale convection rather than episodic fluid movements. Interestingly, the McArthur Basin modelling indicates that such a sustained hydrological system would also allow the interaction of the dense brines with relatively low permeability basement. This is especially true in the region of faults that cut the basin–basement boundary, and in these areas the latter could therefore also be implicated as a potential metal source.

If sandstone-hosted Cu mineralisation is also the product of sulfate reduction (and/or reduced sulfur addition), the most obvious candidate for an organic phase in these deposits would be mobile or trapped hydrocarbons. These would be unlikely to occur where the aquifer is thick and continually flushed by convecting brines, but would be more likely at lateral pinchouts of the lower clastics, which would also be natural pathways for basin dewatering. Hydrocarbon mediated Cu precipitation has proposed for Mufulira (Annels, 1979), and for other sandstone-hosted base metal accumulations such as the Pb-rich deposits of the Swedish Caledonides (e.g. Laisvall; Rickard et al., 1979). In the sandstone hosted ores of the Polish Permian, the sulfides reportedly replace carbonate and sulfate (Ludwig and Rentzsch, 1967). In petroleum systems, the generation of secondary porosity by dissolution of carbonate and sulfate is a classic method of producing effective hydrocarbon reservoirs.

Although the ZCB is more complex, broad similarities exist with the simpler Polish system, especially the focus of the mineralisation around the base of the main reduced seal in the lowermost basin phase in both sandstone- and shale-hosted forms, the latter of which has no obvious structural control. This suggests that syn-diagenetic processes were also an important initial Cu-concentrating factor in the ZCB system, even though much of the metal has been subsequently remobilised, or more has subsequently been introduced, into structurally hosted sites. Interestingly, Hitzman (2000) has calculated that there is not enough clastic sediment beneath the ore shale in the exposed part of the ZCB to source the Cu present, and interprets this to indicate that the host stratigraphy has been tectonically displaced from the actual source rocks. As outlined above, the hydrogeological modelling based on the McArthur Basin suggests another possibility, if large-scale convective fluid flow systems were maintained in the basal clastics for long periods. These rift-stage deposits characteristically infill irregular basement topography controlled by growth faults, an ideal scenario for at least some of the Cu to have been derived from interaction of the circulating brines with basement.

In the case of the AFB, the Cu deposits most often compared in style to the Zambian and Kupfershiefer systems are those hosted in the Tapley Hill Formation (THF) on the Stuart Shelf. However, as discussed above, the THF was deposited considerably later in the relative basin fill history than the basal basin phase that hosts the Polish, and as far as we know the Zambian Cu mineralisation. In fact it occurs in the third major basin phase of the AFB, the Umberatana Group (Fig. 3). It has been argued above that the syn-diagenetic concentration of Cu in the basal basin phase in the well preserved Polish system, suggests that convective fluid flow occurred while the basal arkoses and volcanics retained primary porosity and permeability. However, provided the stratigraphy was intact, at the time when the reduced siltstones and shales of the THF had primary porosity and permeability in the basin depocentre/s, they would have been insulated from the basal (Cu-enriched?) Callana Group succession, by the impermeable platformal carbonates of intervening Burra Group. Preliminary work this field season suggests that exceptions exist where the Burra Group was tectonically removed during accelerated extension (Selley and Bull, this volume), leading to Cu mineralisation both in and around the diapiric breccias and uplifted Callana Group fault blocks that record breaching of the Burra Group, and in the THF and associated reduced Umberatana units.

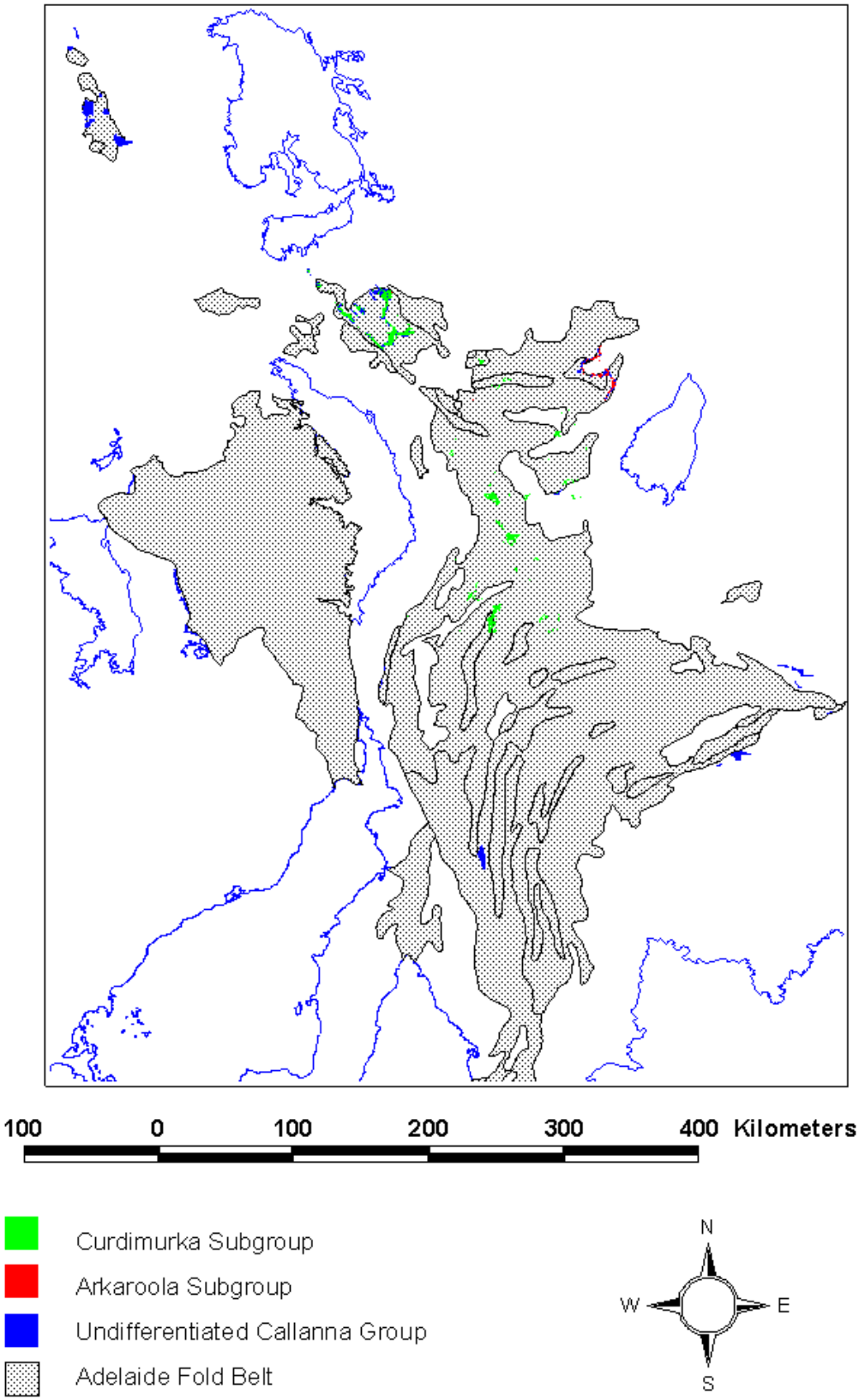

Figure 4
Outcrop of the Callanna Group, Adelaide Fold Belt.

On the Stuart Shelf the THF transgresses basement in many areas, but is locally underlain by inliers of Callana Group sediment. However, even if the basal sediments retained primary porosity and permeability to Umberatana time, their restricted development would seem to provide little potential for the development of large-scale convective fluid flow. Preliminary examination of the Emmie Bluff prospect as part of the current project, and a review of other THF deposits (Selley, 2000), indicates a common vertical metal zonation with respect with both lower and upper unconformable contacts. This suggests the Cu was more likely introduced via fluids moving along the unconformities that bound the THF.

Conclusions

The discussion above raises a number of testable hypotheses that can be used to address some of the major questions raised on the field meeting in June that relate to the basin studies module as follows.

Question. What is the broad structural framework of the Copperbelt?

Hypothesis. The simplest scenario would involve an effectively sheet-like Katangan basin-system, wherein present structural geometry involving "basins" (e.g. Chambishi "basin") and basement inliers ("domes") is solely attributable to the inversion phase.

Hypothesis. A more likely model is that the present structural geometry was inherited largely from a complex basin architecture. On the western flank of the Kafue Anticline at least, thickness variation within the Roan sequence appears to define broadly WNW-ESE trending depocentres. The present configuration of "basins" and basement "domes" may be attributable to oblique inversion of a compartmentalised basin architecture involving subsident troughs and intervening basement highs (?tilt blocks).

Method. Original basin architecture is best deciphered by incorporating thickness and facies variation with existing structural data. This will be undertaken firstly at the mine scale where drilling is sufficiently dense to establish sub-basin geometry. These data will be fed into a broader "basin-scale" model (where drilling data is sparse) and hopefully integrated with available geophysical datasets. Details concerning the inversion history will come largely from deposit-scale mapping at the periphery of the Chambishi "basin".

Lithogeochemical (and geochronological) studies will aid in stratigraphic correlation, potentially with the construction of a chemostratigraphic framework. It is anticipated that variation in geochemical and/or geochronological characteristics will have developed both vertically and laterally in response to contribution from different source areas.

The AFB will be used as an analogue for the ZCB. Although considerably more complex in terms of its history of basin growth, there are distinct similarities in terms of fundamental stratigraphic architecture and style of basin closure.

Question. Why is strain partitioned and what controls this?

i.e. Strain and to some extent metamorphic grade is partitioned both laterally and vertically within Katangan stratigraphy.

Hypothesis. The apparent increase in strain within the Mwashia compared to the Roan package indicates allochthoneity of the former.

Hypothesis. "Decoupling" occurred at the Roan-Mwashia boundary during inversion in response to a change in original basin architecture at this level. This stratigraphic level may record the transition from a compartmentalised, fault-bounded basin morphology to a broader basin system which lacked significant internal structure (?sag).

Hypothesis. The progressive northerly decrease in metamorphic grade (in some cases coinciding with major shear zones) may reflect deeper burial of Roan strata beneath a thicker post-Roan sequence to the

south. The abrupt change in metamorphic grade across major shear zones may indicate that they were originally active as basin-bounding structures, effectively controlling depth of burial of the Roan stratigraphy.

Method. This question will be in part resolved by continuing work of Dave Broughton on structural complexities at the Roan–Mwashia interface. Textural and geometric study of this surface from drill core will be incorporated with the team's work on establishing basin morphology within the lower Katangan. Geochronological and provenance studies undertaken by CODES and UWA will aid in identifying major changes in basin geometry and/or allochthoneity of the post-Roan stratigraphy.

Again, the AFB will be used as an analogue for the ZCB. Similar vertical and lateral partitioning of metamorphic grade and strain occur throughout this system. Importantly widespread detachment surfaces soled within evaporitic strata of the lower AFB developed both during basin growth and inversion.

Question. What lithological/facies/provenance changes are present regionally — both laterally (esp. Lower Roan) and vertically (Roan– Mwashia–Kundelungu)?

Question. What is the sedimentary environment for the different sedimentary packages? (Can we develop facies models to help guide exploration?)

Hypothesis. That where shale-hosted mineralisation occurs in the basal basin phase of a Cu mineralized system, it may be broadly associated with thick clastic packages. Conversely, sandstone-hosted mineralisation may be associated with hydrocarbon traps in condensed sections and lateral pinchouts.

Method. This can only be tested by putting the Katangan deposits in their broader basin context as far as that is possible given the limitations involved. This work is underway in the logging of a fence of holes from the Chambishi Basin, and examining some of the deposits on the basin margin (e.g. Nkana and Chibiluma).

Question. Were there thick evaporites (lacustrine and/or marine) in the sequence? If so, where were they and did they move?

Hypothesis. That the Kupfershchiefer and AFB provide contrasting models for the role of evaporites in the ZCB. In the former, they form part of a regional seal during an initial syn-diagenetic stratiform Cu concentration, and probably also contribute salinity to the convecting basinal brines in the underlying sandstones. In the latter they, are aggressively mobile at some time in the basin history (basin compaction, inversion or deformation?) and facilitate Cu mineralisation by creating cross stratal pathways for saline fluids and thermal conduction.

Method. The AFB provides a magnificent natural laboratory for studying the nature and effects of evaporite mobility, and the relationship of the diapirism to Cu mineralisation. It can help clarify several important problems that exist in Zambia. For example, we require a method of testing whether some of the enigmatic breccias in the upper Roan and Kundelungu are the result of evaporite dissolution. We may be able to the use the geochemistry and/or isotopic composition of carbonate matrix to the AFB diapirs that we know represents evaporitic cement in this system.

Question. Why are different lithologies (shale, siltstone, arkose, and carbonate) ore hosts? What is common to them that allowed sulfide precipitation?

Question. What precipitates copper sulfides? (why is mineralisation in different lithologies?).

Hypothesis. That each of these host packages shared the common elements of high permeability (structural and/or stratigraphic) and the presence of a reactive component, which allowed significant fluid flow whilst also providing an effective chemical gradient to drive ore deposition

Method. Detailed deposit-based studies by the PhD students will provide new insights into the controls on ore formation at Konkola North and Nkana. This information needs to be integrated with the information currently available in the literature, and with the additional new data generated by the research team at other Zambian deposits. Whether one common factor emerges for all of the deposits (be it structural history, secondary porosity, presence of hydrocarbons, etc.), or whether a conjunction of several factors have occurred at any given deposit needs to be established in order to address these questions adequately. Fluid inclusion studies would be of great benefit, if suitable material can be found.

Hypothesis. That the metalliferous brines are oxidised (i.e. aqueous sulfur occurs predominantly as sulfate) and that sulfate reduction and/or interaction with/addition of reduced sulfur are the main processes responsible for ore deposition.

Method. To test whether the mineralising brines are oxidised at any given deposit, it is essential to assess the ore and gangue mineralogy (e.g. hematite, anhydrite, pyrrhotite, organic carbon) for indications of the prevailing redox conditions. This needs to be done in conjunction with an evaluation of the anomalous trace elements in the system, because the presence or absence of anomalous Au, Ba, Mn, Sn, Sb, As, etc. can also provide indications of the redox potential of the mineralising brines. If the brines are oxidised, then sulfur (& carbon?) isotopic analyses can be used to help evaluate whether sulfate reduction occurred. If addition of H_2S from a sour gas reservoir or by replacement of a pre-existing sulfide accumulation were key processes, then textural studies in conjunction with stable isotope analyses should help to evaluate these hypothesis.

Hypothesis. Based on observations of the Kupfershiefer system in Poland, some disseminated shale-hosted Cu mineralisation represents syn-diagenetic infiltration of oxidised fluids via primary or diagenetic, not deformation-generated, porosity and permeability.

Method. Samples were collect on our visit to Poland this year that will be compared with detailed petrological observations of the most similar of the Zambian deposits, Konkola.

Hypothesis. That the reductant and/or reduced sulfur source in the case of the sandstone-hosted mineralisation was trapped hydrocarbons.

Method. At the Century zinc deposit, northern Australia, an intimate association with hydrocarbons is provided by the preservation of pyrobitumen (Broadbent et al., 1998), and also by the extremely fine (angstrom) scale intergrowths of sphalerite and organic carbon detected by transmission electron microscopy (TEM – McKnight and Broadbent, 1993). At the Warrabarty Zn deposit (Northwestern Australia), although organic carbon could not be observed in sphalerite, its presence was detected during laser raman (LR) analyses. In the case of the Zambian Cu deposits, if no macro- or microscopic evidence for the presence of hydrocarbons can be observed, microanalytical techniques such as LR or TEM could be used to assess whether the high grade ore is intergrown with organic carbon at the sub-micron scale.

Question. What is source of Cu?

Hypothesis. If sustained syn-diagenetic brine convection in the basal sandstone package was responsible for initial stratiform Cu concentration in and around the reduced low permeability cap, then metal could also be sourced via brine interacting with the basement at this time, especially in the region of penetrative faults.

Method. There are three possible avenues to approach this problem. One is to examine the literature to determine whether, in a regional sense, all major sedimentary Cu systems overlie Cu mineralised basement (e.g. as is clearly the case for the AFB). The second, to look at an example of spatially related basement and basin Cu mineralisation, is one of the aims of the study of Emmie Bluff on the Stuart Shelf. The third involves using radiogenic isotope studies (Sr, Pb, Os) to assess the relative basement and basinal contributions of these components to the ore and gangue minerals. This approach would require some knowledge of the radiogenic isotopic characteristics of the basement and the basin-fill lithologies.

References

Annels, A. E. 1979. The genetic relevance of recent studies at Mufulira Mine, Zambia. Ann. Soc. Geol. Belg., v 102, p. 431-449.

Broadbent, G. C., Myers, R.E., and Wright, J.V., 1998. Geology and origin of shale-hosted Zn-Pb-Ag mineralisation at the Century deposit, Northwest Queensland, Australia. Economic Geology, 93, 1264-1294.

Garven, G. and Bull, S. 1999. Fluid flow modelling of the HYC ore system, McArthur Basin, Australia. In Stanley, C.J. (ed.) Proceedings of the Fifth Biennial SGA Meeting and the Tenth Quadrennial IAGOD Symposium, Longdon, UK, August 22-25.

Hitzman, M. W. 2000. Source basins for sediment-hosted stratiform Cu deposits: implications for the structure of the Zambian Copperbelt. J. African Earth Sci. v 30 (4), p. 855-863.

Jowett, E. C. 1986. Genesis of the Kupferschiefer Cu-Ag deposits by convective flow of Rotlegende brines during Triassic rifting. Econ. Geol. v. 81, p. 1823-1836.

Ludwig, H. and Rentzsch, J. 1967. Dans Sanderzproblem. Ein beitrag zur genese des Kupfershiefers. Ber. DGGW, Reihe B, p. 1-12.

McKnight, S., and Broadbent, G. C., 1993. Transmission electron microscopy study of bitumens occurring in the Century Zn deposit, north Queensland. Proceedings of Congress on Applied Mineralogy, Perth, 1993, International Council for Applied Mineralogy, p.61.

Neumann N., Sandiford M. & Foden J. in press Regional geochemistry and continental heat flow: Implications for the origin of the South Australian heat flow anomaly.

Pollington and Scott (this volume)

Preiss W. V. (compiler) 1987. The Adelaide Geosyncline-late Proterozoic stratigraphy, sedimentation, palaeontology and tectonics.

Geological Survey of South Australia, Bulletin 53, 438 p.

Rickard, D. T., Willden, M. Y., Marinder, N. E. and Donnelly, T. H. 1979. Econ. Geol. v. 74, p.1255-1285.

Selley, D. 2000. Geological framework and copper mineralisation in South Australia. In AMIRA/ARC project P544, Proterozoic sediment-hosted copper deposits, Report 2.

Selley and Bull (this volume)

Warren, J. K. 1997. Evaporites, brines and base metals: fluids, flow and 'the evaporite that was'. Aust. J. Earth Sci. v. 44, p. 149-183.

Wendorff, M. 2001. New exploration criteria for 'megabreccia'-hosted Cu-Co deposits in the Katangan belt, central Africa. In Piestrzynski et al. (eds.), Mineral Deposits at the Beginning of the 21st Century, proceedings of the 6th biennial SGA-SEG meeting, Krakow, Poland. p. 19-22.

Yang, J., Large, R. and Bull, S. 2001. Numerical simulation of transient hydrothermal fluid migration associated with the formation of mineral deposits in the McArthur basin. In Williams, P.J. (ed.) Extended Abstract of 2001 Hydrothermal Odyssey, 228-229. Townsville, Queensland, May 17-19.